AD-A174 406 DEVELOPMENT AND TESTING OF DRY CHEMICALS IN ADVANCED EXTINGUISHING SYSTEM (U) SAN JOSE STATE UNIV CALIF R L ALTMAN ET AL FEB 83 JTCG/AS-82-T-002 1/3

UNCLASSIFIED NCA2-OR675-806/NSG-2165 F/G 13/12 NL

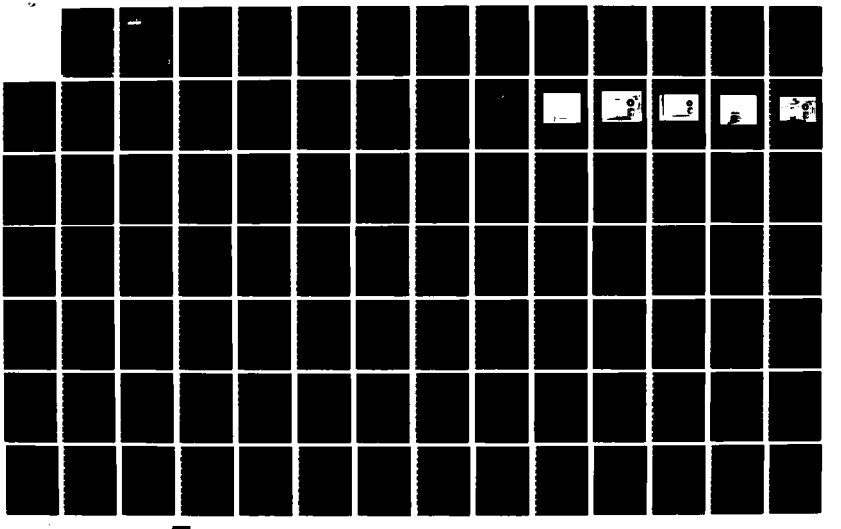

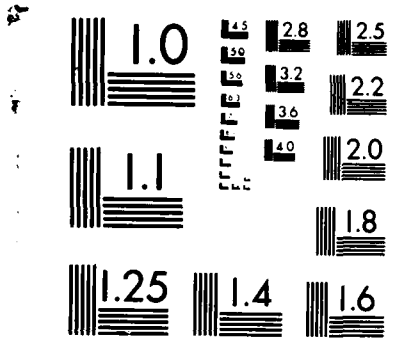

REPORT JTCG/AS-82-T-002

DEVELOPMENT AND TESTING OF DRY CHEMICALS IN ADVANCED EXTINGUISHING SYSTEMS FOR JET ENGINE NACELLE FIRES

Final Report

Robert L. Altman,
A. Campbell Ling,
Ludwig A. Mayer,
Donald J. Myronuk

February 1983

Prepared for

THE JOINT LOGISTICS COMMANDERS
JOINT TECHNICAL COORDINATING GROUP
ON
AIRCRAFT SURVIVABILITY

SECURITY CLASSIFICATION OF THIS PAGE (When Data Entered)

REPORT DOCUMENTATION PAGE		READ INSTRUCTIONS BEFORE COMPLETING FORM
1. REPORT NUMBER JTCG/AS-82-T-002	2. GOVT ACCESSION NO. AD-A174 406	3. RECIPIENT'S CATALOG NUMBER
4. TITLE (and Subtitle) Development and Testing of Dry Chemicals in Advanced Extinguishing Systems for Jet Engine Nacelle Fires		5. TYPE OF REPORT & PERIOD COVERED Final Report 1975-1979 6. PERFORMING ORG. REPORT NUMBER
7. AUTHOR(s) Robert L. Altman, A. Campbell Ling, Ludwig A. Mayer, and Donald J. Myronuk		8. CONTRACT OR GRANT NUMBER(s) NCA2-OR675-806/NSG-2165
9. PERFORMING ORGANIZATION NAME AND ADDRESS Department of Chemistry and Civil Engineering San Jose State University San Jose, CA 95192		10. PROGRAM ELEMENT, PROJECT, TASK AREA & WORK UNIT NUMBERS 505-08-21
11. CONTROLLING OFFICE NAME AND ADDRESS JTCG/AS Central Office, AIR-5164J Naval Air Systems Command Washington, D.C. 20361		12. REPORT DATE February 1983 13. NUMBER OF PAGES 188
14. MONITORING AGENCY NAME & ADDRESS(if different from Controlling Office) National Aeronautics and Space Administration NASA-Ames Research Center Mountain View, CA 94035		15. SECURITY CLASS. (of this report) Unclassified 15a. DECLASSIFICATION/DOWNGRADING SCHEDULE
16. DISTRIBUTION STATEMENT (of this Report) Unlimited		
17. DISTRIBUTION STATEMENT (of the abstract entered in Block 20, if different from Report)		
18. SUPPLEMENTARY NOTES This work was sponsored by AFAPL MIPR 1455700511 and 14557600617.		
19. KEY WORDS (Continue on reverse side if necessary and identify by block number) Fire control Hot surface ignition Dry chemical extinguishants Jet engine fires		
20. ABSTRACT (Continue on reverse side if necessary and identify by block number) (See reverse side.)		

DD FORM 1 JAN 73 1473 EDITION OF 1 NOV 65 IS OBSOLETE
S/N 0102-LF-014-6601

SECURITY CLASSIFICATION OF THIS PAGE (When Data Entered)

National Aeronautics and Space Administration

Development and Testing of Dry Chemicals in Advanced Extinguishing Systems for Jet Engine Nacelle Fires, by Robert L. Altman, A. Campbell Ling, Ludwig A. Mayer, and Donald J. Myronuk San Jose State University. (Department of Chemistry and Civil Engineering). Mountain View, CA, (NASA) for Joint Technical Coordinating Group/Aircraft Survivability. February 1983. 188 pp. (JTCG/AS-82-T-002, publication UNCLASSIFIED.)

This document reports an experimental study of the effectiveness of dry chemical in extinguishing and delaying reignition of fires resulting from hydrocarbon fuel leaking onto heated surfaces such as can occur in jet engine nacelles.

The commercial fire extinguishant dry chemicals tried were, for example, sodium and potassium bicarbonate, carbonate, chloride, and carbamate (Monnex) but we have also tested other metal-halogen and metal-hydroxycarbonate compounds prepared in our own laboratories.

Given in this report are: synthetic and preparative procedures for new materials developed; a new concept of fire-control by dry chemical agents; descriptions of experimental assemblages to test dry chemical fire extinguishant efficiencies in controlling fuel fires initiated by hot surfaces; comparative testing data for more than 25 chemical systems in a "static" assemblage with no airflow across the heated surface, and similar comparative data for more than 10 compounds in a dynamic system with airflows up to 350 ft/sec; and recommendations for future work with one system that fulfills all requirements delineated by the sponsoring agency, and which has been tested in both the Static and Dynamic assemblages with both methodologies confirming it as the most effective system by comparison with the other materials tested.

CONTENTS

Figures:

Tables:

Section 1

INTRODUCTION

When aircraft environmental and operational temperatures increase, as shown in Table 1, the fire hazard from the accidental release of combustible fluids into engine nacelle* compartments following component failure is greatly aggravated. In commercial aircraft with turbine propulsion, 57 such fires occurred in the 18-year period from 1956 to 1974 (Reference 1); however, for military aircraft about 80 to 90 such noncombat fires occurred annually in the USAF from 1965 to 1974 (References 2 and 3), of which about one-half were identified as engine case burn-throughs. To reduce the damage to aircraft due to fire, we have undertaken a program to increase the capability for the suppression and control of those fires that come about from combustible fluids leaking onto heated surfaces.

The current technique for extinguishing such fires began with the injection of gas or liquid systems such as carbon dioxide, carbon tetrachloride, methylene chloride and methyl bromide (References 4–6); later investigations used bromochloromethane, chlorofluoromethane, dibromodifluoromethane, dibromotetrafluorethane, and bromotrifluoromethane (References 7–9). The CAA then initiated an investigation of airflow effects, extinguishant discharge rate and nacelle surface roughness upon successful extinguishment (References 10–14), and development of the Statham analyzer to determine the actual concentration of gaseous extinguishant in the nacelle void space (References 15 and 16). More recent experimental work on fires in engine nacelles, wing fuel tanks, and oil sumps is reported in References 17–21, and a general discussion of the problems of designing gaseous fire extinguishant systems to meet the requirements delineated in Table 1 is given in Reference 22.

The maximum surface temperature and/or bleed air temperature listed in Table 1 is great enough to induce hot surface ignition of fuel. Klueg and Demaree (Reference 23) showed that such ignition can occur when either Jet A (JP-8) or Jet B (JP-4) fuel leaks onto a JT3D-1 turbofan engine case at a 0.3-gpm flow rate with an exhaust gas temperature exceeding 850°F, provided that the secondary airflow was not greater than 0.2 lb/sec for Jet A fuel and not greater than 0.1 lb/sec for Jet B fuel. These flow rates approximate an overall A/F (air/fuel) ratio of six or less. Sommers (Reference 24) also demonstrated that

*A nacelle consists of a pod which encloses the engine, and a pylon which supports the pod if the nacelle assembly is underslung from the lower surface of the wing.

hot surface ignition occurred when Jet A-1 leaked onto a JT-12A-6 turbojet engine whose case temperature was ca. 1150°F. In this instance, the fuel flow rate was about 0.4 gpm and the airflow rate did not exceed 0.15 lb/sec, corresponding to an overall A/F (w/w) ratio of about four. These large scale data support the laboratory scale findings of Strasser et. al. (Reference 25), who report that both JP-4 and JP-8 will ignite on surfaces heated to 1050°F with a fuel flow rate of 0.1 gpm and an airflow rate that produces an A/F (w/w) ratio of 1.3. It should be noted that the minimum ignition temperature increases somewhat with increased air velocity but decreases significantly when the heated surface is increased in area, and is only slightly reduced by preheating the air.

Table 1. Environmental and Operational Parameters for Aircraft Fire Suppression and Control.

	Surface temperature[a]	Bleed air temperature[b]	Ambient air temperature[c]	Airflow velocity[d]	Storage temperature[e]
			Engine nacelle environment		
Advanced	815°F 1500°F	705°C 1300°F	-55 to 345°C -65 to 650°F	105 m/sec 350 ft/sec	-55 to 260°C -65 to 500°F
Current	650°C 1200°F	595°C 1100°F	-55 to 205°C -65 to 400°F	75 m/sec 250 ft/sec	-55 to 120°C -65 to 250°F
			Dry bay area evnironment		
Advanced	290°C 550°F	650°C 1200°F	-55 to 260°C -65 to 500°F	45 m/sec 150 ft/sec (Combat damage)	-55 to 260°C -65 to 500°F
Current	120°C 250°F	540°C 1000°F	-55 to 120°C -65 to 250°F	45 m/sec 150 ft/sec (Combat damage)	-55 to 120°C -65 to 250°F

[a]Maximum turbine engine casing temperature or maximum skin temperature anticipated in the dry bay region

[b]Maximum bleed air temperature in the engine compartment or structural temperature in the dry bay region resulting from duct failure or combat damage.

[c]Maximum air temperature in the engine nacelle or compartment temperatue in the dry bay as per original design.

[d]Maximum air velocity within engine nacelle per original design or in dry bay region resulting from combat damage.

[e]Temperature range for storage of suppressant materials outside the engine nacelle region

NOTE: N.B. engine failure, or combat damage, may lead to still higher temperatures in localized regions than those quoted above.

Figure 1 was redrawn from the data of Reference 23, and substantiated by data from References 10, 13, and 26, indicates that the amount of gaseous fire suppressant, say CF_3Br (Halon 1301), required to extinguish a 0.3-gpm fuel leak fire increases

increased airflow. These data also indicate that the longer a fire is permitted to burn prior to the commencement of extinguishment action, the greater is the quantity of fire extinguishant required to achieve fire control. In these particular tests, the fuel supply was not cut off during the extinguishment phase of the experiment, as had been done in several earlier studies (see References 10, 13). The authors of Reference 23 attribute this need for increased quantities of extinguishant to changes in the airflow pattern (more turbulence?) brought about by deformation of the nacelle wall with prolonged heating, and to overheating of the nacelle walls caused prior to the commencement of the extinguishment process, thus inducing hot surface reignition of the still leaking fuel after initial extinguishment of the flame.

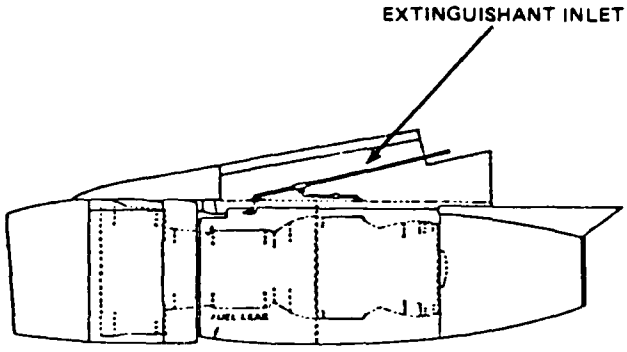

JTB D-1
TURBOFAN
ENGINE & NACELLE

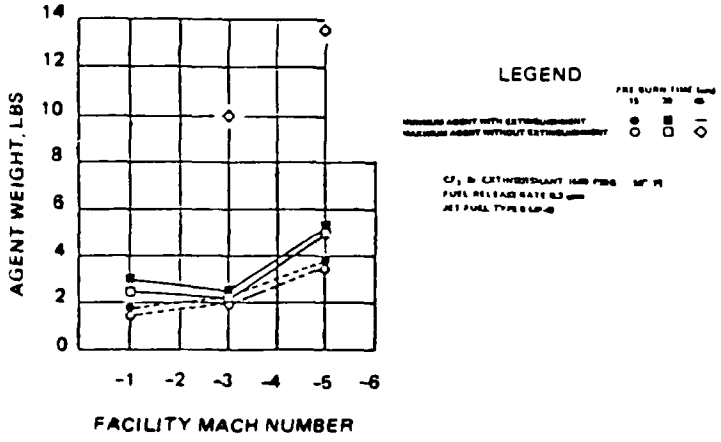

Figure 1. Fire Control of Turbofan Engine Nacelles.
(Redrawn from the Data given in Reference 23)

The authors of Reference 23 tested other gaseous extinguishants besides CF_3Br (Halon 1301) and they report that Halon 1301 was more effective than CF_2Br_2 (Halon 1202), which was better than CF_2ClBr (Halon 1211) or CH_2ClBr (Halon 1011) and that so-called pyrotechnic delivery (References 26–28) was more effective than delivery by stored nitrogen pressure. In an earlier study (Reference 26) Halon 1301 was also rated superior to $C_2F_4Br_2$ (Halon 2402), and this in turn was rated better than Halon 1011. These authors also rated Halon 1301 as more effective than the dry powder fire extinguishants, sodium bicarbonate, and ammonium dihydrogen phosphate, one of the earliest references to dry powder chemical fire extinguishants for nacelle fire control. In another early reference to the use of dry powder fire extinguishants (Reference 4), CCl_4 (Halon 1040) was also found superior to sodium bicarbonate powder and to a water solution of potassium carbonate.

In designing Halon-based fire extinguishers for installation in military aircraft, military specifications MIL-E-5352 and MIL-E-22285 suggest a design based on the relationship:

$$W_e = AW_a + BV \tag{1}$$

where

W_e = Weight of gaseous fire extinguishant required

W_a = airflow rate

V = net volume of the fire zone

A, B = constants depending on the mass and flow units (Reference 29)

A similar equation of this same form has been derived by the authors of Reference 30, and is discussed in Reference 22, this is equation is

$$W_e = (PCM_e)/(RT) \cdot [(W_a t/P_a) + V] \tag{2}$$

where

W_e = weight of gaseous fire extinguishant required

W_a = airflow rate

V = net volume of the fire zone

P = total static pressure

C = volume percent of extinguishant required for fire control

M_e = molecular weight of the extinguishant

R = gas constant

T = absolute temperature

t = extinguishant delivery time

P_a = ambient air density in the fire zone

The density of air can be expressed by the ideal gas equation relationship in the form

$$P_a = (P_a M_a)/(RT) \tag{3}$$

where

P_a = partial pressure of air

M_a = molecular weight of air

Since C is the volume percent of extinguishant required to control the fire, then the partial pressure of air can be written in the form:

$$P_a = (100 - C)\,P \tag{4}$$

and using this, Equation (2) can be written in the form:

$$W_e = C/(C - 100) \cdot (M_e/M_a) \cdot (W_a t + o_a V) \tag{5}$$

Assuming that the model used to derive Equation (2) is valid,* Equation (5) suggests that the value of the term

$$C/(C - 100) \cdot (M_e/M_a) \tag{6}$$

may yield a figure of merit for gaseous fire extinguishant effectiveness in preventing reignition after successful extinguishment, if the flammability peak concentration is used for the value of C in Equation (6), since no fire can exist at concentrations of extinguishant greater than the flammability peak concentration.

*See Reference 31 for discussion of British vs. U.S. extinguishant weight requirements for both military and civilian aircraft.

Data calculated from Equation (6) suggest that Halon 1301 should be about equal to Halon 1201, and should be significantly better than Halon 1211 in delaying hot surface reignition. Similarly, Halon 1202 should be more effective than Halon 2402. Unfortunately, this simple picture does not seem to be supported by experimental facts such as those from the static airflow pan fire test data of Fiala (Reference 33). This author used a hot surface reignition source in the form of one sidewall of a test pan, which was heated by an external flame to 1000°C, and demonstrated that Halons 1301 and 1211 were about equally effective in delaying reignition, and that Halons 1202 and 2402 were also approximately equal in effectiveness. More significantly, this author demonstrated that the latter pair were markedly better than the first pair in delaying reignition. A possible explanation for this may lie in the physical properties of each system at the ambient conditions prevailing. The experimental effectiveness of Halon 1211 relative to Halon 1301 is greater than that predicted by Equation (6), possibly because Halon 1211 is discharged as a liquid, while Halon 1301 is discharged as a gas. Likewise, the greater than predicted effectiveness of Halon 2402 relative to Halon 1202 may be attributed to its lower volatility. In this respect, it is instructive to consider this aspect of volatility further with reference to the current fire control system fitted to the F-111 aircraft.

The extinguishant in current use with the F-111 engine nacelle fire control system is based on Halon 1202, and driven by compressed nitrogen gas. The higher boiling temperature of Halon 2402 presumably means that this Halon will have a lower extinguishant vapor pressure at 260°C (500°F), the maximum quoted temperature for storage of the fire control system; and when the nitrogen driver gas is included also, there will be a significantly lower total pressure in the system as a whole when compared to a Halon 1202 based system used for the F-111. According to McClure & Springer (Reference 22) the F-111 engine nacelle fire control system contains 5.8 Kg of Halon 1202 charged initially with nitrogen to 42 atmospheres pressure at 20°C in a tank volume of approximately 6.3 liters.

Calculating the exact system pressure for Halon based fire control systems depends to a large extent on the availability of experimental values for the vapor pressure of such Halons, and values of the pressures recommended for the driver gases. The following data provide us with an estimate of these parameters. Gerstein and Allen (Reference 30) have estimated the vapor pressures of Halons 1202, 1211, and 1301, and the total system pressure for these systems, at 260°C via a calculation based on the known total system pressure at 20°C of 27 atmospheres, and they showed that

$$P_{1301} > P_{1211} > P_{1202}$$

for both the vapor pressure and the resulting total system pressure at 260°C for each system; but they do not give a corresponding pressure estimate for Halon 2402. DeRouville and Hebenstreit (Reference 27), have measured this latter quantity, yielding data that showed a total system pressure of 102 atmospheres at 260°C when approximately 1.8 moles of Halon 2402 had been loaded into a container of 0.3 liters total volume, and sufficient air added to bring the total system pressure up to 1 atmosphere at 20°C. On repeating this experiment using the same number of moles of Halon 1301, they measured a total pressure of 197 atmospheres at 260°C. They also reported that the Halon 2402 total pressure increased by no more than 4 atmospheres after 10 weeks storage at 260°C.

The total system operating pressure for Halon 1301 at the maximum expected storage temperature of 260°C is unacceptably high. It is therefore of interest at this point to determine whether use of Halons 1202 or 2402 might usefully reduce this total operating pressure for the F-111 fire control system, since both of these independent sets of data indicate that Halon 1202 and Halon 2402 have lower total pressures at 260°C (500°F) than does Halon 1301. To calculate this, we assume that non-ideal gas behavior can be expected for all of the Halons, as well as for the nitrogen driver gas, since relative to other gases and low boiling liquids, the Halons have relatively high critical temperatures. Equally, at the prevailing temperatures, the pressures of the nitrogen driver gas is commensurate with its own critical pressure. We will further assume that van der Waals' equation of state

$$\left(P + n^2a/V^2\right)(V - nb) = nRT \tag{7}$$

will provide a reasonable estimate of non-ideal behavioral characteristics for these systems, and we will use this equation to calculate the final system pressure for these two Halons (Reference 35). The advantage of the van der Waals' equation is that the parameters "a" and "b" can be calculated with sufficient accuracy from the critical parameters of the gaseous fluid, and do not need to be found by an experimental fit. In Equation (7), the values of a, b, and R, are derived from the critical parameters, V_c, P_c, and T_c, by the relations,

$$b = V_c/3 \tag{8}$$

$$a = 27b^2/P_c \tag{9}$$

$$R = 8a/27bT_c \tag{10}$$

where the parameters n, P, and T, are the number of moles of the gaseous fluid at a pressure P and absolute temperature T, respectively.

With this in mind, the parameters of interest pertaining to the F-111 fire control system are as follows:

1. The total volume of the holding container, 6.3 liters
2. The estimated maximum storage temperature, 260°C (500°F)
3. Initial mass of Halon 2402 loaded at ambient temperatures, 5.8 Kg at 20°C
4. Initial total system pressure caused by charging with nitrogen driver gas at ambient temperature, 42 atmospheres at 20°C.

Since the vapor pressure of Halon 2402 is only 0.5 atmospheres at 20°C (293°K), and the liquid density is 2.16 gm/cc, that part of the total pressure due to nitrogen is approximately 41.5 atmospheres; therefore, the 5.8 Kg of Halon 2402 has a liquid volume of ca. 2.7 liters. Hence, assuming that nitrogen gas in insoluble in liquid 2402, the nitrogen gas is contained in the remaining 3.6 liters. Now using the van der Waals' equation (Equation (7)), we can calculate the number of moles of nitrogen gas present from the given temperature,

pressure, and volume. This yields an answer for the number of moles of nitrogen gas of approximately 8.2 moles. Since the maximum estimated storage temperature of 260°C is above the critical temperature for Halon 2402, gaseous nitrogen will now share the entire volume along with the totally gaseous Halon 2402. Its contribution to the total system pressure is now estimated by repeating the calculation just illustrated, but now using a volume of 6.3 liters and temperature of 500°K for 8.2 moles of nitrogen and for 22.3 moles of 2402 (equivalent to the 5.8 Kg loaded originally). The result of these calculations is that the nitrogen driver gas will exhibit a pressure of ca. 45 atmospheres at 260°C, and the pressure contribution from the Halon 2402 contributes an additional 50 atmospheres; thus, the total system pressure will be 95 atmospheres (1400 psig). Similar calculations have been carried out for the other Halons.

Although the calculated total pressures at the maximum estimated storage temperature of 500°F for these Halon based systems are high, Graviner (Reference 37) nevertheless chose Halon 1211 for the new Concorde engine nacelle extinguishant. This is partly mitigated by the fact that the estimated inflight skin temperature of this aircraft lies in the range of -20 to 100°C, and only at the last engine compression stage does the temperature rise to ca. 580°C (1075°F). Graviner has proposed to circumvent the major defect of gaseous fire control systems, which involves the markedly reduced extinguishant weight effectiveness due to increased airspeed in the nacelle, by shutting a pair of flaps upstream of the compressor to physically reduce the nacelle airflow to the minimum leakage rate, 9 lb/sec, before beginning to discharge the cylinder containing 16 pounds of Halon 1211. This is estimated to provide a minimum Halon concentration of 10.5% by volume within 2 seconds after discharge begins, and to maintain this concentration for the next 2 seconds (Reference 31).

Bearing in mind the disparities exhibited between calculated values and experimental data obtained by Fiala (Reference 33) for the apparent effectiveness of various systems, we believe that further development of a gaseous fluid-based fire control system for advanced jet engine nacelles is not a promising proposition, and that further development of other halogen-based liquid or gaseous systems is probably inadvisable. Although the reduced weight effectiveness of fluid-based systems under conditions of high airflow can be mechanically circumvented to some extent (e.g., the method proposed by Graviner for the Concorde), this facet of the overall problem merely adds emphasis to the statement above.

If fluid (gas or liquid) based systems will not provide the needed characteristics, then solid systems should be investigated further. There are many reports in the research and development literature concerning the negative catalytic effects and general inhibition of gas phase phenomena by solid surfaces. For example, the minimum pressure and temperature required for the thermal detonation of a hydrogen-oxygen mixture, or for the ignition of a hydrocarbon-air mixture, is significantly increased when the inner walls of the container are coated with a salt layer such as KCl or CsCl (References 38–41). Since such salts are also known to be effective as fire extinguishants (References 42 and 43), one of our objectives is to develop fire extinguishant materials that will adhere to the walls of a jet engine nacelle, and thus help to nullify this high airflow effect which negates the fire control mechanism of gaseous systems. Further, a second objective will be to develop a solid-based fire control system that will not only extinguish the fire, *but which will prevent reignition*

of the fire even though the conditions that produced the fire initially are still obtaining. The principal aspect here is that even if jet fuel (JP-4) is still leaking onto a hot surface, and thus providing a potentially flammable situation throughout the delay period, the solid extinguishant adhering to the surface should provide a sufficiently high inhibitory effect so as to prevent reignition. It is hoped that a system, or systems, can be developed that will provide a minimum of 5 minutes delay in the reignition time under the conditions prevailing, or expected to prevail, in advanced jet engine nacelles (these conditions are summarized in Table 1). Our experimental approach will involve the development of a laboratory scale test facility to simulate the fuel ignition and flame propagation characteristics of jet engine nacelle fires under both static and moderate airflows.

Section 2

STATEMENT OF EXPERIMENTAL PROBLEM

The primary objective of this research was to find a suitable system, or systems, that will control ignition initiated by fuel leakage onto a hot surface under conditions pertinent to those that obtain, or will obtain, in the engine nacelles of advanced civil/military aircraft. In particular, the system shall extinguish a fire generated by JP-4 fuel contacting hot surfaces at temperatures up to 815°C, and keep this fire from reigniting for a minimum of 300 seconds even though JP-4 fuel continues to contact the hot surface at this temperature. Further, since the extinguishant system will be subject to storage prior to use, the system has to be stable to gain and/or loss in weight due to water absorption (hygroscopic and efflorescent properties) and chemical/physical decomposition (weight loss, vapor pressure increases, or gas evolution) over a temperature range from -55 to 260°C. In general, weight losses and associated changes shall not exceed 5% by weight. A final criterion involves performance under high airflow velocities (up to 350 ft/sec) as would be present through an engine nacelle of an aircraft in flight (see Table 1). As described in the Introduction, fluid systems (CO_2 or Halon based), are deemed to be inadequate, and a prima facie assessment indicates that solid dry chemical systems may provide viable alternatives.

In terms of a search for materials that will fulfill these requirements, two criteria are important; will the system extinguish a fire generated by JP-4 fuel contacting a hot surface maintained at temperatures in excess of 800°C, and/or will the system prevent reignition for long time periods even though the fuel continues to contact the hot surface. From intuitive aspects, it is possible that a component which accomplishes the first task well may not necessarily accomplish the second task in an equally satisfactory manner. Thus, it is probable that a multi-component system approach to the overall objective should be adopted.

In view of the number of parameters that are expected to contribute to, and interfere with fire control, it was decided that a small carefully controlled testing assemblage should be designed, built, and refined, which would allow a prescreening of suitable candidate systems. Those systems that performed well under static laboratory test conditions would then be tested in a larger dynamic simulator, under conditions that would involve exposure to high airflow velocities as well. Prescreening laboratory testing was done via a so-called static assemblage (no airflow velocities for the majority of testing, and a maximum of ca. 10 ft/sec airflow only as an accessible laboratory parameter). Dynamic testing of suitable materials was undertaken in conjunction with a separate experimental assemblage under the auspices of Dr. D. Myronuk of San Jose State University (details are presented in this report).

In order to find a suitable answer to the stated problem, several experimental problems had to be solved, and one assumption taken; namely, that the measured reignition delay time is a characteristic parameter of the system, and that measurement of this parameter will provide self-consistent and meaningful data concerning the systems tested. Based on this assumption, the following experimental questions arise:

1. Can a suitable laboratory testing assemblage be developed that will allow us to determine which experimental parameters contribute to the observed reignition delay time, their relative importance to this process, and whether these contributing variables can be adequately controlled?

2. Assuming that the contributory variables can be adequately controlled, can meaningful self-consistent data be obtained for these reignition delays, and are the reignition delays a meaningful characteristic parameter of the systems under test?*

3. Using the knowledge gained from items 1 and 2, can the nature of the species, and the mechanism controlling reignition, be identified? In particular, can inherent fire control characteristics be predicted and these facts used to design a new system that will provide better performance than has presently been observed?

4. Can the system predicted in item 3 be modified and/or tailored so as to produce both initial extinguishment and subsequent long-term control of the reignition process?

5. Will the systems developed that satisfy item 4 satisfy the performance criteria delineated by the sponsoring agency, and if not, can they be made to do so by chemical and/or physical modifications?

6. Can the new materials developed in item 4 be suitably characterized so as to allow larger scale production and testing in the dynamic simulator, and thence to full-scale testing in real situations?

Experimental methodologies have been developed that attempt to answer these six phases of the investigation, and adequate solutions to the majority of these problems have been formulated. These experimental data are described in the next section.

*An obvious alternate criterion of effectiveness is the mass of a particular extinguishant system that will extinguish a preset and precalibrated fire; the smaller the quantity needed the "better" the system. We have not attempted to use this criterion for the static testing studies, but it does form part of the approach used for the dynamic simulator studies.

Section 3

EXPERIMENTAL PROCEDURES – STATIC TESTING PHASE

The overall experimental program can be subdivided into two major aspects: (1) testing of materials in the static assemblage under conditions of minimal airflow, together with subsequent syntheses and characterization of new materials; and (2) testing of the materials found to be most effective from static testing criteria in a larger dynamic facility which allows evaluation under conditions of high wind velocities such as those that would obtain during inflight engine nacelle fires.

LABORATORY SCALE STATIC TESTING ASSEMBLAGE

In relating fire control effectiveness to the relative magnitudes of the reignition delays induced by various dry chemical systems in flammable situations, it became necessary to develop a testing assemblage. Accordingly, the simple open pan fire concept was used as an initial development point, and a representation of the first such assemblage is shown in Figure 2. It was immediately obvious from preliminary experiments that precise self-consistent data accumulation could not be managed with this simple approach. An extensive and systematic investigation of possible contributing parameters that served to destroy precision and repeatability was undertaken, and culminated in the design shown diagrammatically in Figure 3, and photographically in Figures 4 through 8. This complete assemblage was mounted in a fume hood, to prevent dangerous accumulations of JP-4 fuel vapor. The final refinement of dimensions and ancillary equipment yielded a usable assemblage by 23 July 1976. The final dimensions of the cavity were 15 x 40 x 12 cm, with a 8 x 15 cm vent at the top rear of the cavity, and a total volume of ca. 6 liters.

As a measure of satisfactory performance, the only criterion adopted was a quantitative measure of precision. We chose to use the SD (standard deviation) of a data set calculated from

$$(SD)^2 = \frac{\sum_{i=1}^{i=N} (X_i - \overline{X})^2}{N - 1}$$

where N is the number of data points in the set. Typical values for the standard deviation as a function of the mean X were systematically reduced from values in excess of 500% to final values that were routinely less than 33%, and often as little as 10%. Data points that lay outside the values corresponding to "the mean ± twice the standdard deviation of the mean" were discarded, and a new standard deviation was computed. This degree of precision was deemed sufficient for the purposes of this investigation.

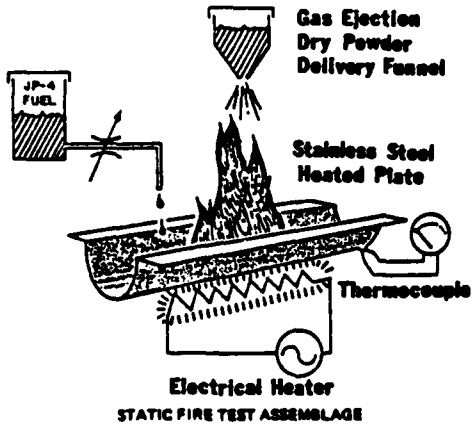

Figure 2. Schematic Diagram of Fire Test Assemblage (Initial Configuration).

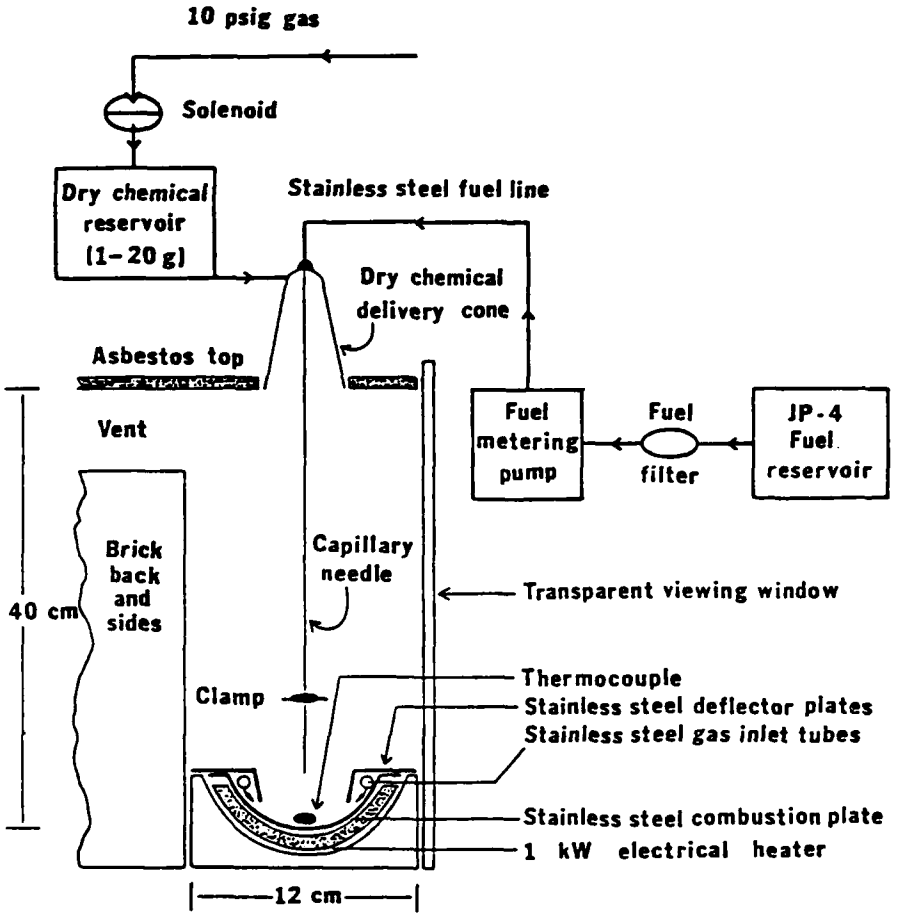

Figure 3. Schematic Representation of the Static Testing Assemblage in its Final Form.

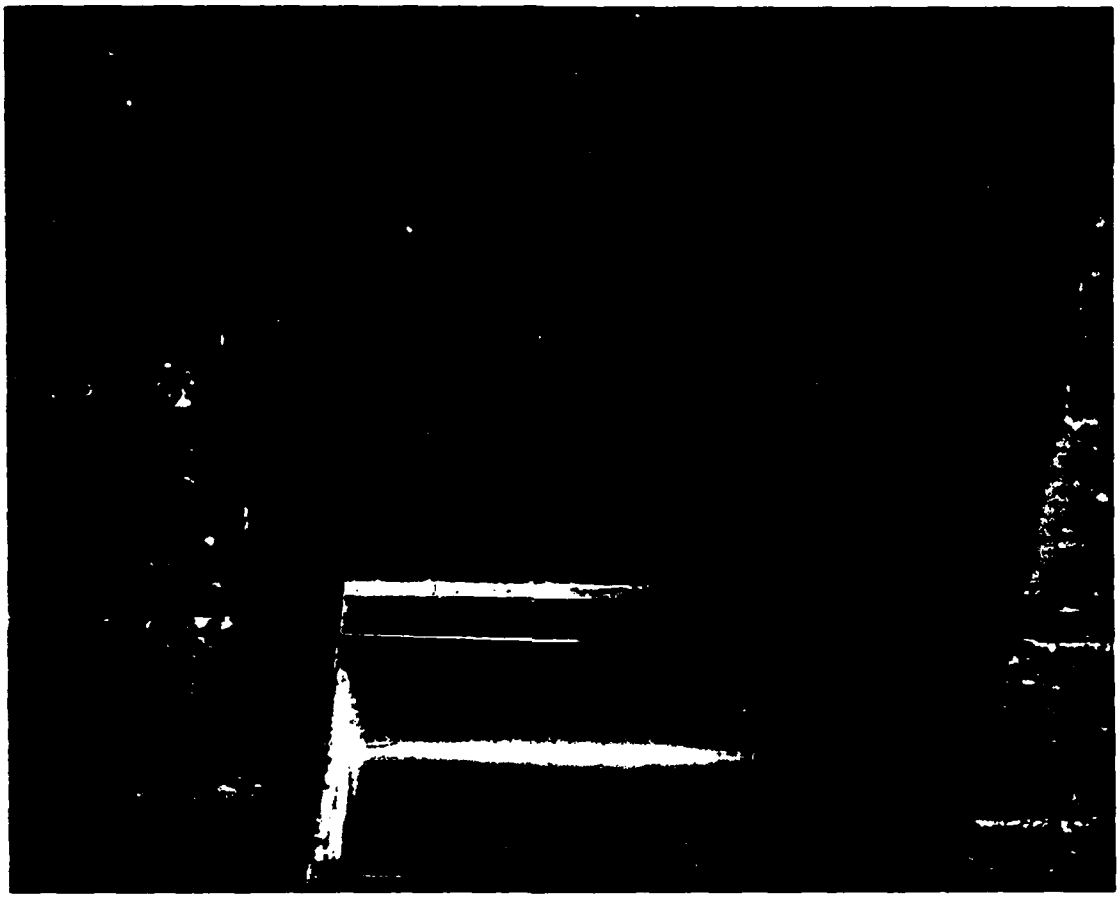

Note: The fuel feed needle can be seen in the center of the photograph, supported rigidly at the end to prevent movement under pressure from the fuel feed pump. The gas inlet tubes (copper in this photograph, but usually constructed from stainless steel) can be seen along the edges of the cavity, with the gas diffuser gauze appearing under the gas deflector plates. The ends of the cavity are sealed with a soft fireproof insulating material ("Fibrefrax").

Figure 4. The Interior of the Cavity Showing the Two Metal-Braid Sheathed Chromel-Alumel Thermocouples Spot Welded to the Heated Plate Surface.

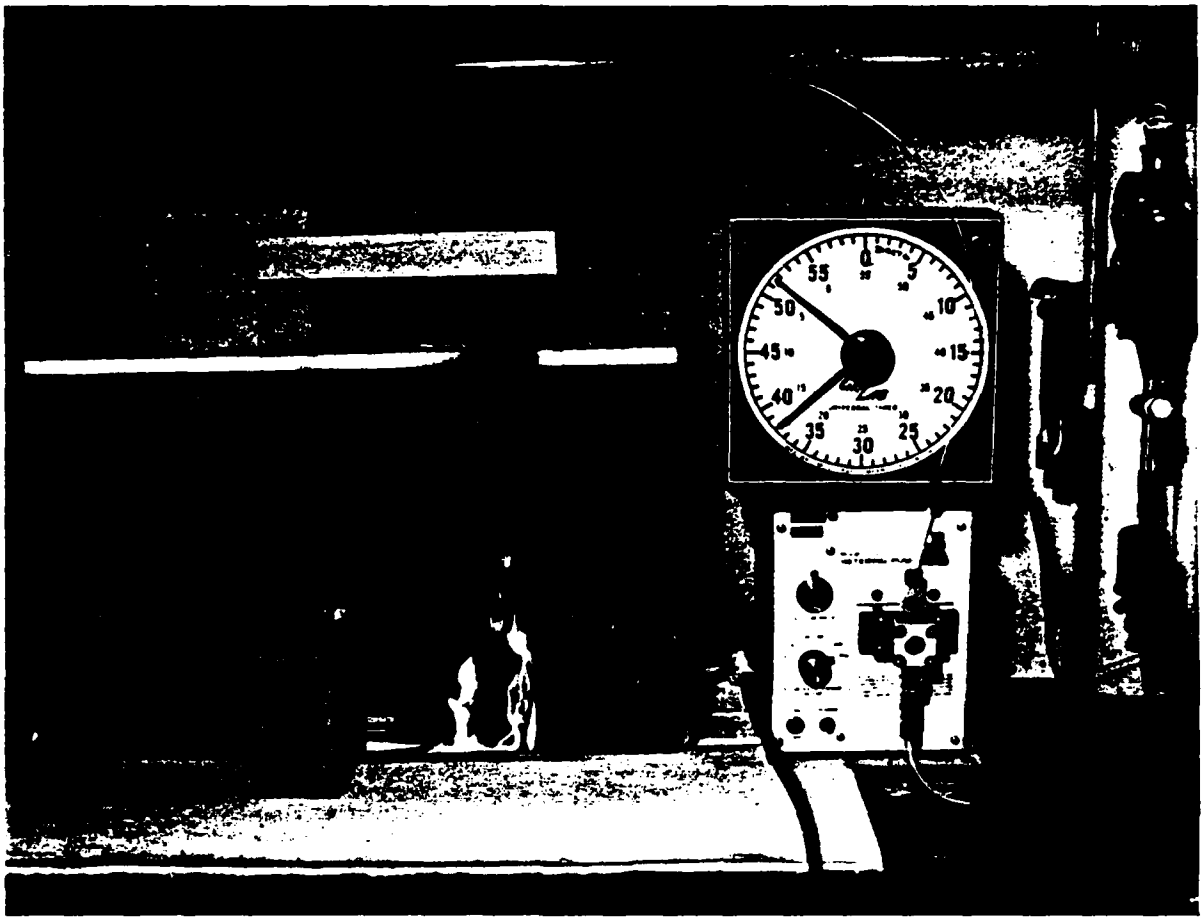

Note: The enclosure is mounted in a fume hood, together with a timing clock, fuel pump, and fuel reservoir on the extreme right of the picture. The front of the cavity is closed with a transparent plastic shield, allowing observation of the flame processes. In this photograph, the fuel has just been turned on, and the flame ignited. The gas feed tubes to the cavity can be seen at the extreme left and right hand sides of the brick enclosure.

Figure 5. The Brick Enclosure Around the Heated Plate.

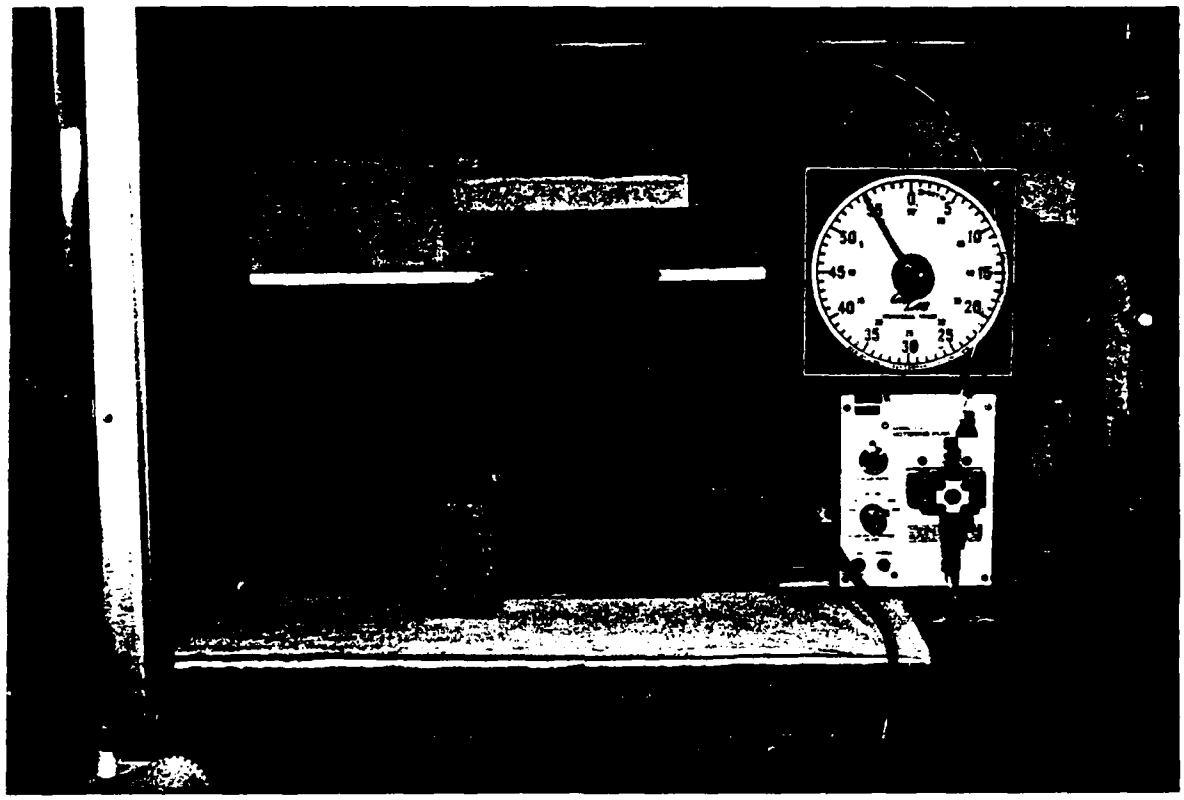

Note: In this photograph, the dry chemical extinguishant has just been discharged (commercially supplied potassium bicarbonate in this particular experiment) and the flame extinguished. The chart recorder used to monitor the temperature of the plate from the chromel/alumel thermocouples can be seen on the left of the fume hood.

Figure 6. Discharge of the Dry Chemical and Flame Extinguishment.

Note: The splash pattern of the fuel stream contacting the heated plate surface can be clearly seen in the center of the plate. This scouring action to cleanse the heated surface is partly due to the momentum of the fuel, and partly to the vigorous boiling action as the volatile fuel contacts the hot surface.

Figure 7. The Interior of the Cavity After Discharge of the Dry Chemical and After the Flame Has Reignited.

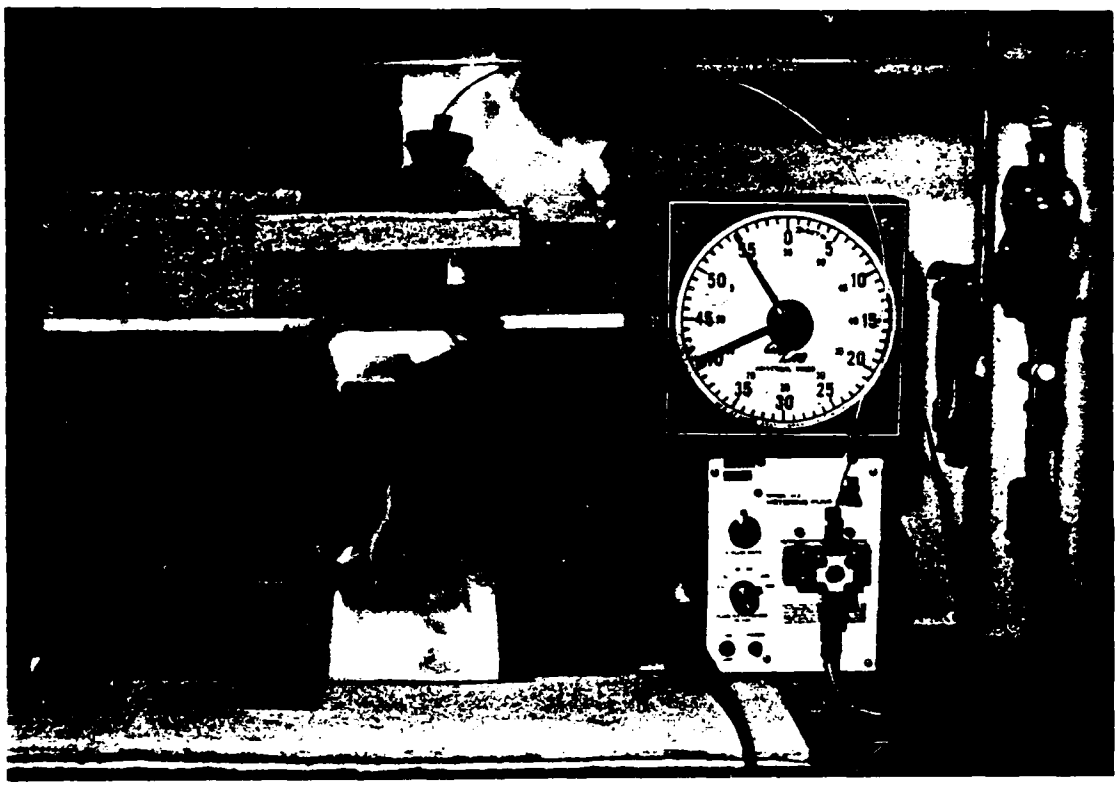

Note: This photograph illustrates the reignition process; the JP-4 fuel vapor has ignited throughout the whole of the cavity, and flames can be seen exiting from the vent in the rear of the cavity. The vivid purple color is from potassium ions from the $KHCO_3$ used to extinguish the flame in this experiment.

Figure 8. The Cavity at the Moment of Reignition.

CONTRIBUTORY VARIABLES

In the course of developing the final successful static testing assemblage, it was found that the precision achieved in the measurement of reignition delay times was influenced strongly by several variables. One major cause of erratic behavior; i.e., lack of repeatability of measured reignition delay times when apparently all parameters of the system were identical, was related to random air currents across the heated surface. In this respect, it soon became apparent that the assemblage should be as tightly sealed as possible. In view of the reignition process, and particularly when oxygen was used to provide a higher partial pressure of oxidant than that available from air combustion (when quite severe concussive reignition was often the rule), a standard vented enclosure was designed. To seal the enclosure against occasional leaks, especially close to the plate surface, a combination of rigid fireproof board ("Transite®" materials) and a soft fireproof woven sheet ("Fiberfrax®", available commercially) were used to ensure a leakproof cavity.

A second set of problems was identified as involving delivery of fuel to the heated plate surface: (1) the rate of fuel delivery has to be standardized; (2) the degree of atomization of the fuel stream supplied to the plate had to be standardized; and (3) the point of initial contact of the fuel stream with the concave heated plate surface had to be standardized. This third factor was attributed to a potential scouring action by the fuel stream travelling tangentially across the heated surface; and particularly for oxygen rich atmospheres, local concentrations of fuel could build up in oxygen rich areas of this cavity, leading to irreproducible data. Use of oxygen diffuser plates and deflector plates, as shown in Figures 3 through 8, helped to alleviate these problems. As development proceeded, gravity feed droplet delivery of the fuel to the plate proved inadequate, and all of these latter facets were found to be controllable by utilizing a constant volume delivery pump to deliver a metered amount of JP-4 fuel, and a long (30 cm) capillary needle (0.2 mm i.d.) to deliver the fuel reproducibly close to the plate surface (end of needle was ca. 5 cm from plate surface). It was found best to deliver the fuel to the center of the plate, such that the stream of JP-4 struck the surface of the heated plate normally (i.e., at an angle of 90 degrees to the surface). Although a slight degree of "splashing" did occur, producing a small shower of ancillary droplets, provided that the momentum of the fuel stream was not too high, this did not create a problem. Further, as shown in Figure 3, the needle was mounted concentrically through the center of the cone that delivered the dry chemical agent to the plate surface. Thus, both dry chemical extinguishant and JP-4 fuel were delivered to the same point on the plate initially.

Apart from these variables, other major parameters of the system expected to contribute to the observed reignition delay from intuitive ideas would include the following:

1. Rate of fuel delivery to the heated surface
2. Partial pressure of the oxygen above the heated surface
3. Mass of extinguishant delivered to the plate surface, together with the associated surface density of the extinguishant over the plate
4. Particle size of the extinguishant powder and/or bulk density of the dry chemical extinguishant
5. Temperature of the heated surface.

Several other variables were identified as the investigation progressed.

TEMPERATURE MEASUREMENTS

Since the temperature of the heated plate surface was one of the major independent variables, accurate values for this parameter were essential, and a knowledge of prevailing temperatures adjacent to the actual surface are also needed. Initial measurements were made using a metal braided chromel/alumel thermocouple held in contact with the surface. A representative profile of the temperatures along the center line of the concave plate surface and vertically above the center of the plate are shown in Figures 9 and 10, respectively. Since the temperature was seen to change so abruptly just off of the heated surface, it was decided that only by directly welding a thermocouple to the plate surface could accurate temperature information be obtained. To obviate thermocouple failure, two chromel/alumel thermocouples were spot-welded to the center of the plate, with each thermocouple junction approximately 1 inch apart (see Figure 4). The thermocouples were read via a 10-inch strip chart recorder, and the strip-chart trace was calibrated directly using a Leeds and Northrup special Chromel/Alumel Thermocouple Potentiometer. Calibration data were taken each morning prior to use, over a range of temperatures from 50°C below the minimum to be used, to 50°C above the maximum to be used, at 50°C increments throughout the range covered (usually, 375 to 700°C, or 600 to 900°C). Severe corrosion of the chromel/alumel thermocouples was noted for all dry chemical reagents at the higher temperatures, and for caustic reagents at all temperatures.

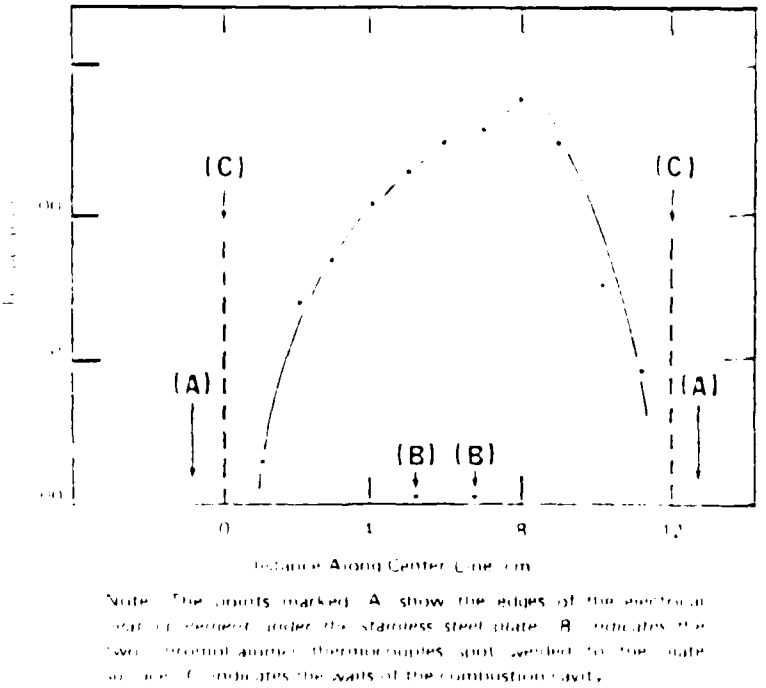

Figure 9. Temperature Profile Along Center-Line of Heated Plate Surface.

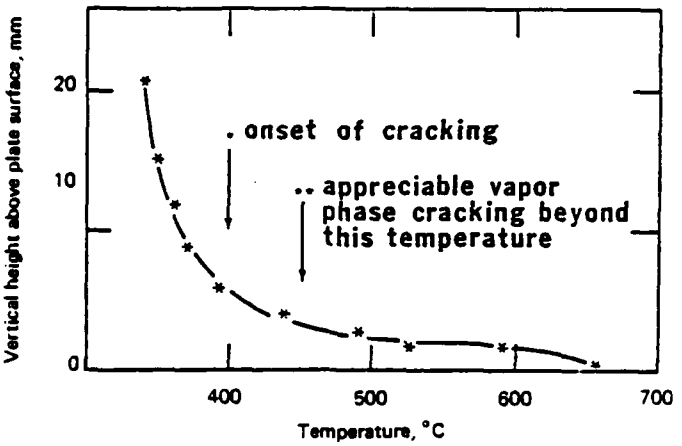

Note: A small moveable chromel/alumel thermocouple junction was used to chart this temperature profile vertically above the center of the heated plate surface.

Figure 10. Temperature Profile Vertically above the Center of the Heated Plate Surface.

EXPERIMENTAL TECHNIQUE

Several experimental techniques were tried, but eventually one was selected over the others and retained for all comparative testing. It was soon noticed that repeatability suffered adversely if the heated surface was not cleaned thoroughly between experiments. This was most apparent for compounds that formed a "crust" over the plate surface, or reacted with (or appeared to react with) the metal surface. Therefore, between successive experiments, the excess dry chemical from the previous run was removed using a vacuum cleaner, the plate was sprayed liberally with distilled water in order to dislodge all particles adhering to the heated surface and/or to dissolve soluble deposits; and while the plate was still drenched with water and before the water could evaporate from the hot surface, the plate was vacuum cleaned again. The front cover to the cavity was replaced, and the plate allowed to reach a steady preselected temperature ready for the next experiment, with the oxidant flow (either pure oxygen, or air, or preselected mixtures of oxygen and nitrogen) adjusted to (usually) 2 SLPM (standard liters per minute) of gas flow. The normal experimental procedure was as follows:

1. A known mass of extinguishant powder was loaded into the reservoir of the discharge funnel, taking care not to dislodge any powder onto the clean plate surface. When a spillage occurred, the plate was recleaned as above and left to temperature equilibrate.

2. The fuel pump was turned on at a preselected flow rate.

3. The fuel would now normally ignite within 1 to 3 seconds depending on the plate temperature. At the moment that ignition occurred, the dry chemical extinguishant was discharged (via a 10-psig compressed air line, later replaced with a compressed nitrogen discharge line) so as to extinguish the flame. If the flame did not extinguish, this run was terminated.

4. If the flame did extinguish, then the fuel pump was allowed to continue pumping fuel onto the heated surface; the time between the moment of extinguishment and subsequent reignition was then measured and noted. If no reignition occurred within (usually) 1000 seconds, the run was terminated by switching off the fuel pump.

The overall technique described by steps 1 through 4 was used for all comparative testing (data described below), and provided a precision for a data set containing up to 12 points corresponding to a standard deviation of less than 30% of the mean for the set, and often as small as 10% of the mean. When data points lay outside the range of the mean by more than two standard deviations, then these points were discarded (essentially Chauvenet's Criterion), and the mean was recomputed. This process was not repeated a second time for any one data set. Other alternative experimental techniques were tried, primarily involving changes in steps 3 and 4; these consisted of the following variations:

5. In step 3, after ignition, the flame was allowed to burn continuously until the temperature measured from the thermocouple which was welded to the plate eventually stabilized. This temperature was always higher (40 to 180°C) then the initial temperature set for the plate, due to the exothermic combustion process itself, and reduced radiative and convective heat losses from the plate by shielding from the flame process. The extinguishant was now discharged, and the reignition delay measured as before.

6. Another variation involved step 3; the fuel flow having been initiated, the extinguishant was discharged immediately, and prior to ignition of the flame, and the time to ignition now measured. Where flame production was very rapid (high temperatures), the extinguishant was discharged, and immediately following this (virtually simultaneously) the fuel flow was turned on and the time to ignition measured.

All methods gave qualitatively similar results; the final variation described in step 6 was rejected since it did not allow experimental verification of the extinguishant power of a chemical, merely the long term ability to control a flame once it was extinguished.

The method described in step 5 gave qualitatively, and quantitatively, similar data to the method adopted (steps 1 through 4, inclusive), but suffered one drawback—lack of knowledge concerning a precise value for the initiating temperature of the plate surface. Although the temperature of the plate did stabilize (±5°C), there was no prior knowledge of this value, and temperature was no longer a truly independent variable under these conditions.

Typical temperature traces from the thermocouple output using the experimental procedure outlined above are shown in Figures 11 and 12; where Figure 11 delineates the trace seen from the experimental procedure adopted (steps 1 through 4), and Figure 12 the trace from the alternate method described in step 5 (flame-on temperature equilibration). Typical data collected by this experimental method are shown in Table 2.

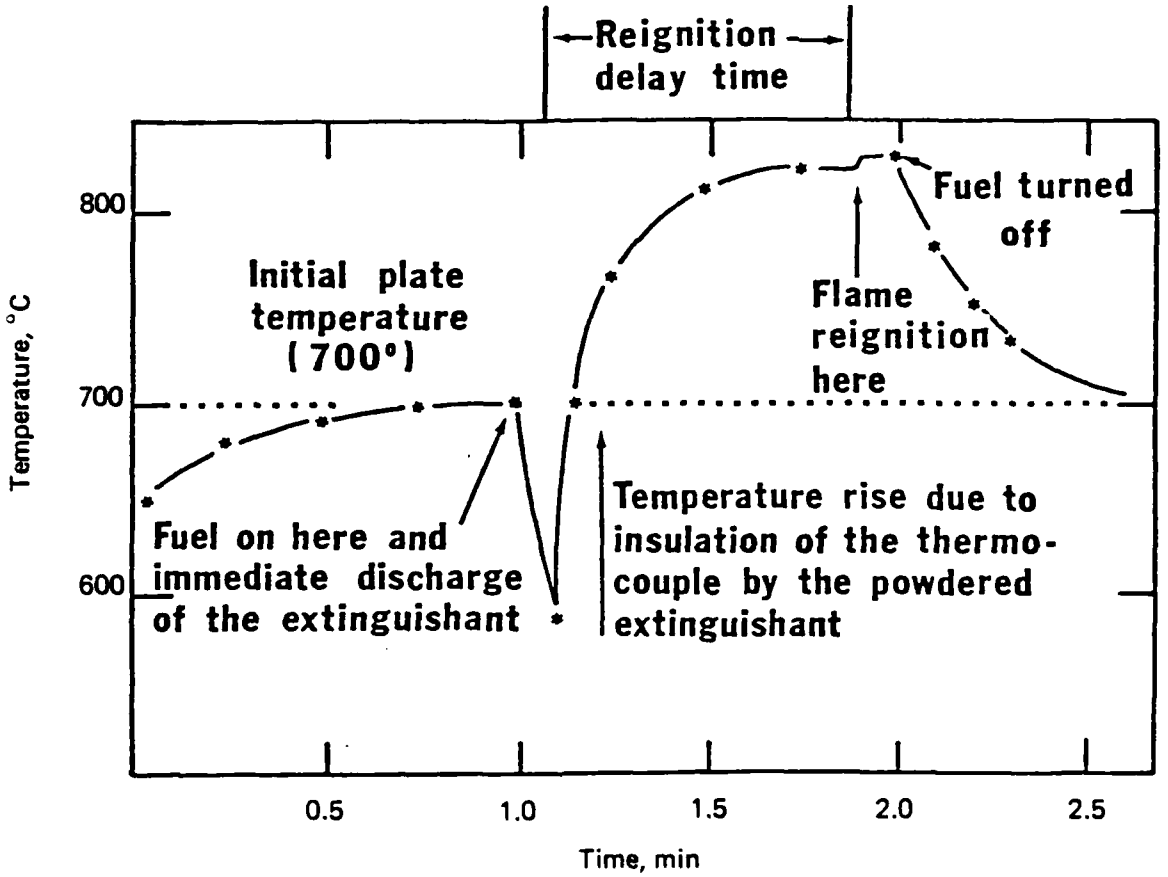

Figure 11. Temperature Profile as a Function of Time for the Experimental Method Adopted for the Comparative Testing of Extinguishants.

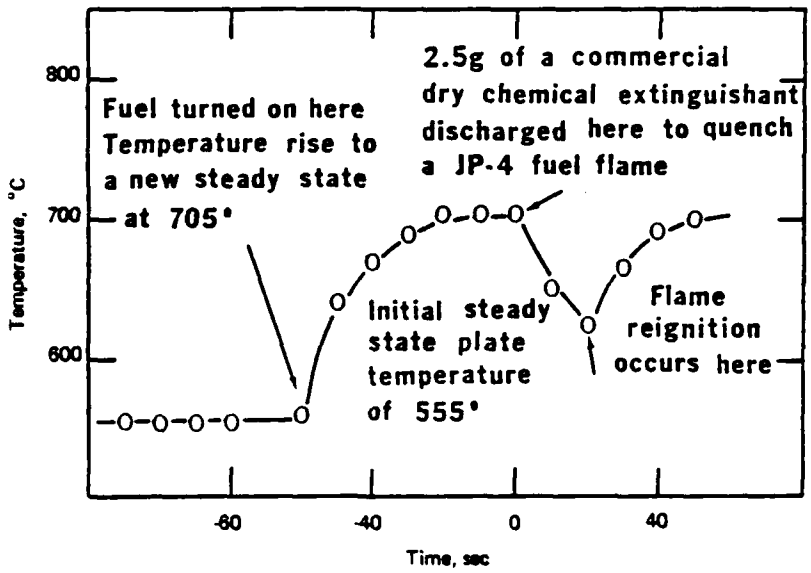

Figure 12. Temperature Profile as a Function of Time for the Alternate Experimental Technique Described in the Text which Involves a "Flame-On" Equilibrium Temperature.

Table 2. Typical Experimental Reignition Delay Data.

Temperature, °C	Reignition delay times, sec							Mean ± SD (%SD)	Data
	1	2	3	4	5	6	7		
675	269	384	436	282	302			335 ± 72 (22)	5
700	231	162	147	142	90	145		153 ± 46 (30)	6
725	117	178	123	96	72			117 ± 39 (34)	5
750	30	29	56	46	37	71	117	63 ± 32 (51)	for 12
	74	126[a]	34	59	72			63 ± 27 (43)	for 11
775	31	29	26	31				29 ± 2 (8)	4
800	22	22	24	20				22 ± 2 (6)	4
825	18	19	17	20				19 ± 2 (5)	4
900	7	8	9	6	8			8 ± 1 (16)	5

[a] Exceeds ± 2 x SD for this data set

NOTE Reignition delays for Potassium Dawsonite; bulk density 0.8 g/ml; 200 ml/hr of JP-4 jet fuel; 10g shots of extinguishant; 2 SLPM air input to cavity plate surface; delay times measured in seconds, temperature in °C.

N.B. calculated SD values and means are rounded values; percent SD reflect true values with no rounding.

FUEL POLYMERIZATION PROBLEMS

JP-4 fuel is well known for polymerizing in a static storage system, and problems were experienced involving deposition of an insoluble "waxy" solid inside the needle. This was particularly prevalent when the assemblage was infrequently used. It was therefore customary to turn on the fuel pump (at the maximum flow rate) for long periods (30 to 60 minutes) prior to the first experimental run of the day. This helped to clear any possible blockage in the needle, and also allowed calibration of the fuel flow rate directly by actual measurements of volume collected over a relatively long time period.

FUEL ATOMIZATION TECHNIQUES

One final experimental modification tried was the incorporation of an electrically driven "vibrator" attached to the fuel supply needle. The rationale for this approach was that fuel - jet atomization might reduce effects attributed to fuel - jet momentum (scouring action, and splashing). This was unsuccessful; leading to an increased observed standard deviation for a data set to the point where the collected data were inadequate for our purposes.

LOADING DENSITY OF EXTINGUISHANT APPLIED TO THE PLATE SURFACE

Since all of the extinguishant is discharged (compressed gas ejection) in one action, the surface density of extinguishant applied to the plate varies from point to point. Surface density distributions were determined via a set of concentric circular containers with diameters of 2.6, 5.2, and 10.0 cm; these were weighted before and after discharge, and the mass collected as a function of distributive area over the plate was determined. The center of the concentric set of collection containers was vertically beneath the center of the extinguishant delivery cone, which itself was approximately 25 cm above the collector surface. Data obtained are shown in Table 3. These data indicate that distributions over the plate surface are relatively uniform, and vary both with bulk density and particle size distributions. It is not clear why the higher bulk density material (commercially supplied potassium bicarbonate) produces an overall lower surface density of powder compared to potassium Dawsonite. However, since the apparent surface density measured for this commercial material is less at the center of the plate when compared to the edges, it is apparent that the powder leaving the discharge funnel disperses more quickly. The higher edge densities probably reflect the fact that the powder has hit the side walls of the cavity and is being collected by the outer concentric vessel following rebound from the cavity walls, thus increasing the observed surface density. Our synthesized material (potassium Dawsonite) has not been treated in any extensive manner to either increase bulk density, or to maximize flow characteristics, and thus leaves the discharge funnel in a more tightly packed dispersion mode. This both increases the central surface density and minimizes the "rebound-collection" behavioral pattern seen for the commercial powder. This is further emphasized when data for different particle size distributions are compared. The smaller the overall

particle size distribution, the smaller the noted surface densities observed. Although two samples are shown that contain 100% Pass #325 ASTM (American Society for Testing and Materials) mesh, we have no knowledge of particle size distributions below this figure, and it is probable that the commercial powder contains a higher percent composition of small particles than does our synthetic potassium Dawsonite. This helps to increase dispersion at discharge, and thus reduce central surface densities at the expense of the larger radii measurements.

Table 3. Surface Densities of Dry Chemical on the Heated Plate Surface.

Dry Chemical Delivery Cone	Purple-K®,[a] 100 P325		Potassium Dawsonite[b]			
			Sieved, 100% P325		Unsieved, 45% P325	
	Shot size applied to the heated plate surface[c]					
35 cm	10g	15g	10g	15g	10g	15g
	Surface densities measured in mg/cm^2					
←2.6→	14 ± 6	37 ± 6	-	54 ± 30	85 ± 20	156 ± 20
←5.2→	26 ± b	47 ± 5	-	53 ± 16	85 ± 10	128 ± 10
←10.0 cm→	31 ± 5	48 ± 5	-	55 ± 12	71 ± 5	96 ± 5

[a] Ansul Corp. $KHCO_3$, all particles will pass an ±325 mesh sieve; bulk density ca. 1.3 g/ml.

[b] Potassium Dawsonite, $KAl(OH)_2CO_3$, bulk density ca. 0.8 g/ml.

[c] Surface densities measured in mg/cm$_2$.

SELF-IGNITION PROBLEMS

To test a dry chemical powder for extinguishant action, the JP-4 fuel has to ignite initially (self-ignition); and for comparative measurements of reignition delays, it is important that any self-ignition delay be negligible compared to the reignition delay. It was found to be impossible to obtain self-ignition spontaneously and reproducibly in times of less than 5 seconds at any temperatures below ca. 650°C, using air as the oxidant. Considerable investigation of fuel flow parameters, fuel delivery modes, fuel droplet sizes, air delivery to the cavity, and changes in fuel identities (JP-4 mixed with varying amounts of methanol, acetone, diethyl ether, ethanol, propanol, ethyl acetate, tetrahydrofuran, and toluene; and pure components) did not change this fact. In order to investigate the temperature dependencies of extinguishant efficiencies over a realistic temperature range (down to 400°C), it was necessary to have successful self-ignition at lower temperatures than 650°C. Thus, oxygen input to the cavity was tried, and found (after some experimental modifications and refinements to the basic cavity) to yield successful repeatable self-ignition at temperatures down to 370°C. However, above approximately 650 to 700°C, the noted reignition delay times were so short that no differentiation could be obtained from system to system. Thus, resort was made to normal air-oxidation above ca. 700°C, and oxygen-input methods below this temperature. It is realized by the authors of this report that

partial pressures of oxygen in excess of 0.21 are not realistic conditions pertaining to fire control in engine nacelles, but this experimental procedure does provide us with a severely differentiating mode of investigation for assessing the effectiveness of any extinguishant, and does provide access to experimental temperatures below 600°C that would otherwise be denied to us. Further, it appears that the ranking order for a set of extinguishants remains substantially unchanged for experiments at ca. 500°C in oxygen, and at ca. 700°C in air, and that temperature dependencies are similar enough to allow such ranking orders to be compared meaningfully. This aspect, and the effects of plate surface temperature as a variable (Arrhenius and non-Arrhenius behavior), will be discussed later.

SHOT-MASS DEPENDENCIES

To determine relative extinguishant efficiencies, it is necessary to determine the functional dependence of the reignition delay on the mass of extinguishant delivered to the fire. If, in the simplest case, a limiting value is apparent, then this parameter can be standardized easily; if not, an arbitrary test quantity must be chosen in the light of other data. Both of these behavioral patterns were seen, depending on whether the fuel jet was incident on the heated surface at angles that were normal (90 degrees) to the surface, or obliquely tangental to the surface so as to provide a strong scouring effect to cleanse the surface of dry powder. Not surprisingly, the tangential scouring action provided by a fuel jet incident on the curved side of the heated plate yielded a shot-mass dependence that exhibited a "plateau effect", the threshold of the plateau being a function of the ability of the dry powder to cling to the heated surface and not be dislodged by the kinetic energy of the fuel jet. Examples of both behavioral patterns are shown in Figures 13 (plateau effect, tangential fuel jet) and 14 (linear dependence with fuel jet normal to surface) for oxygen enriched ignition at temperatures in the range of 400 to 600°C. There are no qualitative changes in behavior at higher temperatures, or for air combustion rather than oxygen enriched atmospheres. Figure 15 shows a more detailed experimental sequence taken at 800°C using an iodide loaded potassium Dawsonite dry chemical under conditions of air oxidation. (Note the absolute magnitudes of the delays recorded for this very effective compound even at these high temperatures, >1,400°F.)

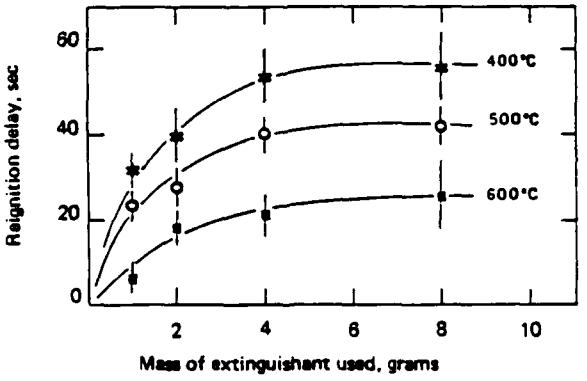

Figure 13. Shot-Mass Dependence for the Reignition Delay Caused by Commercially Supplied Potassium Bicarbonate. (The Fuel Jet is Applied Tangentially to the Heated Plate Surface.)

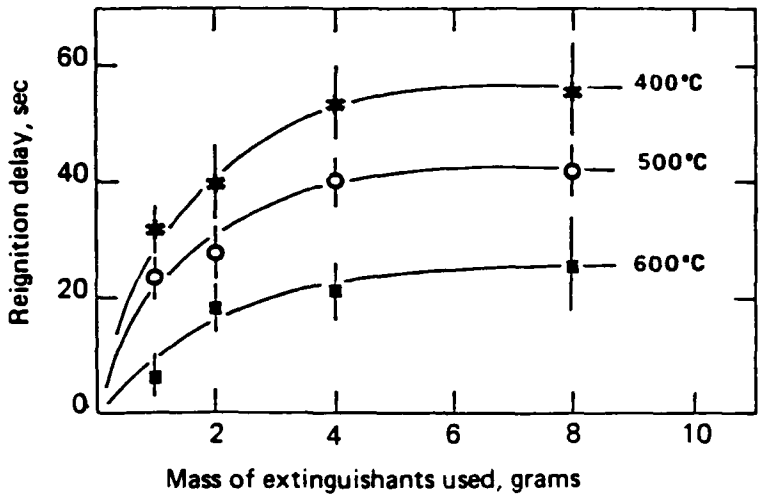

Figure 14. Shot-Mass Dependence for the Reignition Delay Caused by Commercially Supplied Potassium Bicarbonate. (The Fuel Jet is Applied Tangentially to the Heated Plate Surface.)

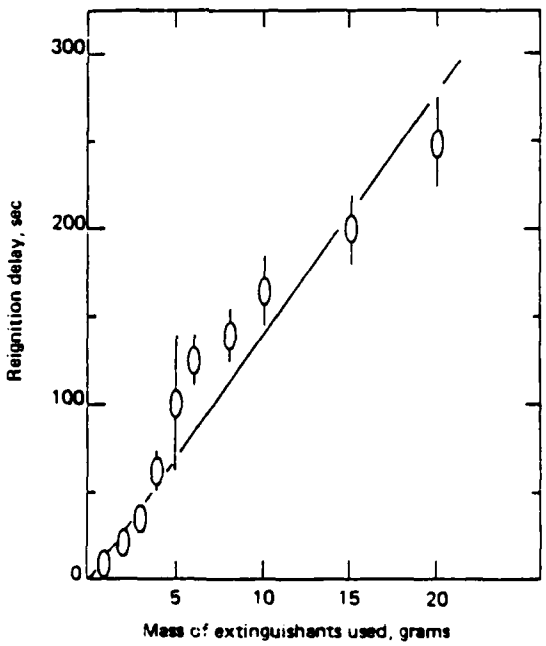

Figure 15. Shot-Mass in Air at 800°C for a Sodium Dawsonite Dry Chemical Loaded with 10% by Weight of Tin Iodide Powder.

POWDER PREPARATION TECHNIQUES

Pure reagent chemicals and those synthesized by us were prepared by ball milling and sieving techniques, using standard procedures. It was usual to add approximately 1% by weight of finely ground fumed silica (supplied commercially—100% will pass a 400-mesh ASTM sieve, bulk density ca. 0.05 g/ml) to enhance flow properties and retard any potential water absorption. Bulk densities were measured by filling a graduated cylinder with a known mass of powder, tapping the base of the capped cylinder gently on a hard surface for 60 seconds, and calculating the apparent density from the final volume achieved. Powders so prepared were either used directly unsieved (typically, ca. 35 to 45% at Pass-325 ASTM mesh, 100% Pass-170 ASTM mesh), or separated into constant fractions containing well defined particle sizes using Numbers 400, 325, 230, and 170 ASTM mesh sieves. No additives to enhance bulk densities were used for any reagent chemicals or synthesized materials, and commercial powders were used directly as received from the manufacturer.

BULK DENSITY AND PARTICLE SIZE EFFECTS

Among the principal physical quenching effects are those attributed to thermal dilution (heat capacity effects pertaining to crystal structure changes, chemical decomposition, phase change phenomena, and thermal reservior effects), and to third-body effects associated with gas phase radical recombination reactions. The first mechanism is a species-dependent phenomenon, and is difficult to investigate in experimental isolation or indeed to separate from purely chemical species-dependent effects. Moreover, it is difficult to distinguish purely physical phenomena such as crystal decrepitation and subsequent thermal reservoir effects produced by chemical decomposition from necessarily associated chemical aspects involving, for example, carbon dioxide gas release from carbonates and consequent "blanketing" effects (a physical mode) induced by the chemical (CO_2 gas) reducing local concentrations of oxidant and/or fuel derived species producing the flame. We have used the rather loose criterion that if a chemical product derived from the extinguishant takes part in (interferes with) any of the flame producing reactions, then this is classified as a chemical effect. Thus, by this definition, local CO_2 gas production and consequent physical occlusion of flame reactions will be classified as a physical quenching mode.

The second general phenomenon mentioned above, that of third-body collision reservoirs, should be a direct function of particle size. Firstly, the more particles per unit mass, the greater the probability of inducing third-body collisions (this will involve both number density effects and surface area effects). Secondly, the smaller the particle, the longer that particle should stay suspended in the gas phase and thus the longer it can affect homogeneous gas phase reactions. Finally, it is possible that physical and chemical decomposition (thermal dilution effects) will be enhanced by smaller particle sizes. An associated phenomenon is one of bulk density. The denser the particles, the more easily they will penetrate to the base of the flame and thus to the core of the flame generation region.

The difficulties of investigating the effects of bulk density independently of the effects introduced by particle size, and vice-versa, needs to be emphasized. The bulk density is a sensitive function of the particle size; changing the particle size distribution by sieving

immediately alters the apparent bulk density of the resulting powder. Accordingly, we elected to separate a test powder into relatively narrow particle size distributions (using ASTM sieves numbered 170, 230, 325, and 400), and adjust the apparent bulk densities of these fractions to a constant value by the addition of a low density (0.05 g/ml) fumed silica flow agent. In a second experimental sequence, we selected one particle size distribution and prepared a sequence of samples with bulk densities varying over the range of ca. 0.35 to 1.4 g/ml by addition of the same fumed silica additive. Preliminary experiments clearly indicated that the fumed silica additive did not of itself act either as an extinguishant or an inhibition agent and could thus be treated as an "inert" additive. For this second experimental sequence, since significant portions of flow agent were added to some of the low density samples, the mass of each shot delivered for each determination of the RIDT values was adjusted such that the quantity of "active" dry chemical delivered was identical and equivalent to that delivered for the highest density sample. Data from these particle size and bulk density studies are summarized in Table 4, Figure 16 (particle size study) and Figure 17 (bulk density study). A commercially supplied potassium bicarbonate based dry chemical was used to obtain the data in Figures 16 and 17, and a reagent grade aluminum hydroxide based material prepared by us was used to obtain the data in Table 4.

Table 4. Investigation of the Effects of Bulk Density and Particle Size on the Reignition Delays for Potassium Dawsonite at Various Temperatures.

KD sample type	750°C	800°C	900°C
1. 100% P325 0.9 g/ml	94 ± 18	42 ± 2	12 ± 3
2. 37% P325 1.2 g/ml	40 ± 14	19 ± 6	12 ± 3
3. 37% P325 0.9 g/ml	27 ± 8	21 ± 2	7 ± 1

NOTE: 10g shot size in each case, 200 ml/hr JP-4 fuel flow, 2 SLPM airflow. Samples contain 1% by weight of commercially supplied flow agent.

These data clearly indicate that bulk density effects are small in our static testing assemblage, although this parameter may become important if the dry powder has to be delivered to the fire over a long distance ("throw"), or if the fire occurs in conditions of considerable turbulence where penetration to the initiation point of the fire is important. However, particle size effects were seen to be important, producing marked changes in the observed reignition delay. This general effect had already been noted by several earlier investigators (Reference 4), although their data were obtained from conventional laboratory mechanistic studies of flame quenching rather than the simulated fire control conditions used herein. However, their data did not exhibit the marked dependence shown

in Figure 16. Since the effect is virtually discontinuous at a particle distribution that passes through a 400 mesh ASTM sieve, and since we know nothing of the particle distribution in this fraction (>38 μm), it is impossible to predict further behavior.

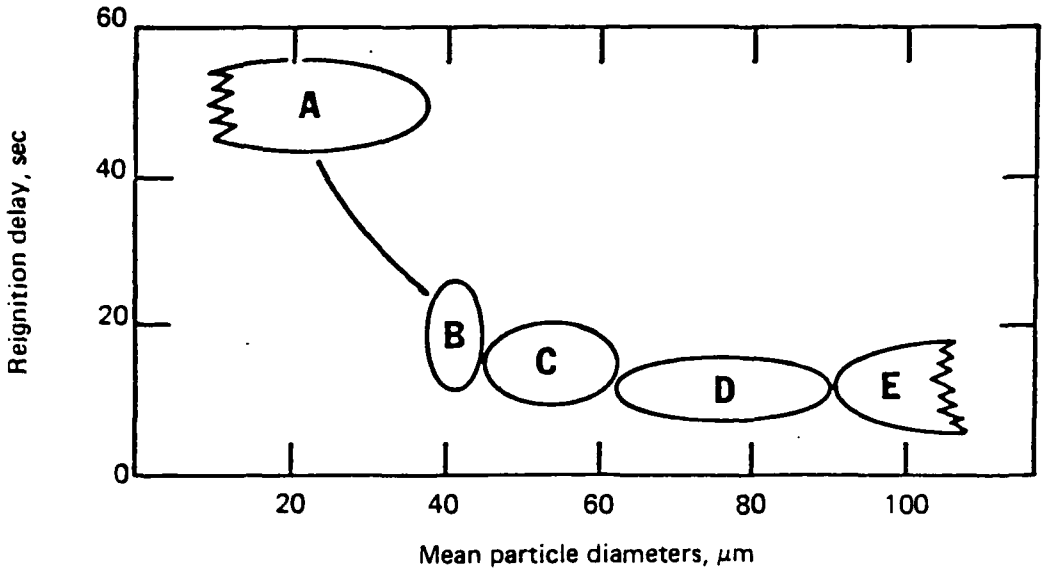

Note: JP-4 fuel flow at 250 ml/hr; oxygen flow rate at 1.5 SLPM; temperature 400°C; shot mass size used for each determination was 4g.

Legend:

A – Pass 400 mesh ASTM sieve	<38 μm particle size
B – Pass 325/not Pass 400 sieve	38 to 45 μm particles
C – Pass 230/not Pass 325 sieve	45 to 63 μm particles
D – Pass 170/not Pass 230 sieve	63 to 90 μm particles
E – Not Pass 170 ASTM sieve	>90 μm particles

Figure 16. Reignition Delay for Commercially Supplied Potassium Bicarbonate as a Function of the Particle Diameter.

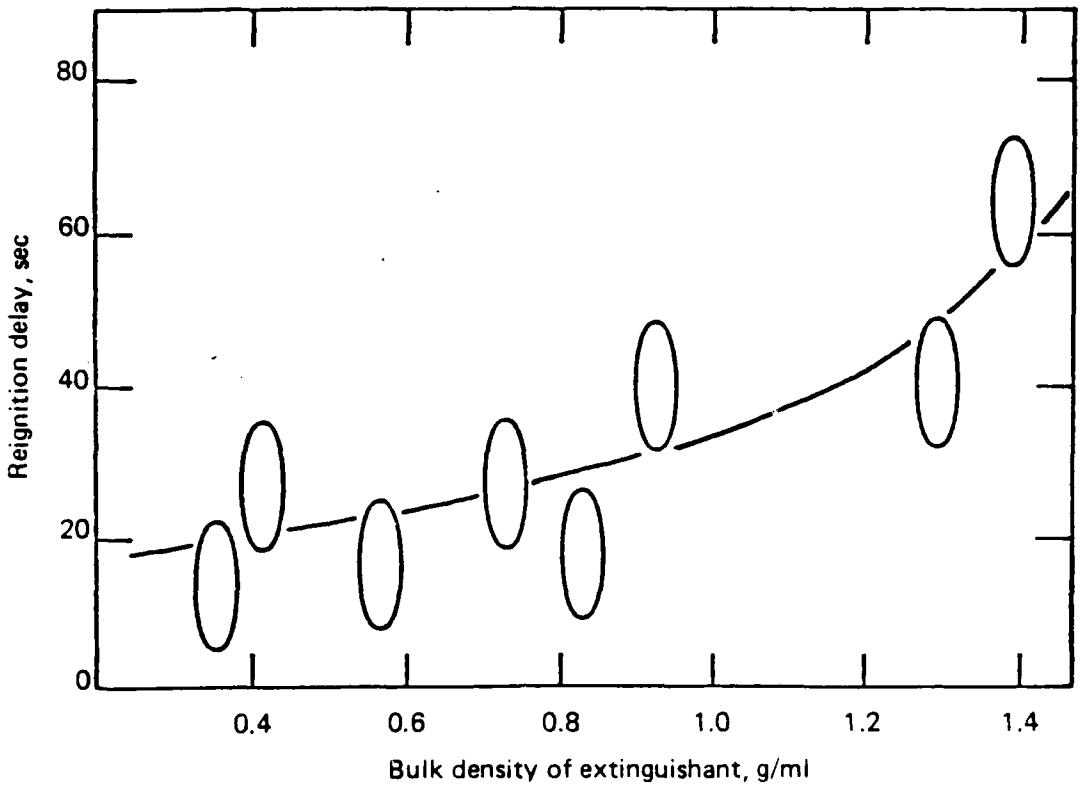

Note: The bulk density was changed by addition of a silica flow agent keeping the particle size distribution constant throughout; JP-4 fuel flow at 250 ml/hr; oxygen flow rate at 1.5 SLPM; temperature 400°C; 4g samples used for each of the determinations.

Figure 17. Dependence of the Reignition Delay on the Bulk Density of a Commercially Supplied Potassium Bicarbonate Dry Powder Extinguishant.

OXYGEN FLOW RATE STUDIES

To attain self-ignition temperatures below 650°C, we found it necessary to inject oxygen into the vapor space above the heated plate surface. Obviously, the partial pressure of oxidant will be a fundamental parameter, and a brief study was initiated to determine the dependence of reignition delays on the effective partial pressure of oxygen (as measured by its flow rate into the cavity) over a range from 1.5 to 3.5 SLPM. These data are shown in Figure 18, where JP-4 fuel at 200 ml/hr was allowed to contact a heated surface at 400°C, the sample used was a commercially supplied potassium bicarbonate dry powder with 5g shots of this chemical being used for each determination.

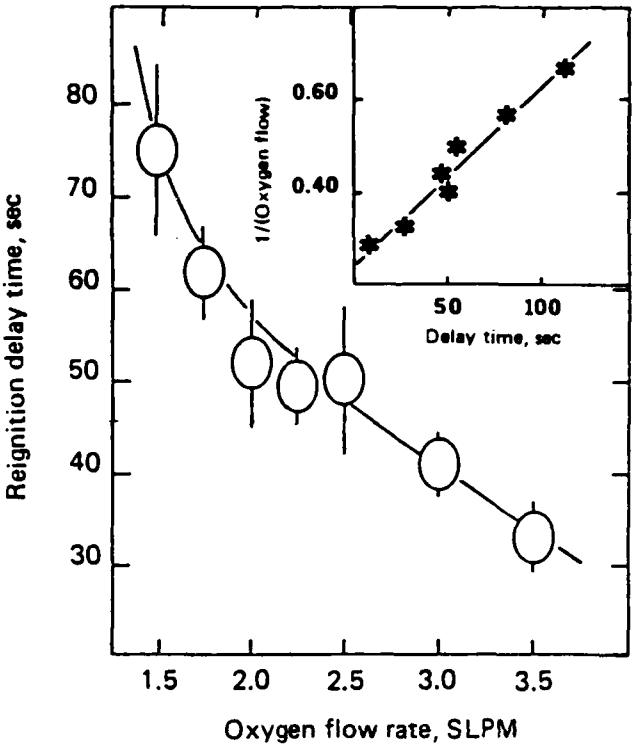

Figure 18. Dependence of the Reignition Delay Time for Commercially Supplied Potassium Bicarbonate Extinguishant as a Function of the Oxygen Partial Pressure Above the Heated Plate Surface (Measured in Terms of the Oxygen Flow Rate Into the Vapor Space Above the Heated Plate).

It should also be noted at this point that use of oxygen flow into the combustion cavity in order to lower the self-ignition temperature provided an excellent "differentiating" effect. Systems that apparently exhibit similar properties under oxidation by air will produce a wide range of reignition delays using oxygen. As will be seen in a later section, ranking of extinguishants in order of effectiveness appears to be independent of oxygen partial pressure. Finally, it should be noted that for low temperatures and/or extinguishants that produce long reignition delays, the JP-4 vaporized fuel concentration can build to high levels in the presence of oxygen atmospheres—a potentially dangerous situation for unvented cavities, or inadequate hood ventilation. Under these conditions, reignition can often be accompanied by a violent detonation. It was noted that detonation was most prevalent for the initial experimental runs in an essentially cold cavity (see "Hysteresis Effects" in a later section of this report) at low temperatures; for temperatures of 500°C and above, reignition took place smoothly, and was a scarcely audible process.

EFFECTS OF AIRFLOW ACROSS THE HEATED PLATE SURFACE

To prevent excess fuel hampering combustion processes (fuel/oxidant ratio effects), a stream of air was supplied to the plate surface. This airstream was supplied at rates ranging from 1.5 to 9.0 SLPM. At high airflows, in excess of 6 SLPM, definite turbulent effects could be seen, and the reignition delay began to increase markedly. For airflows between 1.5 and approximately 6 SLPM, a smooth decrease in reignition delay was seen, similar to that already noted for oxygen inputs to the cavity (described previously). This smooth decrease also followed a "reciprocal concentration" function second-order kinetic plot resembling that shown in Figure 18. Data from this phase of the investigation are shown in Table 5 and Figure 19 (also shown in Figure 19 are self-ignition delays as a function of airflow).

Table 5. Effects of Airflow Across the Heated Plate Surface on the Measured Reignition Delay.

Airflow, SLPM	Airflow velocity, ft/sec	Measured reignition delays,[a] sec	
		Set 1	Set 2
1.5	1.7	39 ± 8 (4)	
2.0	2.3	34 ± 6 (4)	
3.0	3.5	32 ± 3 (4)	
4.0	4.6	24 ± 5 (4)	
5.0	5.8	22 ± 7 (4)	
6.0	7.0	21 ± 4 (3)	24 ± 3 (4)
7.0	8.1	25 ± 5 (4)	22 ± 4 (4)
7.5	8.7	46 ± 17 (5)	
8.0	9.3	65 ± 29 (5)	43 ± 23 (4)
8.5	9.9	44 ± 33 (3)	
9.0	10.4	93 ± 40 (4)	54 ± 25 (4)

[a]Numbers in parentheses are the number of points in each data set, errors shown are calculated single standard deviations over the data set taken.

NOTE. Commercially supplied potassium bicarbonate dry powder; 5g shots used for each reignition delay determination. 200 ml/hr JP-4 fuel flow to heated plate at 750°C.

Using the assumption of nonturbulent flow for the gas stream exiting from the holes in the stainless steel gas entry tubes, an approximate flow rate across the plate surface can be calculated.

For an airflow input of A SLPM to the assemblage, the airflow is divided between two tubes containing 22 exit holes, each ranging between 0.064 and 0.069 inches in diameter, with a weighted mean diameter of 0.065 inch. Assuming laminar (non turbulent)

flow, then a cylinder of air will be propagated at each exit hole with a total volume of (A/22) liters each minute corresponding to 2.774 x A in^3/min. This cylinder will have an area of 3.318 x 10^3 sq in (corresponding to a diameter of 0.065 inch), and thus a propagated length of 836 x A inches each minute, or 1.16 x A ft/sec. This will be an approximate value for the dynamic airflow across the heated plate surface.

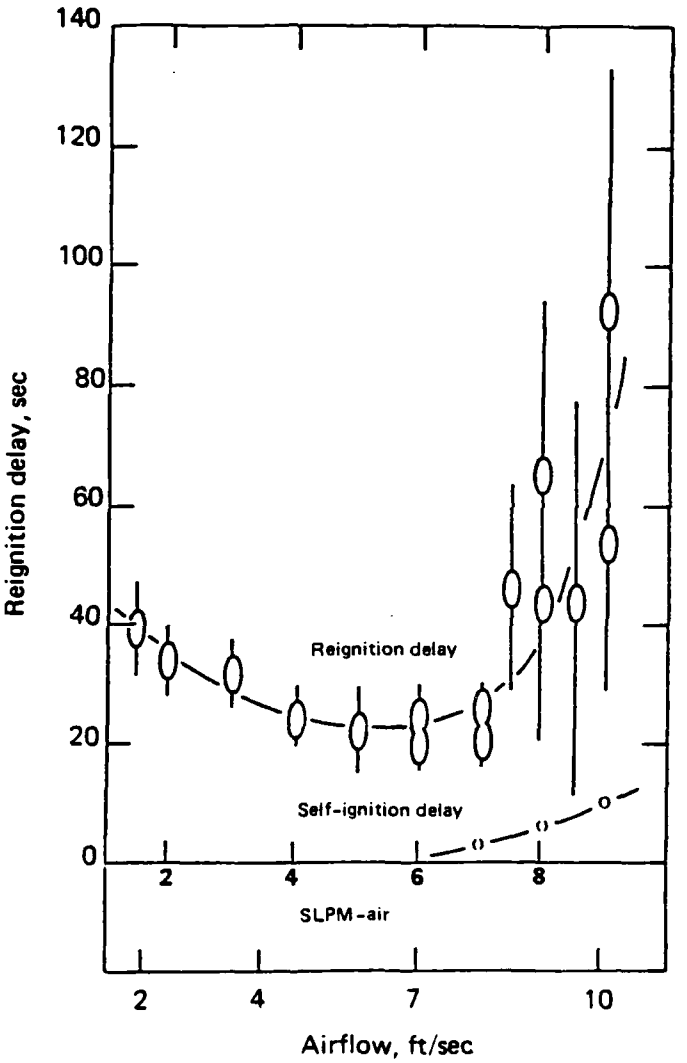

Figure 19. Dependence of the Reignition Delay on the Airflow Velocity Across the Heated Surface.

Although the numbers generated are small (2 to 10 ft/sec) compared to real airflows expected (ca. 350 ft/sec according to Table 1) in aircraft engine nacelles, reignition delay data do reflect interference from this source, and serve to emphasize the need for data from a dynamic facility.

Since self-ignition became a severe problem at high airflow rates (in excess of 9 SLPM), a high testing temperature was chosen (750°C), and data collection was terminated above 9 SLPM airflow. The data exhibit an obvious change at ca. 6 SLPM, and in general, 2 or 3 SLPM airflows were chosen for all measurements. The reignition delay was not particularly sensitive to airflow rates (approximately 4 seconds change per unit SLPM change in airflow), a negligible number compared to actual reignition delays (corresponding to less than 10%/SLPM flow rate, less than the usual standard deviations for data sets). This number may be compared to ca. 25 sec/SLPM change in oxygen flow (corresponding to ca. 50%/SLPM change) noted above.

FUEL FLOW STUDIES

Since the combustibility of fuel/oxidant mixtures depends markedly on the ratio of fuel-to-oxidant, it was necessary to determine the effects of fuel flow rates on the reignition delay. This was done by varying the pumping speed of the fuel delivery assemblage over the range 50 to 500 ml/hr of JP-4 fuel, and measuring the reignition delay as indicated above. Two primary data sets were collected, one for air oxidation, and one for oxygen inputs to the cavity. These data are shown in Figures 20 and 21, respectively. Behavioral patterns are drastically different in each case, reflecting the overall fuel-to-oxygen ratios in each case. However, it should be noted that, within the experimental errors indicated (Figure 20), the magnitude of the fuel flow rate to the heated surface had little effect when combustion took place in air.

HYSTERESIS EFFECTS ON THE REIGNITION DELAY

Since the reignition process probably involves both homogeneous and heterogeneous processes, the cavity walls will influence the reignition delay. It was observed that as the temperature of the cavity walls increased from initial ambient values of the laboratory to temperatures in excess of 200°C at the end of the day (after 8 to 10 hours of use), the reignition delay for a standard system decreased markedly (by as much as 40%). This effect was labelled as a "hysteresis" or "memory" effect, and must be allowed for in formulating a ranking order within a data set. Data are summarized in Table 6.

To obviate such changes during an experimental sequence, it was customary to turn on the heating for the cavity plate several hours prior to the initiation of any experimental work, and allow the cavity to achieve some form of temperature equilibration prior to taking any measurements. Data in Table 6 also serve to illustrate the day-to-day reproducibility obtainable, and the relative precision achieved, with this experimental assemblage.

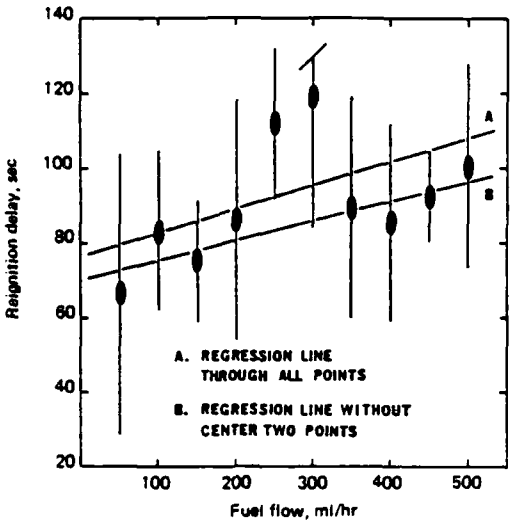

Note: 10g shots of commercially supplied potassium bicarbonate dry powder were used for each determination; 5.0 SLPM of air into cavity; bulk density of powder was 1.3 g/ml; heated plate surface at 700°C.

Figure 20. Dependence of the Reignition Delay for a Commercially Supplied Potassium Bicarbonate Dry Powder on JP-4 Fuel Flow Rate in an Atmosphere of Air.

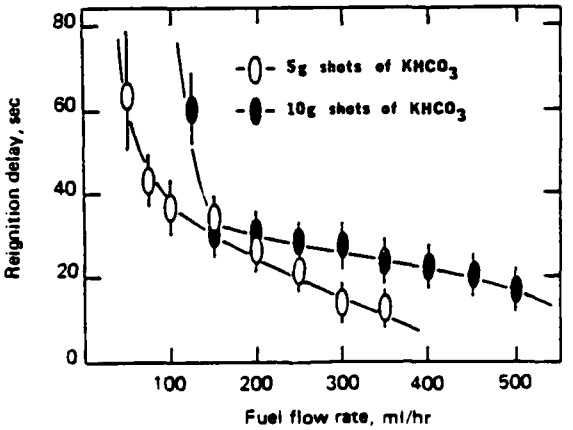

Note: Two data sets are shown, one for 5g shots of the powder, and the other for 10g shots of the commercially supplied potassium bicarbonate dry powder; in each case, the heated surface was at 500°C; bulk density of the powder was 1.3 g/ml; and oxygen flow rate was 2.0 SLPM.

Note the distinctive change in slope at ca. 50 to 100 ml/hr, this corresponds approximately to the stoichiometric barrier for JP-4 oxidation (ca. 60 ml/hr). Such abrupt changes in slope often denote a change in mechanism for a reaction.

Figure 21. Dependence of the Reignition Delay for a Commercially Supplied Potassium Bicarbonate Dry Powder on JP-4 Fuel Flow Rate in an Oxygen Atmosphere.

Table 6. Hysteresis Effects on the Reignition Delay Time.

Day 1 (2 August 1976)		Day 2 (3 August 1976)		Day 4 (5 August 1976)	
Early a.m.	Late p.m.	Early a.m.	Late p.m.	Early a.m.	Late p.m.
67	53	75	52	65	46
60	51	67	43	77	48
59	49	74	48	60	52
60	57	67	53	53	51
71	57	70	51	58	[31][a]
63		72	55		51
			54		48
63 ± 5 (8%)	53 ± 4 (8%)	71 ± 3 (5%)	51 ± 4 (8%)	63 ± 9 (14%)	49 ± 3 (5%)
ratio 1:1.2		ratio 1:1.4		ratio 1:1.3	

[a]Rejected in calculating mean and standard deviation.

NOTE: Measured reignition delays (in seconds) induced by a commercially supplied potassium bicarbonate dry chemical agent. All such material has been passed through a 325 ASTM sieve (<45 microns); 5g sample shots of dry powder were used for each determination. Cavity volume is ca. 5 liters; heated surface at 400°C; 200 ml/hr of JP-4 fuel, with 2.25 SLPM of oxygen into the cavity.

This hysteresis effect also became obtrusive during an experimental run involving several different temperatures. If a sequence was initiated with the dependent variable temperature altered in ascending order, reignition delays would exhibit an "expanded" range compared to those obtained under apparently identical conditions but where temperatures were changed in descending order. Consequently, all experiments delineated in this report were obtained with ascending temperature sequences to provide some degree of comparability.

This demonstration of an apparent "hysteresis" effect also emphasizes the importance of extinguishing a flame at the earliest possible moment, to prevent a general temperature rise in all of the surrounding surfaces, and thus severe curtailment of fire control by a potential extinguishant.

STORAGE STABILITY OF CHEMICALS

The acceptability of potential dry chemical fire extinguishants with respect to delineated storage requriements was judged via compliance with the published physical constants for the compounds concerned, and via TGA (thermogravimetric analysis) data methods obtained by the investigators for each compound tested. Significant weight loss (>5 %) at temperatures below 120°C automatically violates current storage requirements.

and similar weight loss at temperatures up to 260°C would violate those requirements delineated for advanced aircraft. Thus, chemicals with melting points or sublimation temperatures that would conflict with these limits, by producing significant vapor pressures or undergoing a first or second order thermochemical phase change, would prove unsatisfactory for storage. Water loss (effloresence) and water absorption (deliquescent and/or hygroscopic properties) will also preclude compliance with the storage requirements. Some physical parameters for various potential dry chemical fire extinguishants are given in Table 7.

Table 7. Some Physical Parameters of Potential Fire Extinguishants.

Sample description and supplier[a]	Bulk density, [b] g/ml	M. Pt and/or B. Pt, °C
$KHCO_3$ Ansul Corp. "Purple-K"	1.24	100 to 200 decomposition
$KHCO_3$ Ansul Corp. "X" (high density)	1.35	100 to 200 decomposition
K_2CO_3 Ansul Corp. (commissioned)	1.22	891
$NH_4H_2PO_4$ Ansul "Foray"	1.18	190
$NH_4H_2PO_4$ PyroChem TUW-156	1.16	190
NaCl PyroChem "BCD-Orange"	1.36	801
$KC_2H_3N_2O_3$ I.C.I. Ltd. "Monnex"	0.88	---
KCl PyroChem "Super-K"	1.42	776
$SnCl_2 \cdot 2H_2O$ Reagent Grade + 1% w/w f.a.[c]	1.55	38
$Na_2WO_4 \cdot 2H_2O$ Reagent Grade + 1% w/w f.a.	2.11	
Na_2WO_4 Reagent Grade + 50% w/w f.a.	2.17	698
Tin Oxide Reagent Grade	3.26	1080 decomposition
Tin Iodide Reagent Grade	1.77	320 717
Tin Iodide Laboratory Synthesis/1% w/w f.a.	2.69	320 717
KI Reagent Grade + 1.5% w/w f.a.	1.95	686
NaI Reagent Grade + 1.5% w/w f.a.	2.02	651 hygroscopic
KD[d] with 1.0% w/w f.a.	0.75	270 to 320 decomposition
KD with 1.5% w/w f.a.	0.84	270 to 320 decomposition
KD with 2.0% w/w f.a.	0.88	270 to 320 decomposition
KD + 9% tin iodide + 1% w/w f.a.	0.85	270 to 320 decomposition
KD + 17% tin iodide + 1% w/w f.a.	0.96	270 to 320 decomposition
NaD[d] with 1% flow agent	0.85	240 to 290 decomposition
NaD + 1% tin iodide + 1% f.a.	0.88	240 to 290 decomposition
NaD + 5% tin iodide + 1% f.a.	0.89	240 to 290 decomposition
NaD + 10% tin iodide + 1% f.a.	0.93	240 to 290 decomposition
NaD + 20% tin iodide + 1% f.a.	1.04	240 to 290 decomposition
NaD + 40% tin iodide + 1% f.a.	1.28	240 to 290 decomposition
NaD + 60% tin iodide + 1% f.a.	1.42	240 to 290 decomposition
NaD + 80% tin iodide + 1% f.a.	1.74	240 to 290 decomposition

[a] All powders ground, sieved, and passed through an ASTM #325 mesh (<45 μm).

[b] Probable error in bulk density ± 0.03 units.

[c] "f.a." is used for "silica flow agent" (bulk density <0.06 g/ml).

[d] "D" is used for the Dawsonite anion, $[Al(OH)_2CO_3]^-$.

COMPARATIVE TESTING OF POTENTIAL EXTINGUISHANTS

The experimental static testing assemblage described previously was now used to determine the relative effectiveness of various chemicals in extinguishing a flame, and preventing reignition of this flame even though JP-4 fuel was still being pumped onto the hot surface. The reignition delay observed can be related to the competitive scavenging reactions induced by the extinguishant chemical in controlling flame propagation reactions, and is thus a fundamental descriptive parameter of the system from which meaningful deductions can be drawn. Although the absolute magnitude of the reignition delay will depend on the experimental parameters already delineated above, the relative magnitudes for one chemical compared to another will provide us with a true measure of fire control performance. Since we are primarily concerned with relative performance of each system tested, we need to be able to standardize the performance of our experimental assemblage. We chose to do this by measuring the reignition delay for a standard compound each day, or at the beginning of any sequence of self-consistent measurements, whichever occurred sooner. Since potassium bicarbonate proved to be one of the most effective commercially available dry chemical fire extinguishants (Ansul Corp. "Purple-K®"), and we had a large supply in one batch, we chose this as one standard. However, at high temperatures, this chemical was very corrosive to the plate surface and particularly to the thermocouples welded to the plate. To obviate corrosion problems, we used a second standard, aluminum hydroxide ("Gibbsite") supplied by Kaiser Aluminum Corp., again one single large batch was used throughout the 30-month experimental period. Over the 30-month period, the mean for any data set taken did not differ from the mean to all sets taken by more than ±75%, and the mean for one set in a sequence did not differ from the mean to a set of sets taken over the duration of an experimental sequence (extending over a period of as much as 10 days) by more than ±10%. Figure 22 exhibits a limited display of data taken over a period of several months for "Purple-K®".

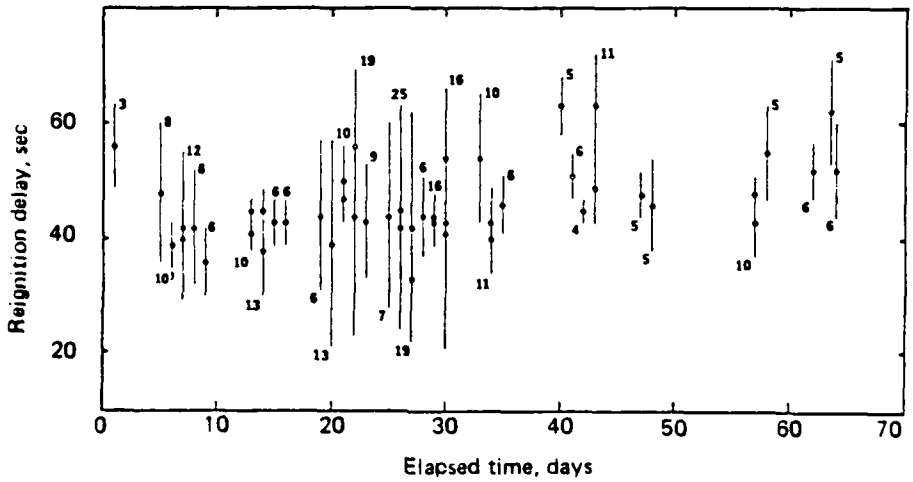

Note: The points are mean values for a data set containing the indicated number of points (number appended at top or bottom of error bar). Error bars are single standard deviations for the data sets. Two (or more) points for any one day show means for multiple data sets during that day.

Figure 22. Quality Control Display of Reignition Delay Data for Standard Compound ("Purple-K®", $KHCO_3$) Taken Over a Period of Several Months.

CHOICE OF POTENTIAL SYSTEMS

In choosing which systems to test, several criteria were used.

1. All current commercially supplied materials were examined directly; obviously, existing technology should be utilized where possible to minimize economic factors.

2. Fundamental chemical knowledge allows us to predict that certain compounds will be effective fire control agents under certain prevailing circumstances.

3. Intuitive concepts of fire control would indicate that other chemicals might successfully provide initial extinguishment ("knock-down") and/or long term control of flammable situations.

Since many compounds have already been tested by other investigators, only those chemicals thought to be more effective than the most effective commercial chemicals were selected for further testing in the static assemblage (a screening process prior to dynamic testing).

In reviewing factors that are thought to provide effective fire control, the following points are worth delineating at this time:

1. Chemicals used to control preignition ("antiknock") in internal combustion engines include lead, tin, manganese, and iron, in the form of lead alkyls (tetra-ethyl lead), tin alkyls (tetra-t-butyl tin), cyclopentadiene-manganese tricarbonyl ("cymantrene"), and bis-dicyclopentadieneiron (ferrocene). Further, tetra-t-butyl tin is used as an antioxidant in plastics and fibers. One seeming characteristic displayed herein is the multiple valency available to each metal, and this has been mentioned in the literature before by several investigators.

2. The solid chemical should provide a prima-facie display of fire control, best exemplified by the thermal decomposition of carbonates and oxalates to provide a CO_2 atmosphere locally and thus to blanket the flame physically in an inert atmosphere. This factor has dominated previous approaches to fire control, and the majority of commercial systems are based on either carbonates or bicarbonates.

3. Intuitive concepts also indicate that the solid chemical has to be volatile enough to penetrate into the gas phase, and thus alkali metal cations and some aluminum salts are more likely to be useful than alkaline earth cations. Equally, standard concepts of gas phase reaction mechanisms would indicate that any radical or ion scavenger should interfere with the chain propagation processes that characterize flames and explosions and should provide a measure of fire control. In particular, halogens and halogen derivatives are well known radical-scavengers, and should form an important part in the testing role and assessment process, with particular emphasis on iodine and the iodides. For these latter compounds, a strongly ionic bond or a weak covalent bond is mandated, to allow scavenging by the halogen entity itself to occur.

4. For obvious reasons, the salt should possess minimum toxicity; although for remote usage in an engine nacelle this is not a property that is particularly important at the time of use. The fire extinguishant system still has to be loaded and installed, and there may be a cleanup operation on successfully combatting the fire. Thus, cations such as mercury and lead should be avoided, and some anions such as cyanide and arsenate are of doubtful efficacy in this respect.

5. Economics will play some part in the overall choice, in that large quantities of the final material will be needed for all uses; thus, chemicals that require many steps to synthesize, or contain large quantities of rare materials, or which require experimental syntheses involving processes that are relatively intractable to bulk production, are not considered prime candidates for the major component in a dry chemical system.

6. On finally assessing the utility of various chemicals, or mixtures of chemicals, attention must be redirected to the storage requirements delineated in Table 1, and other ancillary requirements delineated in standard military specification. These are restated here for classification:

a. The material should be stable to temperatures up to 260°C for advanced aircraft use, corresponding to <5% loss in weight at this temperature (current vehicles dictate 120°C for maximum storage temperatures). A less stringent requirement is stability down to -55°C for storage purposes.

b. The material should exhibit no water absorption properties, or corresponding weight losses by efflorescence.

c. The material should be effective at controlling fires initiated by hot surfaces at temperatures up to 815°C, and it is expected that a 300-second delay or better can be produced by a candidate dry chemical powder applied to a JP-4 fuel fire initiated on an 800°C surface.

Using these criteria, some potential candidate systems would include alkali metal carbonates and bicarbonates, alkali metal halides, tin salts (particularly tin carbonate), aluminum salts, various boron derivatives, and commercially available materials. These choices are limited by the following points:

1. Tin carbonates are not stable entities and cannot be isolated satisfactorily by current technology. Similarly, aluminum carbonates are equally unsatisfactory. To overcome these problems, specific syntheses were initiated to produce a stable complex tin carbonate in the form of an alkali metal carbonate-hydrated tin oxide system. This was unsuccessful. A second preparation involving a mixed salt of potassium oxalate and hydrated tin oxide ("stannic acid") was successful and produced a material with the probable formula $K_2Sn(OH)_4C_2O_4$. No toxicity data are currently available for this compound, but it should be noted that sodium and potassium oxalates are systemic poisons.

2. The availability of a complex sodium-aluminum carbonate as a naturally occurring mineral (Dawsonite), in the form $NaAl(OH)_2CO_3$, prompted us to examine its utility as a fire control agent, since aluminum carbonate itself is not an accessible compound. Three sources of Dawsonite are conveniently available:

a. The natural mineral, essentially the major component in oil shale, can be obtained as a waste product from oil recovery operations.

b. A commercial source of Dawsonite is available from either "antacid" manufacturers (such as "Tums®"), or from water treatment plants where alumina flocculation processes of industrial and recycled water produces this material by precipitation. One such source proved to be the Kaiser Aluminum Corp., who very kindly provided samples of this material.

c. A third source is laboratory synthesis, isolation, and characterization of this material by conventional means; one such preparation being reported in the chemical literature as an existing U.S. Patent. Moreover, since it is usual for potassium salts to be more effective than corresponding sodium salts, a synthetic preparation of potassium Dawsonite was also a potentially useful route to an effective agent.

3. Commercially available systems included various carbonate and bicarbonates, of which the best known are based on potassium bicarbonate. Since potassium carbonate is hygroscopic, and this limits its usefulness, we commissioned the Ansul Corp. to prepare a potassium carbonate based material that would resist water absorption, and this compound also was tested. Other systems available commercially included:

a. A mixture of potassium bicarbonate and urea as a condensed (one water molecule eliminated per pair of molecules) solid, marketed by I.C.I. Ltd., and tradenamed "Monnex®". This material is essentially a carbamate compound.

b. Various phosphate derivatives from many companies are currently being used, one such being "Phos-Chek®" from Monsanto, used for forest fire control, and based on $(NH_4)_2HPO_4$. Phosphates based on $NH_4H_2PO_4$ are sold by other companies for domestic and automobile fire control, such as the Ansul Corp. "Foray®".

c. Currently, I.C.I. Ltd. holds a patent for the use of "cryolite", K_3AlF_6, as a potential dry chemical system for fire control, and this compound was also included in the list of potential agents.

d. Forest fire control has, in the past, used borax (sodium borate in various hydrated forms), and although it is not as effective as the phosphates and bicarbonates, the oxide (B_2O_3) and acid (H_3BO_3) are worth investigating further as potential agents. Similar in chemical properties to borax are the tungstates, $WO_4^=$, and the sodium salts in hydrated and nonhydrated forms could be potential control agents, since tungsten exhibits one of the widest range of valence states of any element (as does uranium, but other factors rule out use of this metal).

e. One final chemical is worth mentioning, carbon tetra-iodide, since carbon tetrachloride was one of the first agents to be used for fire control. Moreover, CI_4 is a solid at room temperature, a potential iodine source in the vapor phase (since C-I bonds are weaker than C-Cl bonds), and iodine is recognized as being the best radical scavenger among the halogens.

f. Since some of the chemicals seemed to be easily dislodged from the heated plate surface by the fuel jet momentum, it was proposed that some form of "sticky" additive be added to assist the particles in adhering to the plate. Since boron compounds tend to form glasses when melted, we decided to test one such sample (potassium Dawsonite) that contains 10% by weight of boron(III) oxide.

COMPARATIVE TESTING OF SINGLE CHEMICALS AT 675 to 900°C

Using the experimental method already described, reignition delay data for various single chemicals and commercially supplied extinguishants were obtained at various temperatures in the range 700 to 900°C for air oxidation, and for various quantities of powder varying between 5 and 20g per sample determination. These data are shown in Table 8.

It is pertinent at this point to mention that tin(II) salts are prone to oxidation by air and/or moisture and that commercially supplied tin(II) salts contained up to 60% tin(II) salts. Thus, we refer in general SnI_x, for example, as being tin iodide (and vice-versa), purchased nominally as the tin(II) salt from commercial sources. Since some of the chemicals tested did not produce significant delays even at 700°C, and virtually none at higher temperatures, an additional nine compounds were tested at 700°C only. Although eight of these additional nine have indifferent performances with respect to fire control capabilities, the exception is the specially prepared (by Ansul Corp.) K_2CO_3 powder, which is deemed slightly superior to the $KHCO_3$ based material already marketed by this corporation. These data are shown in Table 9.

It became apparent that data obtained from 10g samples provided sufficient differentiation between materials (reignition delays ranging from greater than 900 seconds down to less than 10 seconds), and yet provided a small enough sample to allow reasonable prolonged testing sequences for moderate quantities of powder. This was especially important for some materials that were quite "expensive" either in actual costs, or in time to synthesize and prepare. Accordingly, we standardize our next phase of testing to this amount, 10g, and recorded data for an additional five compounds at various temperatures. These data are shown in Table 10.

To provide a self-consistent listing of relative efficiencies in controlling JP-4 fuel fires initiated by hot surface ignition, we have retabulated all compounds examined (data from Tables 8, 9, and 10) in a rank-order determined by their reignition delay at 700°C for 10g sample determinations. This reference temperature was chosen merely because the majority of compounds were tested at this value. It was necessary to estimate reignition delays at 700°C for five compounds; this was done by using a reaction kinetics Arrhenius-style plot

(see next section below). These data are presented in Table 11. It is clear from these data that iodides are, as expected, powerful chemical extinguishants at low temperatures, but that their efficiencies fall rapidly as the temperature rises. Again, as expected, the stabilized (by complexing as a double salt) carbonates provided better performance than simple carbonates (cf. both Dawsonites with respect to potassium carbonate and bicarbonate), indicating perhaps a form of "shielded" or "hindered" carbon dioxide release due to the increased thermal stability induced by double salt formation. This is further exemplified when data taken at 900°C is examined, where the Dawsonites can be seen to be virtually the only chemicals providing any (albeit, very limited) protection at these elevated temperatures.

Table 8. Reignition Delay Data as a Function of Temperature and Shot-Mass for Various Potential Single Chemical Dry Powder Extinguishants: Testing in Air-Combustion Over the Range 700 to 900°C.

1. All reignition delays are given in seconds.
2. 200 ml/hr JP-4 fuel flow and 2 SLPM air into cavity.
3. All dry powders were ball-milled and sieved to pass an ASTM-325 Mesh.
4. All dry powders contain 1% w/w flow agent to prevent caking and moisture uptake.
5. All chemicals are reagent grade materials unless stated.
6. $KHCO_3$ and K_2CO_3 are commercially supplied extinguishants (Ansul Corp.).
7. Na and K Dawsonites were synthesized by the authors, the Dawsonite anion is $\left[Al(OH)_2CO_3\right]^-$.
8. Note that a delay of approximately 4 to 5 seconds is really equivalent to a zero delay, since this time is needed for the fuel to "wash" through to the heated surface and/or for the fuel to reach ignition temperatures due to heat capacity effects from the dry powder.
9. Data are given in the form "Mean Reignition Delay in Seconds ± the Standard Deviation (Number of Points in Data Set)".
10. Tin iodide is referred to as SnI_x.

Temperature, °C	Potassium Dawsonite KD			Ansul Corp.	"Purple-K"	$KHCO_3$
	5g	10g	20g	5g	10g	20g
675	193 ± 38(10)	252 ± 91(5)	>600(5)			
700	73 ± 11(10)	153 ± 15(15)	350 ± 50(10)	30 ± 12(25)	69 ± 20(40)	204 ± 80(30)
725	34 ± 6(10)	98 ± 38(15)	203 ± 25(10)			
750	31 ± 10(10)	81 ± 18(15)	113 ± 11(5)	27 ± 5(10)	50 ± 8(10)	106 ± 45(5)
775	21 ± 4(5)	30 ± 3(5)	82 ± 8(5)			
800	12 ± 2(5)	30 ± 6(15)	38 ± 4(5)	29 ± 7(10)	38 ± 8(10)	102 ± 50(10)
825	10 ± 1(5)	18 ± 2(5)	32 ± 3(5)			
850		19 ± 3(5)			18 ± 3(5)	
900	6 ± 3(10)	10 ± 4(15)	13 ± 3(20)	2 ± 1(5)	7 ± 4(15)	13 ± 3(10)

Table 8. (Contd.).

Temperature, °C	I.C.I "Monnex" $KHCO_3$-urea			PyroChem "BCD-NaCl"		
	5g	10g	20g	5g	10g	20g
700	30 ± 3(5)	55 ± 30(20)	61 ± 12(10)	9 ± 3(10)	33 ± 15(5)	27 ± 2(5)
750	18 ± 5(5)	27 ± 6(5)	63 ± 14(5)	5 ± 2(5)	9 ± 2(5)	11 ± 2(5)
800	5 ± 2(5)	9 ± 2(5)	20 ± 3(5)	5 ± 2(5)	8 ± 3(5)	10 ± 3(5)
900	4 ± 2(5)	7 ± 2(5)	13 ± 3(5)	4 ± 2(5)	5 ± 2(5)	5 ± 2(5)

Temperature, °C	Tin iodide SnI_x[a]			NaD	$Al(OH)_3$	NaI	KI
	5g	10g	20g	10g	10g	10g	10g
700	200 ± 80(15)	380 ± 80(30)		296 ± 50(5)	100 ± 30(30)	600 ± 60(5)	>900
725		244 ± 40(10)				725 ± 75(5)	280 ± 30(5)
750	102 ± 50(20)	102 ± 40(15)		170 ± 50(15)	82 ± 20(30)	262 ± 95(5)	
775	58 ± 3(5)	58 ± 6(15)				195 ± 50(5)	
800	8 ± 2(5)	19 ± 2(10)	32 ± 3(5)	29 ± 5(15)	18 ± 6(30)	10 ± 25(5)	16 ± 6(5)
850		3 ± 2(5)	28 ± 3(5)			16 ± 10(5)	10 ± 5(5)
900		2 ± 2(5)	8 ± 6(10)	6 ± 3(15)	3± 2(15)	3 ± 2(5)	2 ± 2(5)

[a]Tin(II) iodide is very unstable to air or moisture, and commercially supplied materials contained varying proportions of tin(IV) iodide. The majority of tin iodide, supplied nominally as tin(II) iodide appeared to contain approximately 50 to 60% tin(IV) iodide.

Table 9. Reignition Delay Data for Various Single Compound Potential Dry Chemical Extinguishants at 700°C (Air-Combustion).

Ranking order[d]	Compound	5g	10g	20g
1	Ansul Corp. K_2CO_3	65 ± 11	150 ± 80	300 ± 55
2	Pyro-Chem Corp. "Super-K" (KCl)		33 ± 4	26 ± 5
3	$SnCl_x \cdot 2H_2O$	7 ± 2	26 ± 3	81 ± 8
4	$Na_2WO_4 \cdot 2H_2O$	14 ± 2	17 ± 2	22 ± 3
5	SnO		15 ± 5	
6	Cryolite (K_3AlF_6)	8 ± 2	14 ± 5	
7	Ansul Corp. "Foray" ($NH_4H_2PO_4$)	5 ± 2	12 ± 2	38 ± 14
8	Pyro-Chem TUW-156 ($NH_4H_2PO_4$)	5 ± 2	8 ± 3	13 ± 2
9	Na_2WO_4 (dehydrated)		8 ± 2	
10	Carbon tetra-iodide	zero		

[d] Arranged as decreasing effectiveness based on data for 10g shots. All samples were ball-milled, passed through an ASTM-325 (<45 microns), and mixed with 1% w/w of flow agent to prevent caking and moisture uptake.

NOTE: Errors are single standard deviations for a minimum of five data points.

Table 10. Reignition Delay Data for Various Single Compound Dry Chemical Extinguishants for JP-4 Fuel–Air Oxidation Studies at Various Temperatures.

Compound	750°C	800°C	900°C
Al_2O_3 "alumina"	28 ± 12	7 ± 3	zero
AlOOH "Boehmite"	48 ± 35	5 ± 2	zero
B_2O_3	5 ± 3	3 ± 2	2 ± 1
K-Dawsonite + 10% B_2O_3	62 ± 28	18 ± 5	6 ± 2
H_3BO_3	<10>[a]		

[a]Single reading only.

NOTE: 10g shots for each determination, 200 ml/hr JP-4 fuel, 2 SLPM air.

Table 11. Reignition Delay Data for Potential Dry Chemical Fire Extinguishants Ranked According to Their Performance at 700°C.[a]

	Compound	700°C	750°C	800°C	900°C
1.	KI	>900[b]	100 ± 30	16 ± 6	zero[c]
2.	NaI	600 ± 60	262 ± 95	90 ± 25	zero
3.	SnI_x	380 ± 80	102 ± 40	19 ± 2	zero
4.	NaD[d]	296 ± 50	170 ± 50	29 ± 5	6 ± 3
5.	KD	153 ± 15	81 ± 18	30 ± 6	10 ± 4
6.	K_2CO_3 (Ansul Corp.)	150 ± 80			
7.	KD + 10% w/w B_2O_3	<140>[e]	62 ± 28	18 ± 5	6 ± 2
8.	$Al(OH)_3$	100 ± 30	82 ± 20	18 ± 6	zero
9.	$KHCO_3$ (Ansul Corp. "Purple-K")	69 ± 20	50 ± 8	38 ± 8	7 ± 4
10.	$KHCO_3$/urea (ICI "Monnex®")	55 ± 30	27 ± 6	9 ± 2	7 ± 2
11.	AlOOH ("Boehmite")	<55>	48 ± 35	5 ± 2	zero
12.	Al_2O_3 ("alumina")	<55>	28 ± 12	7 ± 3	zero
13.	KCl (Pyro-Chem Corp.)	33 ± 4			
14.	NaCl (Pyro-Chem)	33 ± 4			
15.	$SnCl_x \cdot 2H_2O$	26 ± 3			
16.	$Na_2WO_4 \cdot 2H_2O$	17 ± 2			

Table 11. (Contd.).

	Compound	700°C	750°C	800°C	900°C
17.	$SnO_x \cdot nH_2O$	15 ± 5			
18.	K_3AlF_6 ("cryolite")	14 ± 5			
19.	H_3BO_3	<14>	[10][f]		
20.	$NH_4H_2PO_4$ (Ansul Corp.)	1? ± 2			
21.	$NH_4H_2PO_4$ (Pyro-Chem Corp.)	8 ± 3			
22.	Na_2WO_4	8 ± 2			
23.	B_2O_3	<8>	5 ± 3	3 ± 2	zero
24.	CI_4	zero			

[a]Data for 10g samples, 200 ml/hr JP-4 fuel flow, 2.0 SLPM air input.

[b]Reignition delays in seconds, errors shown are standard deviations.

[c]Less than 2 to 3 seconds delay is considered to be zero inhibition.

[d]Anion D^-, Dawsonite, is $[Al(OH)_2CO_3]^-$.

[e]<x> indicates estimated reignition delay via Arrhenius extrapolation.

[f]Only one measurement taken.

TEMPERATURE DEPENDENCE OF REIGNITION DELAY DATA

As indicated previously, the reignition delay is a kinetic parameter describing the competition between extinguishant scavenging action and chain propagation reactions that typify the flame and/or explosion. It is not surprising, therefore, that reignition delay data as a function of temperature can be correlated by an Arrhenius-type function involving a linear plot of the logarithm of the reignition delay against reciprocal absolute temperature. Two such plots are shown in Figure 23 for potassium bicarbonate and potassium Dawsonite. The slopes of each line vary widely, and reflect to some extent the thermal energy needed to decompose the material, and in kinetic terms, are related to a so-called "activation energy". It is also pertinent here to note that the effectiveness of a dry chemical as a fire control agent falls to zero above the melting point. For example, $KHCO_3$ has a melting point of 891°C, (at 900°C there is virtually no reignition delay observed).

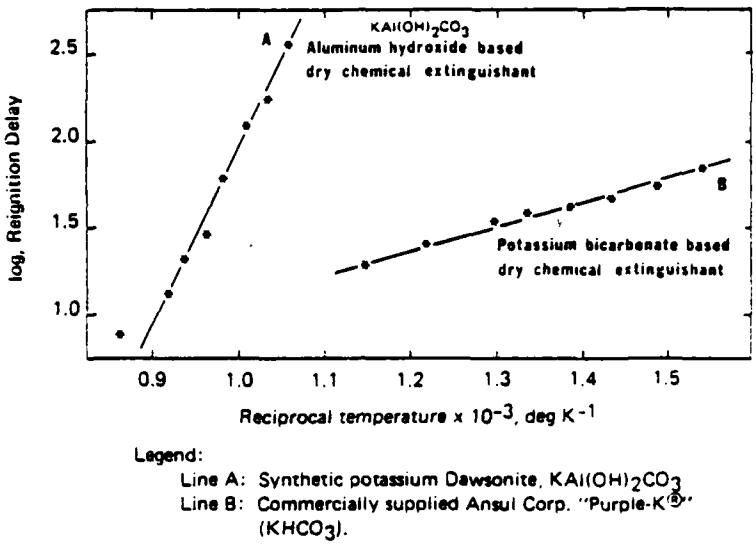

Legend:
Line A: Synthetic potassium Dawsonite, $KAl(OH)_2CO_3$
Line B: Commercially supplied Ansul Corp. "Purple-K®" ($KHCO_3$).

Figure 23. Arrhenius-Style Plot of the Temperature Dependence for Two Representative Compounds.

COMPARATIVE TESTING IN THE RANGE 400 TO 600°C

To extend the range of measurements of reignition delays below 700°C, it was necessary to overcome the self-ignition difficulties. This was accomplished by enriching the oxygen content of the combustion cavity above the normal partial pressure of 0.21 available from air alone. Using pure oxygen introduced through the gas inlet pipes shown in Figure 3 enabled us to extend the self-ignition temperature down to 370°C, allowing data collection in the range 400 to 600°C. Above approximately 600°C, reignition delays became immeasurably short and prevented differentiation between compounds. These low temperatures serve to emphasize thermal activation/degradation effects. For example, these temperatures are now low enough that it is possible to envisage a situation where the extinguishant has little or no effect until a minimum threshold temperature is reached and exceeded. Up to this temperature, the effectiveness of the extinguishant will actually increase as the temperature increases. However, above a sufficiently high temperature, all compounds will exhibit a fundamentally Arrhenius-type behavior. These behavioral patterns are clearly displayed in the data taken for combustion in oxygen enriched atmospheres at temperatures between 400 and 600°C for nine selected compounds (see Table 12). These data are also shown plotted in Figures 24, 25, and 26, and illustrate clearly this non-Arrhenius behavior discussed above. This mode of behavior appears prevalent for compounds whose anion decomposes irreversibly; e.g., carbonates, oxalates, and dehydration of hydroxides. These data also illustrate the catastrophic fall in efficiency seen for volatile compounds such as tin iodide, emphasizing the point already made that above the melting point of a compound the effectiveness rapidly falls to zero.

Table 12. Reignition Delay Data as a Function of Temperature for Various Potential Single Chemical Dry Powder Extinguishants (Testing in Oxygen-Enriched Atmospheres in the Range 400 to 600°C).

Compound[b,c]	Mean reignition delay[a] ± standard deviation (number of data points)				
	400°C	450°C	500°C	550°C	600°C
$KHCO_3$[d]	48 ± 9 (37)	38 ± 7 (28)	31 ± 10 (42)	28 ± 4 (16)	22 ± 5 (22)
SnI_x	90 ± 11 (8)	63 ± 7 (4)	34 ± 5 (7)	41 ± 9 (7)	2 ± 1 (6)
K_2CO_3[d]	30 ± 8 (20)	25 ± 8 (11)	21 ± 4 (10)	14 ± 6 (5)	16 ± 3 (5)
KD	26 ± 8 (5)	18 ± 5 (19)	18 ± 2 (3)	18 ± 3 (4)	14 ± 2 (4)
$K_2Sn(OH)_4C_2O_4$	24 ± 6 (6)	16 ± 4 (7)	19 ± 3 (6)	14 ± 4 (5)	
$Al(OH)_3$	19 ± 3 (5)	10 ± 5 (4)	17 ± 6 (11)	9 ± 3 (10)	
NaD	10 ± 7 (4)	8 ± 2 (4)	94 ± 2 (7)	11 ± 2 (4)	
K_2SO_4[d]	9 ± 1 (3)		3 ± 1 (3)		zero
K_3AlF_6	3 ± 1 (6)		ca. zero		zero

[a] All reignition delays given in seconds.

[b] All determinations for: 5g shot size, 2.25 SLPM oxygen flow rate, and 200 ml/hr JP-4 fuel flow rate.

[c] All dry powders were prepared by ball milling and sieving through an ASTM-325 mesh, all contain approximately 0.5 to 1% w/w SiO_2 flow agent to prevent caking and moisture absorption.

[d] Commercially supplied as extinguishants.

NOTE: Note SnI_2 and $K_2Sn(OH)_4C_2O_4$ were synthesized by the authors. $KHCO_3$, K_2CO_3, K_2SO_4, are commercially supplied dry chemical fire extinguishants. NaD and KD are sodium and potassium salts of $[Al(OH)_2CO_3]^-$.

For comparison purposes, we have ranked these nine compounds in order of their reignition delay observed at 400, 500, and 600°C, in three separate rank-orderings. These data are presented in Table 13, and indicate the problems of ranking a system at only one temperature, since ranking "cross-over" can be seen for several compounds listed therein, and most dramatically for tin iodide. This latter compound is most effective at 400°C and virtually ineffective at 600°C, a facet of its behavior that reflects the volatility of the pure substance, and the temperature dependence of its vapor pressure. Equally dramatic is the change in ranking seen for NaD between 400 and 500°C; apparently the temperature dependence for NaD exhibits a maximum in the curve, and this system is "activated" as the temperature rises. However, the rank-ordering at 400 or 500°C are substantially alike, and resemble the rank-ordering already presented at 700°C for air combustion (Table 11).

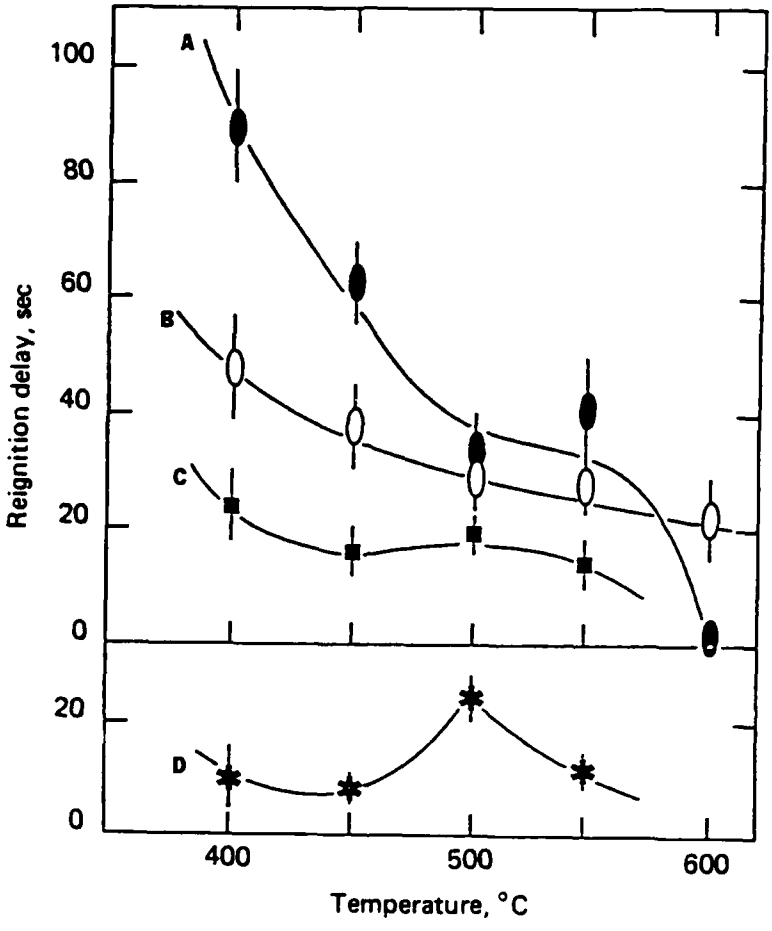

Legend:

Line A: Tin iodide
Line B: Ansul Corp. "Purple-K®" $KHCO_3$
Line C: A potassium-tin complex oxalate
Line D: Sodium Dawsonite

Figure 24. Temperature Dependence of the Reignition Delays for some Potential Dry Chemical Fire Extinguishants in an Oxygen Enriched Atmosphere in the Temperature Range 400 to 600°C.

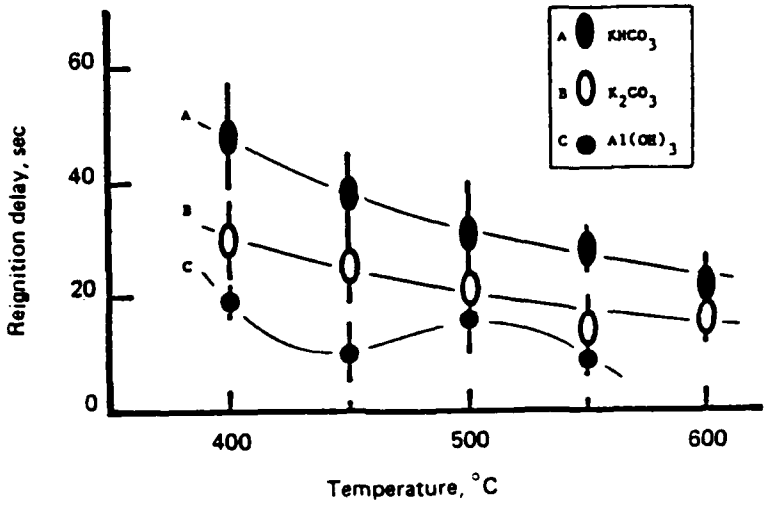

Figure 25. Temperature Dependence of the Reignition Delays for some Potential Dry Chemical Fire Extinguishants in an Oxygen Enriched Atmosphere in the Temperature Range 400 to 600°C.

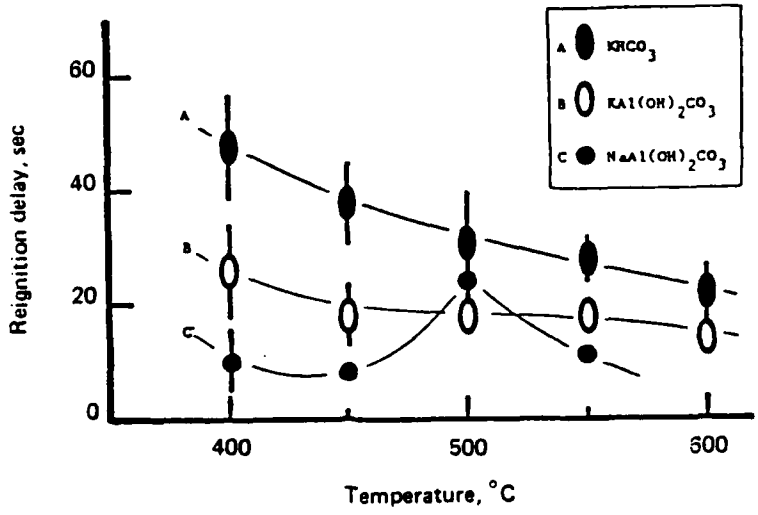

Figure 26. Temperature Dependence of the Reignition Delays for some Potential Dry Chemical Fire Extinguishants in an Oxygen Enriched Atmosphere in the Temperature Range 400 to 600°C.

Table 13. Relative Effectiveness of Various Single Chemical Dry Powder Extinguishants at 400 to 600°C in Oxygen-Enriched Atmospheres.

400°C	500°C[a]		600°C[a]	
1. SnI_x	1. SnI_x	(1)	1. $KHCO_3$	(2)
2. $KHCO_3$	2. $KHCO_3$	(2)	2. K_2CO_3	(3)
3. K_2CO_3	3. NaD	(7)	3. KD	(4)
4. KD	4. K_2CO_3	(3)	4. $K_2Sn(OH)_4C_2O_4$	(5)
5. $K_2Sn(OH)_4C_2O_4$	5. $K_2Sn(OH)_4C_2O_4$	(5)	5. NaD	(7)
6. $Al(OH)_3$	6. KD	(4)	6. $Al(OH)_3$	(6)
7. NaD	7. $Al(OH)_3$	(6)	7. SnI_x	(1)
8. K_2SO_4	8. K_2SO_4	(8)	8. K_2SO_4	(8)
9. K_3AlF_6	9. K_3AlF_6	(9)	9. K_3AlF_6	(9)

[a] Rankings at 400°C are shown in parentheses after compound.

MULTICOMPONENT SYSTEMS AS EXTINGUISHANTS

We have discussed already the possibility that flame extinguishment capability ("knock-down") may not be compatible with long-term time control ("inhibition") of flammable situations. Further, an extinguishant that works well at low fire temperatures (400 to 600°C) may not prove to be effective at higher temperatures (600 to 900°C), a demonstrated fact emphasized by data in Tables 11 and 12, and clearly illustrated in Figure 24 for tin iodide. Although B_2O_3 did not prove any enhancement of fire control properties when admixed with potassium Dawsonite at 10% w/w (see Table 12), we believe that the principle of a component added specifically to help the dry chemical adhere to the heated surface is still a viable one, and will be tested further in Section 5 (Dynamic Assemblage). Moreover, this concept is more pertinent to real situations involving high-speed airflows across the hot surface, and rapid removal of the extinguishant powder from contact with the ignition source. For these reasons, we believe that a multi-component system will become essential for effective fire control in various situations and scenarios.

We have shown that sodium and potassium Dawsonites have intrinsic fire control capabilities superior to other systems, commercial or synthetic. This can be attributed partly to the chemical structure which allows better control over the thermal activiation of the extinguishant powder. Equally, it is quite clear that iodides exert, predicatably so, considerable influence over flammable situations, providing the best long-term control so far observed. It seemed prudent, therefore, to initially test mixtures of various iodides with these Dawsonites, and other carrying agents or matrices such as aluminum hydroxide. Details of these iodide doping experiments are given in the next section.

USE OF IODIDES AS ADDITIVES

Data for both oxygen-enriched atmospheres and air combustion (Tables 8 to 13) clearly indicate the superiority of iodide salts as long-term fire control agents. This is an effect that can be predicted a priori from two properties of these compounds: (1) iodides are volatile (typically, tin iodide has a melting point of 320°C and a boiling point of 717°C listed for Sn(II) iodide) and their vapor pressures at the temperatures used for testing are significant, thus producing appreciable vapor phase concentrations of the molecular species; and (2) iodine is known to be an excellent gas phase, and liquid phase, scavenger of free radicals, ions, and molecular fragments. Moreover, most metal-iodine bonds are weak (e.g., Sn-I at ca. 40 kcal/mol); thus allowing free iodine (atoms and/or ions) to be released into the gas phase and contribute significantly to homogeneous scavenging and radical-recombination catalysis reactions involving flame precursors. However, because these iodides are volatile, their performance at high temperatures is poor, since they are volatilized fast and thus lost from the plate surface and/or system too quickly to provide long-term control. Typically, SnI_x has virtually no fire control capability at temperatures in excess of 750°C.

It was not immediately obvious whether the metal ion itself produced beneficial effects, since it has long been known that if a sodium salt has good fire control properties, the potassium analog would be superior; for example, sodium bicarbonate and potassium bicarbonate, sodium chloride and potassium chloride, sodium and potassium iodides. Further, some zero-valent metals are themselves inherently good fire control agents; e.g., lead as an antiknock agent, and tin has been postulated as a fire control system (most elements exhibiting multiple valences appear to have fire control properties to some degree). Also, the other halogens are known to be gas phase scavengers too, and this aspect needed further investigation. Accordingly, tin chloride was tested relative to tin iodide, and found to be vastly inferior; similarly KCl was found to be inferior to KI, and NaCl far inferior to NaI in performance. Moreover, tin oxide exhibited poor fire control performance when tested alone, and did not enhance the properties of $Al(OH)_3$ when mixed at 10% w/w ratios, nor did it enhance the effectiveness of potassium Dawsonite when added at 20% by weight; thus precluding a significant contribution from the metal ions in each case. The inescapable conclusion is that the iodine is providing the main contribution to long-term fire control ability. It was therefore decided that mixtures of various iodides should be tested with other systems to try and reduce the volatility via a "blanket" effect, and thus prolong the fire control ability (reignition delay) at higher temperatures.

Tin Iodide and Potassium Sulphate Mixtures

Data in Table 12 indicated the poor performance from K_2SO_4 alone, and mixtures of SnI_x in K_2SO_4 produced a direct additive increase in performance as the concentration of SnI_x in the K_2SO_4 was increased. These data are shown in Figure 27 for oxygen enriched atmospheres in the temperature range 400 to 500°C. One interpretation of these data merely indicates that the K_2SO_4 is "diluting" the effect of SnI_x, as no increase in performance is seen from either system, and the dependence of the reignition delay on a molar ratio is akin to Raoult's Law for vapor pressures of regular solutions, exhibiting no maximum or minimum corresponding to an enhancement or interaction of properties by the other component.

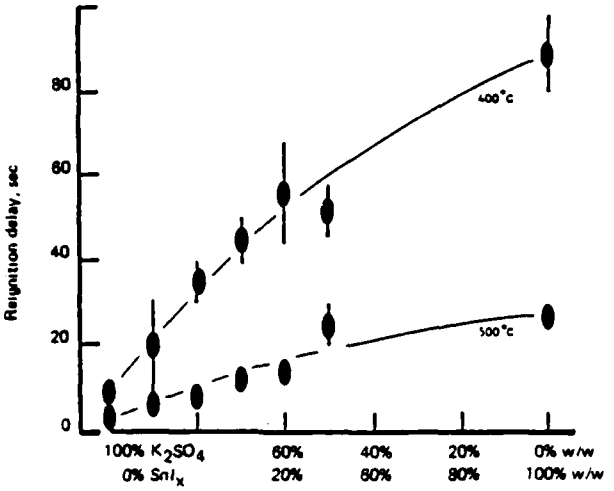

Figure 27. Reignition Delay Data for Mixtures of Tin Iodide in Potassium Sulphate as a Function of Weight Percent Composition.

Iodide Additives to Aluminum Hydroxide

A sequence of mixtures containing varying amounts by weight of both SnI_x in $Al(OH)_3$, and KI in $Al(OH)_3$, was tested for air-oxidation of JP-4 fuel in the range 750 to 800°C. These data are shown in Table 14, and appear to indicate that, unlike for the K_2SO_4 above, each system is improved by the other component, since reignition delay data as a function of composition exhibit a maximum in each case. This mutual enhancement is referred to herein as a "synergistic" effect, since the properties of the mixture are better than the direct sum of individual contributions from the components.

Table 14. Reignition Delay Data for Mixtures for Aluminum Hydroxide With Tin Iodide and With Potassium Iodide.

Composition of mixture	Bulk density, gm/ml	$Al(OH)_3 + SnI_x$		$Al(OH)_3 + KI$	
		750°C	800°C	750°C	800°C
100% $Al(OH)_3$	1.58	82 ± 20	18 ± 6	82 ± 20	18 ± 6
1% w/w iodide	1.33	60 ± 10	15 ± 2	103 ± 12	15 ± 3
5% w/w iodide	1.45	112 ± 25	30 ± 9	80 ± 15	40 ± 4
10% w/w iodide	1.49	157 ± 40	35 ± 4	233 ± 60	70 ± 7
20% w/w iodide	1.60	154 ± 40	45 ± 4	442 ± 140	96 ± 9
100% iodide	3.26	102 ± 40	19 ± 2	100 ± 30	16 ± 6

Iodide Additives to Dawsonites

Since aluminum hydroxide is not a particularly effective fire control agent in its own right, we decided to see whether this synergistic effect was demonstrated for two of the better systems tested, the sodium and potassium Dawsonites. Accordingly, mixtures of iodide at varying proportions by weight with each of the two Dawsonites, were tested individually. These data are shown in Tables 15, 16, and 17. To show that the identity of halide scavenger is of paramount importance, data for a 50% w/w mixture of KCl in potassium Dawsonite are also shown in Table 17 for direct comparison with KD/KI mixtures. It is obvious from these data that the synergistic effect is very strong, exemplified by the data at 800°C for NaD/SnI_x mixtures, and clearly illustrated in Figures 28, 29, and 30.

Table 15. Reignition Delay Data for Sodium Dawsonite/Tin Iodide Mixtures.

Composition of mixture	Bulk density, g/ml	NaD + SnI_x mixtures reignition delay data, sec			
		700°C	750°C	800°C	900°C
100% NaD	0.87	296 ± 50	170 ± 50	29 ± 5	6 ± 3
1% iodide	0.88		238 ± 25	71 ± 7	14 ± 2
5% iodide	0.89		489 ± 50	157 ± 16	19 ± 2
10% iodide	0.93	>900	600 ± 60	201 ± 30	27 ± 2
20% iodide	1.04		600 ± 60	320 ± 65	35 ± 5
40% iodide				374 ± 45	32 ± 4
60% iodide				510 ± 90	52 ± 5
80% iodide				20 ± 4	
100% iodide	2.69	380 ± 80	102 ± 40[a]	19 ± 2	zero
100% KI		>900	100 ± 30	16 ± 6	zero

[a] SnI_x at 725°C, 244 ± 40 sec; SnI_x at 775°C, 58 ± 6 sec.

Table 16. Reignition Delay Data for Potassium Dawsonite/Tin Iodide Mixtures.

Composition of mixture	Bulk density, g/ml	KD + SnI_x mixtures reignition delay data, sec				
		700°C	750°C	800°C	850°C	900°C
100% KD	0.87	153 ± 15	81 ± 18	30 ± 6	19 ± 3	10 ± 4
1% iodide	0.90		193 ± 35	89 ± 15		20 ± 2
5% iodide	0.88		412 ± 30	162 ± 15		35 ± 7
9% iodide	0.88	>900	520 ± 52	113 ± 20	58 ± 6	51 ± 3
17% iodide	0.96		>900	143 ± 14	105 ± 11	63 ± 5

Table 17. Reignition Delay Data for KD/KI Mixtures.

Composition of mixture	Bulk density, g/ml	KD + KI mixtures reignition delay data, sec				
		700°C	750°C	800°C	850°C	900°C
1% iodide	1.20		188 ± 40	24 ± 2		10 ± 2
5% iodide	1.21		517 ± 130	57 ± 9		14 ± 2
9% iodide	1.30	>900	548 ± 70	107 ± 13	27 ± 3	18 ± 6
16% iodide	1.32					
20% iodide			776 ± 30	155 ± 14		17 ± 2
50% iodide					160 ± 30	
100% iodide		>900[a]	100 ± 30	16 ± 6	10 ± 4	zero
KD/KCl 50/50	1.28		28 ± 9	19 ± 3		11 ± 4

[a]KI at 725°C has a reignition delay of 280 ± 30 sec.

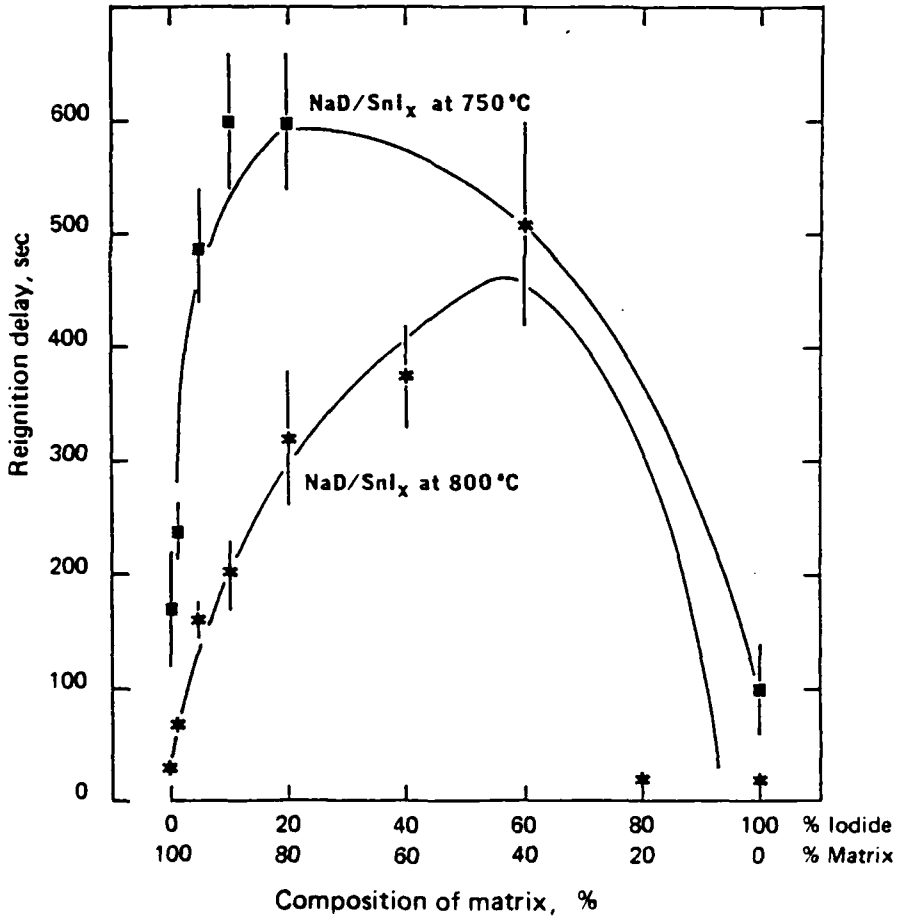

Figure 28. The Synergistic Effect Seen in Fire Control Properties for Sodium Dawsonite Doped With Tin Iodide at Various Temperatures.

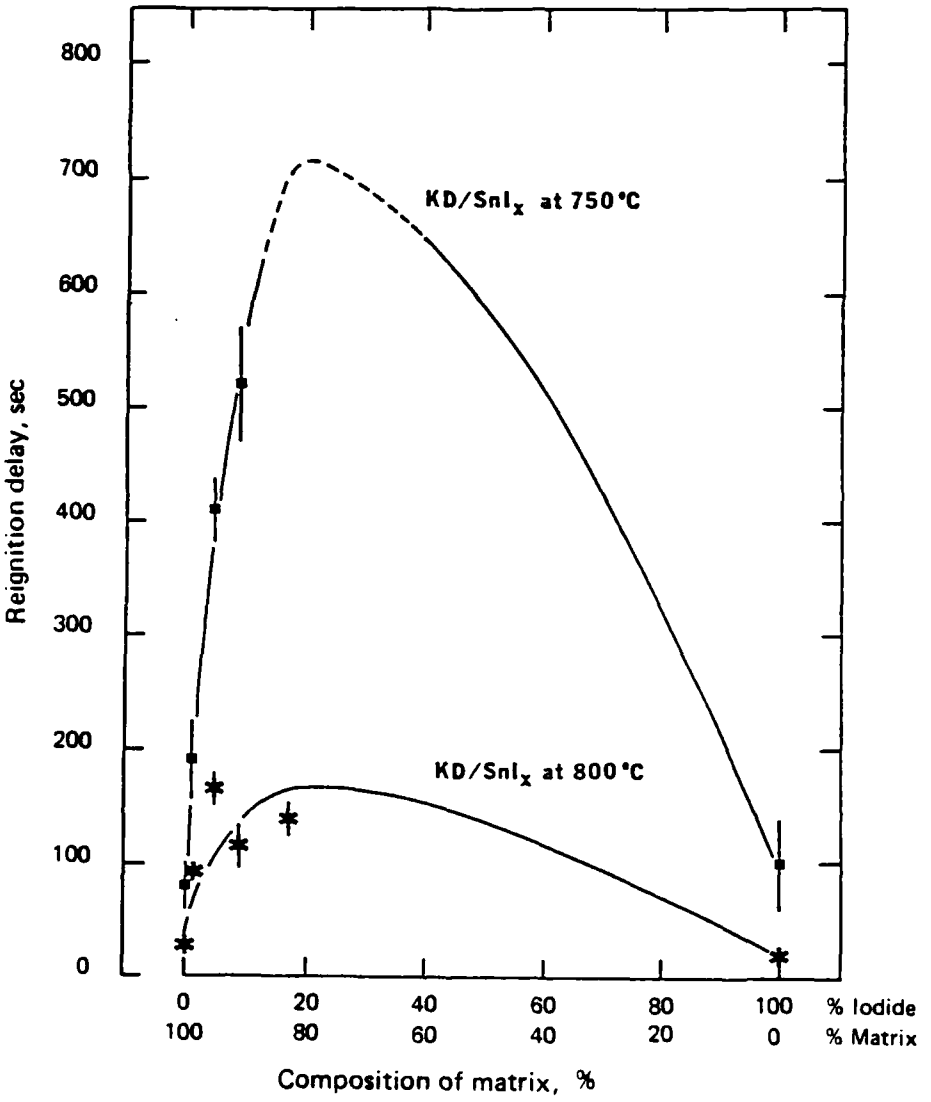

Figure 29. The Synergistic Effect Seen in Fire Control Properties for Potassium Dawsonite Doped With Tin Iodide at Various Temperatures.

Although preliminary experiments were conducted with NaI, and NaI as an additive, these were later abandoned in favor of KI additives even though the reignition delays produced were exceptionally favorable. Sodium iodide is known to be strongly hygroscopic, obviating any sensible storage requirements immediately, and was not considered further as either a single component or an additive.

Since synergism implies nonadditivity of properties in the normal manner, indicating that some interaction has occurred, it is necessary to explore the system more thoroughly in an attempt to elucidate a possible mechanism; this will be described in the next section (A New Concept in Fire Control).

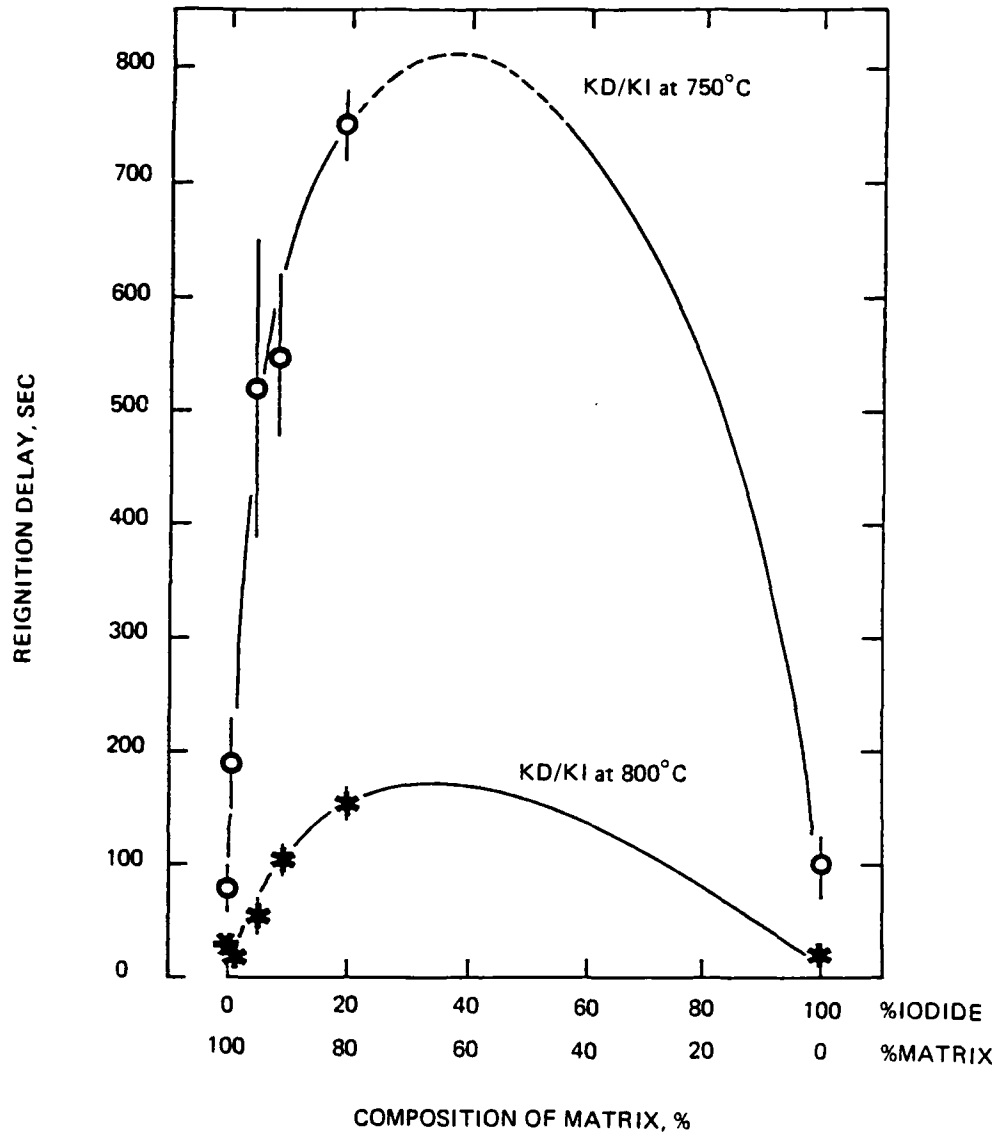

Figure 30. The Synergistic Effect Seen in Fire Control Properties for Potassium Dawsonite Doped With Potassium Iodide at Various Temperatures.

A NEW CONCEPT IN FIRE CONTROL

The synergistic effects seen in the data for iodide additives to Dawsonites and aluminum hydroxide clearly indicates that some form of interaction has occurred between the matrix and the additive. This synergism displayed in Figures 28 to 30 is similar in concept to the non-ideal behavior of vapor pressures correlated by Raoult's Law effects. It is postulated that the volatility of the additive has been suppressed in some way by the matrix

carrier, thus slowing its relase from the carrier to produce long-term time control of the flammable environment. It was thought initially that some form of inorganic crystal clathrate or inclusion complex had been formed in situ on the plate surface, an effect akin to the microencapsulation process utilized in pharmacological sciences to provide time controlled release of drugs. In this case, formation of a crystal inclusion complex that is slowly broken down by thermal effects releasing the fire control additive slowly as the crystal structure is degraded. If this hypothesis were true, then heating the matrix plus doping solids together prior to use would produce the microencapsulation effect sought ahead of time, and thus would produce an effective long-term control agent for the fire. This hypothesis was tested using the same compounds used originally to produce the physical mixtures, accordingly, sodium and potassium Dawsonites were ground (100% pass #325 ASTM sieve) and mixed with varying proportions of tin iodide (also 100% pass #325), heated together at ca. 300°C in the presence of ca. 400 psig CO_2 gas (to prevent decomposition of the Dawsonites) for 12 to 24 hours. This process we refer to as "calcining" or "calcination" Reignition delay data for these calcined solids are presented in Tables 18 and 19. Comparison of these data with those already presented in Tables 15 and 16 for physical mixtures, shows that little or no enhancement of the fire control properties occurs on calcining NaD with tin iodide, but that the high temperature fire control properties of KD calcined with tin iodide are significantly better than those for physically mixed solids– an effect that is expected on the basis of our hypothesis.

Table 18. Reignition Delay Data for Calcined Mixtures of Sodium Dawsonite and Tin Iodide in the Temperature Range 700 to 900°C.

Composition[a] of calcined solid mixture	Bulk density, g/ml	Calcined NaD/SnI_x mixtures reignition delay data, sec[b]			
		700°C	750°C	800°C	900°C
100% NaD	0.87	296 ± 50	170 ± 50	29 ± 5	6 ± 3
1% iodide	0.89		154 ± 6 (15)	46 ± 10 (15)	14 ± 3 (5)
5% iodide	0.88		259 ± 42 (15)	143 ± 16 (15)	19 ± 4 (5)
10% iodide	0.89		450 ± 60 (15)	214 ± 20 (15)	41 ± 15 (5)
20% iodide	0.94		400 ± 40 (15)	217 ± 60 (15)	34 ± 6 (5)
100% iodide	2.69	380 ± 80	102 ± 40	19 ± 2	2 ± 2

[a] By weight

[b] Mean ± standard deviation (number of data points)

Table 19. Reignition Delay Data for Calcined Mixtures of Potassium Dawsonite and Tin Iodide in the Temperature Range 700 to 900°C.

Composition[a] of calcined solid mixture	Bulk density, g/ml	Calcined KD/SnI_2 mixtures reignition delay data, sec[b]			
		700°C	750°C	800°C	900°C
100% KD	0.87	153 ± 15	81 ± 18	30 ± 6	10 ± 4
1% iodide	1.00		67 ± 9	36 ± 8	10 ± 3
5% iodide	1.07		306 ± 100	116 ± 25	37 ± 6
10% iodide	1.40		500 ± 100	250 ± 40	50 ± 5
20% iodide	1.26		550 ± 50	340 ± 40	53 ± 7
100% iodide	2.69	380 ± 80	102 ± 40	19 ± 2	2 ± 2

[a]By weight

[b]Mean and standard deviation (number of data points)

Since NaD does not show significant performance gain on calcination with tin iodide, perhaps reflecting the "softer" matrix compared to KD (thermogravimetric analyses indicate that NaD decomposes at 240 to 260°C, and KD at 290 to 320°C), we decided to examine calcination effects in KD further, together with calcination procedures in $Al(OH)_3$, AlOOH, and Al_2O_3 matrices. Data in Table 17 also indicated that KI was a more effective additive even than tin iodide, and we have confined this phase of the investigation to KI additives alone. Additional reignition data for various calcined solids are given in Table 20. For comparative purposes, reignition delay data for individual components and for physical mixtures of components are also given. To aid in interpreting Table 20, note that we use the nomenclature "KD + KI" to denote a physical mixture of the two solid components and "KD·KI" to denote the calcined solid obtained by heating both solid components in contact with each other. It should also be noted that the Dawsonites can be synthesized by these high-temperature high-pressure solid-phase reactions (calcination), and that this forms a new, hitherto unreported, method of preparing Dawsonites in high yield product clean processes. In general, we form the KD·KI calcined solid by calcining the correct stoichiometric quantities of $KHCO_3$ and $Al(OH)_3$ in the presence of the requisite weight percent of KI in one step.

The data in Table 20 indicate that KI is an extremely effective additive when calcined with either Al_2O_3 or KD, and additional data were collected for reignition delays induced by KD·KI calcined solids containing varying proportions of KI. These data are shown in Table 21, and for comparison purposes, the Al_2O_3·KI calcined solid with 10% w/w of KI are presented again in the same table. It is apparent that a 10% iodide salt content (ca. 7% iodine content) is reasonably close to an optimum value, and that these two calcined solids (Al_2O_3·KI and KD·KI) form the most effective fire control agents tested by us in this static assemblage.

Table 20. Reignition Delay Data for Various Calcined Solids and Physical Mixtures of Potassium Dawsonite and Aluminum Derivatives With Potassium Iodide.[a]

	Bulk density, g/ml	750°C	800°C	900°C
Aluminum Oxide (Al_2O_3)	1.07	28 ± 12	7 ± 3	zero
Al_2O_3 + KI (mixed solids)	1.14	>900	388 ± 31	14 ± 8
Al_2O_3·KI (calcined solid)	1.18	>900	557 ± 92	50 ± 12
AlOOH ("Boehmite")	1.01	48 ± 25	5 ± 2	zero
AlOOH + KI (mixed solids)				
AlOOH·KI (calcined solid)	1.08	131 ± 7	47 ± 12	15 ± 4
$Al(OH)_3$	1.58	96 ± 15	22 ± 10	3 ± 1
$Al(OH)_3$ + KI (mixed solids)	1.49	233 ± 60	70 ± 7	
$Al(OH)_3$·KI (calcined solid)	1.13	72 ± 3	47 ± 8	8 ± 1
KD	0.87	81 ± 18	30 ± 6	10 ± 4
KD + KI	1.30	548 ± 70	107 ± 13	18 ± 6
KD·KI	1.09	>900	665 ± 44	50 ± 14
KI		100 ± 30	16 ± 6	zero

[a]All mixtures, physical or calcined, contain 10% w/w KI in matrix.

Table 21. Reignition Delay Data for Potassium Dawsonite Calcined With Various Proportions of Potassium Iodide.[a]

	Bulk density, g/ml	750°C	800°C	900°C
KD	0.87	81 ± 18	30 ± 6	10 ± 4
KD·KI (1% calcined solid)	1.09	466 ± 79	87 ± 9	26 ± 2
KD·KI (5% calcined solid)	1.03	>900	332 ± 40	30 ± 4
KD·KI (10% calcined solid)	1.09	>900	665 ± 44	50 ± 14
KD·KI (20% calcined solid)	1.36	>900	>900	54 ± 15
KD·KI (30% calcined solid)	1.36	>900	>900	54 ± 15
Al_2O_3·KI (10% calcined solid)	1.18	>900	557 ± 92	50 ± 12
KD·KI (10% calcined solid)	1.09	>900	665 ± 44	50 ± 14
KI		100 ± 30	16 ± 6	zero

[a]All mixtures, physical or calcined, contain 10% w/w KI in matrix.

These data amply support the hypothesis initially put forward that calcination impedes the loss of fire control additive (in this case, iodine, from a potassium iodide precursor), providing long-term control of the flammable situation by slowly releasing small quantities of the fire control agent through thermal activation. One can thus envisage the situation where the exact properties of an extinguishant can be "tailored" to suit any type of flammable situation. In particular, for large conflagration such as forest fires, large concentrations of the fire control agent are needed initially to provide good knock-down capabilities, since rationally, it is not expected that this type of fire will reignite once extinguished and long-term time control is unnecessary. However, for hot surface or electrically initiated fires in the presence of a continuous fuel source (e.g., engine compartment fires for internal combustion engines), reignition is continuous in the absence of an extinguishant. Thus, the extinguishant should degrade thermally to produce sufficient agent to control the fire, but no more, allowing slow consumption of the extinguishant to provide long-term time control of the flammable environment. It is possible that a second additive may be needed to produce good knock-down capabilities, or that this facet of control can be provided from the matrix carrier itself.

NATURE OF TIN IODIDE DOPED SOLIDS

It is pertinent at this point to comment briefly on the nature of tin iodide doped solids, especially calcined solids. As mentioned above, the commercially supplied tin(II) iodide was found (via X-ray diffraction spectrometry crystal analysis) to contain large and varying proportions of tin(IV) iodide. Tin(II) iodide is particularly sensitive to air oxidation, moisture, and light induced reactions. One point noted early in the investigation was that the physical mixtures of SnI_x with any matrix were distinctively colored (pink to deep orange, depending on concentrations of SnI_x added). After calcination, these solids were virtually colorless. Moreover, TGA (thermogravimetric analysis) of these calcined solids exhibited quite different characteristics to the physical mixtures. After extensive investigation (described in the Appendix) it was found that the calcined solid no longer contained any tin iodide at all, merely an amorphous colorless hydrated tin oxide (stannic acid), and potassium iodide (also colorless). Indeed, in retrospect, the fire control properties of tin iodide doped KD calcined solids mimic quantitatively those of KD·KI calcined solid, as they should, since the presence of KI (quantitative conversion based on tin iodide concentrations) in the calcined solid is now firmly established and quite unambiguous. Thus, the use of tin iodide as a dopant was discontinued immediately, and cannot be recommended in any way for use as a fire control additive, nor will it be considered further.

NATURE OF THE CALCINED SOLID

It was initially proposed that the calcined solid was some form of inorganic crystal clathrate or inclusion complex. However, examination of KD·KI and Al_2O_3·KI by TGA discloses that the properties of the calcined solid are additive properties of the components, and not a distinctive new species. Further, X-ray diffration crystal analysis shows quite unambiguously that the calcined solid is merely an intimate mixture of both components,

and no new crystalline form can be detected. Thus the explanation for the vigorously enhanced fire control properties must lie elsewhere, since the hypothesis of microencapsulation via a new crystal inclusion complex is no longer tenable. However, the concept of reducing the volatility of the additive by the carrier matrix is still acceptable and does provide a good explanation for the observed facts. The exact mechanism of this volatility control is not presently understood, although we can advance one possible explanation for the observed behavior.

In making the calcined solid, as compared to simple mixing of two separate solid phases, and particularly for the situation where KD is synthesized in the presence of KI, an extremely intimate mix of particles is produced. The minor component, KI, will find itself in an environment dominated by KD, and each KI particle will be in excellent thermal contact with a larger molecular total of KD. On warming the whole system, preferential thermolysis will occur for the major component, and since KD decomposition is severely endothermic, little or no heat energy will be available for volatilizing KI and/or thermal activation of KI. Thus, the effect postulated as being essential for long-term control, that of volatility reduction, can equally be accomplished via this "heat-sink" hypothesis, rather than the microencapsulation process envisaged initially. It might be inferred, therefore, that calcination procedures could perhaps be replaced by a process where the dopant is dissolved in a suitable solvent, allowed to wash the carrier matrix (obviously the matrix should be insoluble in the solvent), and then evaporation of the solvent could leave all carrier particles coated with the dopant additive. This procedure, analogous to that used to coat stationary phases onto GLC (gas-liquid chromatography) support materials for GLC columns, has not yet been tried. Further, it is possible that a suitable molecular sieve could be found whose pore size would hold a dopant molecule, or perhaps merely the active (iodide/iodine) moiety of the additive itself. Equally, a polymeric anion exchange substrate loaded with an iodide anion may provide similar volatility reductions, provided that the polymer was nonflammable and thermally stable. These processes might reduce volatility by many orders of magnitude. The remaining adjustments needed for tailoring an exact fire control agent to the situation would be to synthesize a suitable molecular sieve (usually naturally occurring ziolites; e.g., molecular sieve 5A with a 5-angstrom pore size, or M.S. 13X with 10-angstrom pores) or a matrix carrier whose thermal degradation temperature was matched to those of the fire. This process would more closely resemble the microencapsulation concept advanced by us earlier. Data from these approaches are not yet available.

SUMMARY

Static Testing Assemblage

The primary purpose of this investigation was to test various existing dry chemical fire extinguishants, to synthesize new ones where possible, and to provide a preliminary ranking of their effectiveness with regard to fire control (particularly, hot surface initiated fuel fires) prior to dynamic testing procedures and evaluation. A secondary purpose was to

recommend potential systems for further study via a dynamic fire test simulator, and to finally recommend systems compatible with the criteria delineated in a previous section (Choice of Potential Systems). Thus, the fire control chemicals should (see Table 1):

1. Be stable to storage at 260°C (advanced systems) or 120°C (current).

2. Possess no hygroscopic or efflorescent properties leading to weight changes that will exceed 5% of the mass of the powder supplied.

3. Induce a reignition delay in a JP-4 fuel fire of greater than 300 seconds at a hot surface temperature of 800°C, and possess knock-down capabilities for the flame in addition to long-term time control.

To test for storage capabilities at temperatures up to 260°C we have simply tested our solid dry chemicals for resistance to thermal degradation by using TGA techniques. Equally, hygroscopic and efflorescent properties were tested directly by weighing powders before and after exposure to air saturated with water-vapor, and to dry air. We may then extract reignition delay data from Tables 8 through 21, inclusive, and rank them subject to the criteria delineated. In view of the comments given for tin iodide, data for mixtures containing this compound have not been included in this section. We also use the term *MARGINAL* herein to imply that the compound formulated will meet all requirements except storage at 260°C (for advanced systems), but will meet storage requirements for current aircraft (storage to 120°C) rather than those predicted for advanced vehicles.

We have chosen to present our data summary in the form of two tabular presentations:

1. A rank-ordered presentation of all data observed for compounds tested in the static combustion assemblage, ranked according to their performance in controlling a JP-4 fuel fire at a nominal temperature of 800°C as measured by the magnitude of the observed reignition delay induced by a 10g sample (arbitrarily chosen sample size). For convenience, sequences involving varying proportions of an additive have been grouped together. It is possible that one member of one group is out of sequence relative to another member of a group above and/or below it. A certain degree of subjective value judgement has been exercised by the authors in ranking group sequences relative to each other. In the light of comments made concerning tin iodide, data for calcined samples of matrices containing tin iodide have been deleted from consideration, although physical mixtures are presented. These data are presented in Table 22, where we also indicate suitability with respect to both current and advanced specifications for storage as delineated in Table 1.

2. We present data for only those systems that produce a reignition delay of 300 seconds (arbitrarily given limit) or more, and also meet the storage requirements. These data are presented in Table 23.

Table 22. Dry Chemicals Rank-Ordered According to Their Performance in Inducing a Reignition Delay at 800°C and Controlling a JP-4 Fuel Fire.

Rank at 800°C	Dry chemical system[a]		Reignition delay, sec	Storage Sutiability[b]	
				Current, 120°C	Advanced, 260°C
1	KD·KI Calcined Solid	1% iodide	87 ± 9	Yes	Yes
		5% iodide	332 ± 40	Yes	Yes
		10% iodide	665 ± 44	Yes	Yes
		20% iodide	449 ± 32	Yes	Yes
		30% iodide	>900	Yes	Yes
2	Al_2O_3·KI Calcined	10% iodide	557 ± 92	Yes	Yes
3	Al_2O_3 + KI Mixture	10% iodide	388 ± 31	Yes	Yes
4[c]	NaD + SnI_x Mixture	1% iodide	71 ± 7	Marginal	No
		5% iodide	157 ± 16	Marginal	No
		10% iodide	201 ± 30	Marginal	No
		20% iodide	320 ± 65	Marginal	No
		40% iodide	374 ± 45	Marginal	No
		60% iodide	510 ± 90	Marginal	No
		80% iodide	20 ± 4	Marginal	No
5	KD + KI Mixture	1% iodide	24 ± 2	Yes	Yes
		5% iodide	57 ± 9	Yes	Yes
		9% iodide	107 ± 13	Yes	Yes
		20% iodide	155 ± 14	Yes	Yes
6[d]	KD + SnI_x Mixture	1% iodide	89 ± 15	Marginal	No
		5% iodide	162 ± 15	Marginal	No
		10% iodide	113 ± 20	Marginal	No
		17% iodide	143 ± 14	Marginal	No
7	$Al(OH)_3$ + KI Mixture	1% iodide	15 ± 3	Yes	Marginal
		5% iodide	40 ± 4	Yes	Marginal
		10% iodide	70 ± 7	Yes	Marginal
		20% iodide	96 ± 9	Yes	Marginal
8	$Al(OH)_3$·KI Calcined	10% iodide	47 ± 8	Yes	Marginal
9	AlOOH·KI Calcined	10% iodide	47 ± 12	Yes	Marginal
10	$Al(OH)_3$ + SnI_x Solid Mixture	1% iodide	15 ± 2	Yes	Marginal
		5% iodide	30 ± 9	Yes	Marginal
		10% iodide	35 ± 4	Yes	Marginal
11	NaI		90 ± 25	No	No
12	$KHCO_3$ Ansul Corp. "Purple-K®"		38 ± 8	Marginal	No
13	KD		30 ± 6	Yes	Yes
14	K_2CO_3 Ansul Corp.		<30 ± 10>	No	No
15	NaD		29 ± 3	Marginal	No
16	SnI_x		19 ± 2	No	No

Table 22. (Contd.).

Rank at 800°C	Dry chemical system[a]		Reignition delay, sec	Storage Sutiability[b]	
				Current, 120°C	Advanced, 260°C
17	KD + KCl 50% w/w		19 ± 3	Yes	Yes
18	$Al(OH)_3$		18 ± 6	Marginal	No
19	KD + B_2O_3 10% w/w		18 ± 5	Yes	Yes
20	K'		16 ± 6	Yes	Yes
21	$KHCO_3$-Urea[e] I.C.I. Ltd. "Monnex®"		9 ± 2	Marginal	No
	KCl		< 9 ± 4 >	Yes	Yes
22	NaCl		8 ± 3	Yes	Yes
	Na_2WO_4		8 ± 2	Yes	Yes
23	Al_2O_3		7 ± 3	Yes	Yes
24	AlOOH		5 ± 2	Marginal	No
	$SnCl_x \cdot 2H_2O$		< 5 ± 3 >	No	No
	$Na_2WO_4 \cdot 2H_2O$		< 5 ± 3 >	No	No
25	$SnO_x \cdot nH_2O$		< 4 ± 2 >	No	No
	K_3AlF_6		< 4 ± 2 >	Yes	Yes
	H_3BO_3		< 4 ± 2 >	No	No
26	$NH_4H_2PO_4$ Ansul Corp.		< 3 ± 2 >	No	No
	$NH_4H_2PO_4$ PyroChem Corp.		< 3 ± 2 >	No	No
	B_2O_3		3 ± 2	Yes	Yes
	K_2SO_4		< 3 ± 2 >	Yes	Yes
27	CI_4		<zero>	No	No

[a] "KD + KI" implies a mixture, "KD · KI" implies a calcined solid.

[b] As delineated in Table 1.

[c] Subjective judgement exercised by authors in ranking sequences of data.

[d] SnI_x implies unspecified mix of SnI_2 and SnI_4.

[e] A carbamate condensation product between these two species.

In summary, only two systems, KD calcined with KI, and Al_2O_3 calcined with KI, meet the strict requirements delineated by the original terms of the investigation. These systems will be tested experimentally in the dynamic combustion assemblage, and data for these compounds and others will be presented in Section 4.

Table 23. Potential Dry Chemicals That Satisfy the Storage Requirements and Produce a Reignition Delay Greater Than 300 Seconds at 800°C.[a]

Rank at 800°C	Dry chemical system		Reignition delay, sec	Storage sutiability	
				Current, 120°C	Advanced, 260°C
1	KD·KI Calcined Solid	5% iodide	332 ± 40	Yes	Yes
		10% iodide	665 ± 44	Yes	Yes
		20% iodide	449 ± 32	Yes	Yes
		30% iodide	>900	Yes	Yes
2	Al_2O_3·KI Calcined	10% iodide	557 ± 92	Yes	Yes
3	Al_2O_3 + KI Mixture	10% iodide	388 ± 31	Yes	Yes

[a]It is possible that some calcined mixtures of NaD·KI will also meet the criterion of 300 seconds reignition delay time, but NaD is of marginal suitability for current storage requirements and unsuitable for advanced systems.

Section 4

DYNAMIC TESTING WITH SIMULATED AIRFLOW*

To provide further data, over and above those from the static combustion assemblage, and to more closely simulate conditions that would obtain in an aircraft engine nacelle in flight, a second experimental assemblage was designed and built. In this second assemblage, the additional variable of air velocity across the heated plate surface was included, and a design fabricated, that allowed this variable to take values in the range 0 to approximately 50 m/sec. Materials recommended from the static assemblage testing phase, recommended by the Arthur D. Little report, and materials available commercially, were tested in this dynamic assemblage, at air velocities up to ca. 150 ft/sec (36 m/sec), and temperatures of 800°C, with some materials tested at 900°C.

INTRODUCTION

In many of the cited references (References 1–25), some form of dynamic testing prevails. Details given in References 17–19 provided much of the background for the design of our assemblage, and we have designed an assemblage that offers greater dynamic range for the variables involved than in previous such facilities. Moreover, previous investigations have not included any data on the effectiveness of dry chemical extinguishants, but have concentrated on the effects of CO_2 and various Halons.

What was shown by previous investigators was the need for a simple laboratory sized fire simulation system that allowed a combustible fuel to contact and ignite on a heated surface capable of holding the flame at surface airflow speeds that ranged from about 0 to 50 m/sec. A quantity of extinguishant dry chemical, liquid or gas injected well upstream of the active fire, would be carried by the airflow to the heated surface igniting the applied fuel, and would preceed to interfere with the flame reactions causing a fire knock-down. Following knock-down, a successful extinguishant candidate should also inhibit reignition of the fuel by continued interference with the combustion processes. In this latter event, even though fuel continued to be applied to a heated surface which is capable of igniting the fuel at a known airflow over the surface, the ignition/combustion processes would be delayed for as long a period as possible. In subsequent experiments, 20 seconds was selected as a delay time goal, when it became obvious that a combination of the following three factors would preclude reignition at any time beyond this limit (20 seconds) even if the extinguishant was quite ineffective: (1) surface cooling due to evaporating fuel, (2) enhanced surface scouring by the airflow resulting in greater convective heat transfer losses, and

*Funded via NASA-Ames Research Grant NSG-2165 made to Professor Donald J. Myronuk of the Civil Engineering Department of San Jose State University.

(3) the relatively low thermal conductivity of the heated surface material which results in a local lowering of the heated surface temperature to values that would no longer be adequate to ignite the fuel.

The implied experimental approach precludes a catastrophic failure of an engine in a nacelle space, or burn-through of a combustion can leaving a massive flame ignition source, or a continuous high-energy spark capable of igniting virtually any fuel/air mixture. The simulation described in this report would more realistically represent a failed fuel, hydraulic or lubrication fluid line, spewing combustible fluid over heated engine surfaces or frictionally heated wheel/brake assemblages leading to ignition and a potentially disastrous fire. The prime function then of a successful extinguishant candidate used in the nacelle-type fire simulator system was to be able to knock down the initial fire and prevent its reignition for as long a period as possible, even though the combustible fuel/air mixture continues to contact a heated surface capable of causing reignition.

FACILITY CONSTRUCTION

A schematic view of the experimentally evolved dynamic fire simulator system, with a close-up sketch of the heated surface, and multiple flame site generators on the surface, are shown in Figures 31, 32, and 33. The final choice for the nacelle fire simulator heated surface utilized a 1-meter long section of 3-inch Schedule-80 stainless steel pipe internally heated with a propane/air flame. The heater had a separate exhaust system. The upper, outer surface of the pipe was extensively drilled and threaded to accept 1.3-cm diameter threaded rods that projected from the outer surface penetrated 2 cm into the interior of the pipe. Acting as thermally conductive pin fins, the rods help to conduct heat from the hotter regions of the air/propane flame to the outer surface of the stainless steel pipe through the pipe interior insulating boundary layer. Without the interior fins, the relatively low value for the thermal conductivity of stainless steel would allow too rapid a cooling of the exterior upper surface, which mandatorily had to remain hot enough to ignite the fuel applied to the surface. A simple trough and two parallel rods welded to the upper surface served to hold the fuel in intimate contact with the heated surface until the combustion process could be well established, especially at the higher airflows. A combination of exterior projections welded to the pipe, as well as the threaded holes for the pin fins (as opposed to welding the internal fins in place), served to minimize tube warpage due to the enormous thermal stresses which occurred when one-third of the upper periphery of a horizontal red-hot (800°C) tube was being repeatedly sprayed with a cold liquid fuel, as well as being scoured by a high-speed airstream over the upper third of the heated surface. The problem of thermal distortion of the heating surface as well as the containment channels and exhaust ducting was minimized by using smoothly curved sections or surfaces for their strength, while at the same time the sections were laterally supported, but were unconstrained in a longitudinal plane to allow motion of the thermally expanding or contracting parts. Sharp corners, or intersecting flat plates, tended to warp badly to the point of self destruction of welds or materials when temperature variation rates of more than 100°C/sec were experienced.

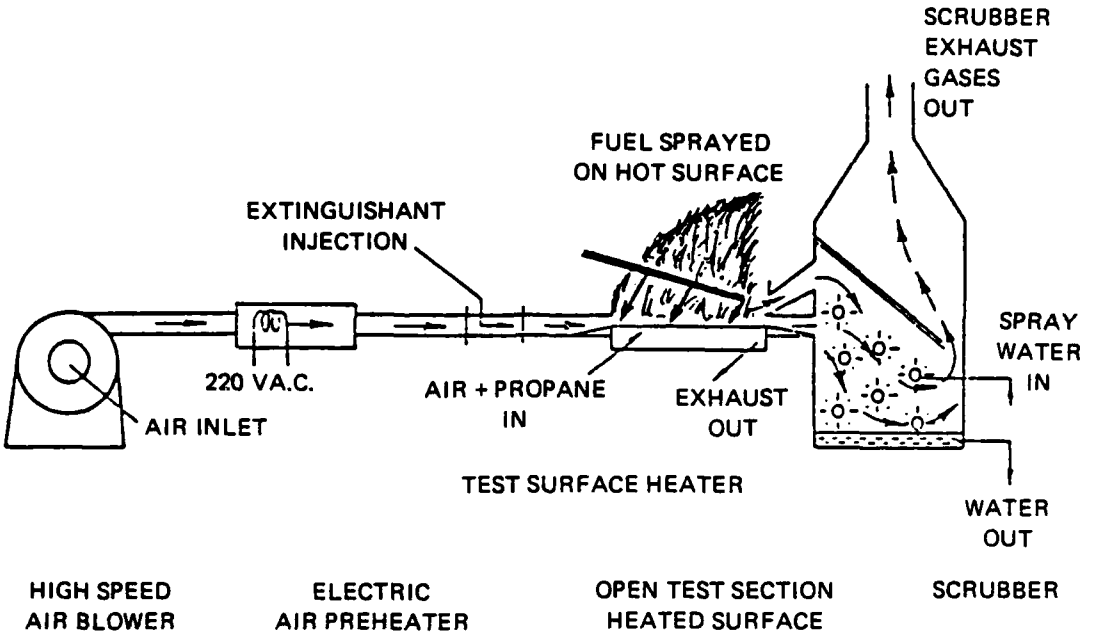

Figure 31. A Schematic Representation of the Dynamic Fire Test Assemblage for Evaluating the Fire Control Performance of Gaseous, Liquid, and Solid Extinguishants.

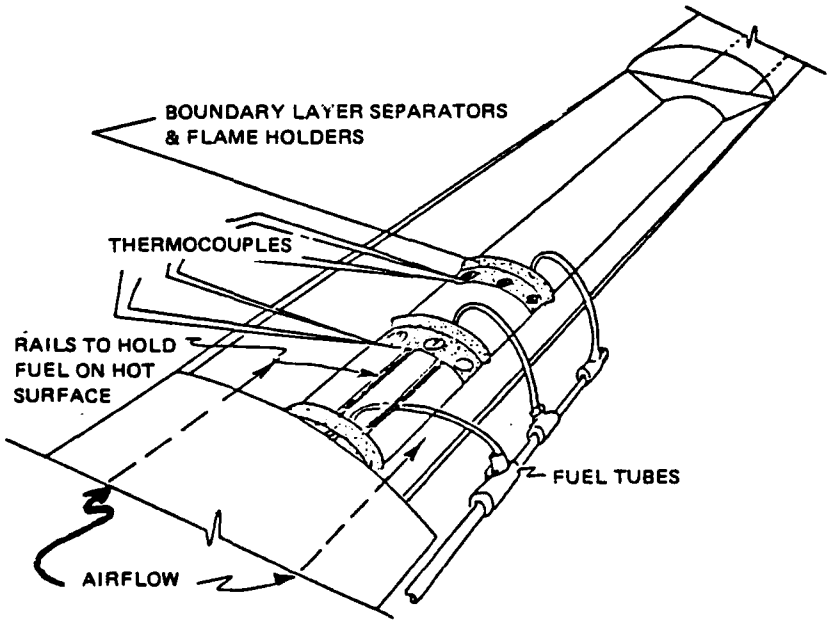

Figure 32. Enlarged View of the Heated Surface and Multiple Ignition Points for the Dynamic Fire Test Assemblage.

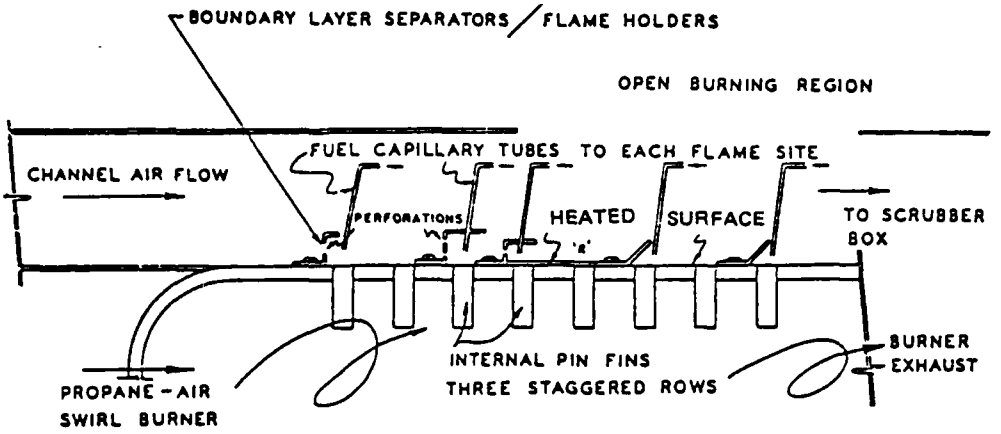

NOTE: Assemblage is approximately 50 cm in length.

Figure 33. Schematic Representation of Heated Ignition Surface Showing Thermal Condition Pins and Boundary Layer Separators for the Multiple Ignition Points.

A major system design problem that was successfully solved involved the selection of appropriate flame holders on the heated surface. When room temperature air velocities were above a few meters per second and flowing over a smooth, visibly red-hot stainless steel surface, it was virtually impossible to ignite the JP-4 fuel by simply spraying it onto the hot surface as a liquid, or as a premixed air/fuel mist. In order to ignite the fuel stream on the heated surface over which air was flowing (without any external spark or open flame source) a stagnation region must be generated in the smooth surface, and a combustible mixture of fuel and air retained in this region. In turn, the air-vapor mixture must be retained in contact with the heated surface until the combustion of the fuel becomes continuous. Sheet metal strips projecting through the boundary layer of the airflow over the heated surface were a simple means of generating mixture stagnation, retention, and ignition zones over the heated surfaces. However, the geometry of such flame holders could range in description from random shards of torn metal or shrapnel, to carefully designed and located reentrant cavities. Each variety could play a very significant role in any subsequent fire extinguishment operation, for if the flame holders were well designed (e.g., reentrant and overlapped, such as downstream-facing cavities or conics) there was no reasonable way to extinguish an established flame without either cutting off the air or fuel supply, or using a great quantity of extinguishant material and flooding the entire fire zone hoping that some of the extinguishant penetrated the stagnation zone. On the other hand, a crude flat or curved sheet metal projection may act as an apparent flame holder on or near a heated surface, especially if a combustible mixture and a source of flame were provided from some other area upstream of the flame holder, or in the neighborhood of the flame holder. However, a vigorous puff of air could blow out the flames, and the inadequate stagnation zone would not allow reignition. In this case, fire knock-down would be immediate; however, chances were the extinguishant played a tiny role in the process, and measurements or observations of relative effects with other extinguishant agents would really have no

meaning. A compromise solution to the problem of flame holder geometry involved a simple reentrant variety with a flap facing downstream, allowing formation of a flame stagnation zone at all test-section channel airspeeds, yet at the same time, it allowed some infiltration of extinguishant material into the stagnation burning zone. Perforations in the boundary layer separators allowed both air and extinguishant to slightly penetrate the cavity formed by the metal strip. Further, the perforation area was of such a value as to provide atmospheric pressure inside the cavity at all airflows over the top of the reentrant stagnation cavity generators. With the modified multiple flame system, the minimum temperature for hot-surface ignition of JP-4 fuel with very low velocity airflows was of the order of 575°C, and ignition occurred within a fraction of a second after application of the fuel to the hot surface.

Initially, a single flame holder on the heated surface in the airstream was used to begin the evaluation of extinguishants. In the subsequent review of 16 mm movie films of the various fire conditions, it was concluded that multiple fire locations would be much more representative of a nacelle fire than a single fuel/fire source. In this latter case, fuel was sprayed into the stagnation region of an appropriate boundary layer interrupter or separator. When an extinguishant agent was applied, fresh, nondecomposed extinguishant would impinge on the single flame region and conditions for successful flame knock-down could be noted. However, a more stringent representative test of knock-down ability would result when there were multiple independent flames combined with an initial extinguishant agent concentration decrease due to agent decomposition in the initial flame, as well as dilution in the open channel of the test section. In the modified fire simulator system, a vigorous flame was established in at least three locations; but in addition, a further stream of fuel was sprayed into the airstream just above the flame rows on the heated surface. While the initial investigation was to involve air flowing at room temperature, a bank of resistance heaters could be used to preheat the flowing airstream, since it has been well established that a fuel can be more easily vaporized in heated air, and hot-surface ignition will then occur more readily than for a cold airstream.

For safety, a scrubber box was built to ingest and remove the flame combustion products, toxic decomposition products of the Halons (HBr, HCl, HF), as well as some dry chemical particulates. In addition, the box water-spray system cooled a potentially explosive fuel/air mixture that was formed in the test section after flame knock-down occurred, and prior to the operator turning off the fuel. A simple water seal, coupled with blowout panels and protective blast screens was designed to provide adequate personnel protection from any minor fuel/air explosion in the scrubber box.

EXPERIMENTAL METHODOLOGIES

The following parameters were experimentally accessible with this dynamic fire testing assemblage:

1. Zero to 50 m/sec airflow velocities at 20°C and 1 atmosphere.

2. Zero to 15 m/sec airflow velocities at 100°C and 1 atmosphere.

3. Zero to 450 g/sec mass flow rates.

4. Stainless steel (Schedule-80 SS-321) heated surface, with 200 cm^2 area, and ambient–1050°C accessible temperature range.

5. Combustible fluids from JP-4, JP-5, Jet-A, Jet-B, and other vehicular fuels, to lubricating and hydraulic fluids, can be used at flow rates up to 250 ml/min at low pressure capillary tube feeds, or 15 to 25 ml/min via spray injection at 6.9 M Pa.

6. Extinguishants can be: powders at 0 to 60 g/sec; liquids at 0 to 100 g/sec; gases at 0 to 100 g/sec.

Specific agents were injected in single bursts, in a sequence of bursts or simultaneously with other solid, liquid, or gaseous agents. Combustion products, extinguishing agent decomposition products (HBr, HCl), and dry chemical particulates were removed by the scrubber box. In the immediate vicinity of the open flame section, some Halon decomposition products escaped to the local atmosphere. Additional ventilation fans prevented these products from diffusing in the room and making contact with operating personnel who normally worked well away from the active burning region of the system. Figure 34 summarizes the general operational parameters for JP-4 burning on a heated stainless steel surface with room temperature air flowing over the heated surface, which is open to the atmosphere. It is believed that these characteristics are representative of general hot-surface ignition of hydrocarbons in a flowing airstream.

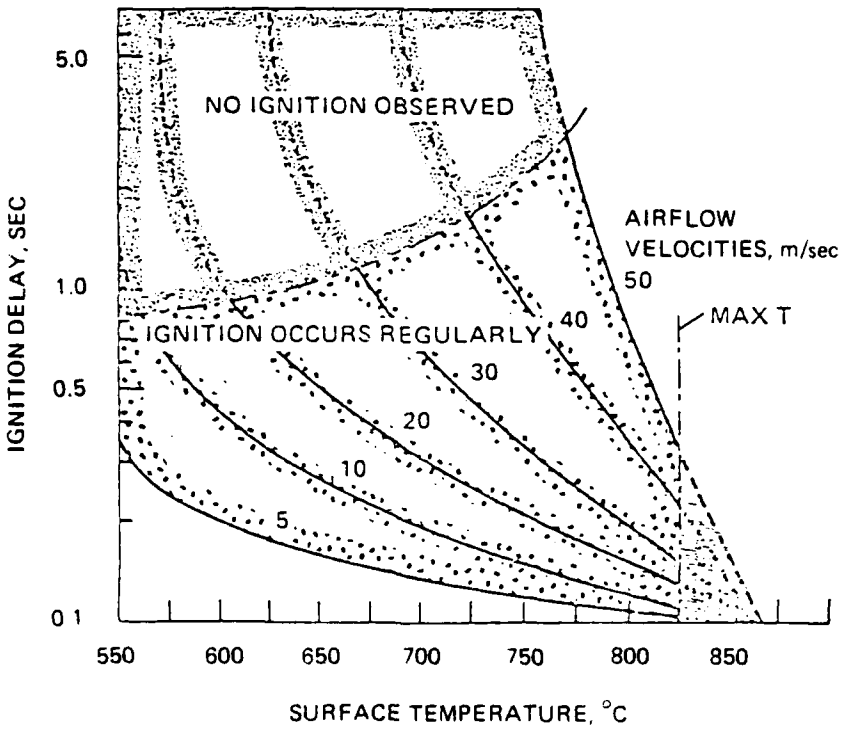

Figure 34. General Operating Parameters for JP-4 Fuel Ignition on a Heated Surface as a Function of Local Air Velocity.

It was noted that the fuel did not ignite immediately upon contacting the heated surface. The liquid first vaporized, and then the air/vapor mixture required adequate contact time with the hot surface before formation of a visible flame was seen to occur. At higher airflow velocities, even with the flame holders generating stagnation regions on the hot surface, the increased surface scouring by the turbulent airflow generating wakes and eddies caused an even greater delay in the ignition of the fuel. Now should ignition be delayed beyond a few seconds at any airflow, a combined effect of local surface cooling due to evaporating fuel as well as the high local airspeed, would cause an additive effect that prevented air/vapor mixtures in the hot-surface boundary layer from ever attaining a threshold ignition temperature, and no self-ignition was observed. With increasing air speeds, higher hot-surface temperatures were required to produce a fire. Finally, ignition temperatures and air velocity relationships became quite independent above 850 to 900°C. At this extreme condition any flame control required continuous applications or single injections of very large quantities of agent.

For this particular simulator system, operational experience has led to the adoption of two parameter values; a fuel flow rate of 250 ml/min (so that excessive quantities of applied evaporating fuel did not cool the entire heated surface to a point where local reignition could not occur), and an arbitrary upper limit to the reignition delay of 20 seconds. In this latter case, the stainless steel surface was cooled by evaporating fuel and surface convection to a point where the surface temperature was no longer capable of igniting the fuel. It is pertinent at this point to comment on this choice of fuel flow rate: liquid fuel was conducted from a pressurized container to the heated surface via capillary tubes, and the fuel released as a liquid into the stagnation region of a boundary layer separator acting as a surface flame holder. In the stagnation zone, film boiling heat transfer effects caused the liquid drops to evaporate, the resulting vapor was mixed with air, and the mixture retained in close contact with the heated surface until combustion occurred. It was possible, by varying the delivery pressure, to deliver from 0 to 1 liter of fuel per minute to the heated surface. However, at 1 l/min, regardless of the chosen airspeed, fuel flooded the heated surface area and either totally quenched the heated surface, or it burned vigorously in the test area, and the downstream channel, and especially in the scrubber box. For lower fuel flow rates (e.g., 100 ml/min) while providing an acceptable reference fire at low airspeeds, at the midrange of system air speeds, the enhanced surface turbulence tended to cause a lean burning condition, and at higher channel airflows, the flame sites were barely able to sustain their local fires. Our choice of 250 ml/min fuel flow rate was an experimentally determined compromise that produced vigorous fires fueled from evaporating fuel patches in the boundary layer separations, and fuel/air mixtures that were not too rich at low airspeeds (6 m/sec) and not too lean at the highest airspeeds (36 m/sec).

It is significant to note that the usual designation of a system air/fuel ratio is no longer applicable when a liquid fuel is being directed onto a heated surface. Should the fuel be vaporized and premixed upstream of the fire sites, then a bulk air/fuel ratio can be descriptive. For example at maximum airflow conditions, with vigorous burning the simulator system had an air/fuel ratio of about 100 to 1, which should be totally nonflammable! In reality, at each flame holder, local conditions of a vaporizing liquid/air interface can be

assumed to exist. Preliminary results also indicated that preheating the airstream to 100 or 200°C had no measureable effect on the hot-surface ignition of the fuel, again attributed to direct channelling of the liquid fuel to the hot surface. If a fuel vapor/air mixture were formed upstream, however, preheating of the air would certainly result in a more stoichiometrically exact fuel/air mixture, which previous studies have shown to be more easily ignited by a hot surface.

Our design, and the intrinsic concept of multiple flame sites proved to be a very important innovation. In real nacelle type fires, the specific location of the fire is not known. However, it is a safe assumption that there would be numerous flame sites in the nacelle space. At best, a cloud of extinguishant could be injected into the intake of the entire nacelle, and it is hoped that a small amount of the extinguishant would penetrate to the flame sites and extinguish them. But an agent which may be successful in knocking down one fire site (and by doing so, be erroneously labled as effective) may be thermally or chemically decomposed by this process, and thus ineffective in knocking down other fires downstream. As a result, the original fire site can be reignited by the unextinguished downstream flames. A more valid test of fire extinguishant capability, in our opinion, is the ability to knock down a sequence of flame sites. The extinguishant performance data of the next section all involves fire control observations for multiple fire sites.

An important aspect of extinguishant performance involves the formation (or lack of it) of a scale on the heated surface as a function of operating surface temperature. Below about 825°C there was very little noticeable surface oxide formation and subsequent spallation (break-up) of the thin oxide layer. However at surface temperatures above 850°C, the oxide layer grows very thick and thermal expansion/contraction stresses and volume expansion stresses result in noticeable spallation. Studies performed by Professor J. K. Tien et. al.* revealed the formation of a thin protective layer of a spinel compound $(FeO)_{0.25}(Cr_2O_3)_{1.75}$ on the surface of austenitic stainless steel (like the heated surface in our fire simulator) at temperatures less than 1500°F (815°C). Surface oxidation was very limited. However, above 1500°F, the spinel fractured and allowed rapid oxidation of the underlying chromium depleted iron-nickel alloy, which resulted in far less protective iron-nickel oxides. For ignition of jet fuels on heated stainless steel, Figure 34, it was noted that a minimum ignition delay was found at the maximum surface oxide spallation condition, regardless of the airspeed over the heated plate surface. Fracture of the oxidation resistant spinel layer was suspected of enhancing the fuel ignition/combustion process via catalytic action, yielding an improved contact opportunity for the fuel on the oxidation prone surface. Subsequent investigations mandated keeping the heated surface at a temperature just below the obvious spallation condition (labelled max T on Figure 34). Obviously, repeated excursions to surface temperatures exceeding 825°C would result in a surface chromium depletion, and a hysteresis effect was noted such that, upon reheating the test surface, higher surface temperatures (25 to 75°C higher) were required to ignite the same fuels on a chromium depleted stainless steel surface. This latter effect was suspected of being caused by the rapid oxidation of the heated surface, followed by the oxides combining with silicon (used as SiO_2 in extinguishant material flow agents) to form relatively adherent coatings on the hot surface ($T > 859$°C). These coatings now protected the surface from further rapid

*Private communication, later published as part of the "Report from the Columbia University School of Engineering and Applied Science and Research", No. 6, June 1973.

oxidation/spallation, as well as interfering with ignition reactions, even after the surface had been cooled and then reheated. These surface accumulations were removed via surface sandblasting during the extinguishant performance comparison tests.

CHOICE OF TEST SYSTEMS

Since the majority of contemporary fire control systems use Halons as their working fluid, we have tested four of these liquid systems and compared their performance directly to gaseous CO_2 injection systems. The four Halons chosen were those used for fire control systems in different countries and different aircraft, and included Halons 1011 (CH_2BrCl), 1202 (CF_2Br_2), 1211 (CF_2BrCl), and 1301 (CF_3Br).

Our choice of dry chemical agents to test depended on recommendations from different sources: (1) systems recommended by data obtained from the Static Test Assemblage, (2) systems available commercially (particularly where they are used for current technology fire control systems), and (3) systems recommended as being particularly effective from data obtained in a similar dynamic fire test assemblage designed, constructed, and operated by the Arthur D. Little Corp. Thus, the dry chemicals tested included the following materials:

1. Potassium bicarbonate based materials such as the Ansul Corp. "Purple-K®", and a special high-density formulation designated as "Ansul-X®".

2. A specially prepared experimental potassium carbonate material commissioned from the Ansul Corp. designed to minimize the hygroscopic properties of K_2CO_3 via a judicious blend of additives.

3. A special potassium bicarbonate-urea condensed polymer (loss of one water molecule per pair of reactant molecules) with an essentially "carbamate" structure marketed by I.C.I. Ltd. under their tradename of "Monnex®".

4. A sodium bicarbonate based material marketed by Ansul Corp.

5. A PyroChem Corp. product based on potassium chloride.

6. A lithium chloride-water eutectic slurry at 0.8/1.0 mole ratio of $LiCl/H_2O$ recommended by the A. D. Little Corp.

7. Potassium iodide, recommended both by A. D. Little and the Static Testing Assemblage data.

8. Potassium Dawsonite based materials, including potassium Dawsonite itself, and this compound doped with 10% w/w of tin iodide, or potassium iodide, were recommended by static testing data.

9. A special formulation of potassium Dawsonite containing 10% w/w B_2O_3 was recommended from the concept of attempting to provide adhesion between the powder and the hot surface in the presence of high local air velocities. Since B_2O_3 melts at ca. 500°C to provide a viscous glassy fluid, it was hoped that this would aid in "sticking" the potassium Dawsonite to the hot surface, keeping it in the presence of the fire, and preventing it from being dislodged from the active zones by >150 ft/sec air velocities.

10. A special formulation of potassium Dawsonite (KD) formed by calcination in the presence of 10% w/w KI was highly recommended by the static testing data, and was tested along with other KD materials.

All powders were tested as received from commercial sources, or as prepared for static testing (details of powder preparation techniques have been given earlier).

PERFORMANCE DATA FOR VARIOUS DRY CHEMICALS

Performance data for various commerically supplied and synthetic/reagent dry chemical fire extinguishants are given in Tables 24 to 38. The majority of chemicals were tested at hot surface temperatures of 800°C, but three compounds (Ansul Corp. K_2CO_3, and reagent grade KI and Li_2CO_3) were tested at 900°C. The choice of these three compounds for special testing procedures was made on the recommendation of data from the A. D. Little Corp. study (for KI and Li_2CO_3), and from data obtained from the dynamic simulator at 800°C which indicated that Ansul Corp. K_2CO_3 was the most effective agent tested. A hot surface at 900°C provides an extreme test of fire control performance (see Static Testing Assemblage data in Section 3), allowing easy differentiation between apparently equivalent systems. A summary of performance data for these materials based on their ability to control multiple JP-4 fuel fires under conditions of high airflow (36 m/sec) at 800°C, and rank-ordered in the listing according to the minimum mass of dry chemical needed to extinguish the flames, is given in Table 39. These data indicate, quite unambiguously, that the comercially prepared K_2CO_3 is superior to commercially prepared $KHCO_3$, and slightly better than the synthetic material obtained by calcining KD with 10% KI. However, this slightly improved performance for the commercial material can easily be accounted for by powder preparation techniques alone, since no special efforts were made to improve either particle size distribution effects, or bulk density effects, in our synthetic material.

Table 24. Performance Data for Ansul Corp. "Purple-K®" Potassium Bicarbonate.

Airflow velocity, m/sec[a]	Shot mass, g[b]	Knock-down observed?[c]	Reignition delay, sec[d]
6	10	No	–
	20	Yes	17.0
	30	Yes	>20.0
16	10	Close[e]	0.5
	20	Yes	6.0
	30	Yes	>20.0
23	10	Close[e]	0.5
	20	Yes	>20.0
	30	Yes	>20.0
36	10	No	–
	20	Close[e]	0.5
	30	Yes	2.0
	40	Yes	10.0
	50	Yes	>20.0

[a] Flow volumes obtained by multiplying by 8.5×10^{-3} m^3/sec.

[b] Ejected with a 1 second burst of compressed gas at 825 kPa (ca. 120 psig).

[c] Multiple flame sites (usually 3).

[d] Time >20 seconds are essentially infinate in length.

[e] See text for explanation of this term.

NOTE: 250 ml/min JP-4 fuel flow to multiple ignition sites. Ambient air (30°C) flows to heated surface at various flow velocities. Stainless steel ignition surface at 800°C.

Table 25. Performance Data for Ansul Corp. "Ansul-X® " Potassium Bicarbonate.

Airflow velocity, m/sec[a]	Shot mass, g[b]	Knock-down observed?[c]	Reignition delay, sec[d]
6	5	Close[e]	0.5
	10	Close	1.0
	20	Yes	>20.0
16	10	No	–
	20	Yes	>20.0
23	10	No	–
	20	Close	1.0
	30	Yes	>20.0
36	10	No	–
	20	Close	0.5
	30	Yes	>20.0

[a] Flow volumes obtained by multiplying by 8.5×10^{-3} m^3/sec.

[b] Ejected with a 1 second burst of compressed gas at 825 kPa (ca. 120 psig).

[c] Multiple flame sites (usually 3).

[d] Time >20 seconds are essentially infinite in length.

[e] See text for explanation of this term.

NOTE: All deposits were easily removed by a wire brush at the conclusion of testing procedures for this compound.

250 ml/min JP-4 fuel flow to multiple ignition sites. Ambient air (30°C) flows to heated surface at various flow velocities. Stainless steel ignition surface at 800°C.

Table 26. Performance Data for Ansul-X JOC Sodium Bicarbonate.

Airflow velocity, m/sec[a]	Shot mass, g[b]	Knock-down observed?[c]	Reignition delay, sec[d]
6	10	No	–
	20	Yes	2.0
	30	Yes	>20.0
16	10	No	–
	20	Close[e]	1.0
	30	Yes	>20.0
23	10	No	–
	20	No	–
	30	Yes	2.0
	40	Yes	>20.0
36	10	No	–
	20	No	–
	30	No	–
	40	No	–
	50	Close	0.5
	60	Yes	>20.0

[a]Flow volumes obtained by multiplying by 8.5×10^{-3} m^3/sec.

[b]Ejected with a 1 second burst of compressed gas at 825 kPa (ca. 120 psig).

[c]Multiple flame sites (usually 3).

[d]Time >20 seconds are essentially infinite in length.

[e]See text for explanation of this term.

NOTE: At higher air velocities there are accumulations of powder in stagnation regions. No flakes or scale appeared to form on the surface, all deposits were easily removed by brushing.

250 ml/min JP-4 fuel flow to multiple ignition sites. Ambient air (30°C) flows to heated surface at various flow velocities. Stainless steel ignition surface at 800°C.

Table 27. Performance Data for Ansul PREP Potassium Carbonate.

Airflow velocity, m/sec[a]	Shot mass, g[b]	Knock-down observed?[c]	Reignition delay, sec[d]
6	5.0	No	–
	7.5	No	–
	10.0	No	–
	20.0	Yes	2
	30.0	Yes	>20
16	5.0	No	–
	7.5	No	–
	10.0	Yes	>20
	20.0	Yes	>20
23	5.0	No	–
	7.5	No	–
	10.0	Yes	>20
	20.0	Yes	>20
36	5.0	No	–
	7.5	Yes	>20
	10.0	Yes	>20
	20.0	Yes	>20

[a] Flow volumes obtained by multiplying by 8.5×10^{-3} m^3/sec.

[b] Ejected with a 1 second burst of compressed gas at 825 kPa (ca. 120 psig).

[c] Multiple flame sites (usually 3).

[d] Time >20 seconds are esstntially infinite in length.

NOTE: 250 ml/min JP-4 fuel flow to multiple ignition sites. Ambient air (30° C) flows to heated surface at various flow velocities. Stainless steel ignition surface at 800° C.

Table 28. Performance Data for I.C.I. "Monnex®" ($KC_2N_2H_3O_3$).[a]

Airflow velocity, m/sec[b]	Shot mass, g[c]	Knock-down observed?[d]	Reignition delay, sec[e]
6	5	Close[f]	0.5
	10	Yes	2.0
	20	Yes	>20.0
16	5	Close	0.5
	10	Yes	Yes
23	5	No	–
	10	Close	0.5
	20	Yes	>20.0
36	5	No	–
	10	No	–
	20	Yes	>20.0

[a] Essentially a carbamate structure.

[b] Flow volumes obtained by multiplying by 8.5×10^{-3} m^3/sec.

[c] Ejected with 1 second burst of compressed gas at 825 kPa (ca. 120 psig).

[d] Multiple flame sites (usually 3).

[e] Time >20 seconds are essentially infinite in length.

[f] See text for explanation of this term.

NOTE: This agent has a bulk volume that is ca. 10% greater than potassium bicarbonate. Small amounts of scale formation were noted on the hot surface, and the residue from testing readily absorbed water. Residue removal was difficult, both on the hot surface, and after cooling to room temperatures.

250 ml/min JP-4 fuel flow to multiple ignition sites. Ambient air (30°C) flows to heated surface at various flow velocities. Stainless steel ignition surface at 800°C.

Table 29. Performance Data for (Pyro-Chem Super-K) Potassium Chloride.

Airflow velocity, m/sec[a]	Shot mass, g[b]	Knock-down observed?[c]	Reignition delay, sec[d]
6	5	No	–
	10	No	–
	20	No	–
	30	Close[e]	0.5
16	5	No	–
	10	No	–
	20	Close	0.5
	30	Yes	>20.0
23	5	No	–
	10	No	–
	20	Yes	>20.0
	30	Yes	>20.0
36	5	No	–
•	10	No	–
	20	No	–
	30	No	–
	40	Close	0.5
	50	Yes	>20.0

[a] Flow volumes obtained by multiplying number by 8.5×10^{-3} m^3/sec.

[b] Ejected with 1 second burst of compressed gas at 825 kPa (ca. 120 psig).

[c] Multiple flame sites (usually 3).

[d] Time >30 seconds are essentially infinite in length.

[e] See text for an explanation of this term.

NOTE: After the test sequence, a glassy residue was noticed in all air stagnation regions on the heated surface. The residue readily dissolved in water and could be removed from the surface with a wire brush.

250 ml/min JP-4 fuel flow to multiple ignition sites. Ambient air (30°C) flows to heated surface at various flow velocities. Stainless steel ignition surface at 800°C.

Table 30. Performance Data for Aqueous Lithium Chloride Slurries.[a]

Airflow velocity, m/sec[b]	Shot mass, g[c]	Knock-down observed?[d]	Reignition delay, sec[e]
6	10	No	–
	20	No	–
	30	No	–
	40	No	–
	50	No	–
	60	No	–
16	10	No	–
	20	No	–
	60	No	–
23	10	No	–
	20	No	–
	60	No	–
36	10	No	–
	20	No	–
	30	No	–
	40	No	–
	50	No	–
	60	No	–

[a](0.8:1.0 $LiCl/H_2O$).

[b]Flow volumes obtained by multiplying number by 8.5×10^{-3} m^3/sec.

[c]Ejected with a 1 second burst of compressed gas at 825 kPa (ca. 120 psig).

[d]Multiple flame sites (usually 3).

[e]Time >20 seconds are essentially infinite in length.

NOTE: A white "cakey" residue remains on all of the cooler parts of the system, none on any of the hot surfaces.

250 ml/ min JP-4 fuel flow to multiple ignition sites. Ambient air (30°C) flows to heated surface at various flow velocities. Stainless steel ignition surface at 800°C.

Table 31. Performance Data for Potassium Dawsonite (Ames Research Center Prep).

Airflow velocity, m/sec[a]	Shot mass, g[b]	Knock-down observed?[c]	Reignition delay, sec[d]
6	5	No	–
	10	No	–
	20	Close[e]	0.5
	30	Yes	>20.0
16	5	No	–
	10	No	–
	15	Yes	2.0
	20	Yes	>20.0
23	5	No	–
	10	No	–
	20	No	–
	30	Yes	>20.0
36	5	No	–
	10	No	–
	20	No	–
	30	Close	0.5

[a] Flow volumes obtained by multiplying number 8.5×10^{-3} m^3/sec.

[b] Ejected with a 1 second burst of compressed gas at 825 kPa (ca. 120 psig).

[c] Multiple flame sites (usually 3).

[d] Time >20 seconds are essentially infinite in length.

[e] See text for explanation of this term.

NOTE: 250 ml/min JP-4 fuel flow to multiple ignition sites. Ambient air (30°C) flows to heated surface at various flow velocities. Stainless steel ignition surface at 800°C.

Table 32. Performance Data for Potassium Dawsonite + B_2O_3 (10%).

Airflow velocity, m/sec[a]	Shot mass, g[b]	Knock-down observed?[c]	Reignition delay, sec[d]
6	5	No	–
	10	No	–
	15	No	–
	20	Close[e]	0.5
	20 (repeat)	Yes	>20.0
16	5	No	–
	10	No	–
	15	No	–
	20	Yes	>20.0
23	5	No	–
	10	No	–
	15	No	–
	20	No	–
	30	Close	0.1
36	10	No	–
	20	No	–
	30	No	–
	30 (repeat)	Yes	>20.0

[a]Flow volumes obtained by multiplying number 8.5 x 10^{-3} m^3/sec.

[b]Ejected with a 1 second burst of compressed gas at 825 kPa (ca. 120 psig).

[c]Multiple flame sites (usually 3.).

[d]Times >20 seconds are essentially infinite in length.

[e]See text for explanation of this term.

NOTE: No visible surface deposits or surface wetting was apparent at 800°C. On cooling the small glassy remains of B_2O_3 could be seen; these were very tenacious deposits and extremely difficult to remove, even by vigorous scraping. Glassy deposits were only really evident when >20g shot masses were used.

250 ml/min JP-4 fuel flow to multiple igntiion sites. Ambient air (30°C) flows to heated surface at various flow velocities. Stainless steel ignition surface at 800°C.

Table 33. Performance Data for Potassium Dawsonite Containing SnI_2 and KI.

Airflow velocity, m/sec[a]	Shot mass, g[b]	Knock-down observed?[c]	Reignition delay, sec[d]
6	5	No	–
	10	Close[e]	0.5
	15	Yes	2.0
	15 repeat	Yes	>20.0
16	5	No	–
	10	Close	0.5
	15	Yes	>20.0
23	5	No	–
	10	No	–
	15	Close	0.5
	20	Yes	>20.0
36	5	No	–
	10	No	–
	15	Close	0.5
	20	Yes	>20.0

[a] Flow volumes obtained by multiplying number by 8.5×10^{-3} m^3/sec.

[b] Ejected with a 1 second burst of compressed gas at 825 kPa (ca. 120 psig).

[c] Multiple flame sites (usually 3).

[d] Time >20 seconds are essentially infinite in length.

[e] See text for explanation of this term.

NOTE: 250 ml/min JP-4 fuel flow to multiple ignition sites. Ambient air (30°C) flows to heated surface at various flow velocities. Stainless steel ignition surface at 800°C.

AD-A174 406 DEVELOPMENT AND TESTING OF DRY CHEMICALS IN ADVANCED EXTINGUISHING SYSTEM (U) SAN JOSE STATE UNIV CALIF R L ALTMAN ET AL FEB 83 JTCG/AS-82-T-002 2/3

UNCLASSIFIED NCA2-OR675-806/NSG-2165 F/G 13/12 NL

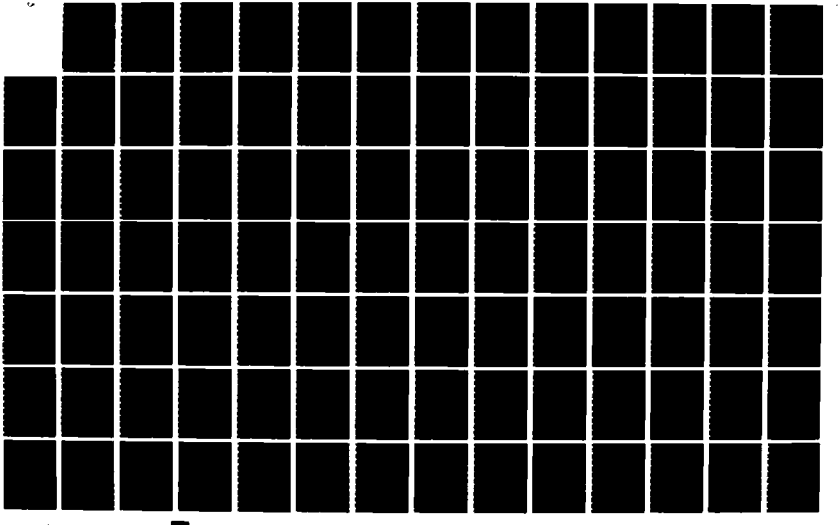

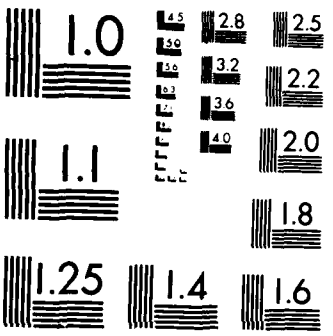

MICROCOPY RESOLUTION TEST CHART
NATIONAL BUREAU OF STANDARDS-1963-A

Table 34. Performance Data for Potassium Dawsonite + KI (10%).

Airflow velocity, m/sec[a]	Shot mass, g[b]	Knock-down observed?[c]	Reignition delay, sec[d]
6	5	No	–
	10	Close[e]	0.5
	15	Yes	>20.0
16	5	No	–
	10	No	–
	15	Close	0.5
	20	Yes	>20.0
23	5	No	–
	10	No	–
	15	No	–
	20	Yes	>20.0
36	5	No	–
	10	No	–
	15	Close	0.5
	20	Yes	>20.0

[a] Flow volumes obtained by multiplying number by 8.5×10^{-3} m^3/sec.

[b] Ejected with 1 second burst of compressed gas at 825 kpa (ca. 120 psig).

[c] Multiple flame sites (usually 3).

[d] Time >20 seconds are essentially infinite in length.

[e] See text for explanation of this term.

NOTE: 250 ml/min JP-4 fuel flow to multiple ignition sites. Ambient air (30°C) flows to heated surface at various flow velocities. Stainless steel ignition surface at 800°C.

Table 35. Performance Data for Potassium Dawsonite·KI (10%).

Airflow velocity, m/sec[a]	Shot mass, g[b]	Knock-down observed?[c]	Reignition delay, sec[d]
6	5	No	–
	10	Close[e]	0.5
	15	Yes	1.0
	20	Yes	>20.0
16	5	No	–
	10	No	–
	15	Yes	>20.0
23	5	No	–
	10	Close	0.5
	10 (repeat)	Yes	>20.0
	15	Yes	>20.0
36	5	No	–
	10	Close	0.5
	10 (repeat)	Yes	>20.0
	15	Yes	>20.0

[a] Flow volumes obtained by multiplying number by 8.5×10^{-3} m^3/sec.

[b] Ejected with a 1 second burst of compressed gas at 825 kPa (ca. 120 psig).

[c] Multiple flame sites (usually 3).

[d] Time >20 seconds are essentially infinite in length.

[e] See text for explanation of this term.

NOTE: Even though material contained significant quantities of KI, no visible surface deposits or corrosion effects were noted.

250 ml/min JP-4 fuel flow to multiple ignition sites. Ambient air (30°C) flows to heated surface at various flow velocities. Stainless steel ignition surface at 800°C.

Table 36. Performance Data for Sodium Carbonate (Arc Prep).

Airflow velocity, m/sec[a]	Shot mass, g[b]	Knock-down observed?[c]	Reignition delay, sec[d]
6	10	No	–
	20	Close[e]	0.1
	30	Close	0.5
16	10	No	–
	20	No	–
	30	Close	0.5
23	10	No	–
	20	Close	0.5
	20	No	–
	30	Close	0.5
36	20	No	–
	30	No	–
	40	No	–

[a] Flow volumes obtained by multiplying number by 8.5×10^{-3} m^3/sec.

[b] Ejected with a 1 second burst of compressed gas at 825 kPa (ca. 120 psig).

[c] Multiple flame sites (usually 3).

[d] Time >20 seconds are essentially infinite in length.

[e] See text for explanation of this term.

NOTE: 250 ml/min JP-4 fuel flow to multiple ignition sites. Ambient air (30°C) flows to heated surface at various flow velocities. Stainless steel ignition surface at 900°C.

Table 37. Performance Data for Potassium Iodide (Arc Prep).

Airflow velocity, m/sec[a]	Shot mass, g[b]	Knock-down observed?[c]	Reignition delay, sec[d]
6	10	No	–
	20	No	–
	30	No	–
	40	Close[e]	0.5
16	10	No	–
	20	No	–
	30	No	–
	40	Close	0.1
23	10	No	–
	20	No	–
	30	No	–
	40	Close	0.1
36	10	No	–
	20	No	–
	30	No	–
	40	No	–

[a] Flow volumes obtained by multiplying number by 8.5×10^{-3} m^3/sec.

[b] Ejected with a 1 second burst of compressed gas at 825 kPa (ca. 120 psig).

[c] Multiple flame sites (usually 3).

[d] Time >20 seconds are essentially infinite in length.

[e] See text for explanation of this term.

NOTE: 250 ml/min JP-4 fuel flow to multiple ignition sites. Ambient air (30°C) flows to heated surface at various flow velocities. Stainless steel ignition surface at 900°C.

Table 38. Performance Data for Lithium Carbonate (Arc Prep).

Airflow velocity, m/sec[a]	Shot mass, g[b]	Knock-down observed?[c]	Reignition delay, sec[d]
6	10	No	–
	20	No	–
	30	Close[e]	0.5
	40	Close	0.5
16	10	No	–
	20	No	–
	30	No	–
	40	No	–
23	10	No	–
	20	No	–
	30	No	–
	40	Close	0.5
36	10	No	–
	20	No	–
	30	No	–
	40	No	–

[a] Flow volumes obtained by multiplying number by 8.5×10^{-3} m^3/sec.

[b] Ejected with a 1 second burst of compressed gas at 825 kPa (ca. 120 psig).

[c] Multiple flame sites (usually 3).

[d] Time >20 seconds are essentially infinite in length.

[e] See text for explanation of this term.

NOTE: 250 ml/min JP-4 fule flow to multiple ignition sites. Ambient air (30°C) flows to heated surface at various flow velocities. Stainless steel ignition surface at 900°C.

Table 39. Rank-Ordered Listing of Dry Chemical Fire Extinguishants According to Their Performance in the Dynamic Simulator Fire Test Assemblage.

Rank	Material	Source	Mass needed, g	Comments
1	K_2CO_3	Ansul Corp.	7.5	Hygroscopic, required >40g at 900°C, experimental system.
2	KD·KI	Synthetic material[a]	10.0	Calcined KD with 10% w/w KI
3	"Carbamate"	I.C.I. "Monnex®"	15.0	$KHCO_3$-Urea condensed polymer
4	KD + KI KD + SnI_x[b]	Reagents/Synthesis Reagents/Synthesis	17.0 17.0	10% w/w KI mixed with KD 10% w/w SnI_x mixed with KD
5	$KHCO_3$ $KHCO_3$	Ansul "Purple-K®" Ansul "X®"	25.0 25.0	Special high bulk density formulation of "Purple-K®"
6	KD + B_2O_3	Reagents/Synthesis	30.0	B_2O_3 added to assist KD in adhering to heated plate
7	KD	Synthesis	35.0	
8	KCl	PyroChem Corp.	45.0	
9	$NaHCO_3$	Ansul Corp.	55.0	
10	$LiCl/H_2O$ Slurry	Reagents	>60.0	Recommended by A. D. Little Corp. at 0.81/1.0 mole ratio $LiCl/H_2O$
X	Li_2CO_3	Reagents	>40.0	Only tested at 900°C, recommended by A. D. Little Corp.
Y	KI	Reagents	>40.0	Only tested at 900°C, recommended by both A. D. Little Corp. and Static Testing Assemblage

[a] Synthetic materials prepared as indicated in previous section.

[b] Tin(II) iodide purchase from commercial sources was found to be significantly contaminated with tin(IV) iodide.

250 ml/min JP-4 fuel flow to multiple ignition sites. Ambient air (30°C) flows to heated surface at various flow velocities. Stainless steel ignition surface at 800°C.

Rank estimated from data in previous tables, and based on the minimum quantity of material needed to produce "knock-down" at the highest airflow velocity used for testing.

DISCUSSION OF DRY CHEMICAL PERFORMANCE DATA

An attempt was made to quantify the relative agent performances via an EEF (extinguishant effectiveness factor). The EEF was the numerical product of reignition delay time in seconds; inverse mass of agent injected in grams^{-1}; and an arbitrary knock-down factor whose value on a scale of 1 to 10 depended on the ability to initially knock down the multiple flame sites. No knock-down ability was assigned a value of 1, complete knock down a value of 10, and what evolved as an "almost" or "close to" flame removal situation was given a value of 5 for this arbitary factor.*

The mass injected was controlled at 5, 10, 15, 20, 30, 40, 50, and 60g, no attempt was made to make further divisions (e.g., 7 1/2g), hence an "almost" situation evolved when it was generally agreed by observers that, while 10g of agent did not achieve flame knock-down, flame intensity and/or visibility was marked by reduced, such that perhaps as little as an extra gram of agent would have achieved complete flame knock-down. In every case the dry chemical injection period was 1 second with dry nitrogen injection pressures of 825 kPa (about 120 psig).

With regard to the values calculated for this EEF factor, the longest reignition delay time would be 20 seconds; the shortest observed time for momentary loss of visible flame was 0.5 second; and a lower bound delay time value for any agent effects at all on the flame (decreased intensity, some visible flame size reduction) was assigned a simiarbitrary value of 0.1 second. Hence for 5g of any agent, the maximum EEF calculated would be 40 corresponding to the relationship:

$$EEF = \frac{(20 \text{ seconds max delay}) \times (\text{knock-down factor} = 10)}{(5\text{g injected})} = 40$$

while for a minimally effective agent, a value of 0.02 for our EEF would be obtained, i.e.:

$$EEF = \frac{0.1 \text{ second min delay} \times (\text{knock-down factor} = 1)}{5\text{g injected}} = 0.02$$

If a plot is made of EEF values against reciprocal mass needed to control multiple JP-4 fuel fires at each air velocity across the plate, then an observed trend upwards and to the right indicates the more effective fire control agents. We have taken the mean data for each compound and plotted their calculated EEF values against reciprocal minimum mass (in g^{-1}) needed to control the fires set in our Dynamic Testing Assemblage, these data are shown in Figure 35. What emerges from Figure 35 is a behavior pattern that emphasizes the desirable features sought in an effective fire extinguishant, namely, the ability of a small amount of agent to extinguish and control (inhibitation) multiple location JP-4 fuel fires ignited via a hot surface.

*This situation is described as "Close" in all data tables (Tables 24 to 38), and a corresponding reignition delay of either 0.1 or 0.5 second appears alongside this descriptive term.

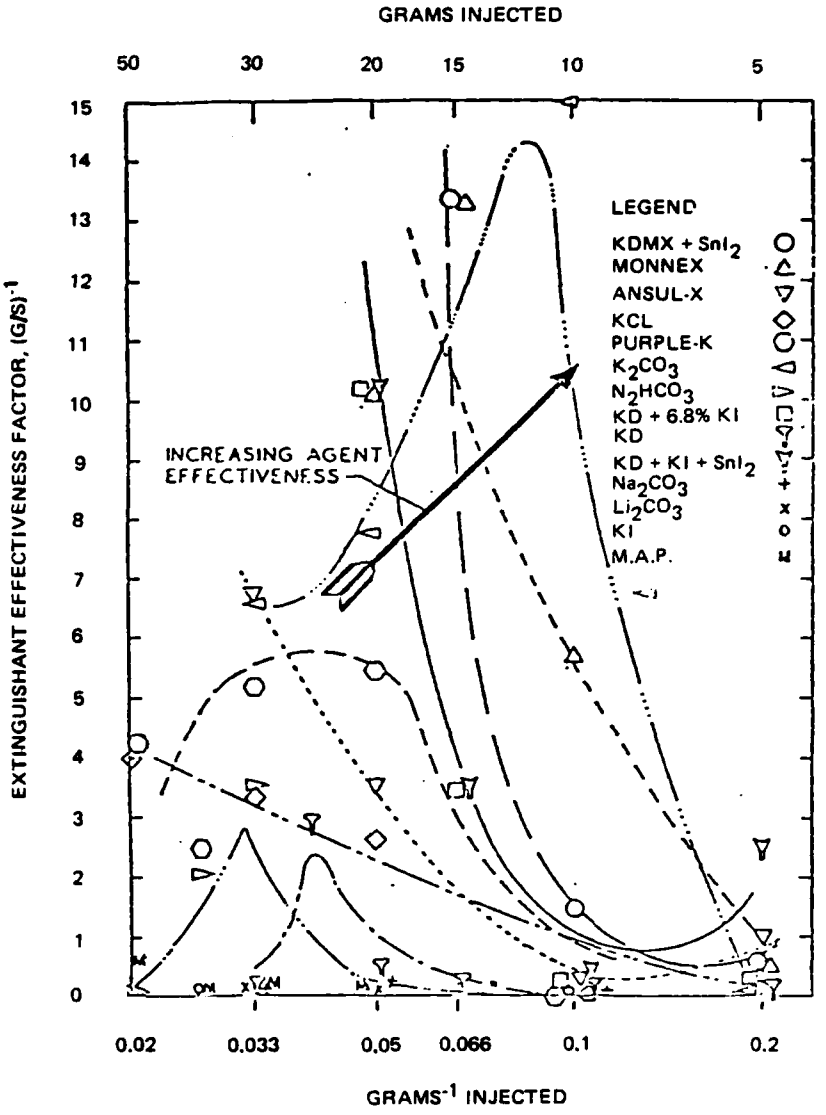

Figure 35. Relative Extinguishant Performance for Some Dry Chemicals Tested in the Dynamic Fire Test Assemblage.

The test program did not involve studies of other factors relevant to a desirable extinguishant, such as corrosion problems with the agent or its decomposition products, long term storability and thermal decomposition, compaction during storage, flow properties at high and low temperatures, pressure, and humidity conditions, and any adverse biological effects attributable to the use of the particular agent at the site of the fire, or in loading/servicing any engineering system needed to inject the agent. Agents which brought

about premature failure of the unsheathed "Chromel-Alumel" thermocouple leads heated to incandescence by the initial fire stream, or left tenacious surface deposits, or residues which made surface cleanup difficult, were noted. Examples were KCl, K_2CO_3 and $KHCO_3$ based agents. On the other hand, a few noncommercial agents, notably some Dawsonite compounds, were easily brushed off the heated surface after suppressing the controlled fires. Thus, corrosion problems of engine surfaces will be minimized for these latter reagents. The limited extinguishant abilities of potassium chloride, and to an even lesser extent potassium iodide, lithium carbonate, sodium bicarbonate and sodium carbonate, are reflected in their low EEF values. At the same time, potassium carbonate, K_2CO_3, appeared to work well at lower values of mass injected; and it is interesting to note that injecting increased quantities of material did not enhance the initial excellent fire suppression performance (plateau effect similar to that noted in the Static Testing Assemblage). The potassium bicarbonate based agent, "Ansul-X®", demonstrated a similar trend, whereas nominally similar chemically based agents, "Purple-K®" and "Monnex®", appeared to function more effeciently at high mass injections. These latter commercial extinguishing agents became reference standards of performance for new formulations.

One of the experimental candidates, Potassium Dawsonite (KD), described in the earlier sections of this report, showed great promise in the Static Testing Assemblage although it was considerably less impressive under more dynamic test conditions. The KD performance was markedly improved by the addition of small quantities of potassium iodide or tin iodide. The EEF values for the KD plus tin iodide shown in Figure 35 confirmed its effectiveness as a potential fire control agent. Further, despite the addition of iodide compounds, the KD agent maintained its overall noncorrosive performance and relative ease of cleanup of the heated surfaces.

PERFORMANCE DATA FOR VARIOUS HALONS

Fire control performance as measured by the magnitude of the observed reignition delay for Halon 1011, 1202, 1211, and 1301, are given in Tables 40, 41, 42, and 43, respectively. For comparative purposes, similar test data for carbon dioxide are given in Table 44. More complete experimental data are available for Halon 1301, but even for this compound they are insufficient for reliable interpolation of the data to be used. Nevertheless, bearing in mind the incomplete state of the data arrays presented, we can use the data from the more extreme testing conditions at 36 m/sec airflow (and secondarily from 23 m/sec airflow studies), to provide a measure of the relative effectiveness of each compound. Examining these data in Tables 40 to 43, we can device an approximate and partly subjective rank-ordering of these four Halons with respect to their fire control capabilities via the minimum mass that will produce a so-called "infinite" delay (defined as greater than 20 seconds) at airflow velocities of 36 m/sec. Where these data indicate approximately equal masses for two compounds, then a second criterion based on weight effectiveness is used. Where these criteria are still insufficient, or where reinforcement of our partly subjective rank-ordering presented are needed, then resort is made to the data recorded at 23 m/sec airflow velocities. In this manner, we have managed to rank the four Halons in fire control effectiveness, and these data are shown in Table 45. It should be noted that the data given in

Table 45 (taken from Tables 40 to 44) has been corrected to the nearest 5g unit of mass, and to the nearest 0.5% unit of volume-percent mixture. Moreover, because of the paucity of data at intermediate points, for example, for Halon 1011, the value listed for 36 m/sec airflow of "less than 60g and less than 3.5%" could mean 59g and 3%, or it could mean as little as 10g and 1%. If this latter situation obtained, then Halon 1011 will be *the* most effective Halon of the four tested. However, the statement "greater than 5.5%" at 23 m/sec airflow for Halon 1011 is used to justify the position of Halon 1011 as Number Four in the ranking. Similarly, Halon 1202 is justifiably Number One in this ranking, from airflow data at both 36 and 23 m/sec. Nevertheless, the data for Halons 1211 and 1301 are ambiguous, and more experimental work is needed to clearly distinguish between these two compounds.

Table 40. Performance Data for Halon 1011 (CH_2BrCl).[a]

Airflow velocity, m/sec[b]	Shot mass size[c]		Knock-down observed?[d]	Reignition delay, sec[e]
	Volume, percent mixture	Grams injected		
6	11.8	38.6	Yes	2
16	6.1	55.6	Yes	1
23	5.3	60.0	Yes	>20
36	3.6	60.0	Yes	>20

[a] Molecular weight 129.4; boiling point 67°C; specific gravity 1.93.

[b] Flow volumes obtained by multiplying number by 8.5×10^{-3} m^3/sec.

[c] A 1 second pulse of nitrogen gas used to atomize Halon.

[d] Multiple flame sites (usually 3).

[e] >20 seconds are essentially infinite reignition delays.

NOTE: 250 ml/min JP-4 fuel flow to multiple ignition sites. Ambient air (30°C) flows to heated surface at various flow velocities. Stainless steel ignition surface at 800°C.

Table 41. Performance Data for Halon 1202 (CF_2Br_2).[a]

Airflow velocity, m/sec[b]	Shot mass size[c]		Knock-down observed?[d]	Reignition delay, sec[e]
	Volume, percent mixture	Grams injected		
6	4.3	21.0	Yes	2
16	1.7	24.5	Yes	1
23	1.6	28.5	Yes	>20
36	1.5	39.9	Yes	>20

[a] Molecular weight 209.8; boiling point 24°C; specific gravity 2.28.

[b] Flow volumes obtained by multiplying number by 8.5×10^{-3} m^3/sec.

[c] A 1 second pulse of nitrogen gas used to atomize Halon.

[d] Multiple flame sites (usually 3).

[e] >20 seconds are essentially infinite reignition delays.

NOTE: 250 ml/min JP-4 fuel flow to multiple ignition sites. Ambient air (30°C) flows to heated surface at various flow velocities. Stainless steel ignition surface at 800°C.

Table 42. Performance Data for Halon 1211 (CF_2BrCl).[a]

Airflow velocity, m/sec[b]	Shot mass size[c]		Knock-down observed?[d]	Reignition delay, sec[e]
	Volume, percent mixture	Grams injected		
6	6.0	24.0	Yes	2
16	2.8	32.0	Yes	1
23	2.6	37.0	Yes	1
36	1.9	40.0	Yes	>20

[a] Molecular weight 165.4; boiling point -3°C; specific gravity 1.83.

[b] Flow volumes obtained by multiplying number by 8.5×10^{-3} m^3/sec.

[c] A 1 second pulse of nitrogen gas used to atomize Halon.

[d] Multiple flame sites (usually 3).

[e] >20 seconds are essentially infinite reignition delays.

NOTE: 250 ml/min JP-4 fuel flow to multiple ignition sites. Ambient air (30°C) flows to heated surface at various flow velocities. Stainless steel ignition surface at 800°C.

Table 43. Performance Data for Halon 1301 (CF_3Br).[a]

Airflow velocity, m/sec[b]	Shot mass size[c]		Knock-down observed?[d]	Reignition delay, sec[e]
	Volume, percent mixture	Grams injected		
6	2.6	8.6	No	–
	9.5	34.5	Yes	2
	15.5	60.0	Yes	3
	20.0	83.0	Yes	4
16	0.9	8.6	No	–
	3.6	34.5	Yes	2
	6.0	60.0	Yes	2
	8.2	83.0	Yes	3
23	0.7	8.6	No	–
	2.8	34.5	No	–
	4.7	60.0	Yes	>20
	6.4	83.0	Yes	>20
36	1.8	34.5	No	–
	3.2	60.0	Yes	>20
	4.3	83.0	Yes	>20
	5.3	104.0	Yes	>20

[a] Molecular weight 148.9; boiling point 72°C; specific gravity 1.57. After continued injection, noticeable scale build up on the hot surface (propably iron bromide). This Halon is stable to 800°C.

[b] Flow volumes obtained by multiplying number by 8.5×10^{-3} m^3/sec.

[c] A 1 second pulse of nitrogen gas used to atomize Halon.

[d] Multiple flame sites (usually 3).

[e] >20 seconds are essentially infinite reignition delays.

NOTE: 250 ml/min JP-4 fuel flow to multiple ignition sites. Ambient air (30°C) flows to heated surface at various flow velocities. Stainless steel ignition surface at 800°C.

Table 44. Performance Data for Carbon Dioxide.

Airflow velocity, m/sec[a]	Shot mass size[b]		Knock-down observed?[d,e]	Reignition delay, sec[f]
	Volume, percent mixture	Grams[c] injected		
1.5	50	24.8	Yes	–
3	34	24.8	No	–
6	20	24.8	No	–
16	10	24.8	No	–
23	7	24.8	No	–
36	5	24.8	No	–

[a]Flow volumes obtained by multiplying number by 8.5×10^{-3} m^3/sec.

[b]A 1 second pulse of nitorgen gas used to atomize Halon.

[c]Continuous injection rate of 24.8 g/sec into flow stream.

[d]Multiple flame sites (usually 3).

[e]Continuous suppression only as long as CO_2 gas flow maintained.

[f]>20 seconds are essentially infinite reignition delays.

NOTE: 250 ml/min JP-4 fuel flow to multiple ignition sites. Ambient air (30°c) flows to heated surface at various flow velocities. Stainless steel ignition surface at 800°C.

Table 45. A Rank-Ordered Listing of Halons According to Their Performance as Fire Control Agents in the Dynamic Fire Test Assemblage.

Rank	Material	Minimum mass needed, g		Equivalent minimum volume, %[a]	
		23 m/sec	36 m/sec	23 m/sec	36 m/sec
1	Halon 1202 CF_2Br_2	<30	<40	<1.5	<1.5
2[b]	Halon 1211 CF_2BrCl	>35	<40	>2.5	<2.0
2[b]	Halon 1301 CF_3Br	<60	<60	<4.5	<3.0
4	Halon 1011 CH_2BrCl	<60	<60	<5.5	<3.5
	Carbon dioxide	>25	>25	>7.0	>5.0

[a]Needed to produce a greater than 20 second reignition delay.

[b]Ambiguous ranking, data does not allow sufficient distinction.

NOTE: 250 ml/min JP-4 fuel flow to multiple flame sites. Local air velocities across heated plate surface at 23 and 36 m/sec. Stainless steel hot-surface ignition source at 800°C.

DISCUSSION OF HALON PERFORMANCE DATA

In general, gaseous agents, or well atomized liquid Halon extinguishants, demonstrated only slight ability to prevent reignition of the fuel after initial fire knock-down has been achieved, although knock-down capabilities are good. This reflects directly the enormous dilution effects caused by the airstreams crossing the heated surface. The agents were injected into the flowing airstream of the dynamic simulator, well upstream of the fire sites. As a function of agent container pressure, a calibrated quantity of material was delivered to a cylindrical injector pipe whose axis was parallel to the airflow and directed downstream. Prior to release of the agent, a pulse of nitrogen gas at 700 kPa (100 psi) was used to atomize the liquid agent stream, and allow good mixing of the agent and nitrogen. Nigrogen flow began 0.2 second before the liquid flow, and continued 0.2 second after the agent flow was terminated at the solenoid valve. The quantity of nitrogen gas used did not have any observable effect by itself on the fire sites. However, a most interesting effect was noted that involved the magnitude of the nitrogen atomization pulse pressure and the performance of the various agents. Specifically, the nitrogen pulse driving pressures varied from 350 to 2000 kPa (50 to 300 psi) and a measurable change in agent performance could be observed. For 1211 and 1202, the best extinguishant performance occurred with an atomization pressure of about 700 to 900 kPa, respectively; while Halons 1011 and 1301 were about 25% more weight effective at about twice these atomization pulse pressures. On the other hand at higher nitorgen pressures, 1000 to 2000 kPa, the Halon 1211 weight effectiveness decreased by at least 10 to 15% (i.e., more agent was required to knock down the reference fires when the nitrogen pulse pressure was raised to 1500 kPa). For Halon 1202, a higher nitrogen-pulse pressure of about 900 kPa appeared to be the most effective for flame knock-down. For even higher atomization pulse pressures, the weight effectiveness of 1202 then declined, and about 10% more agent was required for established flame knock-down performance.

It had been suggested that the higher the boiling point of the liquid agent (the boiling points for Halons 1011, 1202, and 1211 are 67, 24, and -3°C, respectively), the more atomization pressure is required to disperse the flowing liquid agent. Surface tension effects and viscosity variations probably enter the picture as well. Also, it was believed agent droplet size should be considered in greater detail. Observations of the free jet of Halon 1211 and the atomizing pulse of nitrogen gas at 700 kPa, shows that the jet plume contains visible droplets, mists and agent vapor. The "throw" capability of this mixture was 3 to 4 meters. Here a measure of agent "throw" was to observe droplets impinge and then evaporate from a flat black surface. At 1500 kPa, the free jet of agent and nitrogen was much more vigorous, well mixed, and vaporized. However, no droplets were observed and the "throw" has decreased considerably (about 1 meter or so). For Halon 1011, the result of increasing the atomization pressure from 700 to 2000 kPa, was to provide a better agent/nitrogen mixture, while maintaining a good proportion of droplets that yielded longer "throw" values at higher pressures, unlike Halon 1211, or to a lesser extent Halon 1202.

From a dynamic fire point of view, an extinguishing agent vapor has much less chance of penetration into the boundary layer where fuel and air are being combusted, than has a higher momentum-carrying droplet. The droplet then serves as a mechanism to transport

the agent into the active combustion zone, where ensuing vapors can now interfere with the flame processes. With stratification of a fuel vapor/air mixture burning on a hot surface, the extinguishing agent vapor alone has little probability of penetration into the burning zone. Agent vapors are transported by the airstream beyond the fize zones, where they serve no purpose. At the same time, if agent atomization is poor, the presence of droplets that are too large results in more rapid initial fallout of the agent from the fire air supply stream, and at the fire sites, discontinuous bombardment of the combustion zone. These locally scattered high agent-vapor concentrations are only partially successful in interfering with the flame chemistry and soon the combustion processes will have vigorously reestablished themselves over the entire burning surface. The need for additional weight (more than twice the weight of 1202) of Halon 1301 agent (boiling point: 60°C, with a room temperature vapor pressure of about 3300 kPa) appears to substantiate the need to have some droplets capable of pentrating the flame boundary layers in order to interfere with flame radical chemistry.

Each liquid extinguishant appears to have an optimum pressure for injection atomization, that results in a good distribution of droplet sizes in the fire air supply stream for maximum weight effectiveness. For a dynamic fire, we conclude it is possible to apply a liquid agent such as Halon 1211 too vigorously (i.e., use of too high an injection pressure or use of injection nozzles that promote too fine a particle atomization). As in the case of Halon 1011, too little mechanical atomization resulted in less than maximum performance.

Halon 1011 which is a simple liquid at room temperature, was injected under pressure into the test section and finely atomized and dispersed by a simultaneous pulse of nitrogen gas. About 50 to 100% more Halon 1011 agent was required to perform the same fire extinguishing tasks as Halon 1211. In a few cases where Halon 1011 failed to knock down the vigorously burning multiple fires, it was suspected that some of the decomposition products from this Halon were capable of flashing and burning. An aluminum cowling, which had survived numerous hours of operational burning in the simulator, partially melted during what was suspected to be a unique instance of some additional energy release in the combustion zone.

For general reference purposes only, CO_2 was also tested in the Dynamic Fire Assemblage. It is important to note the difference in injection techniques for CO_2 compared to that adopted as a standard procedure for Halon application in the facility. The CO_2 was injected continuously such that the predetermined concentration of CO_2 and air by volume was reached at the fire site. Air speeds were low. Even at 30% volume mixture of CO_2 and air, the multiple fire sites continued to burn vigorously. At 40 to 50% CO_2/air concentrations, the fire could be knocked down and suppressed only as long as the high CO_2 flow rate was maintained. The CO_2 capability is contrasted with, for example, Halon 1211 performance, wherein much smaller quantities of agent in a single injection creates a short plug of mixture in the flow stream that, upon reaching the fire sites, promptly knocks down the flames. As the agent concentration rapidly dropped with the passing of the plug, the fire registers a slight delay, and then reignites. However, it may be assumed that the fire would remain suppressed if, upon achieving knock-down, the 1211 agent continued to be injected even in rather small concentrations. This suggests that for a fixed weight of extinguishant, more effective fire control could be achieved with a series of pulses of agent injection rather than a single massive injection as is now the case in aircraft nacelle fires. The same method used to determine an EEF for the dry chemicals was applied to the Halon agents and the mean results plotted in Figure 36.

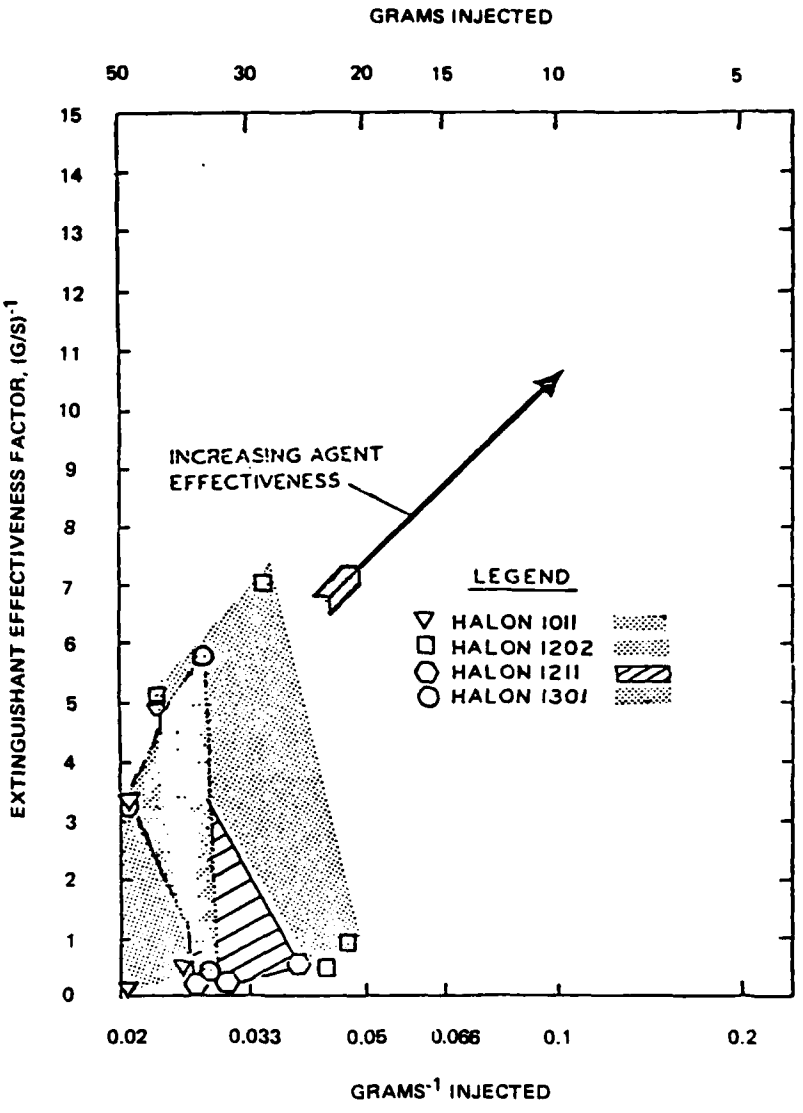

Figure 36. The Relative Fire Control Effectiveness of Various Halon Fire Extinguishants as Determined by Data from the Dynamic Fire Test Assemblage.

SUMMARY OF DYNAMIC TESTING DATA

Data obtained clearly indicate the superiority of the calcined KD·KI dry chemical fire extinguishant synthesized by us, exhibiting both excellent knock-down performance and good inhibition effects, confirming the Static Testing Assemblage data for this compound. Also, addition of an arbitrarily chosen "sticking" agent (in an attempt to counteract the severe scouring effects of high local air speeds across the heated plate surface) did seem to show some merit, in that 10% B_2O_3 added to potassium Dawsonite was judged to be slightly more effective than KD alone. Similary, unambiguous evidence indicates that Halon 1202 is more effective than the other three Halons tested. However, even though knock-down capabilities are excellent for these Halons, the severe volume dilution effects intrinsic to gaseous and/or liquid systems under conditions of high local air velocities, allows virtually no inhibition capability, and reignition delay times are minimal in all cases.

Section 5

DISCUSSION AND CONCLUSIONS

PROPERTIES NEEDED FOR EFFECTIVE FIRE CONTROL

The intrinsic properties of gaseous and liquid fire control agents make them quite unsuitable for situations involving high airflow velocities due to the consequent dilution effects that operate. Thus, dry chemical systems, provided that they can be localized to the actual scene of the fire, provide a viable alternative. Since it is believed that the effective dry chemical agents act to control fire via chemical mechanisms and not via physical effects, the fire control process is a molecular one (chemical scavenging and interference with chain propagation processes). The chemical system of choice has to satisfy several criteria, which we find convenient to classify under two major subdivisions, Passive Phase and Active Phase, in fire control.

Passive Phase Criteria for Dry Chemical Fire Extinguishants

Mandatorily, the dry chemical system has to be formulated and then loaded into some form of discharge mechanism. It is probable that the chemical system will remain in this stored state for a long period prior to discharge and subsequent use. These facets of formulation/loading, storage, and discharge comprise the so-called Passive Phase of the fire control process, and necessarily involve severe restrictions on the choice of chemical system to be used.

1. The chemical should be easily available, or capable of synthesis by a single stage process, in order to satisfy economic restraints.

2. The chemical should be "processable" with respect to grinding, sieving, and optimization of bulk density, particle size distribution, and flow properties.

3. The chemical should be nontoxic, or of minimum toxicity, to enable all steps in the processing and subsequent loading into an engineering system to be accomplished safely, both at the chemical synthesis plant, and locally at the extinguishant system site (aircraft engine nacelle).

4. The chemical should be noncorrosive to the engineering system that will deliever it to the fire, so that special handling apparatus or specially lined containers and hoses are avoided.

5. Storage of the chemical prior to use mandates that the chemical system shall not:

   a. Lose or gain weight significantly; thus precluding hygroscopic (water absorption) and efflorescent (water loss) solids, solids that react with water or air, solids that react with other components contained in them (matrix carrier reactions with solute dopants), and in particular, gas evolution shall be virtually nonexistent.

b. The material chosen has to be of limited volatility to obviate vapor pressure changes with ambient temperature.

c. The material chosen has to be thermodynamically and kinetically stable with respect to chemical change to temperatures of 260°C, which is postulated as the maximum probable temperature of any storage environment of a normally operating engine nacelle of advanced aircraft. Less stringently, the chemical system must be stable down to -55°C, corresponding to the lowest probable ambient temperature of an engine nacelle in a parked aircraft.

d. The chemical solid, after grinding/sieving/loading operations has to be capable of being discharged via a compressed gas ejection system, implying that the powder will not cake, or throttle any discharge orifice (flow properties).

6. The dry powder also has to be engineered to provide dispersion over the target region (particle size distribution), sufficient penetration (trajectory aspects and bulk density) to reach the seat of the ignition process, and still retain fluid properties (powder packing phenomena) to allow complete discharge from the reservoir container.

Active Phase Criteria for Dry Chemical Fire Extinguishants

The dry powder chemical fire extinguishant must provide two major properties, initial fire knock-down, and long-term inhibition. It is recognized that these two properties may be mutually exclusive as a worst case, and probably independent properties at best. It is probable that chemical fire suppression occurs via a scavenger intermediate derived from the extinguishant, this specie (or species) breaks the fire propagation chain that characterizes hydrocarbon oxidation equilibrium we recognize as the flame and/or explosion. When the concentration of this scavenger (or scavenger set) reaches a critical minimum value, the fire can no longer propagate. When the extinguishant has been consumed ("exhaustion"), the concentration of this scavenger falls below the critical minimum value, and the flame reignites. If the extinguishant provides large concentrations of this scavenger early on, then rapid knock-down will occur, but the extinguishant will be consumed rapidly and soon exhausted. However, if the extinguishant degrades slowly to give only small concentrations of this active scavenger, then the concentration will be maintained for long periods, the reignition process will not occur till the extinguishant has been exhausted, and long reignition delays will be observed. Note carefully, however, that if the extinguishant degrades so slowly that the concentration of active scavenger is small, even though this concentration exceeds the critical minimum needed to extinguish the flame, the initial knock-down capability may be so impaired as to be nonobservable. Of course, concentration levels that do not even reach this critical value will produce neither knock-down nor inhibition. These effects will be severely aggravated by high air velocities and severe volume dilution effects consequent upon this factor, and concentrations of scavenger species may exceed this critical minimum on an averaged basis, but yet local and/or momentary concentration fluctuations will negate either or both of the knock-down and inhibition functions.

In addition to these two primary functions, other properties may become important. One such property is the ability of the dry powder to adhere to smooth hot surfaces scoured by up to 50 m/sec local air velocities. Hence it may be necessary to induce some degree of "stickiness" in the powder via another minority compound.

To retard the degradation of the extinguishant species that provides the active scavenger, particularly at high temperatures, the matrix carrier should possess good thermal conductivity and an endothermic pyrolysis mode. It would also help if the degradation products from the matrix also act as fire control agents, by producing additional scavengers (chemical control), or by producing an inert gas blanket such as CO_2 (physical control), or by being highly endothermic and providing local temperature quenching effects (endothermic physical changes such as crystal decrepitation and crystal phase changes). From a practical standpoint, the majority degradation product from the system following pyrolysis should also be easy to clean up, and not cause severe corrosion of hot surfaces exposed to the dry chemical agent. Thus, powders that decompose to strongly acidic/basic products with deliquescent or hygroscopic properties will cause severe damage to exposed surfaces.

CRITERIA FOR FIRE CONTROL PERFORMANCE

We find it convenient to classify fires into two types: Type I fires, typified by forest fires and dwelling fires, begin by an unspecified event and would burn until either their fuel supply is exhausted, or they are extinguished (deliberately or accidentally). In particular, once extinguished, they are not expected to reignite spontaneously, since no continuous ignition source is present. Type II fires, typified by fuel fires in an engine compartment, are initiated by an ignition source which is present continuously, would reignite spontaneously if extinguished, and will continue to reignite after extinguishment as long as both fuel and ignition source remain. An obvious criterion of effectiveness for a fire control agent for Type I fires is "weight efficiency", where the smaller the quantity of agent needed to extinguish a specified fire, the "better" the agent ("only milligrams needed to extinguish a forest fire", and an "index of performance" related to the quotient "exothermicity controlled/mass needed"). This is not a meaningful criterion for Type II fires, and it is suggested that the longer an agent can keep a flame extinguished in the presence of both ignition source and fuel supply the "better" the agent. Beyond this basic criterion, weight efficiency factors can also be incorporated into an overall "index of performance" defined in terms of the quotient:

$$\frac{\text{(Reignition delay induced) (exothermicity of fire controlled)}}{\text{(mass needed to induce delay)}}$$

These factors are summarized schematically in Figure 37.

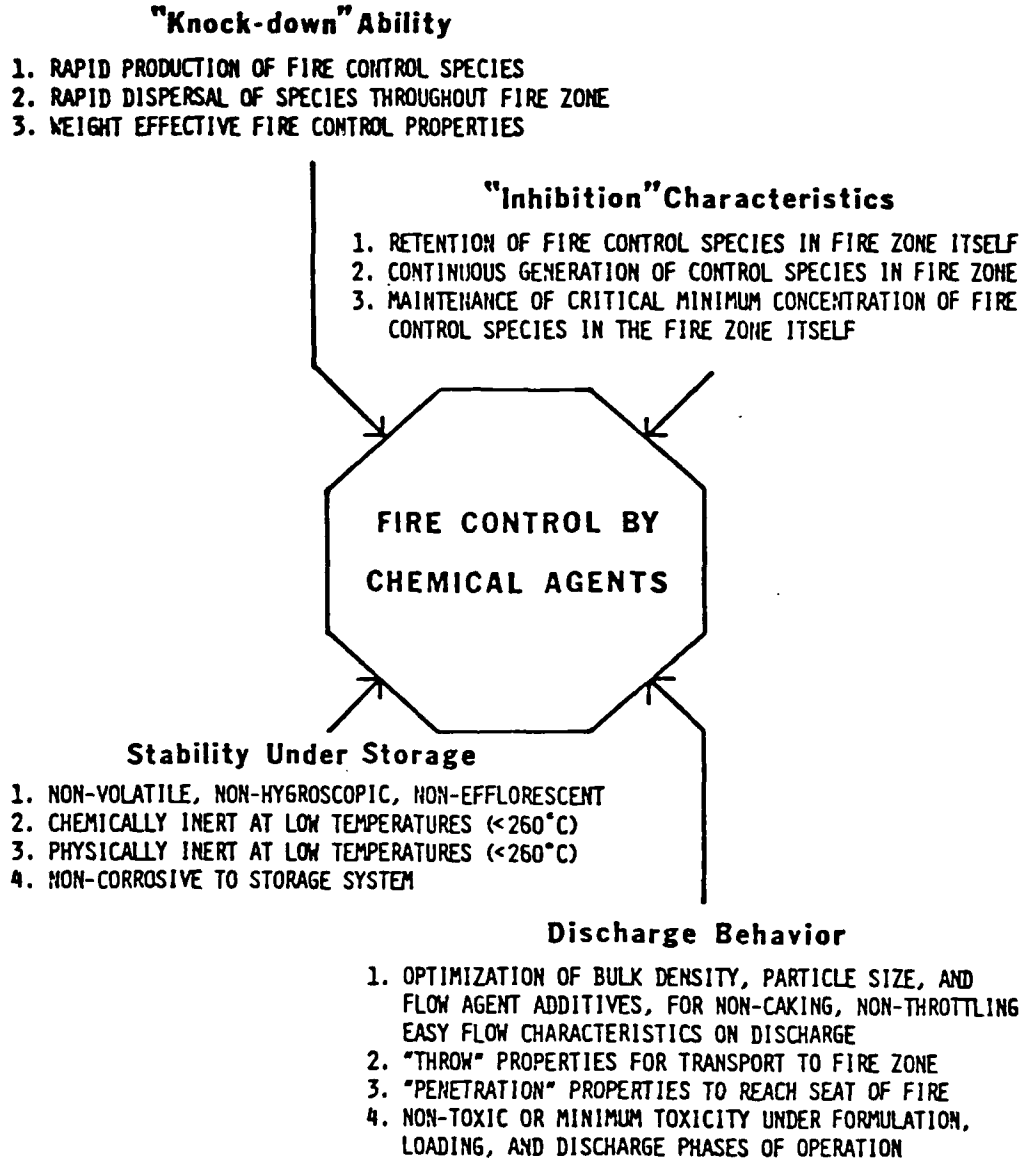

Figure 37. A Schematic Representation of the Criteria Needed for an Effective Dry Chemical Fire Extinguishant System.

SUITABILITY OF SYSTEMS TESTED

The rigorous storage requirements delineated in Table 1 allow us to eliminate all but two species from consideration. These two acceptable systems are potassium Dawsonite (KD) containing various percentage compositions of potassium iodide as simple physical mixtures (KD + KI), and potassium Dawsonite calcined with KI (KD·KI).* The calcined solid appears to have a slightly better performance (as measured from the reignition delay induced in a standard fire). Moreover, since potassium Dawsonite must be synthesized in the first place, and the most attractive synthetic method utilizes calcination, it is recommended that synthesis of KD be accomplished via calcination in the presence of KI directly in one step. The final product, calcined KD·KI, exhibited superior fire control performance in both the static assemblage and the dynamic assemblage. This system also fulfills the other ancillary requirements involving minimum toxicity, easy cleanup after use, noncorrosive properties** (particularly to magnesium/aluminum alloy engine casings prevalent in aircraft, and which are particularly prone to damage by caustic chemicals derived from Na or K compounds such as $KHCO_3$ which degrade to oxide/hydroxide species), and easy synthetic availability.

It is pertinent to comment on some of the other systems tested, both from the viewpoint of data from the static assemblage, and from the complementary information available from the dynamic assemblage.

The concept of an additive designed to "localize" the dry powder to the scene of the fire in the presence of high velocity airflows is worth a brief comment. We selected arbitrarily to use a material known to form a viscous liquid (glass) at the temperatures expected in the fire zone (500 to 900°C), and chose B_2O_3 as a preliminary experimental system. Data clearly indicated that B_2O_3 had virtually no fire fighting ability of its own and the static testing procedure also indicated that it reduced the efficacy of KD when added at 10% by weight (a pure dilution effect, similar to the simple additive effects seen for K_2SO_4 and SnI_x mixtures). However, dynamic assemblage experimental data did confirm the slightly better performance expected for KD + B_2O_3 when high air velocities scoured the heated plate surface. Other high temperature "adhesive" agents can be postulated, and would be worth investigation, the most obvious examples are high temperature asphalts/tars, or synthetic organic or inorganic nonflammable polymeric materials. It should be noted that addition of these "sticky" agents to the chemical system immediately negates criteria associated with ease of cleanup operations, and may perpetrate high temperature corrosion effects.

Tin iodide as an additive may be dismissed quite summarily. It is a volatile system intrinsically, and all physical mixtures regardless of the matrix carrier fail to fulfill the storage requirements (high volatility, corrosive, temperature instabilities at 120°C and

*A marginally acceptable system could substitute sodium Dawsonite as the major component in oil shale, and some solid sludges from water processing plants for potassium Dawsonite, but this will only satisfy current storage requirements. However, economically, this may be an attractive alternate to the special synthetic preparation of the potassium analog.

**However, note that the end product after use is probably aluminum oxide, which possesses extreme crystal "hardness", and thus could cause severe physical damage to reciprocating/rotating surfaces.

above). Further, a solid phase reaction occurs between the additive (SnI_x) and carbonate carriers such as the Dawsonites, resulting in CO_2 release, which is significant at ambient temperatures of 40°C, and very rapid above 100°C. Finally, calcination of SnI_x with KD results in formation of KI, and merely provides an expensive method of preparing KI from these two precursors (SnI_x and KD)!

The I.C.I. Ltd. product "Monnex®", although producing excellent results in the dynamic phase of testing, did not satisfy the advanced storage requirements, and did suffer the disadvantages associated with high temperature corrosivity and particularly poor cleanup operations.

The experimentally formulated and commercially supplied K_2CO_3 powder offered high performance in both the static and dynamic apparatus, better than the corresponding $KHCO_3$ compounds. However, high-temperature performance was poor (phase change effects), and the inherent hygroscopic character could merely be reduced, and not eliminated, thus obviating use in humid atmospheres.

Although Al_2O_3 mixtures with KI (calcined and simple mixtures) exhibited superior performance in the static phase, dynamic testing did not confirm this promise. Similarly, $Al(OH)_3$ and AlOOH carriers did not prove to be superior to KD.

Sodium Dawsonite (NaD) mixtures with iodides did offer excellent performance in the static testing sequences, but NaD itself will not satisfy the advanced storage requirements. However, commercial sources are available (liquid phase solution precipitation reactions to provide a low density powder used for antacids such as "Tums®"; precipitated sludges from water treatment plants utilizing alumina flocculation and pH-carbonation control; bulk component in U.S./Canada oil shale residues).

COMMENTS ON POTENTIAL IODIDE DOPED SYSTEMS

Our data provide unambiguous evidence for the efficacy of iodide loaded dry chemical systems, and it appears that the prime matrix carrier of choice is KD. However, the choice of iodide dopant is more diverse. Our choice of KI was dictated by economic/availability reasons, and by the fact that NaI is strongly hygroscopic. An equally valid choice would be LiI. In addition to these aspects, prima facie reasoning would seem to indicate that the weaker the metal-iodine bond, the greater the available iodine concentration that might be propagated into the vapor phase, and thus the greater the degree of interference that might ensue among the flame reactions. However, KI is strongly ionic (as too is LiI), and the concept of bond strength is a poor one when ionic bonds are considered. Of the covalent halides that exist, particularly the iodides, tin salts offered the best compromise between cationic toxicity (eliminating lead and mercury) and weakness of bond (Sn-Cl at ca. 76 kcals/mole, Sn-Br at ca. 47 kcals/mole, and Sn-I at ca. 40 Kcals/mole). Thus, tin iodide was our second choice for an iodide dopant (it has already been noted that multivalent metals seemed to possess antioxidant properties, and that tetrabutyltin was used as an antioxidant polymer stabilizer). A third choice, not tested, was cadmium iodide, since bond strengths are even lower for

cadmium than for tin (Cd-Cl at ca. 50 Kcals/mole, Cd-Br at ca. 38 kcals/mole, and Cd-I at only 33 kcals/mole). However, cadmium is toxic to the extent that the U.S. EPA (Environmental Protection Agency) restricts levels of Cd in drinking water to 10 ppb (parts per billion), compared to lead metal at 50 ppb, and mercury to 2 ppb. Although the relative weight effectiveness for iodine content for a fixed iodide salt content reduces in the order $SnI_x > CdI_2 > KI$, potassium iodide is biologically acceptable at low levels, and is only toxic from the iodide anionic content at relatively high concetrations.

Based on the efficacy of iodide dopants, it might be useful to examine other ways of incorporating iodine into a dry chemical, and other potential systems that might be suggested include the following:

1. Iodine (as I_2) held in a suitable molecular sieve as a true clathrate or inclusion complex; or a molecular sieve loaded with CH_3I or CF_3I.

2. Preparation of a "coated" carrier (rather than the calcined approach used) using a volatile solvent held iodide slurry (KI in methanol, or from a solubility viewpoint, LiI in methanol/ethanol) to coat a finely ground precipitate of matrix carrier (KD) which is insoluble in the solvent, and subsequent removal of the solvent by freeze drying or vacuum pumping. This process is analogous to the preparation of stationary phase coatings for GLC column preparation.

3. Use of an iodide loaded anion exchange resin as an additive. It is possible that the anion exchange resin could provide the third component postulated to provide "adhesive" qualities to the powder at high temperatures in high airflow situations.

4. Use of high molecular weight quaternary ammonium iodides as additives, either directly, or as bound entities to silica gel or alumina. Technology is now available for the formulation of anion exchange granules whose majority component is a ceramic or silica material.

CONCLUSIONS

In general, no single component system offers fire control ability that is acceptable. KD alone is the only marginal system that even remotely provides potential control capability and satisfies the delineated storage requirements. Equally, dynamic testing of some Halons merely served to confirm previously stated shortcomings inherent to gaseous and liquid systems, and their performance was generally inferior to dry chemicals. Since CO_2 provided virtually no fire control capability either, indicating that physical quenching effects are unimportant relative to chemical scavenger effects, it is clear that the Halons inhibit by interacting chemically with the flame, and do not merely "blanket" the combustion process by displacing the oxidant from the combustion zone. In the light of the data from iodine doping, it is probable that an iodine containing Halon will prove even more effective than Halon 1202. However, the excellent knock-down capabilities of Halon 1202 (a function of the rapid dispersal through the fire zone, and the ease of pyrolysis to provide

a fire control agent in large concentration) can be usefully employed to augment the lesser knock-down capability of dry chemicals which, in general, possess superior inhibition control properties. Use of Halon 1202 as the discharge/driver gas for a calcined KD·KI dry powder extinguishant (with or without some "sticky" agent such as B_2O_3) would seem to offer a logical approach for real simulations of engine nacelle fire scenarios.

Finally, it is further suggested that one of the Halons could be used in an auxilliary fire detection role. Since many fire warning/detection systems suffer shortcomings due to a multiplicity of invalid alarms (particularly prevalent in engine nacelles where ambient temperatures are already high), it is suggested that small quantities of a suitable Halon be injected upstream of the potential fire zone,* and a simple halide detector (HBr) be mounted beyond the fire zone in one of the many inert downstream sites. A fire would produce breakdown products from the Halon that could not be produced by a mere hot surface at normal engine surface/nacelle operating temperatures. Thus, any indication of HBr formation would be accepted as a true "fire", and not a false alarm. This indication could be used to trigger the main extinguishment system automatically, or a visual and/or audible warning. Since C-I bonds are weaker than C-Br bonds, an iodine containing Halon would provide greater sensitivity in conjunction with an HI detector.

*It would be possible to utilize either a continuous flux of Halon from a reservoir with several milliliters per minute flow rate of gaseous component, or pulsed injection at preset time intervals. For example, a 10 ml/min continuous Halon flow rate from a 1 gallon liquid pressurized container would provide approximately 10,000 hours of operating time.

Section 6

RECOMMENDATIONS FOR FUTURE WORK

1. This program has already shown that some commercial dry chemical fire extinguishants have a greater weight effectiveness in suppressing hot surface initiated fuel fires than the gaseous or liquid Halons currently in use. Therefore, the tailoring and development of dry powder delivery systems, using either stored pressure or explosive gas generation, and which meets the requirements given in Table 1, should be undertaken.

2. If this improved fire control capability is confirmed in the larger scale dynamic facility currently being built at Wright-Patterson AFB, then a more detailed program to develop the presently noncommercial chemicals described in this report should be initiated as well.

3. The concept that fire control occurs through the agency of competitive chemical reactions between the flame propagation species and the interfering scavengers supplied by the extinguishant has been around for more than 40 years. However, it cannot answer why the effectiveness of potassium compounds seems to exceed that of corresponding sodium compounds, and there are other similar anomalies that need further elucidation. It is suggested that a new academic involvement in flame chemistry and flame control be initiated.

4. Extensive time was spent reviewing directly relevant, and less directly relevant materials, culled from many government reports and contracted research publications. It would be appropriate to engage a faculty member experienced in writing a text to review all of this literature, and others, and make clear what has been done before in the field of fire control. This would have the additional benefit of making some of the more obscure reports and publications more easily available in the general literature.

In the light of these data presented in this report, obtained from both static and dynamic testing procedures, it appears that iodide doped sodium and potassium Dawonites offer the most promise for fire control in high velocity airstreams. We recommend that the following aspects be considered further:

5. Carry out scaled up testing procedures for Dawsonite/iodide mixes.

6. Determine the effects of bulk density, particle size, and physical characteristics of the dry chemical powder, on the performance of the dry powder system in the dynamic simulator.

7. Advance the current kinetic model for ignition delay phenomena.

8. Initiate basic studies into the strategies for volatility control of halogen additives, in order to provide controlled concentrations of an active agent over long time periods.

9. Perform fundamental studies using thermogravimetric analysis techniques, mass spectrometry, electron spin resonance spectrometry, and product analyses via GC and GLC, to ascertain the identities of the active species that control flame propagation from the more efficient dry chemical powder extinguishant systems.

10. Attention is redirected to the comments given previously in Section 5, concerning other potential iodide doped systems, and to the use of multicomponent systems to effect initial flame knock-down, long-term flame control, and localization of the dry chemical agent to the flame region via a "sticky" additive.

Finally, it is also recommended that the U.S. Department of the Interior be alerted to the possibility of using sodium or potassium Dawsonite systems, with or without iodide doping, to aid in the control of forest fires. It is envisaged here that a massive knock-down capability will be needed, rather than long-term control of the flame. This is probably a property that is more closely attuned to the behavior of tin iodide doped systems than those derived from potassium iodide. However, it is clearly demonstrated that single component Dawsonite systems, and those systems doped with iodide, are vastly more efficient in controlling flammable situations than are the ammonium phosphate systems currently in use for forest fire control.

Appendix A

SYNTHESIS AND CHARACTERIZATION OF POTASSIUM DAWSONITE AND IODIDE DOPED POTASSIUM DAWSONITE

PRIOR LITERATURE

Although numerous references have appeared in the technical and patent literature concerning the preparation, characterization, structure, properties, and uses of Dawsonite (sodium aluminum dihydroxide carbonate, as in $NaAl(OH)_2CO_3$), a naturally occurring mineral, considerably less attention has been directed at the potassium and other alkali metal analogs. The first references to the potassium analog were in the German patents issued in 1882 and 1892 (Reference 52 and 53). This and subsequent literature dealing in whole or in part with the potassium analog of Dawsonite address one or more of the following aspects: synthesis and composition (References 45–47, 50–53, 55–57); integral TGA (thermogravimetric analysis), DTG (differential thermogravimetric) analysis, DTA (differtial thermal analysis) (Reference 48, 55, 57); IR (infrared) analysis (References 46, 49, 55, 57); solubility and hydrolytic decomposition properties (References 54 and 58), and X-ray diffraction characteristics (References 46, 48, 55, 56).

To date, all published procedures for the synthesis of the potassium analog involve solution methods where the aluminum component is derived from one of the following: elemental aluminum (Reference 55), Gibbsite (References 45 and 55), aluminum hydroxide (References 45, 50, 51, 55), aluminum salts (References 45, 47, 50–53) or aluminum alkoxylates (References 50 and 51). The aluminum component, either as a solid, liquid or aqueous solution is usually combined with an aqueous carbonate and/or bicarbonate system. The composition of the precipitated product, depending on solution temperature during the synthesis, corresponds to a substance having either the formula $KAl(OH)_2CO_3 \cdot 1/2H_2O$ or $KAl(OH)_2CO_3$, the latter being formed at higher solution temperatures (References 45 and 55) and the former capable of dehydration to the latter upon heating to about 100°C (Reference 48).

Based on integral and differential thermogravimetric analysis data as well as differential thermal analysis, it has been suggested that the composition of the potassium analog of Dawsonite is consistent with the formula $KAlO(OH)HCO_3$, as opposed to $KAl(OH)_2CO_3$ (Reference 48). The final product in a complete thermal decomposition of $KAlO(OH)OHC_3$

has been shown to be potassium aluminate (Reference 48). The overall reaction can be formulated as follows (see Figure A-1 for typical TGA, DTG and DTA profiles for the potassium analog (References 48 and 55) of Dawsonite):

$$KAlO(OH)HCO_3 \longrightarrow KAlO_2 + H_2O + CO_2$$

A detailed study of the differential (thermal analysis and isothermal integral weight loss data as given in Reference 48 is in accord with the reaction sequence shown in Table A-1. (NB—for convenience the stoichiometry of the potassium analog of Dawsonite will be expressed as $KHCO_3 \cdot AlO(OH)$).

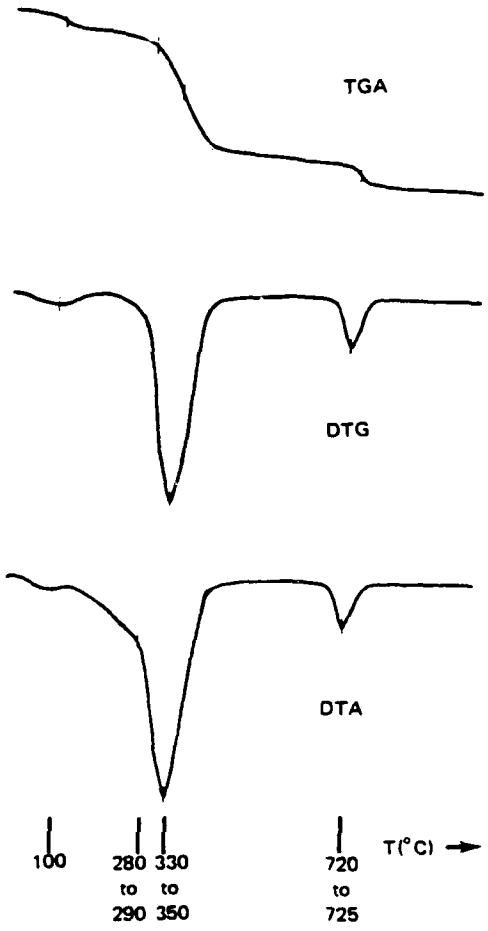

Figure A-1. Typical Integral, Differential Gravimetric, and Differential Thermal Analysis Curves for the Potassium Analog of Dawsonite.
(Based on References 48 and 55)

Table A-1. Thermolytic Degradation of Potassium Dawsonite.
(Postulated Model)

Cumulative experimental weight loss (Reference 48)	Theoretical weight loss/step (cumulative)	Equation	DTA
		100° = 270°C	
1.78%	0%	$8[KHCO_3 \cdot AlO(OH)] \longrightarrow 8[KHCO_3 \cdot AlO(OH)]'$	Gradual endothermic transition
		270° = 370°C	
23.60%	22.2%	$8[KHCO_3 \cdot AlO(OH)]' \longrightarrow 4K_2CO_3 \cdot 2Al_2O_3 \cdot 4AlO(OH) + 6H_2O + 4CO_2$	Large sharp endotherm
		370° = 670°C	
31.90%	9.7% (31.9%)	$4K_2CO_3 \cdot 2Al_2O_3 \cdot 4AlO(OH) \longrightarrow 2K_2O \cdot 2K_2CO_3 \cdot 4Al_2O_3 + 2H_2O + 2CO_2$	---
		670° = 730°C	
35.40%	3.4% (35.3%)	$2K_2O \cdot 2K_2CO_3 \cdot Al_2CO_3 \longrightarrow 3K_2O \cdot K_2CO_3 \cdot 4Al_2O_3 + CO_2$	Small sharp endotherm
		730° = 1000°C	
39.00%	3.4% (38.9%)	$3K_2O \cdot K_2CO_3 \cdot 4Al_2O_3 \longrightarrow 4K_2O \cdot 4Al_2O_3 + CO_2$ (or: $8KAlO_2 + CO_2$)	---

The IR (infrared) spectra and band frequencies as published in References 45, 46, and 49, and shown in Table A-2, are essentially analogous. In addition to the strong or very strong stretching vibrations of the $-(OH)_n$ groups in the 3400 cm^{-1} region, it is observed that all four normal vibrational modes of the planar carbonato group are active. It is concluded that the very strong frequencies in the 1540 and 1400 cm^{-1} regions represent the strongly spilt asymmetric stretching frequencies ($v_3 = v_5 + v_6$), a presumed consequence of the carbonato lattice site symmetry (References 49 and 57). Carbonato symmetric stretching, out of plane and in plane deformation (v_1, v_2 and v_4, respectively) have been assigned in the case of the potassium analog (see Table A-2) (Reference 49).

The infrared activity of the symmetry forbidden symmetric stretch v_1 is attributed to its crystallographic site symmetry and a complementary carbonato-hydroxo group hydrogen bonding relationship. The site symmetry and hydrogen bonding relationship combine to confer upon the carbonato group a bicarbonate-like configuration. The bicarbonate-like thermal decomposition of the potassium analog (see Table A-1) is thus in accord with its infrared properties, giving further credence to the representation of the potassium analog as $KAlO(OH)HCO_3$ (References 48, 49, 57).

Table A-2. Frequencies (in cm^{-1}) and Assignment of the Principal Bands of the Potassium Analog of Dawsonite.

Reference 45	Reference 49		Assignment[a]
3440	3440	s	OH Stretch
	3412		
	1975	w	
	1825	vw	
1540	1544	vs	v_6 Asymmetric
1408	1412	vs	v_5 Stretch
1102	1108	m	v_1 Symmetric Stretch
1000	1000	s	
867	872	m	v_2 Out of plane deformation
844	848	w	
	764	w	v_4 In plane deformation
	744		
	660	mb	
	516	s	
	470	m	
	404	vw	

[a] = See Reference 49

Legend:
s = strong
m = medium
b = broad
v = very

The potassium analog of Dawsonite is not subject to purification by recrystallization since optimum conditions for its formation require a high $KHCO_3$:K_2CO_3/Al_2O_3 ratio (References 45, 55, 57). It is also susceptible to hydrolysis, yielding carbonates and bicarbonates in the aqueous phase and amorphous $Al(OH)_3$ in the solid phase (Reference 58).

X-ray powder diffraction characteristics for the substance with stoichiometry $KAlO(OH)HCO_3$ have been determined by two independent investigations (References 46 and 55). Neither investigation has reported unit cell dimensions, indexing based on the lattice parameters, crystal class system or space group assignment. Moreover, certain interplanar spacings not only lack correlation between the two different studies, but even within one reported study (Reference 55) spacings are not consistently observed. Table A-3

summarizes the reported "d" spacings. The "d" spacings for the substance with stoichiometry $KAlO(OH)HCO_3 \cdot 1/2H_2O$ have also been reported (References 55 and 56) and similarly appear to lack consistency. However, the similarity in "d" spacings between $KA1O(OH)O_3$ and $KA1O(OH)HCO_3 \cdot 1/2H_2O$ that does exist, and the retention of this similarity upon dehydration of the lattter to the former, suggests that the hydration of the latter is not water of constitution (References 48 and 49).

Table A-3. Interplanar Spacings (in A. U.) for the Potassium Analog of Dawsonite.

(Reflections for 2-θ between 0 and 50°C.)

Reference 55		Reference 46
Specimen 3	Specimen 4	
5.58	5.55	5.58
4.08	4.10	
3.34	3.33	3.37
3.18	3.14	3.15
2.83	2.82	2.79
2.65	2.65	2.65
2.53	2.50	2.50
2.21		2.24
2.17	2.15	2.17
1.98	1.98	1.99

Although previous investigations have sought to compare "d" spacings and h, k, l, assignments known for Dawsonite with the potassium analog, the correlation is tenuous and inconclusive (References 46 and 55).

In conclusion, the potassium analog of Dawsonite prepared by solution precipitation methods has been shown by a number of investigations to be a unique substance. It has been characterized according to its composition, infrared, and thermolytic properties, but only partially characterized according to its X-ray diffraction characteristics.

SYNTHESIS AND CHARACTERIZATION OF POTASSIUM DAWSONITE

GENERALIZED PROTOCOL

A novel method for the synthesis of the potassium analog of Dawsonite was investigated and optimized. Accordingly, the formation of a high purity potassium analog of Dawsonite can be achieved by means of a single step, high-temperature, high-pressure solid-state procedure typical of the following generalized protocol:

1. Equimolar quantities of Gibbsite and potassium hydrogencarbonate as dry, ground powders (particle size <90 μm) are intimately mixed and transferred to a cylindrical open-top aluminum reaction vessel.

2. The reaction vessel is placed in a 2 liter PARR High Pressure Reactor (see Figure A-2).

3. The reactor, after securing, is flushed with gaseous carbon dioxide and then pressurized to 240 psig.

4. The reactor temperature is then raised as quickly as possible to 245°C ± 5°C and maintained at that temperature for 4.5 hours.

5. After cooling and depressurization, the product is removed and vacuum oven-dried overnight at 50°C.

DETAILED PROCEDURE

Aluminum hydroxide, $Al(OH)_3$, obtained from The Kaiser Chemical Corp. at approximately 99% purity, was used directly without further purification. (This material is equivalent to the H-36 grade of alumina trihydrate, $Al_2O_3 \cdot 3H_2O$, currently being marketed by Kaiser Chemical Corp.) The particle size distribution of Kaiser $Al(OH)_3$ was as follows:

Mesh	Weight retained, %
120	0
230	45
325	11
Pan	44

Note: Obviously, this $Al(OH)_3$ will all pass an ASTM #35 mesh, a minimum criterion used in this report for all of the powders processed or used.

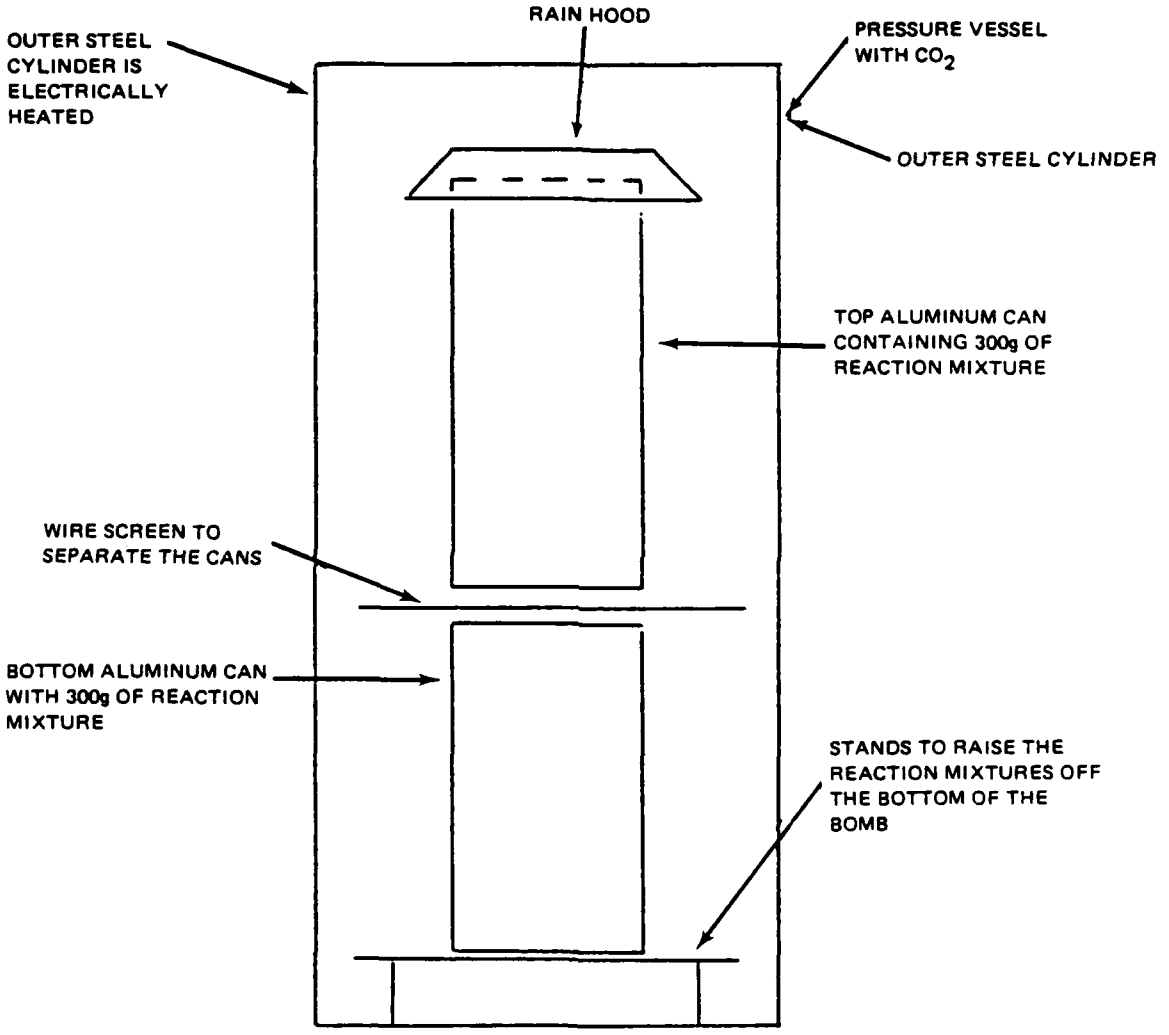

Figure A-2. Pressurized Bomb for the Synthesis of Dawsonite.

Potassium bicarbonate, $KHCO_3$ (supplied as a granular analytical reagent by Mallinckrodt; assay ($KHCO_3$) ... 99.7 to 100.3%) was processed in the following manner before use:

1. It was dried overnight (>16 hours) in a vacuum oven operating at <0.1 mmHg and at 42 to 45°C as a thin layer over the bottom of an aluminum pan with a surface area exceeding 200 cm^2 at a depth of less than 1 cm.

2. The dried $KHCO_3$ was ground in a ball mill for 16 hours. Typically, one pound of the dried powder was added to a 0.3 gallon ceramic pot (diameter 5 5/8 inches), and 12 grinding spheres (ceramic balls; 0.78 to 0.87 in diameter, mass 15.4g) were used. Critical speed of this ball mill used was 124 rpm. The desired speed for efficient grinding was 80% of 124 rpm. The actual revolution rate for the ball mill used was 92 rpm (74% of critical speed). Drying and grinding in this fashion effectively reduces the size of all particles in the $KHCO_3$ powder such that it will pass an ASTM #35 mesh.

3. The ground $KHCO_3$ was placed in a common pool and used as needed. The common material after some time (24 hours and longer) in the storage container would exhibit a degree of water absorption as evidenced by visible caking, and should be dried again in a vacuum oven (as above) just prior to immediate use. $KHCO_3$ was repeatedly dried because of the concern for the reagent weights, since weight loss after reaction provides a convenient measure of extent of reaction.

Step 1. Weigh out the desired amount of each reactant in the ratio 100.12/78.00 for the reactants $KHCO_3/Al(OH)_3$, respectively.

Step 2. Place both the $KHCO_3$ and $Al(OH)_3$ into a 0.3 gallon ball mill container (i.e., 178g total mass per 0.3 gallon volume of mill container). Seal the container without adding any grinding balls and mix for approximately 15 minutes. It is important that a relatively homogeneous mixture of the two solid components be obtained prior to reaction.

Step 3. The resultant solid mixture from Step 2 above was sieved through an ASTM #35 sieve to break up the over-size "lumps". These latter appeared to be mainly $KHCO_3$ coated with a fine dust of $Al(OH)_3$. The $KHCO_3$ lumps are broken up by forcing them through the sieve. The reactants must be mixed again to eliminate any concentration variations of $KHCO_3$ throughout the reaction mixture. The sieved (Pass #35) mixture was returned to the milling pot for further mixing without adding any grinding balls to the pot (mixing time was approximately 15 minutes).

Step 4. Divide reaction mixture among reaction vessels. Determine the mass of reactants in each vessel prior to initiating the reaction. Store the reaction vessels charged with the reactants in a sealed glass container or in a pressurized reaction assemblage until ready to begin the calcination process.

REACTION VESSEL

The vessels used for the calcination process have been the object of much investigation. It was found that glass ("Pyrex®" 250 m beakers), aluminum foil lined glass beakers, and aluminum foil itself, are all unsatisfactory. Glass beakers shatter as the product expands, sometimes even fusing to the product. This makes removal of glass difficult and dangerous. Aluminum foil is too thin for support and reacts to some extent, making for a source of error in aluminum analysis.

It has been found that the bottom half of an all aluminum 12-ounce beverage container (beer and/or soft drink) is satisfactory, with truncation of the container at approximately the midway point. However, concern over potential contamination from volatiles released from the liners of these containers has prompted preparation of the containers as follows.

Reaction Vessel Preparation

Step 1. The aluminum can is cut in such a manner as to produce a container 3 inches high, and with a total volume of approximately 250 m. A clean cut, horizontal edge should be obtained.

Step 2. The containers are now dipped fully into a oxidizing cleaning solution such as "Chromerge®", or a similar vigorous chromic acid based cleaner (i.e., potassium chromate and concentrated sulphuric acid) for 5 minutes or until coatings are observed to have been removed.

Step 3. The cleaned cans are then washed with several liters of water to remove all traces of the chromic acid dip, and residues produced by the oxidation processes induced by the chromic acid dip. The cans are air dried, and then are ready for use.

Some specific brand names were found to be more acceptable than others, due to reasons that were probably tied to surface coatings and/or metal alloy composition, but which were not investigated in any way.

Beverage Container Acceptability for the Synthesis of Dawsonite

Acceptable/preferred[a]	Acceptable	Not acceptable
Budweiser	Dr. Pepper	Coors
7-Up	Colt-45	Schlitz
Pepsi Cola		Miller

[a] Acceptability was defined in terms of criteria associated with visual contamination of the final product (discoloration) and obvious visual signs of chemical reaction induced in exterior and interior walls of the reaction vessel.

CALCINATION ASSEMBLAGE

The calcination assemblage is shown in diagrammatic representation in Figure A-2. A commercially supplied pressure reaction vessel was used, manufactured by the Parr Corp., capable of withstanding ca. 1100 psig, and of being operated at temperatures up to 350°C with temperature control of approximately ±5°C at any temperature between ambient and the maximum.

Calcination Procedure

Step 1. The aluminum reaction containers are positioned in the vessel to be used for the high-pressure/high-temperature calcination procedure.

Step 2. The assemblage is sealed as recommended by the manufacturer of the pressurized calcination apparatus.

Step 3. The sealed pressure vessel should be flushed well with CO_2 gas to remove most of the air that might be present. For the small Parr Reaction Vessel, 60 seconds flushing at a flow rate of 13 SLPM (standard liters per minute) CO_2 was used. The apparatus is then charged with 240 psig pressure of CO_2 gas for this preparation.

Step 4. The sealed and pressurized assemblage containing the reaction vessels with the reactants inside is now placed in the heating unit, and the temperature brought quickly up to 245°C in approximately 60 minutes without allowing any overshoot in the temperature. Recommended "Variac®" settings are difficult to delineate because of several factors that determine final "Variac®" setting for proper temperature.

Step 5. When the reaction has proceeded for the desired time period (4.5 hours), the heater is returned to its zero setting, and the whole assemblage removed from the heating jacket, placed on an asbestos board, and allowed to cool towards room temperature. This process can be accelerated by use of an air draught from a fan, or similar unit. The assemblage and reaction mixture contained within it are left pressurized until the temperature of the assemblage reaches 50°C. At this point the pressurization may be released, and the reaction gases allowed to escape slowly through the release valve.

Step 6. When the pressure has reached equilibrium with atmospherie, the assemblage may be opened and the contents removed.

PRODUCT SEPARATION AND WORKUP PROCEDURES

Drying

The reaction products are dried while still in the aluminum can reaction container, and they may be weighed after this procedure to ascertain the extent of reaction. The recommended drying procedure involves the use of a vacuum oven at <0.1 mmHg and

temperatures not exceeding 50°C or less than 40°C for not less than 16 hours. By the foregoing procedure, crude potassium Dawsonite is obtained in a 96% yield. Yields were computed by comparing observed versus theoretical weight losses that accompanied the calcination reaction.

Grinding

1. Remove all of the material from the reaction vessel by peeling away the aluminum can with the aid of a pair of metal cutters and some form of hand vise (beware of the very sharp aluminum edges subsequently exposed). Use a sharp knife to scrape off all material that is still clinging to the bulk of the product. Unwanted impurities will be colored grey or black: the product is a clean white powder.

2. Use a large conventional mortar and pestle to reduce the size of the pieces recovered from the reaction vessel to a particle size that will all pass through an ASTM #35 sieve.

3. Place the approximately 350g (two reaction vessels with total capacity of approximately 170g each were calcined simultaneously in the calcination assemblage) into a 0.3 gallon milling container, add 18 spheres (ceramic, individually 0.78 to 0.87 inch in diameter and 15.4g mass), and mill for at least 2 hours (as before: critical speed of ball mill is 124 rpm; desired speed for efficient grinding is 80% of the critical revolution rate of 124 rpm). Actual revolution rate used by us was 92 rpm, corresponding to 74% of the critical speed. Representative samples can be taken at this point for analysis or reference purposes.

4. Open up the milling pot, remove the 18 grinding balls, and add approximately 1% by weight of a solid flow agent such as "Tullanox 500®" (supplied commerically by Tulco, Inc.) in the form of a finely dispersed (100% Pass an ASTM #400 mesh) hydrophobic, fumed, SiO_2 powder. Add six solid rubber mixing spheres (0.76 inch in diameter, 5.5g in weight) and mix for 15 minutes to disperese the flow agent through the reaction mixture containing Dawsonite.

After a flow agent has been added, particle size distribution and bulk density of the resulting material can be determined, and the powder is then ready for use (prepared powder was stored in a plastic bag inside a sealed metal gallon can).

In addition to the conditions specified in the foregoing protocol, the formation of the potassium analog under variable time, temperature, and pressure parameters was investigated. Product speciation was determined by X-ray diffraction and is tabulated in Table A-4 and summarized in Figure A-3. The bottom of Figure A-3 shows the temperature, pressure, and time conditions for which the potassium analog of Dawsonite is the principal resultant specie. At temperatures below 200°C the reaction time increases to days and at 150°C or less no reaction occurs. In the absence of carbon dioxide pressure or insufficient carbon dioxide pressure, the principal phenomenon is decomposition of the reactants.

Table A-4. Formation of the Potassium Analog of Dawsonite by Calcining. (Product Speciation as Determined by X-ray Diffraction.)

Sample designation	Temperature, °C	Time, hr	$P_i(CO_2)$	Identified species and estimated relative amounts[a]
I	250	0.5	360	D>b
II	245	4.5	360	D>>B~b
II(washed)	245	4.5	360	D>>B
III	245	4.5	240	D>>B~b
IV	245	4.5	120	D>>B
V	231	14.0	240	D>>B
VI	200	4.5	240	G≳D ~ B≳b
VII	200	4.5	120	D~B~b≳G
VIII	200	4.5	60	D≳B≳G~b
IX	155	4.5	360	G>b~X≳D
X	155	45.0	360	G≳b~X≳D>c1.5H_2O~c~B
XI	155	45.0	240	G>b~X≳D~c1.5H_2O

Legend:
- D = Potassium Dawsonite
- G = Gibbsite
- B = Boehmite
- b = Potassium bicarbonate
- c = Potassium carbonate
- X = Unknown compound not in ASTM

[a] >> means about 10:1
> means about 5:1
≳ means about 3.2 to 2:1
~ means about 4:5 to 5:4

NOTE: The relative amount of each component was estimated assuming the following:

1. The principle peak height for each substance is of comparable intensity, and
2. The relative amount present was inproportion to the height of its major peak compared to the height of the largest principle peak.

Contrasted to the inherent complexities of a refined quantitative X-ray diffraction approach, the above procedure offers little in the way of quantitative information; thus, ~ and ≳ relationships should be interpreted accordingly.

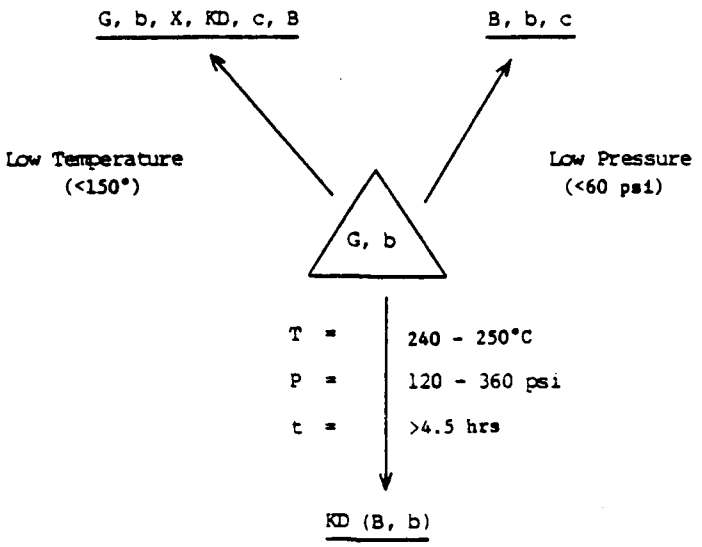

Legend: G = Gibbsite; $Al(OH)_3$
b = Bicarbonate, Potassium
KD = Dawsonite, Potassium Analog
c = Carbonate, Potassium
B = Boehmite; AlO(OH)
X = Unknown Specie

Figure A-3. Potassium Analog Syntheses. (Product Speciation as a Function of Experimental Variables)

ANALYTICAL METHODOLOGIES FOR POTASSIUM DAWSONITE

Quantitative Analytical Methods

The analytical characterizations of the resultant products realized from the calcination of equimolar potassium bicarbonate/Gibbsite mixtures under varying conditions are tabulated in Table A-5. The experimentally determine weight percents were obtained by the following methods: (1) potassium–atomic absorption, (2) aluminum–EDTA titration using Eriochrome-T indicator, and (3) carbonate–acidification followed by absorption of liberated CO_2 by "Ascarite$^{\circledR}$".

Table A-5. Formation of the Potassium Analog of Dawsonite by Calcining. (Analytical Characterizations)

Sample designation	% K^+	% Al^{3+}	% $CO_3^=$
Theoretical	24.42	16.85	37.48
II	25.8	17.03	37.7
II(washed)	25.1	17.59	37.3
III	24.4	16.97	37.4
IV	26.0	16.74	37.5
V	25.1	17.02	37.8
VI	25.3	17.84	31.5
VII	23.5	18.31	31.6
VIII	25.5	16.92	34.6
IX	23.8	16.72	32.3
X	23.9	16.89	32.6
XI	24.1	17.92	29.0
Uncertainty	±0.5	±0.5	±0.5

Hypothetically, the intended objective in the calcining process is the realization of the potassium analog of Dawsonite according to Equation (1) of Table A-6. In addition to the Dawsonite formation reaction, a series of probable competitive decomposition reactions is shown. The variety of species resulting from varying the calcination conditions, as identified in the X-ray diffraction spectra taken of the crude products obtained, is consistent not only with the postulated formation reaction (1), but with the competitive decomposition reactions (2), (3), and (4) as well. It can be ascertained from Table A-7 and Figure A-4, that in the case for crude product analyses, the carbonate content would be the most sensitive indicator of the contribution of conversion types (3) and (4). To the extent that conversion types (1) and (2) predominate, carbonate analyses of the crude product would be an insensitive prarameter with which to distinguish the relative extent of conversion (1) versus (2); however, carbonate analyses performed after purification by low temperature washing would be highly sensitive to the (insoluble carbonate/soluble carbonate) proportion, a characteristic that would be a sensitive measure of the ratio.

$$\frac{\text{Percent conversion for reaction 1}}{\text{Percent conversion for reaction 2}}$$

Table A-8 compares typical analyses for crude and purified potassium Dawsonite. It can be concluded that within the limits of uncertainty of the methodologies utilized, conversion reaction (1) occurs almost exclusively. The existence of unidentified species in systems IX, X, and XI precludes application of the above approach as a diagnostic procedure.

Table A-6. Calcination of Potassium Bicarbonate/Gibbsite Mixtures.
(Possible Type of Conversions)

(1) $KHCO_3 + Al(OH)_3 \longrightarrow KAl(OH)_2CO_3 + H_2O$

(2) $KHCO_3 + Al(OH)_3 \longrightarrow KHCO_3 + AlO(OH) + H_2O$

(3) $KHCO_3 + Al(OH)_3 \longrightarrow 0.5K_2CO_3 + AlO(OH) + 1.5H_2O + 0.5CO_2$

(4) $KHCO_3 + Al(OH)_3 \longrightarrow 0.5K_2CO + Al(OH)_3 + 0.5CO_2$

Conversion (1) is the formation of the potassium analog of Dawsonite.
Conversion (2) is the decomposition of Gibbsite.
Conversion (3) is the decomposition of Gibbsite and potassium bicarbonate.
Conversion (4) is the decomposition of potassium bicarbonate.

Table A-7. Reactant and Product Composition as a Function of Conversion Type.
(Calcination of Potassium Bicarbonate/Gibbsite Mixtures)

Initial composition

Conversion type	% K^+	% Al^{3+}	% $CO_3^=$
(1)	21.95	15.15	33.69
(2)	21.95	15.15	33.69
(3)	21.95	15.15	33.69
(4)	21.95	15.15	33.69

Final composition

Conversion type	% K^+	%Al^{3+}	% $CO_3^=$
(1)	24.42	16.85	37.48
(2)	24.42	16.85	37.48
(3)	30.29	20.90	17.05
(4)	26.58	18.34	14.96

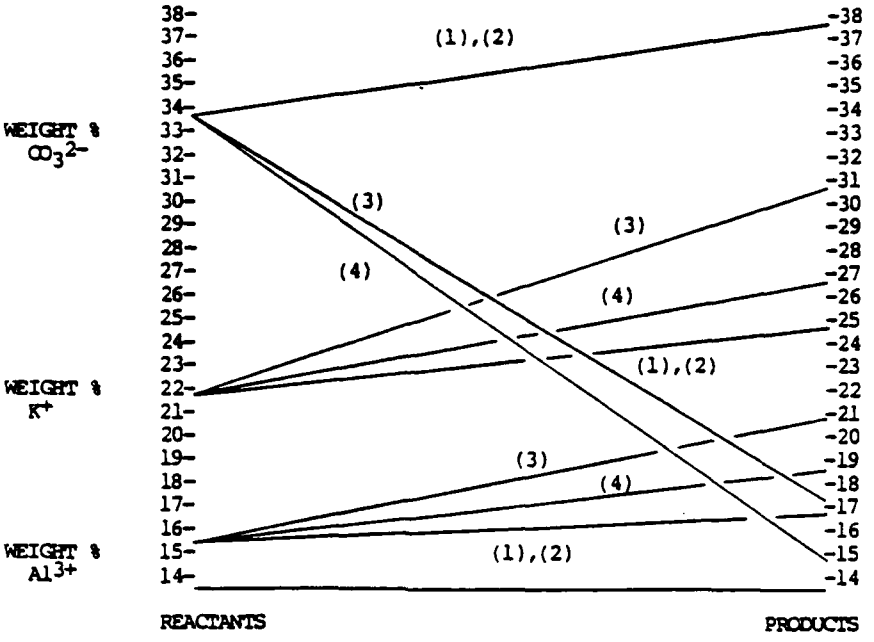

Legend:

(1) = Potassium Dawsonite formation reaction
(2) = Gibbsite decomposition
(3) = Bicarbonate and Gibbsite decomposition
(4) = Bicarbonate decomposition

Figure A-4. Reactant and Product Composition as a Function of Conversion Type.

Table A-8. Potassium Analog Analyses: Crude/Purified Comparison.

	$KAl(OH)_2CO_3$[a]		
	% K^+	% Al^{3+}	% $CO_3^=$
Theoretical	24.42	16.85	37.48
Crude	24.4	17.0	37.4
Purified	24.7	17.0	37.3

[a] K – by atomic absorption.
Al – by EDTA titration.
CO_3 – by acidification and ascarite absorption.

NOTE: All uncertainties < ±0.5%.

INFRARED ANALYSIS

Figure A-5 is a typical spectrum of the potassium analog of Dawsonite synthesized by calcination; Figure A-6 is a characteristic spectrum obtained from a product synthesized by solution preparation methodology analogous to that of the previously published literature (References 45–47, 50–53, 55–57). Table A-9 lists the experimentally observed band frequencies that appear in Figures A-5 and A-6. It can be readily concluded from the data of Table A-9 and Figure A-5 and A-6 that the spectrum of the calcined product and the spectrum of the solution preparation product are virtually identical. The data of Table A-9 is also quite comparable to the previously published infrared band frequencies of the potassium analog of Dawsonite as summarized in Table A-2.

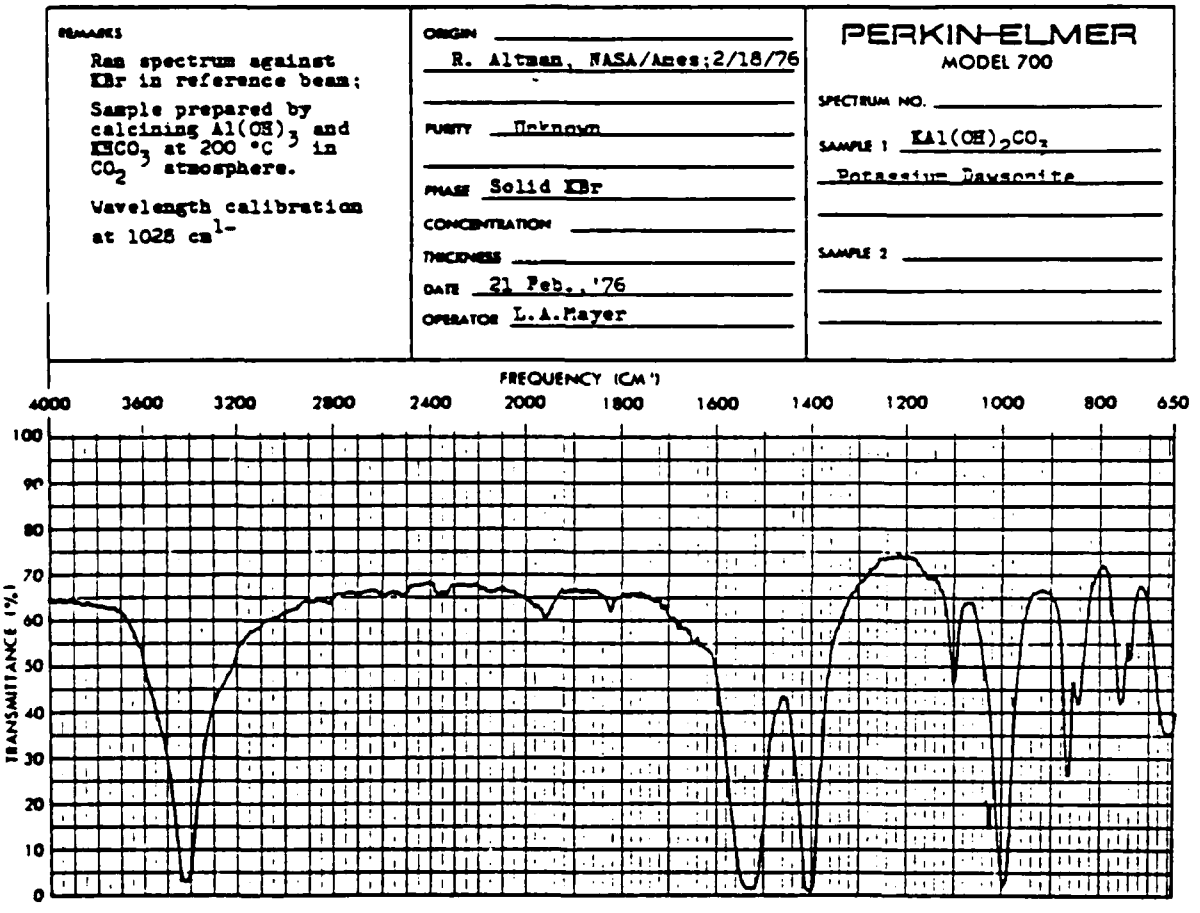

Figure A-5. Infrared Spectrum of the Potassium Analog of Dawsonite Synthesized by Calcination.

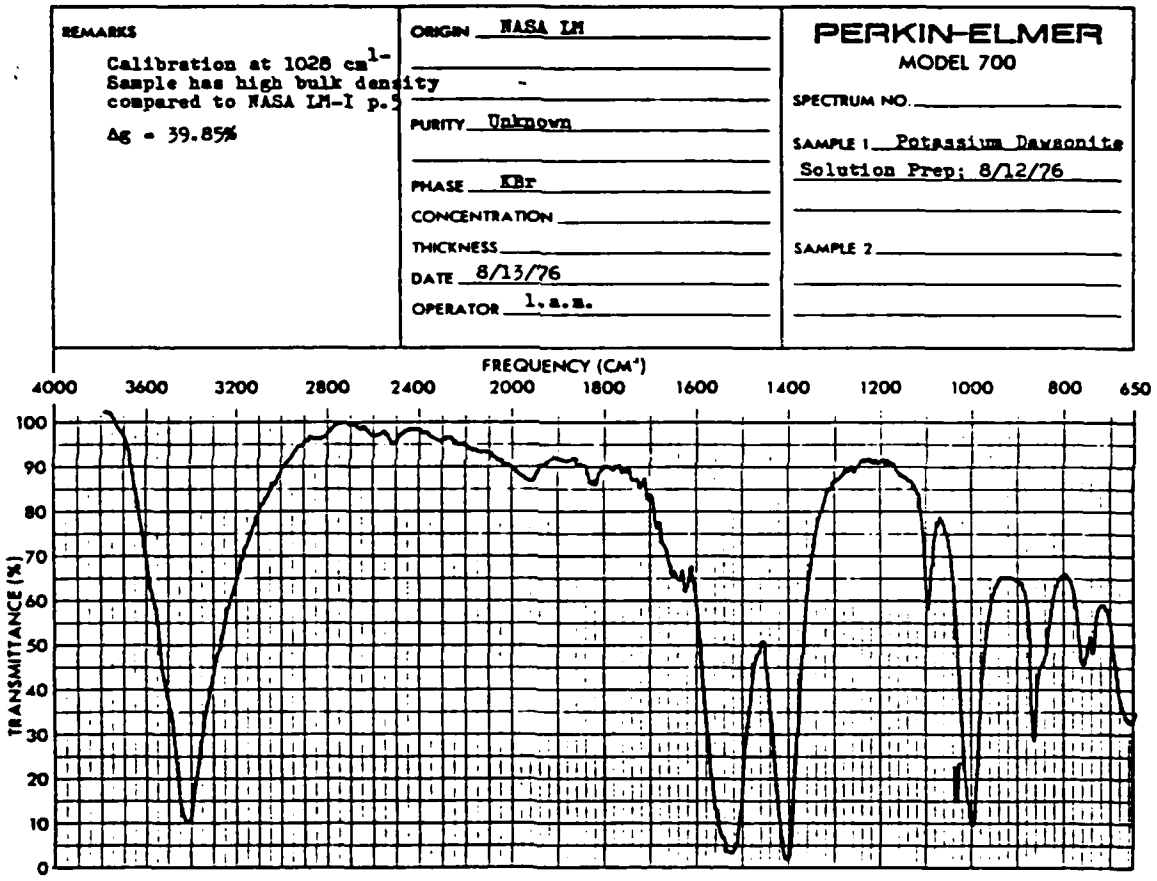

Figure A-6. Infared Spectrum of the Potassium Analog of Dawsonite Synthesized by Solution Precipitation.

Table A-9. Comparison of the Infrared Bank Frequencies of the Potassium Analog of Dawsonite Prepared by Calcining and Solution Precipitation.

Calcining method, cm^{-1}	Intensity	Solution preparation method, cm^{-1}
3423	s	3420
1533	vs	1525
1408	vs	1405
1103	w	1095
1000	s	1000
870	m	865
846	w	840(sh)
761	w	760
743	w	740

Legend:
s = strong
vs = very strong
w = weak
m = medium

THERMOGRAVIMETRIC ANALYSIS

Figures A-7, A-8, and A-9 show the experimentally determined integral weight loss TGA curves obtained for the potassium analogs of Dawsonite formed by low temperature soluiton preparation (T = 80°C), high temperature solution preparation (T = 135°C) and calcination methods, respectively. Temperature versus percent weight loss data at selected intervals was taken directly from the original traces and recorded in Table A-10. It is concluded from this data that the analog prepared by calcination exhibits an overall weight loss profile more analogous to the model postulated in Table A-1. Compared to calcining, the products obtained by solution precipitation methods show diminished thermal stability prior to the first major endothermic decompostion that occurs at approximately 300°C. Figures A-10 and A-11 show combined typical differential as well as integral weight loss curves characteristics of analogs prepared by low temperature solution methods and calcination methods, respectively. Thus, it has been shown that the product obtained by the process of calcination possesses greater thermal stability prior to the major endotherms and the transition temperatures attending these decompositions are measurably higher.

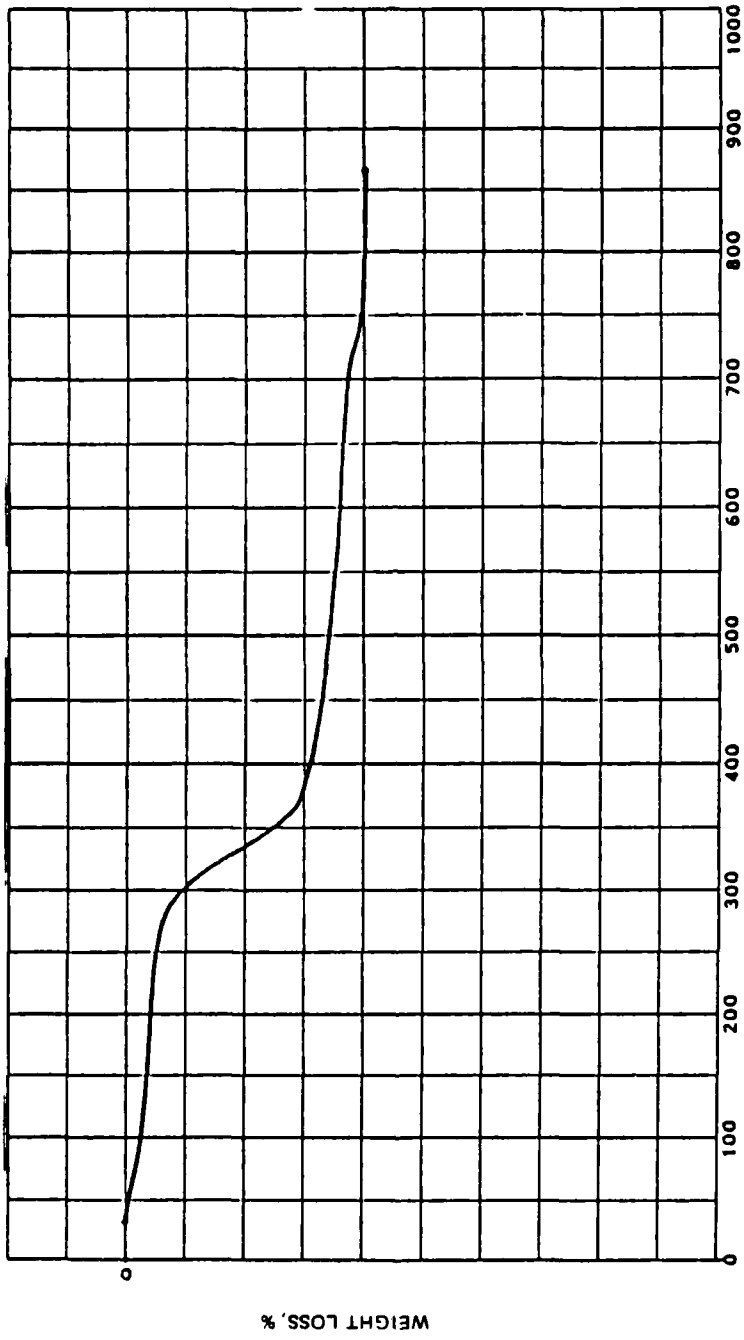

Figure A-7. TGA Curve for Potassium Analog of Dawsonite (Low Temperature Solution Preparation).

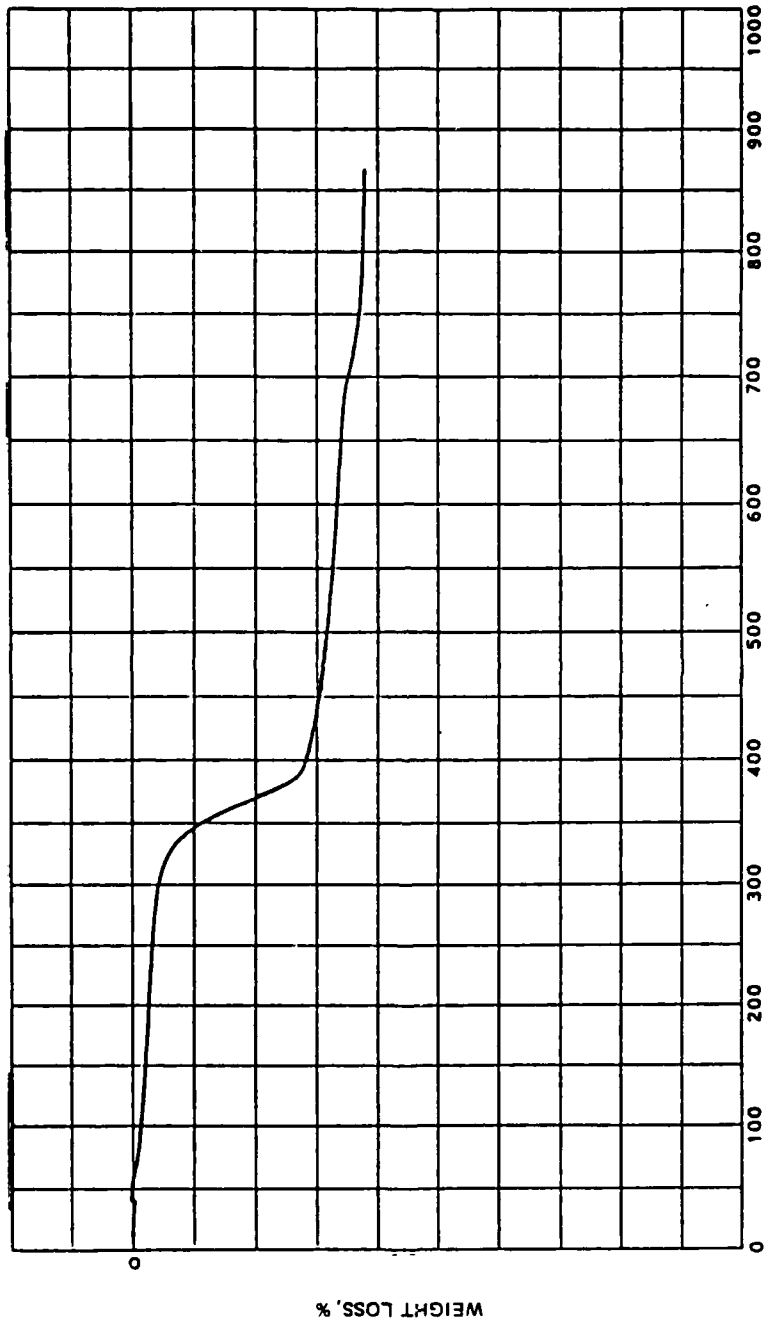

Figure A-8. TGA Curve for Potassium Analog of Dawsonite (High Temperature Solution Preparation).

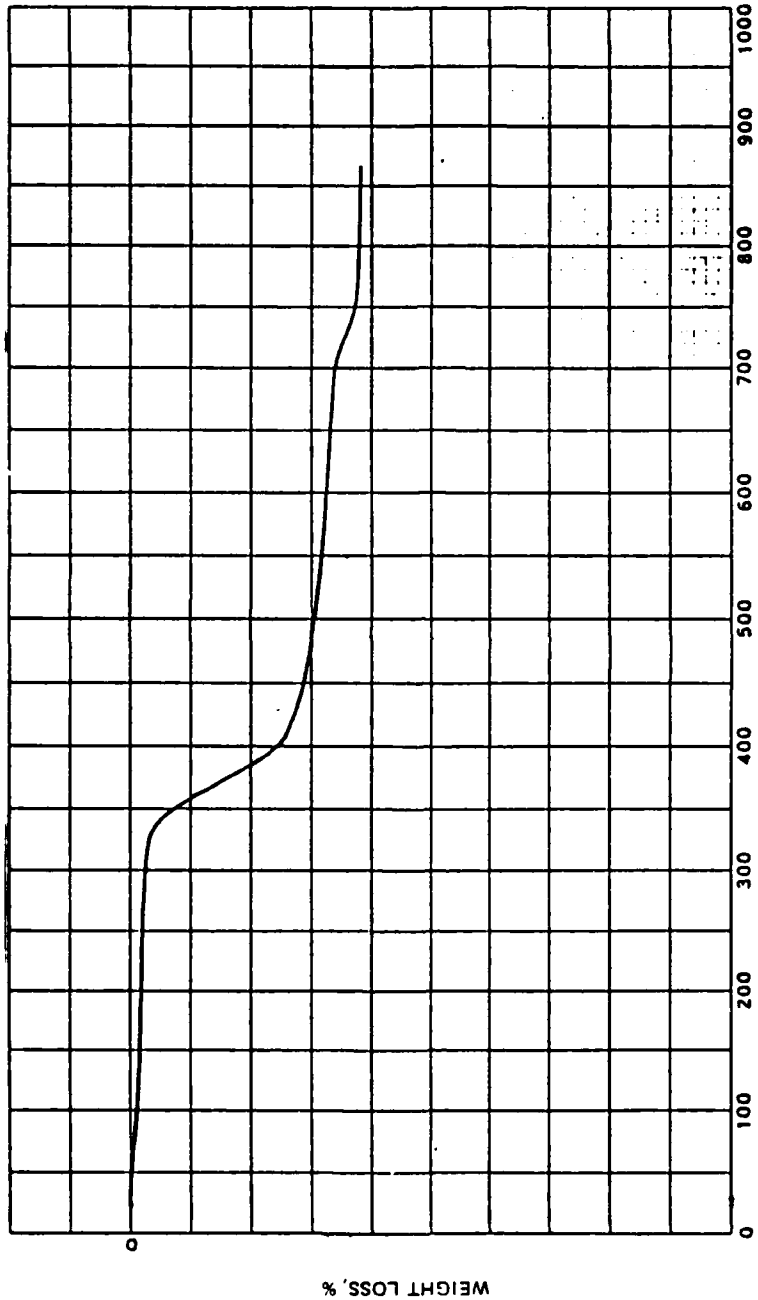

Figure A-9. TGA Curve for Potassium Analog of Dawsonite (Calcination Preparation).

Table A-10. Thermolysis of the Potassium Analogs of Dawsonite Formed by Solution Precipitation and Calcination. (Comparative Weight Loss Profiles)

Point	Low temperature solution preparation		High temperature solution preparation		Calcination preparation	
	Percent	Temperature, °C	Percent	Temperature, °C	Percent	Temperature, °C
A	6	290	4	330	3	340
B	18	330	16	360	16	375
C	32	370	30	390	29	410

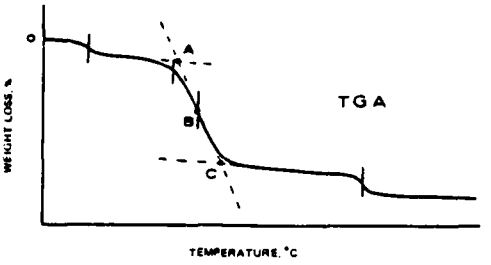

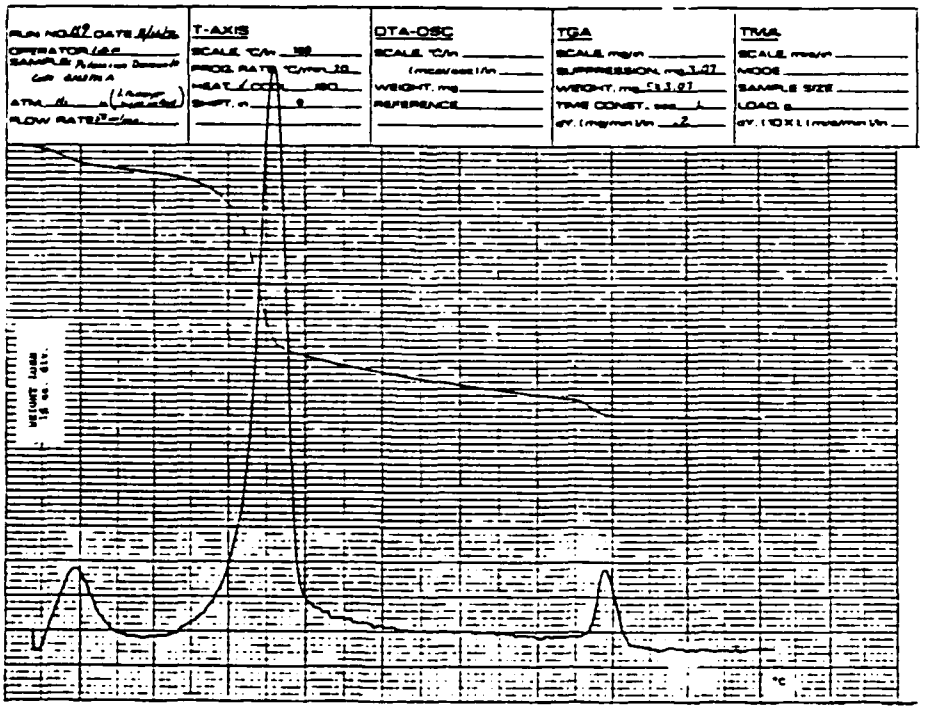

Figure A-10. Integral and Differential Gravimetric Analysis Curves for the Thermolysis of the Potassium Analog of Dawsonite Prepared by Low Temperature Solution Precipitation.

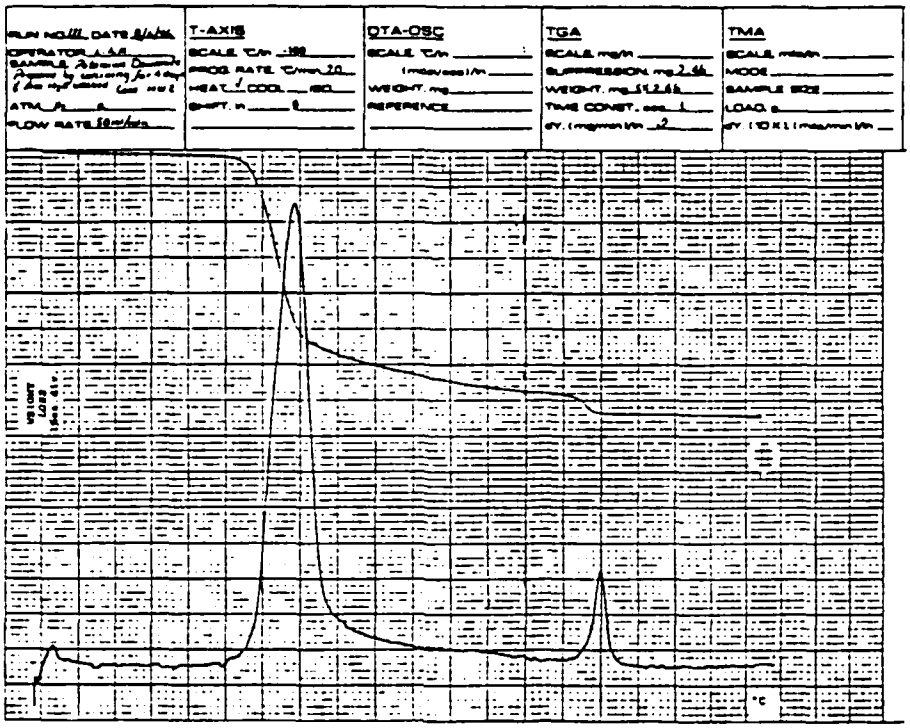

Figure A-11. Integral and Differential Gravimetric Analysis Curves for the Thermolysis of the Potassium Analog of Dawsonite Prepared by Calcination.

THERMOCHEMICAL BEHAVIOR

Using DSC (differential scanning calorimetry) techniques and potasium hydrogen carbonate as a reference comparison, the heat changes attributable to the first major endotherm of potassium Dawsonite decomposition was measured and determined to be 30 ± 2 kcal/mole, a change equivalent to that upon going from System I to System IV as shown below. The endothermic minimum occured at 340°C. Although at high temperatures (725°C), the final decomposition species is potassium aluminate, $KSlO_2(c)$, it is probable that the decomposition phase at 340°C is amorphous (References 48 and 80) and has a composition corresponding to System IV (see Table A-1).

ENDOEXO	ΔH_f° (Kcal/mol)
I	-551 $KAlO(OH)HCO_3(c)/H_2O(l)$ (min. est.)
II	-536 $KHCO_3(c)/Al(OH)_3(c)$
III	-533 $KHCO_3(c)/AlO(OH)(c)/H_2O(l)$
IV	-521$(0.5K_2CO_3 \cdot 0.25Al_2O_3 \cdot 0.5AlO(OH))(am)/0.5CO_2(g)/1.75H_2O(l)$ (min. est.)

In the inset above, System I comprises products in the potassium Dawsonite calcination synthesis; System II consists of the reactants, whereas System III represents the products of a competitive decomposition side reaction.

The formation enthalpies for Systems II and III were computed from thermochemical data of Reference 81. A min. est. (minimum estimate) for System IV was arrived at by computing the formation enthalpy for the following:

$$0.5K_2CO_3(c)/0.25Al_2O_3(c)/0.5AlO(OH)(c)/0.5CO_2(g)/1.75H_2O(l)$$

To be sure, this computation underestimates the actual formation enthalpy by an amount equilvalent to the enthalpy of species interaction minus a smaller enthalpy change attributable to the change in lattice structure, according to the equation below.

$$0.5K_2CO_3(c) + 0.25Al_2O_3(c) + 0.5AlO(OH)(c) \longrightarrow$$

$$0.5K_2O_3 \cdot 0.25Al_2O_3 \cdot 0.5AlO(OH)(am)$$

Utilizing, the minimum estimate for System IV and the measured value of the change on going from I $\longrightarrow$ IV, it can be concluded that the formation of the potassium analog of Dawsonite form Gibbsite and potassium hydrogencarbonate is in fact exothermic, confirming recent observations (Reference 82).

X-RAY DIFFRACTION ANALYSIS

A typical X-ray diffraction spectrum of the potassium analog of Dawsonite prepared by the method of calcining is depicted in Figure A-12. The 12 major peaks observed at reflections between 10 and 50 degrees are compared in Table A-11 to the previously published data. Various differences between the observed data disclosed in this investigation and the previously published data are summarized below.

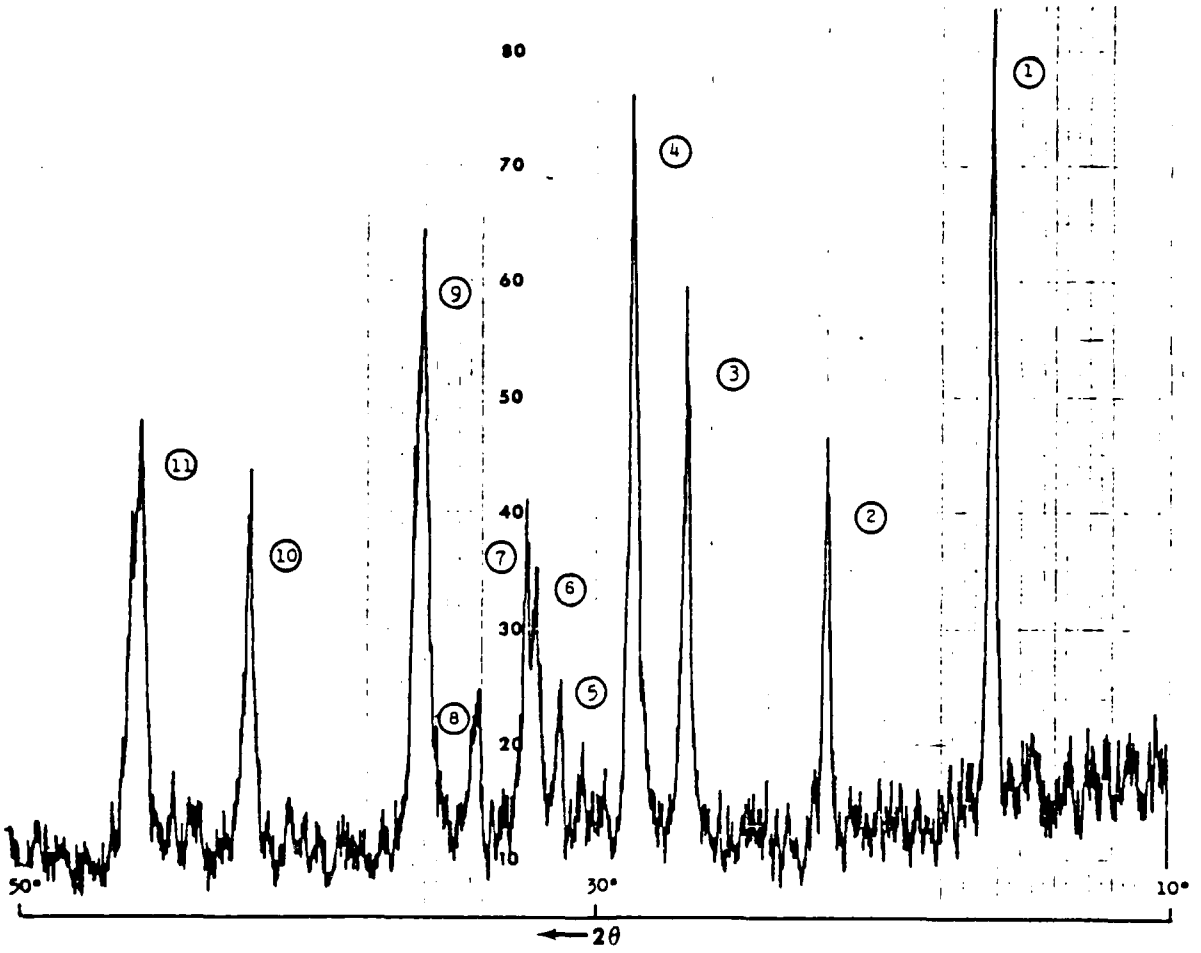

Figure A-12. Typical X-ray Diffraction Spectrum of the Potassium Analog of Dawsonite Prepared by Calcination.

Table A-11. Comparison of "d" Spacings for the Potassium Analog[a] of Dawsonite Prepared by Different Methods.

Solution Preparation Methods				Composite literature average	Calcining Method NASA empirical values
Reference 55			Reference 46		
Specimen 2	Specimen 3	Specimen 4			
5.68					5.985 (1)
5.55	5.58	5.55	5.58	(5.57)	5.574 (2)
4.13	4.08	4.10	*b*	(4.10)	4.105 (3)
3.39	3.34	3.33	3.37	(3.36)	3.370 (4)
3.14	3.18	3.14	3.15	(3.15)	3.153 (5)
				c	2.889 (6)
2.82	2.83	2.82	2.79	(2.82)	2.818 (7)
				c	2.788 (8)
2.64	2.65	2.65	2.65	(2.65)	2.644 (9)
2.53	2.53	2.50	2.50	(2.52)	2.518 (10)
	2.21		2.24	(2.23)	*d*
2.15	2.17	2.15	2.17	(2.16)	2.168 (11)
1.96	1.98	1.98	1.99	(1.98)[e]	1.996 1.985 (12)

[a]For substances having composition $KAl(OH)_2CO_3$.

[b]Although a reflection at 2θ = 21.65 degrees (4.105A) is not reported by the French work of Reference 46, a potassium analog of Dawsonite synthesized according to their published method did yield an X-ray diffraction spectrum analogous to the NASA empirical spectrum, including the reflection at 2θ = 21.65 degrees.

[c]Although neither the 30.92 degree nor the 32.11 degree lines are reported in the prior literature (corresponding to d = 2.889 and 2.788A, respectively), when the potassium analog of Dawsonite is prepared according to the literature methods of References 46 and 55, these lines are seen in the materials resulting from both preparations. Earlier studies may have ascribed these lines to closely matching potassium bicarbonate and potassium carbonate lines, respectively, although neither line corresponds to the principal peak of either of these substances. Experimentally, the 30.92 and 32.11 degree lines cannot be removed by washing; calcining experiments in which the bicarbonate or carbonate was present as a limiting reactant and Gibbsite was present in 25% molar excess yielded products that displayed both of these reflections.

[d]It is to be noted that a reflection corresponding to 2.23A is reported by both previous studies. However, a repeat of the method published in Reference 55 whereby the potassium analog of Dawsonite is formed from elemental Al(s) added to aqueous hot potassium carbonate solution, yielded a product which showed significant amounts of potassium Dawsonite, Gibbsite, and Bayerite, the most intense line of the Bayerite occurring at 2.22 A.U. It was subsequently established by our studies that pure potassium Dawsonite showing no Gibbsite or Bayerite (and no line corresponding to 2.22 A.U.) can be obtained by simply prefiltering the reaction mixture prior to the solution precipitation of potassium Dawsonite, which occurs slowly.

Previous X-ray diffraction and electron microscopy studies (Reference 73) on $KAlO_2$ (aq)/CO_2 systems have established unequivocally that Bayerite and Gibbsite can both form concurrently. Bayerite and Gibsite are different crystal structure forms of $Al(OH)_3$(c) (i.e., a formula that can be written as $Al_2O_3 \cdot 3H_2O$(c)). The formation ratio of these product species is temperature dependent, the Gibbsite/Bayerite ratio increasing with increasing temperature in the 60 to 100°C range. The solution concentrations and concentration ratios of reacting species in this system were, by design, not optimized in favor of Dawsonite analog precipitation.

[e]The reflection in our spectra near 1.99A is usually seen as a broad asymmetric peak that most frequently is observed as a partially resolved pair; infrequently it appears resolved into a trio of peaks, whereas at other times it is observed as a single peak.

LATTICE PARAMETERS

Computer analysis of the powder pattern reflection data of the potassium analog of Dawsonite by the method of J. W. Visser (References 74 and 75) has yielded probable sets of unit cell parameters. Thus, existence of a well defined phase behavior of the potassium analog has been established. Limitations in instrumental precision and the accuracy of the method of internal standards did not allow unambiguous assignment of the unit cell parameters, hence, Table A-12, which compares lattice parameters of Dawsonite (References 62, 76–78) with its potassium, rubidium (Reference 79), and cesium (Reference 80) analogs, depicts two equally probable solutions. Although the two solutions shown in this table came from different samples, no correlation between calcination conditions and unit cell parameters was observed for the numerous indexings that were achieved. Whenever solutions and indexing was achieved for a sample, an orthorhombic system was the most likely of all crystal systems to be assigned and invariably has a higher figure of merit than other solutions.

Table A-12. Dawsonite and Its Analogs.
(Lattice Parameters Summary for General
Formula $\underline{M}Al(OH)_2CO_3$)

Metal $\underline{M}$	System		Unit cell	
		a° b° c°	alpha beta gamma	Volume A^3
Na	Ortho	6.7(4) 10.4(0) 5.5(8)	90.00 90.00 90.00	392
K	Mono/Ortho	11.945/6.310 6.309/11.976 5.644/5.645	90.00/90.00 90.325/90.00 90.00/90.00	425/427
$Rb \cdot 1/2H_2O$	Ortho	6.77 12.7 5.70	90.00 90.00 90.00	490
$Cs \cdot H_2O$	Ortho	7.04 13.1 5.74	90.00 90.00 90.00	554

MOISTURE PICKUP/LOSS CHARACTERISTICS

Potasssium Dawsonite prepared according to the detailed procedure previously described, was subjected to a set of hyper-humidity and hypo-humidity studies. In the high-humidity test, the material was confined to a closed system (desiccator) into which had been placed a reservoir of water sufficient in quantity to provide maximum moisture saturation at ambient temperature, ca. 23°C. During the test periods of 24 and 48 hours, the percent weight gain was 0.98 and 1.62%, respectively. In the low-humidity test, the material was similarly confined, however, a reservoir of concentrated sulfuric acid replaced the water and provided a dehydrating environment. During the test periods of 24 and 48 hours, the percent weight loss was observed to be 0.34 and 0.40%, respectively.

SUMMARY

The prior literature on the potassium analog of Dawsonite has been reviewed and summarized. Previously reported work addresses the following aspects: solution procedures for the synthesis of the analog; composition studies; themogravimetric decomposition behavior; infrared analysis; solubility and hydrolysis properties; and partial X-ray diffraction characterizations.

The work reported herein discloses the investigation and optimization of a new and efficient single-step method, (viz, calcination) for the synthesis of the potassium analog of Dawsonite in high purity and high yield. The analog obtained by calcination was characterized according to its composition, infrared, thermogravimetric, and X-ray diffraction properties, and also compared and contrasted to the corresponding product obtained via solution precipitation procedures.* In nearly all respects, the characteristics of the potassium analog of Dawsonite prepared by calcination are comparable to those of the material obtained via high-temperature solution precipitation; a measurable property differential is observed, however, in their repective TGA profiles. Whereas the analog prepared by calcination exhibits an overall weight loss profile closer to a postulated model, the product obtained by solution precipitation shows diminished thermal stability and greater weight loss prior to the first major endothermic decomposition that occurs around 300°C.

The effort accorded the investigation and characterization of the potassium analog of Dawsonite formed via calcination has thus realized the following:

1. The technological basis for an efficient and simple means of its production in reasonable quantities.

2. Definitive characterization of the product produced in the above manner.

3. A foundation for further investigations of iodide doped potassium Dawsonite systems.

*Crystalline phase behavior has been established and probable lattice parameters have been determined.

SYNTHESIS AND CHARACTERIZATION OF IODIDE DOPED POTASSIUM DAWSONITE

INTRODUCTION

The premise underlying halogen doping of the potassium analog of Dawsonite rests on the well known scavenging of radical flame species by halogens. Potentially, highly effective and efficient fire suppressants and reignition retardants might consist of radical scavenging and recombination catalysts that, as "guests" in a host substance are thermally released upon entry into and partial retention within a combustion zone. A substance of this type or combination of substances would not only have the potential to quench a fire, but the potential to suppress the reignition of the conflagration through a modulated release of quenching components. Substances having these properties could potentially be achieved by stoichiometric encapsulation of an active fire retardant within the structure of a crystalline inorganic substance. An effective fire retardant agent of this type might utilize a layered-structure host compound which, it is asserted, would allow a guest compound such as an inorganic halon, to become inserted into or substituted within available lattice sites. The host compound should have the potential to decompose in the combustion zone with the attendant release of the guest compound (flame-quenching agent). Alternatively, a microcrystalline nonstoichiometric enclathration of an active flame retardant by the crystalline environment of a thermally labile host compound might also serve to modulate the release of quenching components into the combustion zone. A third type of system might involve the use of a simple physical mixture of an active component which is nonadhesively interspersed in the particle voids of the host compound.

It is the first of these three hypotheses that is to be investigated here. Such a flame retardant guest/host compound is to be sought by a solid-phase synthetic procedure utilizing conditions of elevated temperature and pressure. The resultant species realized from these procedures are to be characterized by various spectrophotometric, gravimetric, and chemical analysis techniques with the intention of gaining information as to the nature of their composition and microenvironments. This will lead to an increased understanding of the method of modulation of flame quenching components. The system currently being investigated as the host environment is the potassium analog of Dawsonite. The use of iodides as potential guest agents within the potassium Dawsonite structure will be examined. Iodides are well known as flame quenching agents and are therefore good candidates for interstitial encapsulation or enclathration. Tin iodides and potassium iodide will serve as potential sources for the iodide. In particular, tin(IV) iodide has a high volatility, which is desirable for rapid release of the iodide into the combustion zone. Relative ease of synthesis also makes this compound a favorable choice.

The method of synthesis in pursuit of these guest/host compounds will follow the procedure for the synthesis of potassium Dawsonite as described in a previous section of this paper. Varying mole ratios of KD/SnI_4* will be physically mixed. Each mixture will be

*KD refers to potassium Dawsonite.

divided into two samples with one sample to be calcined at high temperature and pressures. The physical mixtures and their calcined counterparts will be characterized by infrared spectrometry, X-ray diffraction spectrometry as well as chemical analysis and TGA. For reasons to be enumerated subsequently, SnI_2 was not the subject of this guest/host investigation.

Tin(II) Iodide and Tin(IV) Iodide

Under normal conditions tin iodide can exist in two forms. Stannous iodide has the formula SnI_2 and the other moiety, stannic iodide, has the formula SnI_4. Both can be prepared by the direct combination of tin metal and elemental iodine (References 85, 88). Stannic iodide volatilizes at 180°C while stannous iodide remains fixed at red heat (Reference 81). At 327°C, stannic iodide has a vapor pressure 3000 times that of stannous iodide (Reference 82). Stannous iodide has a melting point of 320°C and a boiling point of 720°C. Stannic iodide has a melting point of 143.5°C and a boiling point of 340°C. SnI_2 and SnI_4 have densities of 5.29 and 4.70 g/cm^3, respectively (Reference 81). When crystallized from aqueous solution, stannous iodide contains 2 molecules of water. When dried over sulfuric acid the monohydrate is formed (Reference 81). The crystal structure of both moieties have been reported (Reference 83–85). Meller and Fankuchen report stannic iodide as belonging to the space group Pa3. The unit cell is cubic with $a_0 = 12.26A$. An earlier work by Dickinson reports $a_0 = 12.23A$. Howie, et. al. report stannous iodide as being monoclinic with cell dimensions of:

$a = 14.17$
$b = 4.535$
$c = 10.87$
$\beta = 92.0°$

Stannous iodide belongs to the space group C2/m (Reference 85). Infrared studies on stannic iodide indicate only two active bands at 219 cm^{-1} and 71 cm^{-1} (Reference 86). Observed Raman shifts for stannic iodide occur at $v_1 = 149\ cm^{-1}$, $v_2 = 47\ cm^{-1}$, $v_3 = 216\ cm^{-1}$, and $v_4 = 63\ cm^{-1}$ (Reference 87). Stannic iodide is stable in air, under prolonged contact with moist air SnO_2 is formed (Reference 88). Stannous iodide is known to be sensitive to atmospheric oxidation (Reference 85). Exposure to X-rays also accelerates the decomposition of stannous iodide (Reference 85). X-ray diffraction spectra of both SnI_2 and SnI_4 have been reported, see Tables 37 and 38 (Reference 89).

EXPERIMENTAL

PREPARATION OF TIN IODIDES

Recrystallization of Stannous Iodide

Stannous iodide was obtained from ROC/RIC chemical supplier. Purity was checked by chemical as well as X-ray diffraction analysis. Stannous iodide was then purified by recrystallization from 2 M HCl. The recrystallization procedure follows that as described by Howie, et. al. (Reference 85). The purified product was stored in a nitrogen-filled brown glass bottle which was kept in a vacuum desiccator. Recrystallized product identity and purity were established by X-ray diffraction and TGA.

Synthesis of Stannic Iodide

Pure stannic iodide was prepared by the direct combination of tin and elemental iodine in carbon tetrachloride solvent (Reference 88). The carbon tetrachloride solvent was evaporated off by gentle heating. The stannic iodide obtained was stored in a nitrogen-filled brown glass jar which was placed in vacuo over calcium chloride. Product purity and identity were confirmed by elemental analysis for tin and iodine, and by X-ray diffraction and TGA.

Reactions of Tin Iodides with Potassium Dawsonite

Varying mole ratios of tin(IV) iodide and potassium Dawsonite were mixed and subjected to calcination. The reaction bomb is the same as that used for potassium Dawsonite syntheses. Potassium Dawsonite and tin(IV) iodide were finely ground and made to pass through an ASTM #325 mesh sieve. Samples of each were weighed accurately and various mole ratios were mixed together. The physical mixtures were ground and mixed together until the mixture was homogeneous. The mixture was placed in a 20-ml glass beaker with a watch glass placed on top. The beaker with sample was placed into the reaction vessel along with 10 ml of water which was placed on the bottom of the reaction vessel. The reaction vessel was sealed and flushed with carbon dioxide gas. Carbon dioxide pressure was brought to 240 psi at room temperature. The reaction vessel was allowed to come to a constant temperature of 240 ± 5°C with a corresponding CO_2 and H_2O pressure of 600 ± 25 psi. The calcination was allowed to continue for 18 ± 2 hours. The reaction bomb was cooled rapidly (approximately 1/2 hour) and the sample was removed when bomb conditions came to equilibrium with the surrounding evnironment. The sample was dried in vacuo over calcium sulfate at room temperature. Products obtained were ground in a mortar and were passed through a 325 mesh sieve. Products were characterized by infrared spectrometry, TGA, and X-ray diffraction. Physical mixtures of the same mole ratios of SnI_4/K-Dawsonite were made homogeneous and characterized by IR, TGA, and X-ray diffraction.

Calcination of Aluminum Hydroxide, Potassium Bicarbonate and Potassium Iodide

A physical mixture of aluminum hydroxide, $Al(OH)_3$, potassium bicarbonate, $KHCO_3$, and potassium iodide, KI, was ground and made homogeneous in the mole ratio of 1 mole $Al(OH)_3$ to 1 mole $KHCO_3$ and a corresponding amount of KI that would be necessary to equal the amount of iodine in a mixture of potassium Dawsonite and 10% SnI_4 (the relative proportions by weight are 100.12/78.00/15.7, respectively, $KHCO_3$/$Al(OH)_3$/KI). The mixture was calcined under the same conditions as that of the calcination of potassium Dawsonite as described earlier. The calcined product was characterized by X-ray diffraction.

PRODUCT SEPARATION PROCEDURES

Separation of Components of 1:1 Mole Ratio (Potassium Dawsonite/Tin Iodide) Calcined Product

Components of the above product were separated according to their selective solubilities in carbon tetrachloride and water. Hot carbon tetrachloride was used to extract out any unreacted tin(IV) iodide. Cold water was used to remove any water soluble iodide. The remaining components were not soluble in either hot carbon tetrachloride or cold water. Components were characterized by X-ray diffraction.

Iodine Content of Potassium Carbonate/ Aluminum Hydroxide/Potassium Iodide Calcined Product

The KI of the $KHCO_3/Al(OH)_3$/KI calcined product was extracted with water from the remaining components. The iodine content was determined using a procedure described subsequently in this paper.

Infarared Spectra

The infrared spectra of potassium Dawsonite, crude product before cold water washing, and washed potassium Dawsonite were taken using a Perkin Elmer 700 IR spectrophotometer. Samples for infrared were prepared by grinding a small quantity of the sample into a ten-fold amount of thoroughly dried KBr. The KBr/potassium Dawsonite sample was completely mixed and a pellet was made using a pellet press. A reference pellet of KBr was used during the infrared measurements in order to cancel out any effects of KBr in the sample pellet. The products obtained from the potassium Dawsonite/tin(IV) iodide calcinations also had their infrared spectra obtained by the same procedure as described above.

Thermogravimetric Analysis

A duPont 990 thermal analyzer in conjunction with a duPont 951 thermogravimetric analyzer was used to obtain integral as well as differential thermogravimetric curves. Temperatures ranged from room temperature to 900°C. A heating rate of 10°C/min was used. Sample weights varied from 10 to 25 mg. Platinum pans, usually used for such procedures, were replaced with silica pans because of the high reactivity of platinum with iodine at elevated temperatures.

X-Ray Diffraction

A Norelco X-ray diffraction unit was used for obtaining X-ray powder diffraction patterns. Copper radiation with a K-alpha value of 1.5418 nm was used as the X-ray source. All samples were prepared in the following manner: each sample was finely ground until the entire sample passed through a 325 mesh sieve. An aluminum sample holder with a rectangular hole was placed on a glass slide (large enough to block the entire opening in the aluminum sample holder). The Pass-325 mesh sample was placed into a 120 mesh sieve which covered the aluminum holder (exposed hole facing up). The sample was sifted through the sieve until it totally covered the hole in the aluminum sample holder. The sample was tamped down lightly and the excess carefully removed with a razor blade. The excess was placed into the 120 mesh sieve and the process repeated. The whole process was repeated another time, except that the sample was firmly pressed into the hole before the excess was removed. The exposed side of the sample holder was then covered with another glass slide and the "sandwiched" sample holder was intverted. The uppermost glass slide (originally the lower) was removed, and the newly exposed sample surface was used for the X-ray diffraction analysis. The aluminum holder plus sample was placed into the X-ray diffractometer and subjected to X-rays over a 20 range of 10 to 50 degrees. LiF was used as an internal standard.

Chemical Analysis

Chemical analysis procedures were developed for potassium, aluminum, carbonate, tin, and iodine content. For potassium Dawsonite samples, potassium content was measured by atomic absorption; aluminum content was determined by EDTA titration; total carbonate was determined by making samples acidic and collecting the CO_2 gas on an "Ascarite®" column and measuring weight gain. Tin analyses were carried out on the tin iodides as follows:

1. A small quantity of a sample to be analyzed was weighed accurately and dissolved in concentrated NH_4OH. The solution was heated until only a white residue remained. The solution was allowed to cool whereupon dilute nitric acid was added dropwise until the solution turned red using methyl red indicator. Dilute NH_4OH was added dropwise until the solution just changed to a yellow color. After reheating for a few minutes, the precipitate was filtered using Whatman #40 filter paper. The precipitate (SnO_2) was

washed with warm 2% NH_4OH. Both the precipitate and filtrate were collected quantitatively. Ashing of the filter paper and ignition at 1000°C for 1 hour, followed by cooling in a desiccator yielded pure SnO_2. The iodine content of the sample remained in the filtrate. Concentrated NH_4OH was added to the filtrate until the final volume was approximately 300 ml. A small excess of $AgNO_3$, required to precipitate all of the iodide, was added to concentrated NH_4OH (50 ml). This was added to the filtrate slowly using a thymolphthalein indicator. The solution was heated for 2 hours, whereupon it was allowed to cool to room temperature and stand overnight (placed in the dark). AgI was filtered through a fine sintered glass crucible, washed with cold water and dried at 110°C for 3 to 4 hours. The sample was weighed as AgI.

RESULTS

CHEMICAL ANALYSIS

Purification of Stannous Iodide by Recrystallization

Chemical analysis of the tin(II) iodide as received by the supplier was significantly inconsistent with the calculated values (see Table A-13). X-ray diffraction spectra indicated that in addition to the presence of tin(II) iodide, there was considerable tin(IV) iodide as well as some unidentified species. Recrystallization according to the method of Howie, et. al., yielded a crystalline yellow-orange product. All purified samples were stored in nitrogen-filled brown glass containers which were placed into a vacuum desiccator. Although purified tin(II) iodide exhibited TGA and X-ray diffraction characteristics closely resembling literature data (see Figure A-13 and Table A-14), routine exposure of the purified product to ambient conditions of temperature, light, air, and/or moisture initiated rapid degradation of the product.

Table A-13. Chemical Analysis of Stannous Iodide and Stannic Iodide.

Stannic Iodide (SnI_4)	
Theoretical, %	Washed product, %
Sn = 18.95 I = 81.05	Sn = 19.27 ± 0.1 I = 80.79 ± 0.1
Stannous Iodide[a]	
Theoretical, %	Sample, %
Sn = 31.86 I = 68.14	Sn = 34.11 ± 0.3 I = 63.71 ± 0.1

[a] SnI_2 from the supplier was found to be impure due to oxidation.

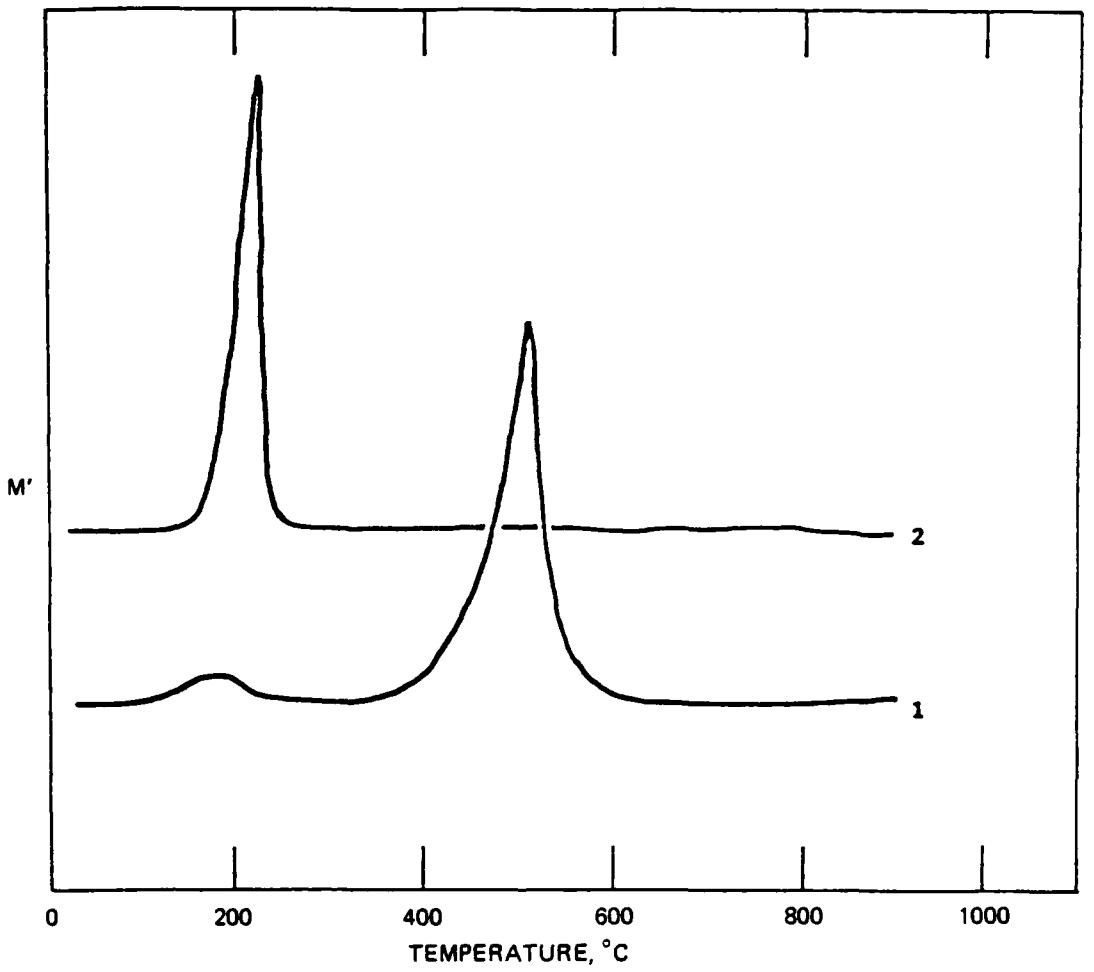

Legend:
Line 1: Stannous Iodide
Line 2: Stannic Iodide

Figure A-13. Differential Gravimetric Analysis Curves for the Thermolysis of Stannous Iodide and Stannic Iodide.

Stannic Iodide Synthesis

Tin(IV) iodide synthesized according to the method of McDermot (Reference 88), yielded an orange-red product whose elemental analysis, TGA, and X-ray diffraction spectrum as shown in Table A-13, Figure A-13, and Table A-15, respectively, are consistent with authentic SnI_4. Tin(IV) iodide obtained from laboratory synthesis was found to be relatively insensitive to laboratory environmental conditions. Moist air, however, is reported to slowly hydrolyze it, therefore the product was also stored in the same manner as tin(II) iodide. Stannic iodide stored this way remained unchanged for months. Since stannic iodide exhibits considerably less environmental sensitivity than stannous iodide, calcination reactions with potassium Dawsonite were performed with stannic iodide and not stannous iodide.

Table A-14. 2θ Values and Relative Intensities for the X-ray Diffraction Spectra of Tin(II) Iodide (SnI_2). (Laboratory Preparation and Literature Reference[a])

2θ		Relative intensity	
Observed	Literature	Observed	Literature
15.30	15.20	50	40
24.70	24.59	34	35
25.23	25.16	18	40
26.85	26.77	35	40
27.32	27.27	83	100
28.22	28.15	100	90
28.79	28.89	29	40
29.62	29.58	12	20
31.78	31.71	15	20
32.74	32.62	19	25
39.42	39.31	28	40
41.10	41.04	30	70
41.80	41.74	14	40
	41.84		30
42.38	42.29	19	30

[a]The relative intensities are taken from the indexed ASTM catalog card number 25-975. The 2θ values were calculated using a lambda value of 1.5418.

Table A-15. 2θ Values and Relative Intensities for the X-ray Diffraction Spectra of Tin(IV) Iodide (SnI_4). (Laboratory Preparation and Literature Reference[a])

2θ		Relative intensity	
Observed	Literature	Observed	Literature
	12.48		3
	16.14	10	
17.75	17.70	10	15
25.20	25.13	100	100
	26.18		5
29.18	29.09	25	32
31.78	31.78	2	3
33.40	33.46	3	6
34.30	34.26	4	5
39.52	39.54	4	5
	40.24		4
41.68	41.62	28	41
41.75		25	
49.28	49.24	20	26
49.40		5	

[a]The relative intensities are taken from the indexed ASTM catalog card number 6-0232. The 2θ values were calculated using a lambda value of 1.5418.

CALCINATION REACTIONS

Tin(IV) Iodide with Potassium Dawsonite

Potassium Dawsonite was calcined with stannic iodide using mole ratios of 1:1, 2:1, 4:1, 5:1, and 8:1 potassium Dawsonite/stannic iodide. The 1:1 and 2:1 mole ratio calcined products were orange-brown and green-brown in color, respectively. The 4:1 calcined product was light yellow, the 5:1 and 8:1 products were white in color. All products were placed into small glass containers and stored in a desiccator. All of the precalcined physical mixtures were orange-white in color.*

Calcination of Aluminum Hydroxide, Potassium Carbonate and Potassium Iodide

Potassium Dawsonite was synthesized by calcining $Al(OH)_3$ with $KHCO_3$ in the presence of KI. The product obtained was dried in vacuo overnight and stored in a desiccator. The final product was a fine white powder.

INSTRUMENTAL ANALYSIS

Infrared Spectroscopy

Stannic iodide is not active in the infrared range from 4000 to 650 cm^{-1} (Reference 86). Potassium Dawsonite is active in this range and shows strong absorption bands at 3440, 1544, 1412, 1000, and 516 cm^{-1}. Refer to Figure A-5 for the IR spectrum of potassium Dawsonite, and Table A-2 shows the IR frequencies and assignments for potassium Dawsonite.

Infrared spectra of the 1:1, 2:1, and 4:1 mole ratio potassium Dawsonite/stannic iodide calcined products are shown in Figure A-14. The 1:1 and 2:1 mole ratio products show no potassium Dawsonite absorption bands. See Tables A-16, A-17 and A-18 for IR band assignments. The 5:1 and 8:1 mole ratio products show significant absorption bands in the strong absorption regions of potassium Dawsonite, as shown in Figure A-15. The 5:1 product has strong IR bands at 3440, 1528, 1405, and 998 cm^{-1}. The 8:1 calcined product has strong IR bands at 3425, 1525, 1410, and 995 cm^{-1}. These absorption bands correspond well to the potassium Dawsonite absorption bands at 3440, 1544, 1412, and 1000 cm^{-1}. Tables A-19 and A-20 show the IR frequencies and assignments for the 5:1 and 8:1 products. The infrared spectrum of the 4:1 mole ratio (potassium Dawsonite/stannic iodide) calcined product shows a very small excess of potassium Dawsonite. Refer to Figure A-16 for the infrared spectrum of the 4:1 calcined product as compared to the species as identified and assigned in Table A-18. Figure A-16 includes the infrared spectrum of Boehmite (AlO(OH)), β-stannic acid, and stannic oxide (SnO_2). Table A-21 gives the IR frequencies of Boehmite, stannic oxide, and β-stannic acid.

*It should be noted that tin(IV) iodide and potassium Dawsonite, when mixed and stored together as dry powders at room temperature and pressure, spontaneously generate an internal pressure within the storage container; thus, the amounts stored, the handling procedures and the type of storage container must be selected accordingly.

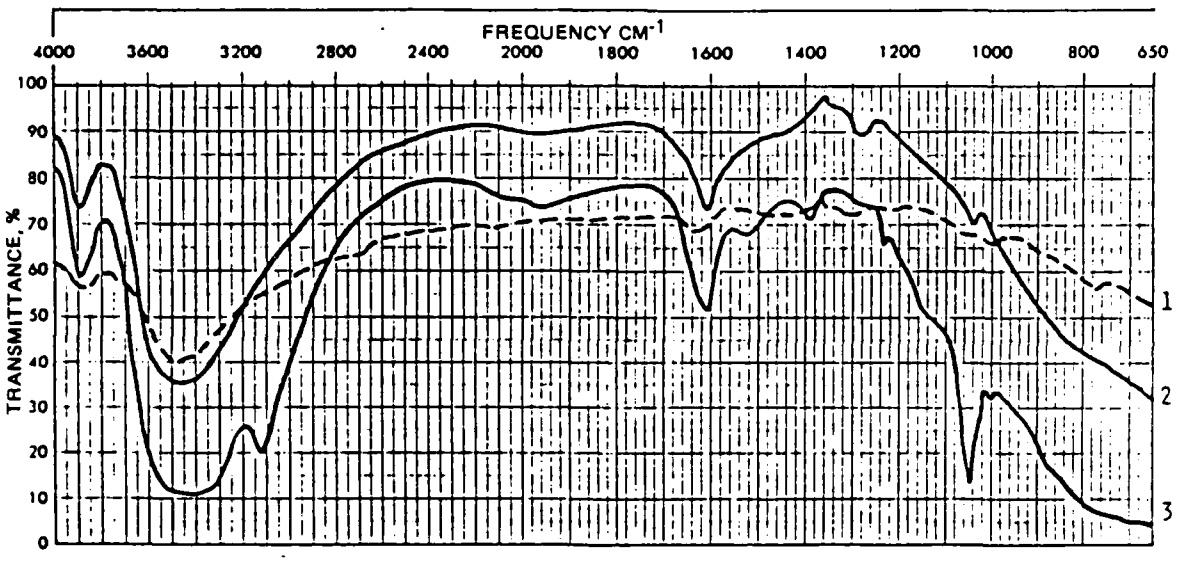

Legend:
Line 1: 1:1 MOLE RATIO
Line 2: 2:1 MOLE RATIO
Line 3: 4:1 MOLE RATIO

Figure A-14. Infared Spectra of the 1:1(1), 2:1(2), and 4:1(3) Mole Ratio (Potassium Dawsonite/SnI_4) Calcined Products.

Table A-16. IR Frequencies (in cm^{-1}) and Assignments of the Principal Bands for the 1:1 Mole Ratio (K-Dawsonite/SnI_4) Calcined Product.

IR frequencies		Assignment
Literature	Observed	
3880 m	3880 w	β-Stannic Acid/AlOOH
3880 m		
3410 s	3450 mb	β-Stannic Acid
3262 s		AlOOH
3079 s		AlOOH
1620 m	1630 w	β-Stannic Acid/SnO_2
1260 w		SnO_2/AlOOH
1145 w		AlOOH
1073 m	1070 w	AlOOH

Legend:
s = strong
m = medium
w = weak
v = very
b = broad

Table A-17. IR Frequencies (in cm^{-1}) and Assignments of the Principal Bands for the 2:1 Mole Ratio (K-Dawsonite/SnI_4) Calcined Product.

IR frequencies		Assignment
Literature	Observed	
3880 m	3880 m	β-Stannic Acid/AlOOH
3880 m		
3410 s	3430 mb	β-Stannic Acid
3262 s		AlOOH
3079 s		AlOOH
1620 m	1610 m	β-Stannic Acid
1260 w	1290 w	SnO_2/AlOOH
1145 w		AlOOH
1073 m	1070 w	AlOOH

Legend:
s = strong
m = medium
w = weak
v = very
b = broad

Table A-18. IR Frequencies (in cm^{-1}) and Assignments of the Principal Bands for the 4:1 Mole Ratio (K-Dawsonite/SnI_4) Calcined Product.

IR frequencies		Assignment
Literature	Observed	
3880 m	3875 m	β-Stannic Acid/AlOOH
3880 m		
3410 s	3415 s	β-Stannic Acid
3262 s		AlOOH
3079 s	3100 s	AlOOH
1620 m	1615 m	β-Stannic Acid
1260 w	1260 w	SnO_2/AlOOH
1145 w	1150 w	AlOOH
1073 m	1070 m	AlOOH

Legend:
s = strong
m = medium
w = weak
v = very
b = broad

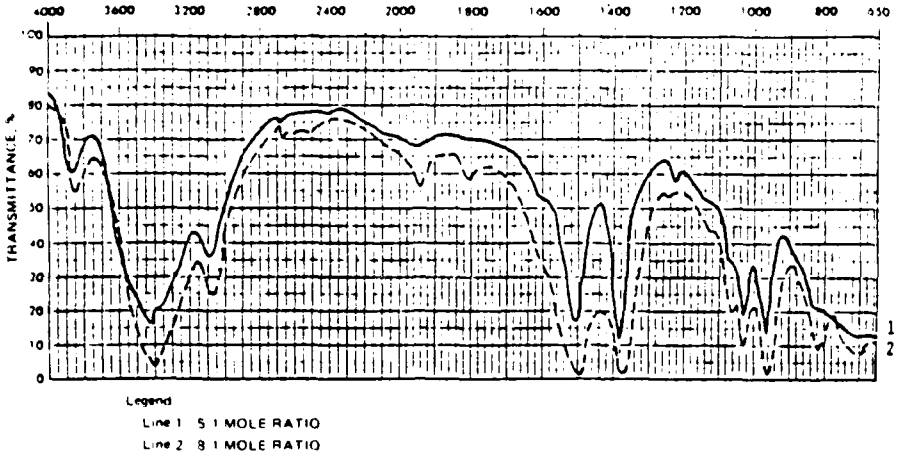

Figure A-15. Infrared Spectra of the 5:1 and 8:1 Mole Ratios of Potassium Dawsonite/SnI_4) Calcined Products.

Table A-19. IR Frequencies (in cm^{-1}) and Assignments of the Principal Bands for the 5:1 Mole Ratio (K-Dawsonite/SnI_4) Calcined Product.

IR frequencies[a]		Assignment
Literature	Observed	
3880 m	3880 w	β-Stannic Acid/AlOOH
3880 m		
3440 s	3440 sb	K-Dawsonite
3410 sb		β-Stannic Acid
3262 s		AlOOH
3079 s	3090 s	AlOOH
1620 m	1625 w	β-Stannic Acid
1544 vs	1528 vs	K-Dawsonite
1412 vs	1405 vs	K-Dawsonite
1260 w	1255 w	SnO_2/AlOOH
1145 w	1140 w	AlOOH
1073 m	1065 m	AlOOH
1000 s	998 s	K-Dawsonite

Legend:
s = strong
m = medium
w = weak
v = very
b = broad

[a] IR literature for AlOOH (Reference 11), β-Stannic Acid, and SnO_2 (Table 44) KDawsonite (Table 29).

Table A-20. IR Frequencies (in cm^{-1}) and Assignments of the Principal Bands for the 8:1 Mole Ratio (K-Dawsonite/SnI_4) Calcined Product.

IR frequencies[a]		Assignment
Literature	Observed	
3880 m	3880 w	β-Stannic Acid/AlOOH
3440 s	3425 sb	K-Dawsonite
3410 sb		β-Stannic Acid
3262 s		AlOOH
3079 s	3080 s	AlOOH
1620 m	1620 w	β-Stannic Acid
1544 vs	1525 vs	K-Dawsonite
1412 vs	1410 vs	K-Dawsonite
1260 w	1260 w	SnO_2/AlOOH
1145 w	1140 w	AlOOH
1073 m	1060 m	AlOOH
1000 s	995 s	K-Dawsonite

Legend:
s = strong
m = medium
w = weak
v = very
b = broad

[a]IR literature for AlOOH (Reference 90), β-Stannic Acid, and SnO_2 (Table 44) K-Dawsonite (Table 32).

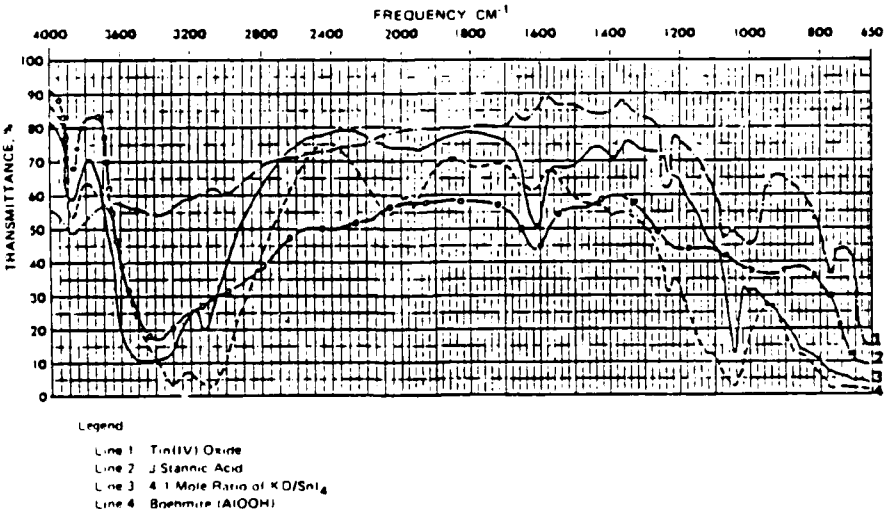

Figure A-16. Infrared Spectra for Various Solid Dry Chemicals.

Table A-21. IR Frequencies (in cm^{-1}) and Assignments of the Principal Bands of Boehmite (AlO(OH)), β-Stannic Acid ($SnO_2 \cdot xH_2O$), and Stannic Oxide (SnO_2).

Boehmite[a]	β-Stannic acid[b]	Stannic oxide
3880 m	3880 w	1260 w
3262 s	3410 sb	1080 m
3079 s	1620 m	1060 m
2080 m		790 m
1960 w		
1640 w		
1260 w		
1145 w		
1073 m		

Legend:
s = strong
m = medium
w = weak
v = very
b = broad

[a] IR frequencies for Boehmite are from Reference 90.

[b] IR frequencies for β-Stannic Acid and Stannic Oxide are from Figure 46.

Thermogravimetric Analysis of Potassium Dawsonite and Tin Iodides

The differential TGA curve of potassium Dawsonite, before washing and after washing with cold water, is shown in Figure A-17. The small peak at 150°C is absent in the washed potassium Dawsonite sample.

The TGA's of both SnI_4 and SnI_2 were taken using freshly prepared samples. This was to ensure product purity, as SnI_2 is well known for its rapid oxidation (Reference 85). Both SnI_4 and SnI_2 had only one principal weight loss peak each, as indicated in Figure A-13. SnI_2 remained relatively stable upon heating until a temperature of 390°C. At 510°C, SnI_2 undergoes its most rapid weight loss. The small weight loss at approximately 170°C is due to SnI_4 impurity in the sample. The TGA of SnI_4 shows only one large weight loss peak due to evaporation, spanning a range of 165 to 240°C. The greatest weight loss occurs at 230°C. The total weight loss was 98% for SnI_4 and 94% for SnI_2.

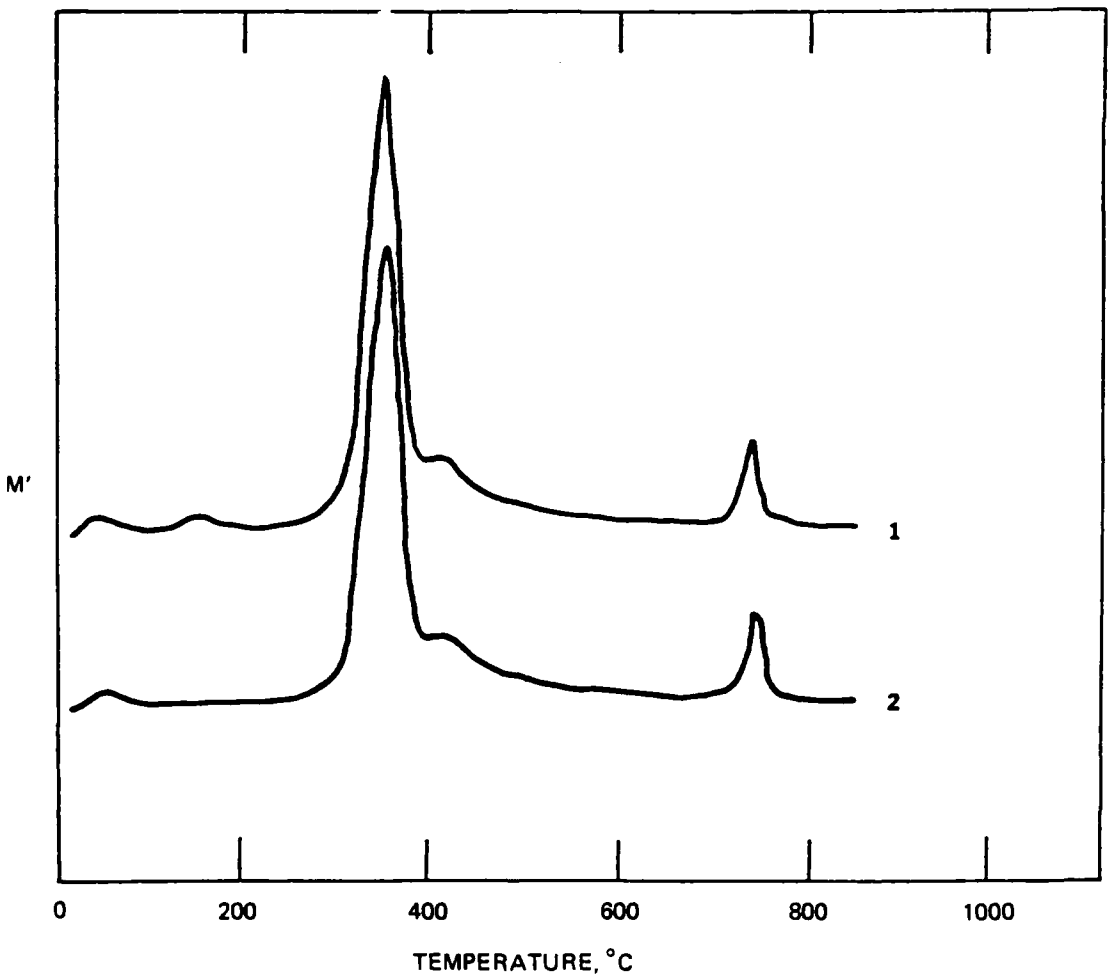

Legend:
Line 1: Before washing
Line 2: After washing

Figure A-17. Differential Gravimetric Analysis Curves for the Thermolysis of Potassium Dawsonite.

Thermogravimetric Analyses of K-Dawsonite/Tin(IV) Iodide Physical Mixtures and Calcined Mixtures

Integral and differential TGAs of physical mixtures, calcined mixtures and probable products of calcined mixtures are shown in Figures A-18, A-19, A-20, A-21, and A-22.

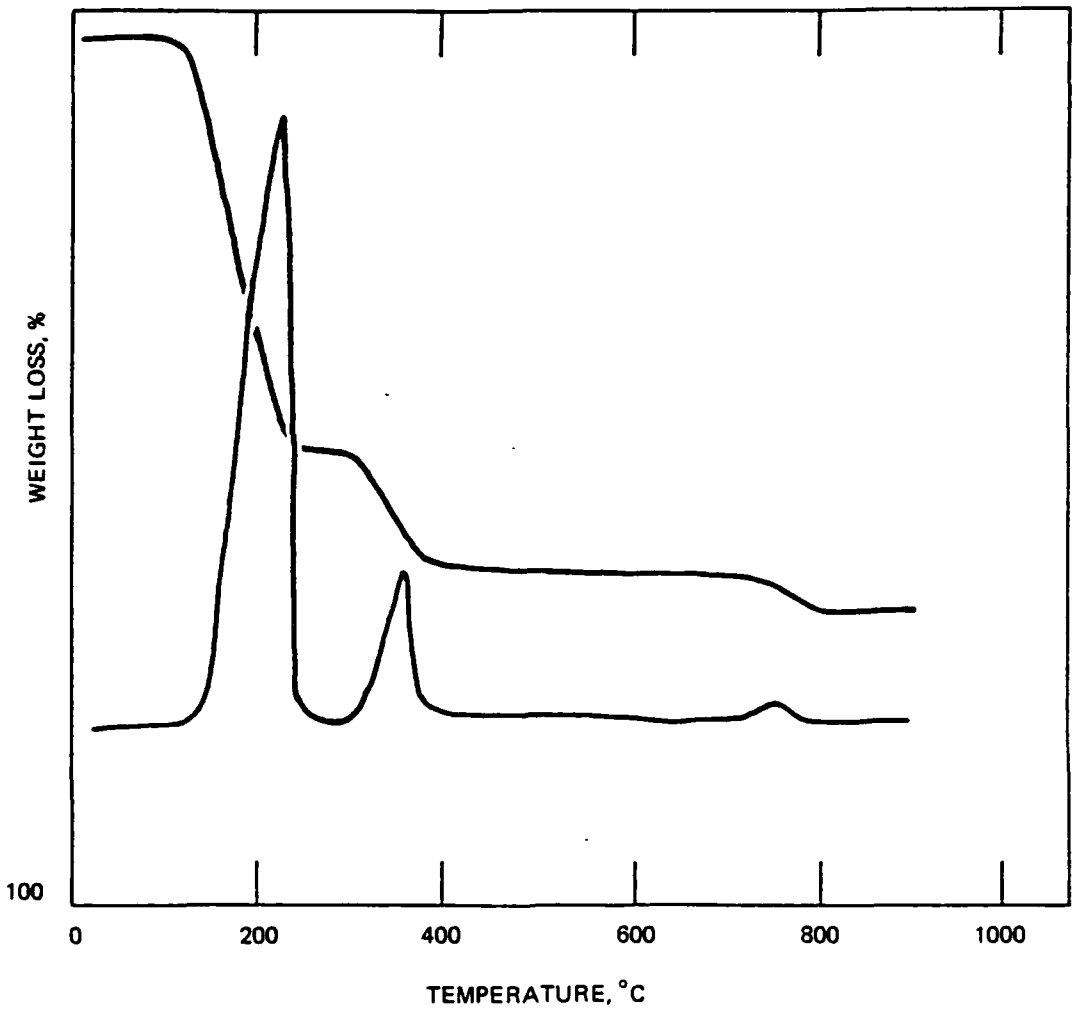

Figure A-18. Integral and Differential Gravimetric Analysis Curves for the Thermolysis of the 4:1 Mole Ratio Potassium Dawsonite/Stannic Iodide Physical Mixture.

The 4:1 physical mixture integral and differential curves as shown in Figure A-18 are characteristic of all mixtures employed, differing from other mole ratio systems only in relative peak heights of the two components. As expected, the major weight loss rates were observed at about 230 and 360°C for the SnI_4 and potassium Dawsonite, respectively.

As depicted in Figures A-19, A-20, and A-21, the integral and differential TGAs of the calcined systems of varying mole ratios reveal a common high temperature weight loss around the 850 to 890°C region. The lower mole ratio systems, 1:1 and 2:1, exhibit weight losses primarily in the 230°C region whereas the higher mole ratio systems, 5:1 and 8:1, show characteristic weight losses in the 350°C zone. The most prominent feature of the 4:1 system is the 850 to 900°C weight loss.

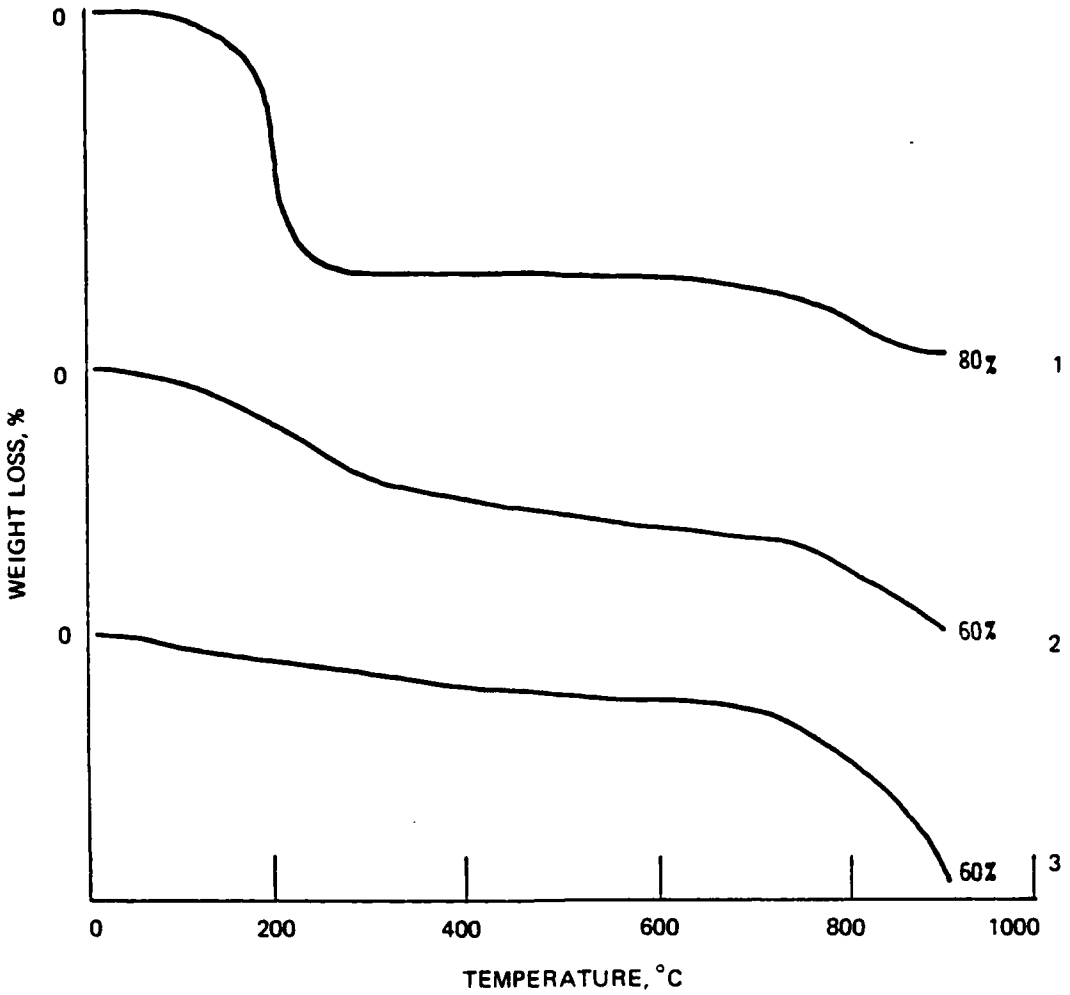

Legend:

Line 1: 1:1 MOLE RATIO
Line 2: 2:1 MOLE RATIO
Line 3: 4:1 MOLE RATIO

Figure A-19. Integral Gravimetric Analysis Curves for the Thermolysis of the 1:1(1), 2:1(2), and 4:1(3) Mole Ratio Potassium Dawsonite/SnI_4 Calcined Product.

Figure A-22 includes the integral TGAs of potassium iodide, β-stannic acid, and Boehmite. Boehmite (AlO(OH)) decomposes to form Al_2O_3. Beta-stannic acid undergoes successive water losses from 50 to 500°C. Reference 91 describes this dehydration more completely. Potassium iodide is very stable to weight loss up to a temperature of 700° C. It then rapidly loses virtually all of its weight from 700 to 900°C.

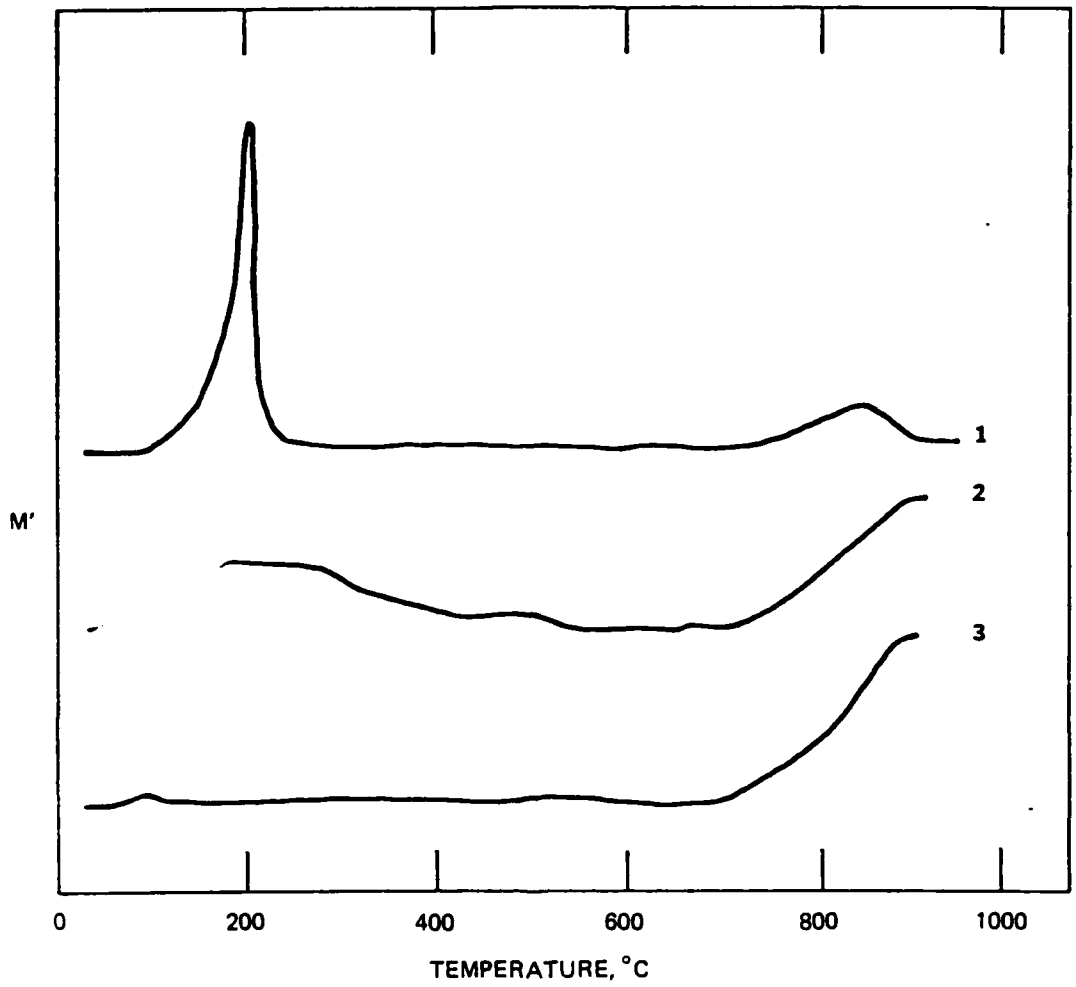

Legend:
Line 1: 1:1 MOLE RATIO
Line 2: 2:1 MOLE RATIO
Line 3: 4:1 MOLE RATIO

Figure A-20. Differential Gravimetric Curves for the Thermolysis of the 1:1(1), 2:1(2), and 4:1(3) Mole Ratio Potassium Dawsonite/SnI_4 Calcined Product.

X-Ray Diffraction Analysis

Potassium Dawsonite SnI_2 and SnI_4, were analyzed by X-ray diffraction. Refer to Table A-22 for potassium Dawsonite 2θ observations with relative intensities, Table A-15 for SnI_4 2θ assignments, and Table A-14 for 2θ assignments of SnI_2. Figure A-12 shows the X-ray diffraction spectrum of potassium Dawsonite. Table A-23 shows the 2θ assignments

with relative intensities for the 1:1 mole ratio K-Dawsonite to SnI_4 calcined product and physical mixture. The 2θ assignments and intensities for the 4:1 calcined product are listed in Table A-24. Tables A-25, A-26, and A-27 list the 2θ assignments and intensities for the 2:1, 5:1, and 8:1 calcined products, respectively. Literature 2θ values and relative intensities for potassium iodide and SnO_2 are listed in Table A-28. Figure A-23 compares the major X-ray diffraction peaks of the 2:1, 4:1, and 8:1 calcined products with the major X-ray diffraction reflections of KI, SnI_4, K-Dawsonite, and SnO_2. All of the spectra were taken using LiF as an internal standard.

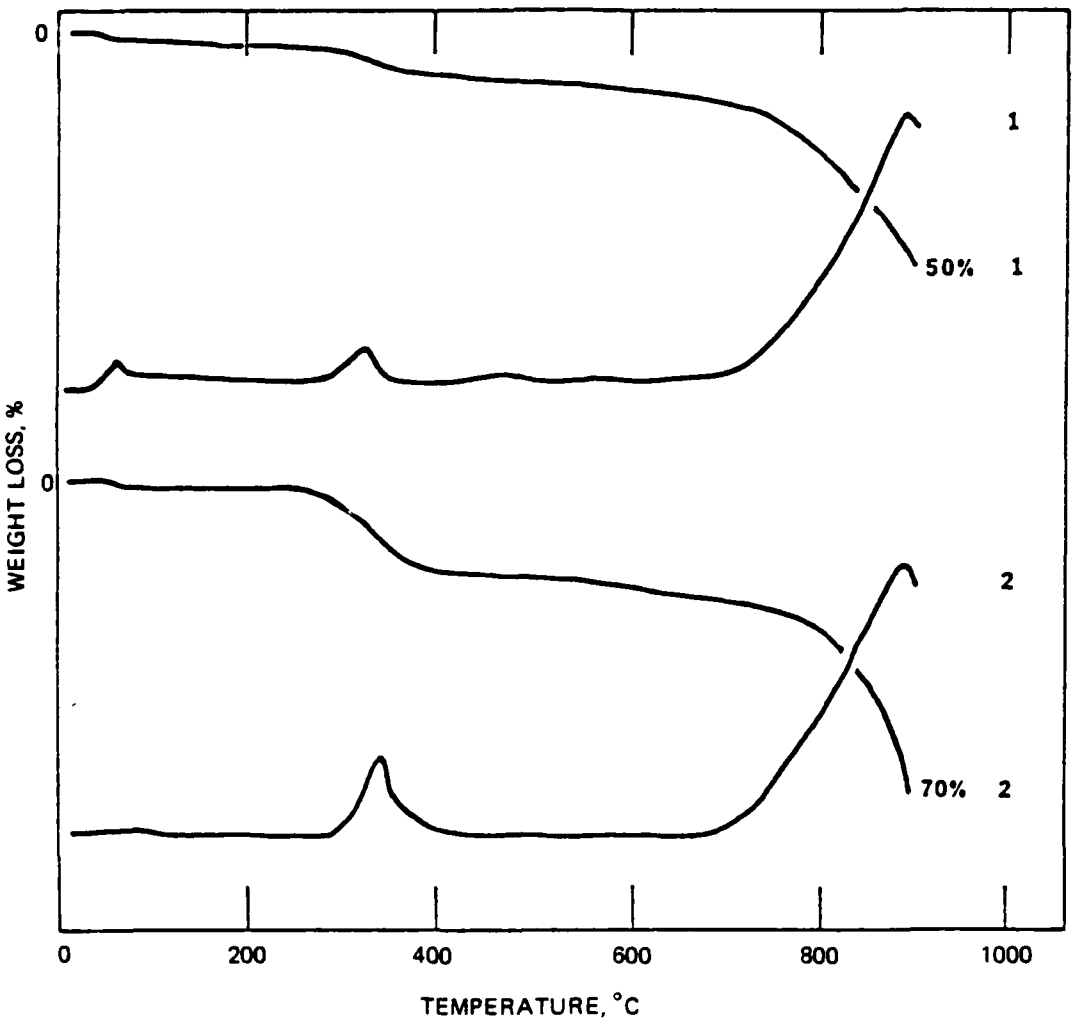

Legend:
Line 1: 5:1 MOLE RATIO
Line 2: 8:1 MOLE RATIO

Figure A-21. Integral and Differential Gravimetric Analysis Curves for the Thermolysis of the 5:1(1) and 8:1(2) Mole Ratio Potassium Dawsonite/SnI_4 Calcined Product.

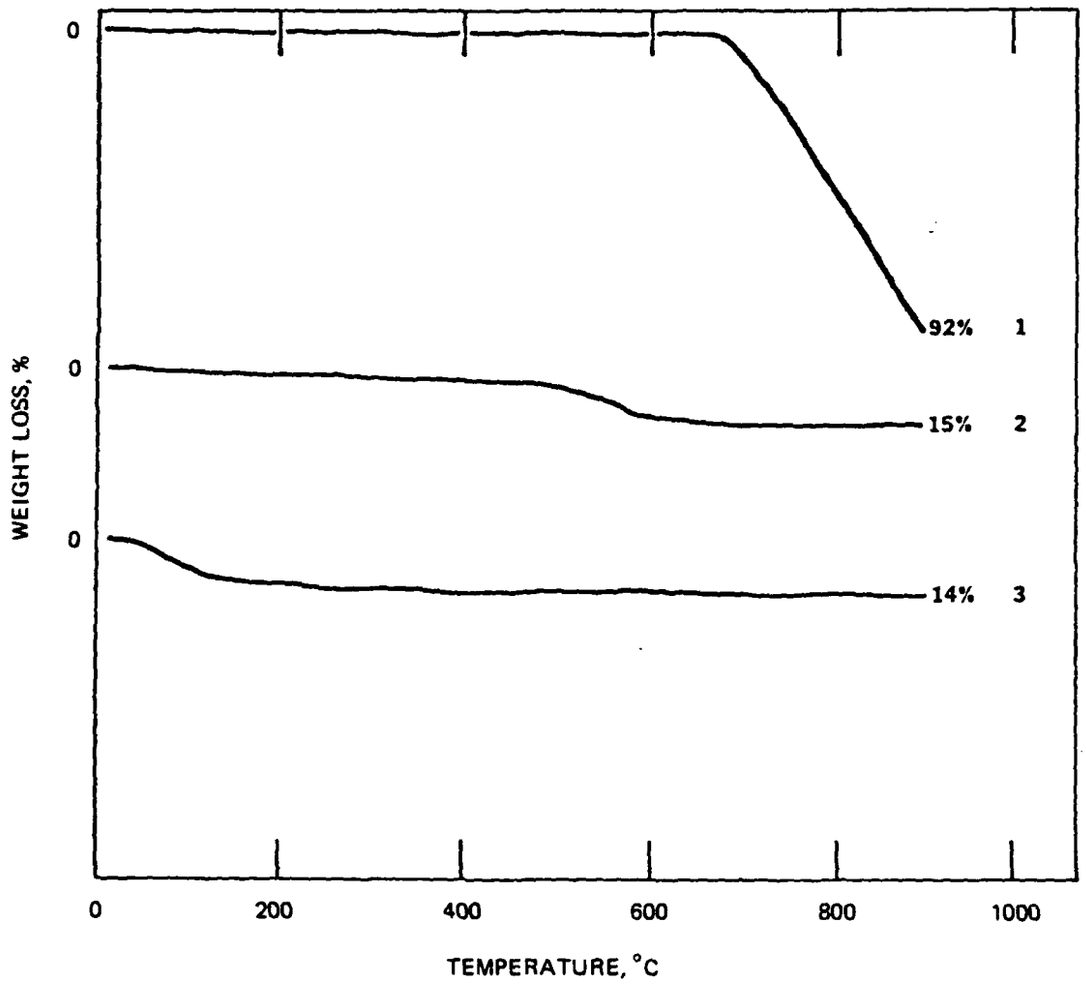

Legend:

Line 1: Potassium Iodide
Line 2: β-Stannic Acid
Line 3: Boehmite

Figure A-22. Integral Gravimetric Analysis Curves for the Thermolysis of Potassium Iodide(1), Beta-Stannic Acid(2), and Boehmite(3).

Table A-22. 2θ Values, Corresponding "d" Spacings and Relative Intensities for the X-ray Diffraction Spectrum of Potassium Dawsonite.

d Spacing	2θ	Relative intensity
(1) 5.577	15.89	100
(2) 4.105	21.65	56
(3) 3.368	26.46	71
(4) 3.150	28.33	94
(5) 2.892	30.92	16
(6) 2.820	31.73	39
(7) 2.787	32.11	40
(8) 2.643	33.92	28
(9) 2.514	35.71	73
(10) 2.164	41.73	42
(11) 1.990	45.56	54

Table A-23. 2θ Values, Assignments, and Relative Intensities for the X-ray Diffraction Spectra of the 1:1 Mole Ratio (K-Dawsonite/SnI_4) Physical Mixture and Calcined Product.

Physical mixture 1:1 mole ratio			Calcined product 1:1 mole ratio			
2θ	Assignment	Relative intensity	2θ		Assignment	Relative intensity
			Literature	Observed		
15.94	KD	14	21.78	21.73	KI	47
16.19	SnI_4	9	25.13	25.17	SnI_4	100
			25.23		KI	
17.72	SnI_4	14	26.60	26.58	SnO_2	11
21.74	KD	7	29.09	29.08	SnI_4	7
25.20	SnI_4	100	33.90	33.90	SnO_2	6
26.48	KD	8	35.95	35.93	KI	63
28.38	KD	12	41.62	41.58	SnI_4	10
29.15	SnI_4	12	42.42	42.43	KI	28
30.88	KD	2	44.43	44.33	KI	26
31.82	KD	6	49.24	49.25	SnI_4	5
32.33	KD	4				
33.48	SnI_4	4				
34.30	SnI_4	4				
35.70	KD	9				
35.93		9				
39.60	SnI_4	4				
41.65	SnI_4	26				
41.75	KD	13				
45.60	KD	7				
49.25	SnI_4	12				

Table A-24. 2θ Values and Relative Intensities for the X-ray Diffraction Spectrum of the 4:1 Mole Ratio (K-Dawsonite/SnI_4) Calcined Product.

2θ		Assignment	Relative intensity
Literature[a]	Observed		
21.78	21.76	KI	40
25.23	25.20	KI	100
26.60	26.57	SnO_2	10
33.90	33.93	SnO_2	8
35.95	35.92	KI	85
42.42	42.40	KI	30
44.43	44.40	KI	20

[a]The relative intensities are taken from the indexed ASTM catalog card number 4-0471 for KI and 21-1250 for SnO_2.

Table A-25. 2θ Values and Relative Intensities for the X-ray Diffraction Spectrum of the 2:1 Mole Ratio (K-Dawsonite/SnI_4) Calcined Product.

2θ		Assignment	Relative intensity
Literature[a]	Observed		
21.78	21.75	KI	40
25.13		SnI_4	
25.23	25.17	KI	100
26.60	26.56	SnO_2	8
29.09	29.08	SnI_4	12
33.90	33.90	SnO_2	6
35.95	35.95	KI	85
41.62	41.58	SnI_4	20
42.42	42.44	KI	32
44.43	44.40	KI	27
49.24	49.25	SnI_4	15

[a]The relative intensities are taken from the indexed ASTM catalog card number 4-0471 for KI, 21-1250 for SnO_2, and 6-0232 for SnI_4.

Table A-26. 2θ Values and Relative Intensities for the X-ray Diffraction Spectrum of the 5:1 Mole Ratio (K-Dawsonite/SnI_4) Calcined Product.

2θ		Assignment	Relative intensity
Literature[a]	Observed		
21.78	21.76	KI	42
25.23	25.22	KI	100
26.60	26.60	SnO_2	8
33.90	33.92	SnO_2	6
35.95	35.94	KI	80
42.42	42.40	KI	25
44.43	44.45	KI	23

[a]The relative intensities are taken from the indexed ASTM catalog card number 4-0471 for KI and 21-1250 for SnO_2.

Table A-27. 2θ Values and Relative Intensities for the X-ray Diffraction Spectrum of the 8:1 Mole Ratio (K-Dawsonite/SnI_4) Calcined Product.

2θ		Assignment	Relative intensity
Literature[a]	Observed		
21.78	21.82	KI	35
25.23	25.25	KI	100
26.60	26.58	SnO_2	10
28.33	28.35	KD	8
33.90	33.90	SnO_2	8
35.95	35.98	KI	80
41.73	41.75	KD	5
42.42	42.45	KI	22
44.43	44.42	KI	18
45.56	45.55	KD	5

[a]The relative intensities are taken from the indexed ASTM catalog card number 4-0471 for KI, 21-1250 for SnO_2, and 6-0232 for SnI_4. 2θ literature values for KD (potassium Dawsonite) are from Table 2.

Table A-28. 2θ Values, Corresponding "d" Spacings and Relative Intensities for the X-ray Diffraction Spectrum of Potassium Iodide and Stannic Oxide.

KI[a]			SnO_2[a]		
d Spacing	2θ	Relative intensity	d Spacing	2θ	Relative intensity
4.08	21.78	42	3.35	26.60	100
3.53	25.23	100	2.644	33.90	80
2.498	35.95	70	2.369	37.98	25
2.131	42.42	29			
2.039	44.43	27			
1.767	51.73	15			

[a] "d" spacing and relative intensities for KI and SnO_2 are from indexed ASTM catalog card numbers 4-0471 and 21-1250, respectively. 2θ values were calculated using a lambda value of 1.5418.

Chemical Analysis

The purity of the calcined potassium Dawsonite and the laboratory preparation of SnI_4 as determined by chemical analysis gave results in good agreement with theoretical values. Also, SnI_2 as obtained from ROC/RIC supplier was analyzed. Refer to Table A-13 for experimental and theoretical values.

A chemical determination was performed on the 4:1, 5:1, and 8:1 calcined products for total water soluble iodine content. The total water soluble iodine of the 4:1 calcined product, expressed as KI, was determined to be 61.10% of the total weight. The theoretical value for total iodine, calculated as KI, is 60.88%. The other calcined products of mole ratios 5:1 and 8:1 had total KI by weight 54.79 and 39.28%, respectively. The corresponding theoretical values for total KI are 53.09 and 38.36%.

Separation of Components of 1:1 Mole Ratio (K-Dawsonite/Tin(IV) Iodide) Calcined Product

The components of the 1:1 calcined product were separated and purified by solvent extraction. Unreacted SnI_4 was extracted with hot carbon tetrachloride crystallized upon cooling. Product potassium iodide was extracted with cold water; the residue phase contained insoluble aluminum and tin components. The X-ray diffraction pattern of these phases was recorded and is shown in Table A-29.

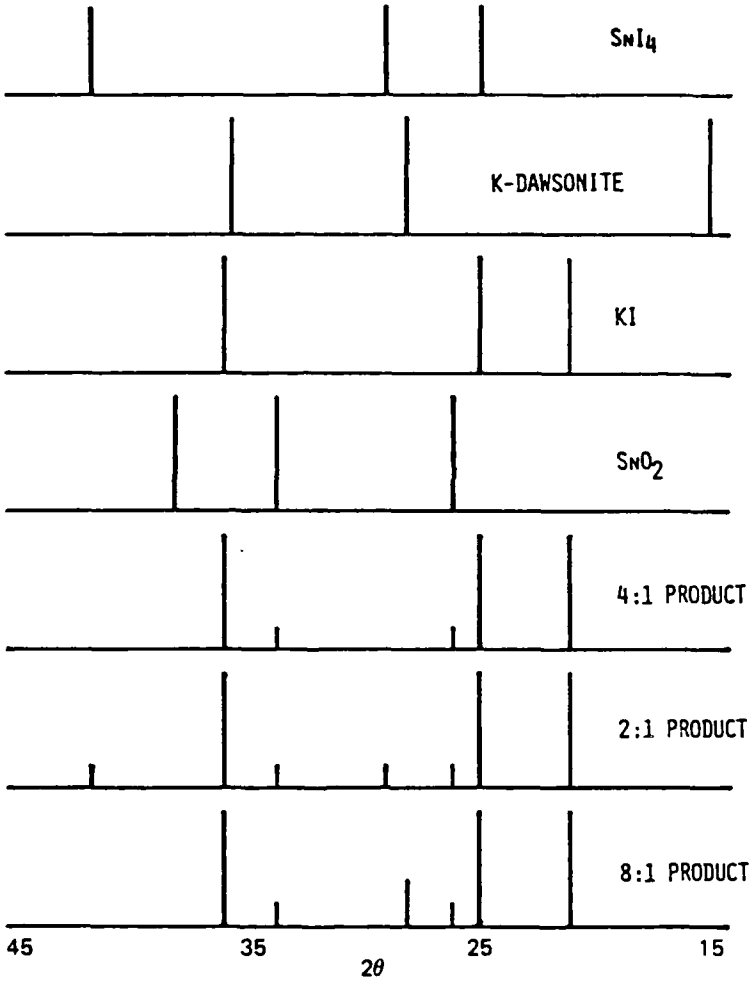

Figure A-23. 2θ Values for the Principal Peaks of SnI_4, K-Dawsonite, KI, SnO_2, 4:1, 2:1, and 8:1 Calcined Products.

Table A-29. 2θ Values and Relative Intensities for the X-ray Diffraction Spectrum of the 1:1 Mole Ratio (K-Dawsonite/SnI_4) Calcined Product--Both Extracted and Residue Phases.

Compound B (SnI_4)				Compound C (Residue phase)				Component D (KI)			
2θ		Assignment	Relative intensity	2θ		Assignment	Relative intensity	2θ		Assignment	Relative intensity
Literature[a]	Observed			Literature[a]	Observed			Literature[a]	Observed		
16.14	16.18	SnI_4	12	26.60	26.58	SnO_2	100	21.78	21.80	KI	50
17.70	17.73	SnI_4	14	33.90	33.86	SnO_2	80	25.23	25.25	KI	100
25.13	25.15	SnI_4	100	37.98	37.92	SnO_2	20	35.95	35.98	KI	65
26.18	26.20	SnI_4	4					42.42	42.46	KI	18
27.19	27.25	SnI_4	3					44.43	44.45	KI	16
29.09	29.09	SnI_4	22								
31.78	31.82	SnI_4	4								
33.46	33.48	SnI_4	8								
34.26	34.30	SnI_4	7								
40.24	40.25	SnI_4	3								
41.26	41.64	SnI_4	52								
49.24	49.27	SnI_4	20								

[a] 2θ literature values are taken from indexed ASTM catalog cards.

The Iodine Content of the PotassiumBicarbonate/Aluminum Hydroxide/Potassium Iodide Calcined Product

The iodine content, expressed as KI, was determined by chemical methods. The results of total KI measured as 8.54% compared to a theoretical value of 8.74% are in good agreement with each other. The aluminum and carbonate content were also determined. The experimentally determined value of Al was 17.51% compared to a theoretical value of 16.86%. Total carbonate was measured as 36.77% compared to a theoretical value of 37.49%. The 2θ assignments for the above calcined product are shown in Table A-30.

Table A-30. 2θ Values and Relative Intensities for the X-ray Diffraction Spectrum of the $KHCO_3/Al(OH)_3/KI$ Calcined Product.

2θ		Assignment	Relative intensity
Literature[a]	Observed		
15.89	15.89	KD	65
21.65	21.68	KD	45
21.78	21.80	KI	60
25.23	25.22	KI	100
26.46	26.45	KD	50
28.33	28.35	KD	65
30.92	30.90	KD	10
31.73	31.72	KD	30
32.11	32.13	KD	25
33.92	33.95	KD	22
35.71	35.72	KD	55
35.95	35.95	KI	80
41.73	41.70	KD	25
42.42	42.45	KI	20
44.43	44.42	KI	25
45.56	45.55	KD	45

[a] 2θ literature values are taken from the indexed ASTM catalog card number 4-0471 for KI, 2θ literature values for KD are from Table 45.

DISCUSSION

SYNTHESIS OF STANNIC AND STANNOUS IODIDES AND THE CALCINED PRODUCTS OF POTASSIUM DAWSONITE/TIN(IV) IODIDE

Although, as documented elsewhere in this report, promising results from static as well as dynamic testing of reignition retardant efficacy had been obtained using calcined KD/SnI_x, where "x" had been presumed to be two, preliminary X-ray diffraction and TGA studies indicated that the resultant material was comparable to that obtained by calcination of KD/SnI_4. Consequently, further study of the environmentally sensitive and unstable KD/SnI_2 system was contra-indicated, since the stannous iodide readily oxidized to SnI_4, probably according to the following reaction:

$$2SnI_2 + O_2 \longrightarrow SnI_4 + SnO_2$$

Stannic iodide was considerably more stable than stannous iodide. The calcined products of mole ratios 1:1 and 2:1 K-Dawsonite/SnI_4 were nonwhite in color whereas the 5:1 and 8:1 products were white in color. This seems to indicate an excess of SnI_4 in the 1:1 and 2:1 products and an excess of potassium Dawsonite in the 5:1 and 8:1 products.

CALCINATION OF ALUMINUM HYDROXIDE/POTASSIUM CARBONATE WITH KI

The calcination reaction with the above components was carried out using the same conditions as used in the potassium Dawsonite synthesis. The weight loss after calcination was equivalent to one mole water loss, thus indicating potassium Dawsonite formation. The reaction proceeded as follows:

$$Al(OH)_3 + KHCO_3 + KI \longrightarrow KAlO(OH)HCO_3 + KI + H_2O$$

INSTRUMENTAL ANALYSIS

Infrared Spectroscopy

From Figures A-14 and A-15 it becomes clear that potassium Dawsonite is the limiting reactant for the 1:1 and 2:1 calcined products, whereas potassium Dawsonite is in excess in the 5:1 and 8:1 calcined products, with SnI_4 being the limiting reactant. The 4:1 calcined product is in the marginal zone with potassium Dawsonite only in a very slight excess. This might be due to incomplete reaction. The stoichiometry of potassium Dawsonite/SnI_4 reaction appears to be in the mole ratio of 4:1 K-Dawsonite/SnI_4. From Figure A-16, the

4:1 calcined product appears to be a mixture of Boehmite (AlO(OH)) and stannic acid and/or stannic oxide. Potassium and iodine are not accounted for via IR, and X-ray spectrometry was used to identify the potassium and iodine species.

Thermogravimetric Analysis

Potassium Dawsonite was washed free of excess bicarbonate with cold water. The decomposition peak at 150°C in Figure A-17 is due to a small excess of bicarbonate. After washing with water the soluble bicarbonate was absent and the decomposition peak at 150°C is no longer present. The two other peaks that remain even after washing are due to potassium Dawsonite decomposition. One peak occurs at 365°C and the other at 745°C. Both are due to H_2O and CO_2 loss. The final residue from potassium Dawsonite decomposition is $KAlO_2$. Figure A-13 shows a weight loss for SnI_4 which occurs over a small temperature range. SnI_2 had some SnI_4 impurity and two weight loss peaks appeared.

All of the calcined products show a prominent potassium iodide weight loss peak at 750 to 900°C. The 1:1 and 2:1 calcined products have an excess of SnI_4 as shown by the weight loss peak at 170 to 240°C. Potassium Dawsonite decomposition peaks appear in the 5:1 and 8:1 products. This indicates that SnI_4 is the limiting reactant for the 5:1 and 8:1 reactions and potassium Dawsonite is the limiting reactant for the 1:1 and 2:1 mole ratio reactions. The 4:1 calcined product is in the transition zone between these two limiting reactants and this is probably where the stoichiometry of the reaction occurs. The 4:1 calcined product appears to contain potassium iodide, stannic acid and possibly some AlO(OH). This is shown in Figures A-19 and A-20.

X-ray Diffraction Analysis

All of the major 2θ peaks for the 1:1, 2:1, 4:1, 5:1, and 8:1 calcined products have been identified and are in Tables A-16 through A-20. The 1:1 and 2:1 calcined products show a small excess of SnI_4 with diffraction peaks at 2θ values of 29.08, 41.58, and 49.25. The major 2θ peak at 25.17 is occluded by the major potassium iodide peak at 25.23. The 4:1, 5:1, and 8:1 calcined products do not show any SnI_4 diffraction peaks. Potassium Dawsonite X-ray diffraction peaks do appear at 2θ value of 28.35, 41.75, and 45.55 in the 8:1 calcined product. Potassium Dawsonite was not detectable in the other calcined products. All of the calcined products show major 2θ value belonging to potassium iodide. The 4:1 calcined product shows only potassium iodide and stannic oxide 2θ reflection values. The 4:1 product appears to consist of potassium iodide and stannic oxide. The alumina phase must be amorphous because no reflection values could be found for AlO(OH), although AlO(OH) was detected by infrared spectroscopy. Figure A-23 shows the starting reactants SnI_4 and potassium Dawsonite, and the products obtained by calcination, KI and SnO_2. The 2:1 product has excess SnI_4 and the 8:1 product has excess potassium Dawsonite. The 4:1 mole ratio appears to be the correct stoichiometry for the potassium Dawsonite–SnI_4 reaction.

CHEMICAL ANALYSIS

The potassium iodide content of the 4:1, 5:1, and 8:1 calcined products were in good agreement with theoretical values for KI, therefore KI appears to be the iodide component of the calcined products.

Separation of Components of 1:1 Mole Ratio (K-Dawsonite/ Tin(IV) Iodide) Calcined Product

Three components or sets of components were separated from the 1:1 calcined product. One component was pure SnI_4, the second component was potassium iodide and the third component, which was mostly amorphous, was $SnO_2 \cdot xH_2O$ and AlO(OH). Table A-29 shows the 2θ values for the X-ray diffraction of these components. This 1:1 calcined product had potassium Dawsonite as its limiting reactant, therefore SnI_4 was in excess after the reaction. The AlO(OH), stannic acid and/or stannic oxide and potassium iodide were formed during calcination.

The Iodine Content of the Potassium Carbonate/Aluminum Hydroxide/Potassium Iodide Calcined Product

Potassium iodide did not interfere with the formation of potassium Dawsonite when the starting reactants were $KHCO_3$, $Al(OH)_3$, and KI. Table A-30 supports this conclusion. Only potassium Dawsonite and potassium iodide are observed in the X-ray diffraction spectrum. The iodine content of the calcined product, measured as KI, is in good agreement with the theoretical value of KI.

CONCLUSION

A new interstitial guest/host type of compound was not formed by the calcination of K-Dawsonite and SnI_4; rather, the resultant mixture underwent a reaction to form a new iodide specie. The stoichiometry of the potassium Dawsonite/SnI_4 reaction is in the mole ratio of 4:1 for the (K-Dawsonite/SnI_4), respectively. The overall reaction proceeds according to the following equation:

$$4KAl(OH)_2CO_3 + SnI_4 \longrightarrow 4KI + 4AlO(OH) + SnO_2 \cdot xH_2O + 4CO_2 + (2-x)H_2O$$

The potassium iodide is a crystalline phase and appears as the prominent part of the X-ray diffraction spectrum. The stannic acid ($SnO_2 \cdot 2H_2O$) has some crystalline characteristics and appears as SnO_2 in the X-ray diffraction powder pattern. AlO(OH) appears to be amorphous. It has a strong IR spectrum but fails to show any diffraction pattern in the X-ray analysis.

An iodide doped sample of potassium Dawsonite can be directly synthesized from aluminum hydroxide, $Al(OH)_3$, and potassium bicarbonate, $KHCO_3$, in the presence of potassium iodide, KI. The long reigition delay times achieved with this KD/KI calcined mixture may be due to the slow release of iodide into the combustion zone. As the flame or heat penetrates the potassium Dawsonite, the iodide volatilization is suppressed by the endothermic decomposition of the potassium Dawsonite; contiguous adhesion of the radical to the potassium Dawsonite by enclathration would optimize thermal exchange between the two phases.

REFERENCES

1. 1955-74 AGARD Conference Proceedings 166, *A Study of Transport Aircraft Accidents*, by A. F. Taylor, April 1975.

2. Air Force Aero Propulsion Laboratory. *Recent USAF and FAA Developments in Aircraft Fire Detection Systems*, by R. G. Hill and C. L. Delaney. Wright-Patterson AFB, OH, AFAPL, 1974, (AFAPL-SF).

3. Air Force Aeropropulsion Laboratory. *Fire Detection System Performance in USAF Aircraft*, by C. L. Delaney, Wright-Patterson AFB, OH, AFAPL, August 1972. (AFAPL-TR-72-49.)

4. "Determination of Means to Safeguard Aircraft from Powerplant Fires in Flight. Part I", by A. W. Dallas and H. L. Hansberry, September 1943. (CAA TDR 33).

5. "Ibid, Part II", by G. L. Pigman, October 1943. (CAA TDR 37.)

6. "Ibid, Part III", by H. L. Hansberry, April 1944. (CAA TDR 38.)

7. Air Force Wright Aeronautical Laboratories. *Fire Protection of Jet Engine Aircraft*, by N. P. Muench and H. A. Klein, Wright-Patterson AFB, OH, AFWAL, 21 July 1949. (MCREXE-664-466-K.)

8. "Aircraft Fire Extinguishment, Part I, A Study of Factors Influencing Exinguishing System Design", by C. M. Middlesworth, October 1952. (CAA TDR 184.)

9. "Fire Extinguishing Studies of the Northrup F-89 Powerplant", by A. V. Young, October 1958. (CAA TDR 365).

10. "Aircraft Fire Extinguishment, Part II, The Effect of Airflow on Extinguishing Requirements of a Jet Power-plant Fire Zone", by C. A. Hughes, June 1953. (CAA TDR 205.)

11. "Determination of a Means to Safeguard Aircraft From Power-plant Fires in Flight, Part VI", by C. M. Middlesworth, March 1954. (CAA TDE 221.)

12. "Aircraft Fire Extinguishment, Part IV, Evaluation of a Bromochloromethane Fire Extinguishing System for the XB-45 Airplane", by C. A. Hughes and C. M. Middlesworth, June 1954. (CAA TDR 240.)

13. "The Halogenated Extinguishing Agents", National Fire Protection Association Report Q48-8, (October 1954).

14. "Aircraft Fire Extinguishment, Part V, Preliminary Report on High-Rate-Discharge Fire Extinguishing Systems for Aircraft Power Plants", by H. L. Hansberry, February 1956. (CAA TDR 260.)

15. "Aircraft Fire Extinguishment, Part III, An Instrument for Evaluating Extinguishing Systems", by J. D. New and C. M. Middlesworth, June 1953. (CAA TDR 206.)

16. "Aircraft Installation and Operation of an Extinguishing Agent Concentration Recorder", by J. E. Demaree and P. R. Dierdorf, September 1959. (CAA TDR 403.)

17. "The Extinction of Fires in Aircraft Jet Engines, Part I, Small-Scale Simulation of Fires", by R. Hirst, P. J. Farenden, and R. F. Simmons, Fire Technology, 12(4), 266 (November 1976).

18. "The Extinction of Fires in Aircraft Jet Engines, Part II, Full Scale Fire Tests", by R. Hirst, P. J. Farenden, and R. F. Simmons, Fire Technology, 13(11), 59 (February 1977).

19. "The Extinction of Fires in Aircraft Jet Engines, Part III, Extinction of Fires at Low Airflows", by J. H. Dyer, M. J. Majoram, and R. F. Simmons, Fire Technology, 13(2), 126 (May 1977).

20. Joint Technical Coordinating Group on Aircraft Survivability. *Airflow Effects on Fuel Fires*, by C. G. Gebhard, Washington, D. C., JTCG/AS, October 1976. (JTCG/AS-75-T-001.)

21. National Aeronautics and Space Administration. "Aircraft Engine Sump-Fire Studies", in Aircraft Safety and Operating Problems, by W. R. Loomis, 18 October 1976. (NASA SP-416.)

22. National Aeronautics and Space Administration. *Advanced Fire Extinguishant for Aircraft*, April 1974 (JTCG/AS-74-T-001) and *Environmental and Operating Requirements for Fire Extinguishing Systems on Advanced Aircraft*, November 1974 (JTCG/AS-74-T-002) by J. D. McClure and R. J. Springer, Washington, D. C., JTCG/AS.

23. Federal Aviation Administration. *An Investigation of In-Flight Fire Protection With a Turbofan Powerplant Installation*, by E. P. Klueg and J. E. Demaree, April 1969. (FAA Report Na-69-26(DS-68-28).)

24. Federal Aviation Administration. *Fire Protection Tests in a Small Fuselage-Mounted Turbojet Engine and Nacelle Installation*, by D. E. Sommers, November 1970. (FAA Report RD-70-57.)

25. Air Force Aeropropulsion Laboratory. *Ignition of Aircraft Fluids by Hot Surfaces Under Dynamic Conditions*, by A. Strasser, N. C. Waters and J. M. Kuchta, Wright-Patterson AFB, OH, AFAPL, November 1971. (AFAPL-TR-71-86.)

26. Navy Bureau of Aeronautics. "Simulated Flight Test Investigation of the Effectiveness of a Lightweight, Aircraft, Fixed, Fire-Extinguishing System", 23 June 1964. (Contract N600 (19) 59752.)

27. Air Force Aeropropulsion Laboratory. *Investigation of Pyrotechnic Generated Gas Discharge Fire Extinguishing System*, by M. deRouville and L. V. Hebenstreit, Wright-Patterson AFB, OH, AFAPL, May 1968. (AFAPL-TR-68-47.)

28. Air Force Aeropropulsion Laboratory. *Development of Full Scale Pyrotechnic Generated Gas Discharge Fire Extinguishing System*, by L. V. Hebenstreit, M. deRouville, and K. Rogers, Wright-Patterson AFB, OH, AFAPL, April 1969. (AFAPL-TR-69-66.)

29. *Aircraft Applications of Halogenated Hydrocarbon Fire Extinguishing Agents*, by B. P. Botteri, R. E. Cretcher, and W. R. Kane, in NASA Symposium Proceedings, "An Appraisal of Halogenated Fire Extinguishing Agents" (11 April 1972).

30. Air Force Aeropropulsion Laboratory. *Fire Protection Research Program for Supersonic Transport*, by M. Gerstein and R. D. Allen, Wright-Patterson AFB, OH, AFAPL, December 1964. (AFAPL-TDR-64-105.)

31. *Final Report of Studies Related to Aircraft Fires and Extinguishment*, by R. F. Simmons, British Ministry of Defense Contract KM/F/129/CB/0b, May 1974. (Report N. D. 739.)

32. "Halogenated Fire Suppressants", by R. G. Gann, Washington, D. C. (ACS Symposium Series 16, pp. 31), 1975.

33. *Contribution to the Selection of Fire Extinguishing Systems and Agents for Aircraft Fires*, by R. Fiala, AGARD Conference Proceedings on Aircraft Fuels, Lubricants and Fire Safety, 10 May 1971. (AGARD CP-84-71.)

34. "Investigations of Fire Extinguishing Powders by Means of a New Measuring Procedure", by R. Fiala and G. Winterfield, (Ibid.).

35. "Physical Chemistry, 2nd Ed.", by W. J. Moore, (Prentice-Hall, Inc., Englewood Cliffs, New Jersey, 1955), pp. 10-16.

36. *A Study of Vaporizable Extinguishants*, by D. L. Engibous and T. R. Torkelson, January 1960. (WADC-TR-59-463.)

37. "Fluobrene, Infoirmazioni Technische", (Montecantini Edison S.p.A. Divisione Petrolchimica Alogini e Derivati N, 006), Arthur Kaufman, private communication.

38. R. A. Davis, Aircraft Engineering, 43(5), 26(1971).

39. "The Foundations of Chemical Kinetics", by S. W. Benson, (McGraw-Hill Book Co., New York, 1960), pp. 452.

40. "Chemical Kinetics of Gas Reactions", by V. N. Kondratyev, (Pergamon Press, Oxford, 1974), pp. 611.

41. "Chemistry of Combustion Reactions", by G. J. Minkoff and C. F. H. Tipper, (Butterworths, London, 1962), pp. 22, 32, 34, 109.

42. "Combustion, Flames & Explosions of Gases, 2nd. Ed." by B. Lewis and G. von Elbe, (Academic Press, New York, 1961), pp. 61-4, 117, 124.

43. Air Force Wright Aeronautical Laboratories. *Inhibition of Flame Reactions.* by A. Van Tiggelen, Wright-Patterson AFB, OH, AFWAL, October 1963, (RTD-TDR-63-4011).

44. M. Friedrich, "Mode of Action of Dry Fire Extinguishing Agents", VFDB Zeit. Forschung u. Technik im Brandschutz, Sonderheit 9(2), 1(1960). (NRL Translation 804).

45. H. Besson, S. Caillere, and S. Henin, "Synthesis and Properties of Dawsonite and of a Potassium-Containing Equivalent", C. R. Acad. Sci., Ser. D 275 (18), pp. 1943-5, (1972), (Fr.).

46. H. Besson, S. Caillere, S. Henin, and R. Prost, "Experimental Formation and Conditions for Deposit of Dawsonite, C. R. Acad. Sci., Ser. D 277 (3), pp. 261-4, (1973), (Fr.).

47. H. Benson, S. Caillere, and S. Henin, "Transformation of Some Minerals in Alkaline Media", Pro. Int. Clay Conf. 1972, pp. 361-5, (Pub. 1973), (Fr.).

48. A. S. Berger and N. P. Tomilov, "Thermal Decomposition of Alkali Metal Hydroalumino Carbonates", Izv. Sib. Otd. Akad. Nauk. SSSR, Ser. Khim., Nauk., No. 4, pp. 74-81, (1969).

49. A. S. Berger and N. P. Tomilov, and I. A. Vorsina, "Interpretation of Infrared Spectra of Alkali Metal Hydroalumino Carbonates", Zh. Neorg. Khim. 16(1), pp. 81-6, (1971): (Eng. Trans.) Russ. J. Inorg. Chem., 16 42, (1971).

50. I. W. Grote, Antacid and Method of Making the Same, by I. W. Grote, U. S. Patent 2,783, 127.

51. Method of Making Dihydroxy Aluminum Carbonate Compounds, by I. W. Grote, U. S. Patent 2,783,124.

52. C. Lowig, German Patent 19,784 (1882).

53. C. Lowig, German Patent 70,175 (1982).

54. M. N. Smirnov, M. V. Mishanina, "Solubility of Sodium and Potassium Hydroalumino Carbonate in Soda and Soda Potash Solution", Tsvet. Metal 44, (8), pp. 33-5 (1971).

55. N. P. Tomilov and A. S. Berger, "Synthesis and Some Properties of Potassium Hydroalumino Carbonate", Izv. Akad, Nauk. SSSR, Neorgan. Mater., 4, (6), pp. 964-8, (1968).

56. N. P. Tomilov and A. S. Berger, "Formation Conditions for Hydroalumino Carbonates During the Interaction of Aluminum with Solution of Alkali Metal Carbonates", Zh. Neorg. Khim, 14 (3), pp. 674-9, (1969); Eng. Trans., Russian Journal of Inorganic Chemistry, 14, pp. 352-355 (1969).

57. N. P. Tomilov and A. S. Berger, "Chemical Analogs of Dawsonite", Tr. Soveshch, Eksp. Tekh. Mineral. Petrogr., 8th 1968, pp. 182-9, (Pub. 1971), (Russ.).

58. N. P. Tomilov, A. S. Berger and V. L. Elchina, "Hydrolytic Decomposition of Sodium and Potassium Aluminate Carbonate Hydrates", Tsvet. Metal, 46 (7), pp. 29-32 (1973).

59. H. G. Hirschberg, Aircraft Engineering, 43(3), 22(1971).

60. Z. Tamura and Y. Tanasawa, Seventh Symposium (International) on Combustion, (Butterworth's Scientific Publications, London, 1959), 509.

61. C. Duval Mikrchim. Ichnoanal. Acta 1963, pp. 348-54, Chem. Abstr. 58, 13105g (1963).

62. *Synthesis and Characterization of Dawsonite*, by J. Jackson, Jr., C. W. Huggins, and S. G. Ampian, USBM Report of Investigation 7664, (1972).

63. J. W. Smith and N. B. Young, Colorado School of Mines Quarterly, 70(3), 69 (1975).

64. K. C. Salooja, Comb. & Flame 5, 243 (1961).

65. H. C. Barnett and R. R. Hibbard, Ed., *Basic Considerations in the Combustion of Hydrocarbon Fuels with Air*, NACA Report 1300 (1959).

66. "Fire Fighting Agents for Large Aircraft Fuel Fires", by R. Fiala and K. Dussa, AGARD Conference Proceedings on Aircraft Fire Safety AGARD (CP-166) (April 1975).

67. G. Lask and G. G. Wagner, Eighth Symposium (International) on Combustion, Williams & Wilkins, Baltimore, 1962, pp. 432.

68. J. Bardwell, Combustion & Flame 5, 71(1961).

69. E. M. Bulewicz and P. J. Padley, Thirteenth Symposium (International) on Combustion (The Comb. Institute, Pittsburgh, 1971), pp. 73.

70. K. E. Jensen, J. Chem. Phys. 51, 4674(1969).

71. T. L. Cottrell, "The Strengths of Chemical Bonds", (Butterworths, London, 1958), pp. 249, 259.

72. C. L. Mantell, "Tin", (Chemical Catalog C., New York 1929), pp. 285-6.

73. H. Ginnsber, W. Huttig, H. Stiehl, Z. anorg. u. allgem. Chem., 309, pp. 233-44 (1961).

74. J. W. Visser, J. Appl. Cryst., 2, 89 (1969).

75. Personal Communication: version number seven of the program of Reference 74, obtained from Dr. Gerald G. Johnson, Jr., The Pennsylvania State University, Materials Research Laboratory, University Park, Pennsylvania 16802.

76. C. Lauro, Atti. acc. naz. Ital., ser. 7, 3 146 (1941).

77. J. A. Mandarino, D. C. Harris, Canada Mineral., 8, pp. 377-81 (1965).

78. A. J. Frueh, J. P. Golightly, the Canadian Mineralogist, 9, pp. 51-56 (1967).

79. N. P. Tomilov, A. G. Merkulov, A. S. Berger, Izv. Sib. Otd. Akad. Nauk. SSSR Ser. Khim. Nauk, 3, pp. 55-59 (1969).

80. N. P. Tomilov, A. G. Merkulov, A. S. Berger, Russian Journal of Inorganic Chemistry, 14 (11) 1581 (1969).

81. C. L. Mantell, "Tin - Its Mining, Production, Technology, and Applications"; pp. 262-299 (1929).

82. R. J. Zollweg and L. S. Frost, Journal of Chemical Physics; 50, pp. 3280-3284 (1969).

83. F. Meller and I. Frankuchen, Acta Cryst., 8, pp. 343-344 (1955).

84. R. Dickinson, Journal of the American Chemical Society, 45, pp. 958-962 (1923).

85. R. Howie, W. Moser, and I. Trevena, Acta Cryst., 828, pp. 2965-2971 (1972).

86. F. K. Butcher, W. Gerrard, E. Monney, R. Rees, H. Willis, A. Anderson, and H. Gebbie, Journal of Organometallic Chemistry, 33, 1963-1964.

DISTRIBUTION LIST

Air Force Wright Aeronautical Laboratories
Wright-Patterson AFB, OH 45433
Attn: AFWAL/MLPJ (S. Lyon)
Attn: AFWAL/FIESE (R. W. Lauzze)
Attn: AFWAL/POSH (R. G. Clodfelter) (10 copies)

Applied Technology Laboratory
Army Research & Technology Laboratories (AVRADCOM)
Fort Eustis, VA 23604
Attn: DAVDL-ATL-ASV (H. W. Holland)
Attn: DAVDL-ATL-ASV (C. M. Pedriani)

Federal Aviation Administration Technical Center
Atlantic City, NJ 08405
Attn: ACT-330 (L. J. Garodz)

NASA - Ames Research Center
Army Research and Technology Laboratories, Headquarters
Mail Stop 207-5
Moffett Field, CA 94035
Attn: DAVDL-AS (V. L. J. DiRito)

NASA - Johnson Space Center
Houston, TX 77058
Attn: Code EC (Dr. F. S. Dawn)

Naval Air Development Center
Warminster, PA 18974
Attn: Code 2012 (M. Mitchell)
Attn: Code 6013 (A. E. Simkins)

Naval Air Systems Command
Washington, D. C. 20361
Attn: AIR-00D4 (Tech. Library)

Naval Postgraduate School
Monterey, CA 93940
Attn: Library, Code 1424 (R. Escobido)

Naval Safety Center
Naval Air Station
Norfolk, VA 23511
Attn: Code 055 (M. B. Jones, Librarian)

87. H. Stammreich, R. Forneris, and Y. Tavares, Journal of Chemical Physics, 25, pp. 1278-1279 (1956).

88. F. McDermot, Journal of the American Chemical Society, 33, 1863-1964.

89. T. Sevastyanova and N. Karpenko, Russian Journal of Inorganic Chemistry, 14, pp. 1649-1651 (1969).

90. L. Frederickson, Analytical Chemistry, 26, pp. 1883-1885 (1954).

91. E. Giesekke, H. Gutowsky, P. Kirkov, and H. Laitinen, Inorganic Chemistry, 6, pp. 1294-1297 (1967).

92. S. Batsonov and N. Shestakova, Izv. Akad. Nauk. SSSR, Neorgan Materialy, 2, pp. 92-97 (1966).

Naval Weapons Center
China Lake, CA 93555
Attn: Code 3383 (K. W. Bailey) (2 copies)
Attn: Code 3381 (C. Padgett) (2 copies)

Naval Weapons Support Center
Crane, IN 47522
Attn: Code 5041 (K. Sanders)

Pacific Missile Test Center
Point Mugu, CA 93042
Attn: Code 6862 (Naval Air Station, Technical Library)

AVCO
Lycoming Division
550 S. Main St.
Stratford, CT 06497
Attn: Richard Euerk

Bell Helicopter - Textron
P. O. Box 482
Fort Worth, TX 76101
Attn: J. R. Johnson (Dept. 81) (Mail Drop 11)

Boeing Vertol Company
A Division of the Boeing Company
Boeing Center
P. O. Box 16858
Philadelphia, PA 19142
Attn: J. P. Donnelly, M/S P32-18

The Boeing Company
P. O. Box 3707
Seattle, WA 98124
Attn: J. G. Avery, M/S 41-10
Attn: K. F. Brettmann, M/S 4E-64
Attn: J. H. Howard, M/S 4E-64

Boeing Military Airplane Company
A Division of The Boeing Company
3801 S. Oliver
Wichita, KS 67210
Attn: J. Komula, M/S K75-25
Attn: J. Stovall

AD-A174 406 DEVELOPMENT AND TESTING OF DRY CHEMICALS IN ADVANCED EXTINGUISHING SYSTEM (U) SAN JOSE STATE UNIV CALIF R L ALTMAN ET AL FEB 83 JTCG/AS-82-T-002 3/3

UNCLASSIFIED NCA2-OR675-806/NSG-2165 F/G 13/12 NL

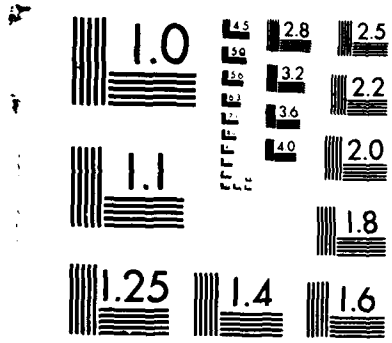

E-Systems Inc.
P. O. Box 1056
Greenville, TX 75401
Attn: L. D. Nelson CBN34
Attn: Librarian, (L. Phelps CBN38)

Falcon Research and Development Co.
One American Drive
Buffalo, NY 14225
Attn: Security Officer

Ford Aerospace and Communications Corp.
Ford Road, P. O. Box A
Newport Beach, CA 92663
Attn: Library

General Dynamics Corp.
P. O. Box 748
Fort Worth, TX 76101
Attn: J. K. Trotter, M/Z 2655

General Electric Co.
Aircraft Engine Group
1000 Western Ave.
Lynn, MA 01910
Attn: Security Officer/E. L. Richardson
Attn: S. Moltz, Drop 24001

Goodyear Aerospace Corp.
Engineered Fabrics Division
1210 Massillon Rd.
Akron, OH 44315
Attn: Library, D/152G2 (L. Lariccia)

Grumman Aerospace Corp.
South Oyster Bay Rd.
Bethpage, NY 11714
Attn: J. P. Archey, Jr., Dept. 662, M/S C31-05
Attn: Technical Information Center, Plant 35 L01-35 (T. Wilkins)

HTL Advanced Technology Division
1800 Highland Avenue
Duarte, CA 91010
Attn: R. P. Smith

IIT Research Institute
10 West 35th Street
Chicago, IL 60616
Attn: Jeannette Harlow

McDonnell Douglas Corp.
Douglas Aircraft Company
3855 Lakewood Blvd.
Long Beach, CA 90846
Attn: Technical Library, C1-250/36-84 AUTO 14-78

McDonnel Douglas Corp.
McDonnell Aircraft Company
P. O. Box 516
St. Louis, MO 63166
Attn: R. D. Detrich, Dept. 022 B/33 L/1
Attn: E. L. Zust, Dept. 345, Bldg. 270E, Level 5

D. W. Mowrer
221 W. Stanton Road
Quarryville, PA 17566

Northrop Corp.
Aircraft Division
One Northrop Avenue
Hawthorne, CA 90250
Attn: K. Christensen, N3895/94
Attn: Library, 3360/82

Northrop Corp.
Ventura Division
1515 Rancho Conejo Blvd.
P. O. Box 2500
Newbury Park, CA 91320
Attn: Tech. Info. Center (M. Raine)

Sikorsky Aircraft Division
United Technologies Corporation
North Main Street
Stratford, CT 06002
Attn: D. P. Bartz, Chief Survivability

Southwest Research Institute
6220 Culebra Road
P. O. Drawer 28510
San Antonio, TX 78284
Attn: Dr. W. D. Weatherford, Jr.

Survice Engineering Company
P. O. Box 693
Bel Air, Md 21014
Attn: Security Officer

Sverdrup Technology, Inc.
AEDC Group
Arnold AFS, TN 37389
Attn: Library, M/S 100

United Technologies Corporation
United Technologies Research Center
400 Main St.
East Hartford, CT 06108
Attn: UTC Library (M. E. Donnelly)

END

12-86

DTIC